A Translational Investigation into Palmitoylethanolamide in Skeletal Muscle Repair

By

Paige Louisa Cole

A thesis submitted in partial fulfilment of the requirements of Liverpool John Moores University for the Degree of Doctor of Philosophy

Date: 3rd November 2025

Authors Declaration

I declare that the work in this thesis was carried out in accordance with the regulations of Liverpool John Moores University. Apart from the help and advice acknowledged, the work within was solely completed and carried out by the author.

Any views expressed in this thesis are those of the author and in no way represent those of Liverpool John Moores University and the School of Sport and Exercise Science.

This thesis has not been presented to any other University for examination either in the United Kingdom or overseas. No portion of the work referred to in this research project has been submitted in support of an application for another degree or qualification of this or any other university or institute of learning.

Signed: 

Date: 3rd November 2025

Abstract

Palmitoylethanolamide (PEA), an endogenous fatty acid amide with analgesic and anti-inflammatory properties, has recently emerged as a potential alternative to non-steroidal anti-inflammatory drugs (NSAIDs) for the management of exercise-induced muscle damage (EIMD). Widespread reliance on NSAIDs among athletes, combined with growing concerns surrounding their efficacy and long-term safety, has underscored the need for safer strategies. This thesis aimed to investigate PEA from four distinct, yet interrelated perspectives: (i) the prevalence and perceptions of NSAID use among endurance athletes, to evaluate usage behaviours and attitudes towards potential alternatives, (ii) the mechanistic influence of PEA on skeletal muscle *in vitro*, (iii) its comparative effects with ibuprofen on protein metabolism *in vitro,* and (iv) it's potential to alleviate symptoms of EIMD *in vivo.* A survey of ultra-endurance runners first established the high prevalence of NSAID consumption and highlighted an openness to consider safer alternatives. *In vitro* investigations using C2C12 skeletal muscle cells demonstrated that PEA supported myogenic differentiation while modulating transcriptional pathways involved in inflammation. These findings were extended through dynamic proteomic analyses comparing PEA and ibuprofen, which revealed that both compounds stimulated ribosomal biogenesis, with PEA uniquely increasing synthesis of proteins associated with the small ribosomal subunit. Finally, a randomised, placebo-controlled trial examined the effects of PEA supplementation compared to ibuprofen and placebo in alleviating EIMD symptoms using a muscle-damaging downhill running protocol. Although no significant group differences were observed in muscle function or renal outcomes, both PEA and ibuprofen were associated with an earlier reduction in muscle pain perception. Taken together, these findings provide novel insights into the actions of PEA on skeletal muscle at both the gene and protein level, while offering preliminary evidence of its potential role in mitigating EIMD-related pain. This thesis contributes important context to the emerging conversation on alternatives to NSAID use in sport and exercise and provides a foundation for future research into the therapeutic potential of PEA.

Table of Contents

Contents

Chapter 1 – General Introduction 1

Chapter 2 – Literature Review 7

2.1 Skeletal Muscle Damage 8

2.1.1 Mechanisms of Exercise-Induced Muscle Damage 8

2.1.2 Primary Damage 11

2.1.3 Secondary Damage 12

2.1.4 Markers of Muscle Damage 13

2.2 Skeletal Muscle Repair 18

2.2.1 Degeneration 19

2.2.2 Regeneration 19

2.2.3 Satellite Cells 20

2.3 Solutions to Reduce Damage and Soreness 21

2.3.1 Nutritional Supplementation 21

2.3.2 Pharmacological Interventions 24

2.4. Palmitoylethanolamide (PEA) 26

2.4.1 A novel alternative to NSAIDs 26

2.4.2 Discovery of PEA 27

2.4.3 Pre-clinical investigations of PEA 28

2.4.4 Clinical use of PEA 29

2.4.5 Pharmacokinetic Characteristics of PEA 30

2.4.6 Mechanism of action 33

2.4.7 Direct Molecular targets of PEA 34

2.4.8 Indirect Molecular targets of PEA 35

2.5 Thesis Aims and Objectives 37

Chapter 3 – General Methods 39

3.1 Cell Model of Myogenesis 40

3.2 Cell Culture 40

3.2.1 Cell Culture Reagents 40

3.2.3 Plasticware 41

3.2.4 C_2C_{12} Skeletal Muscle Cells 41

3.2.5 Passaging C_2C_{12} myoblasts 41

3.2.6 Cell Counting by Trypan Blue Exclusion 42

3.2.7 Cell Cryopreservation and Resuscitation 43

3.2.8 Microscopy and Live Imaging 43

3.4 MTT Cell Viability Assay 43
3.4.1 General Principle 43
3.4.2 General Protocol 44
3.5 Flow Cytometry 45
3.5.1 General Principle 45
3.5.2 General Protocol 47
3.6 Propidium Iodide (PI) Assay 48
3.6.1 General Principle 48
3.6.2 General Protocol 49
3.7 Immunofluorescence (IF) Imaging 50
3.7.1 General Principle 50
3.7.2 General Protocol 50
3.7.3 Measuring Myotube Number and Area 51
3.7.4 Measuring Number of Nuclei 52
3.7.5 Measuring Number of Nuclei Per Myotube 52
3.8 Cell Cycle Analysis with PI 52
3.8.1 General Principle 52
3.8.2 General Protocol 53
3.9 Gene Expression Analysis 53
3.9.1 RNA-Seq General Principle 53
3.9.2 RNA Isolation 54
3.9.3 RNA Quantification 55
3.9.4 RNA Library Preparation and Sequencing 55
3.10 Proteomic Analysis 55
3.10.1 LC-MS General Principle 55
3.10.2 Protein Extraction and Digestion 56
3.10.3 Protein Identification and Quantification 57
3.10.4 Dynamic Proteome Profiling 57
3.11 Location of Testing and Ethical Approval 58
3.12 General Screening and Inclusion Criteria 58
3.13 Blood Sampling 59
3.14 Muscle Biopsy Procedure 59
3.15 Assessment of Peak Oxygen Uptake ($VO2_{peak}$) 60
3.16 Muscular Function Tests 60
3.16.1 KE Isometric MVT 60
3.16.2 Voluntary Activation (VA) 61
3.16.3 Torque-Frequency Relationship 62

Chapter 4 – The Prevalence and Perceptions of Non-Steroidal Anti-Inflammatory Drug Use Among Ultra-Endurance Runners 63

4.1 Abstract 64

4.2 Introduction 65

4.3 Methods 67

4.3.1 Ethical Approval 67

4.3.2 Survey Design 67

4.3.3 Participants 68

4.3.4 Data Collection and Handling 69

4.3.5 Thematic Analysis 70

4.4 Results 71

4.4.1 Participant Characteristics 71

4.4.2 NSAID Consumption 72

4.4.3 NSAID Information and Awareness of Adverse Drug Reactions 75

4.4.4 Considerations and Attitudes Towards NSAID Use 76

4.4.5 Consideration of NSAID Use Amongst Female Athletes 80

4.5 Discussion 80

4.6 Limitations 84

4.7 Conclusion 85

Chapter 5 – Palmitoylethanolamide (PEA) Regulates Cell Cycle Progression and Promotes an Anti-Inflammatory Transcriptomic Singature in C2C12 Skeletal Muscle Cells 87

5.2 Introduction 89

5.3 Materials and Methods 91

5.3.1 Chemicals, Reagents and Plasticware 91

5.3.2 Cell Culture 91

5.3.3 Dose Tolerability Experiments 91

5.3.4 Metabolic Activity Assay (MTT) 92

5.3.5 Cell Viability assay (Propidium iodide exclusion) 92

5.3.6 Next Generation RNA Sequencing 93

5.3.7 Immunofluorescence (IF) Staining 95

5.3.8 Image Acquisition 96

5.3.9 Cell Cycle Analysis with Propidium Iodide 96

5.3.10 Statistical Analysis 97

5.3.11 Bioinformatics 98

5.4 Results 100

5.4.1 Dose Tolerability 100

5.4.2 Myotube Morphology 100

5.4.3 Myoblast Cell Cycle Phase Analysis....102
5.4.4 Acute Transcriptomic Response to PEA in C2C12 Myotubes....103
5.4.5 Transcriptional Response of PEA Metabolising Enzymes in Skeletal Muscle....105
5.4.6 PEA modulates the expression of interleukin genes, their receptors and inflammatory pathways....105
5.5 Discussion....107
5.6 Limitations....109
5.7 Conclusion....110
Chapter 6 – Comparative Effects of Palmitoylethanolamide and Ibuprofen on the Abundance Profile and Synthesis Rate of Proteins in C2C12 Skeletal Muscle Myotubes....112
6.1 Abstract....113
6.2 Introduction....114
6.3 Methods....116
6.3.1 Chemicals, Reagents and Plasticware....116
6.3.2 Cell Culture....117
6.3.3 Cell treatments....117
6.3.4 Proteomic Analysis....118
6.3.5 Liquid chromatography-tandem mass spectrometry....119
6.3.6 Label-Free Quantification of Protein Abundance....120
6.3.7 Dynamic proteome profiling....120
3.6.8 Statistical and Bioinformatic Analysis....121
6.4 Results....123
6.4.1 Dynamic proteome profiling of C2C12 myotubes....123
6.4.2 Mixed Protein Fractional Synthesis Rates (FSR)....124
6.4.3 Alterations in proteome dynamics in response to Ibuprofen....124
6.4.4 Alterations in proteome dynamics in response to Palmitoylethanolamide....127
6.4.5 Ibuprofen and PEA increase ribosomal protein abundance and turnover....129
6.4.6 Relationship between changes in protein synthesis and proteome remodelling 131
6.5 Discussion....132
6.6 Limitations....137
6.7 Conclusion....138
Chapter 7- Exploring the Efficacy of Palmitoylethanolamide (PEA) versus NSAIDs in Alleviating Exercise-Induced Muscle Damage: A Comparative Investigation in Downhill Running....140
7.1 Abstract....141
7.2 Introduction....142

7.3 Methods 144
7.3.1 Ethical Approval 144
7.3.2 Participants 144
7.3.3 Study Design 145
7.3.4 Training Programme Overview 145
7.3.5 Experimental Protocol 148
7.3.6 Treatments 149
7.3.7 Stable Isotope Labelling 149
7.3.8 Food Provision 149
7.3.9 KE Isometric MVT 150
7.3.10 Voluntary Activation (VA) 150
7.3.11 Torque-Frequency Relationship 151
7.3.12 Perceived Muscle Pain 151
7.3.13 Kidney Function Tests 152
7.3.14 Muscle Biopsy 152
7.3.15 Statistical analysis 153
7.4 Results 154
7.4.1 Maximal Isometric Voluntary Contraction 154
7.4.2 Voluntary Muscle Activation 155
7.4.3 Resting Control Doublet Force 156
7.4.4 Torque Frequency Relationship 157
7.4.4 Pain 160
7.4.5 Kidney Function 161
7.5 Discussion 163
7.6 Limitations 167
7.7 Conclusion 168
Chapter 8 – Thesis Synthesis 169
8.1 Realisation of Aims 170
8.1.1 Aim 1 – To investigate the prevalence and perceptions of NSAID use among ultra-endurance runners to assess the need for safer alternatives in managing EIMD. 170
8.1.2 Aim 2 – To investigate the effects of PEA on C2C12 skeletal muscle myogenesis and gene expression in vitro. 171
8.1.3 Aim 3 – To investigate the effects of PEA and the NSAID Ibuprofen on protein synthesis and protein abundance in C2C12 skeletal muscle myotubes in vitro. 172
8.1.4 Aim 4 – To investigate the potential of PEA as an alternative to NSAIDs for alleviating symptoms of EIMD using an in vivo downhill running model. 173
8.2 Final Conclusions 175

List of Tables

Table 2.1. Classification of exercise-induced muscle damage into mild, moderate and severe categories, based on structural changes, force loss and expected recovery time. Categorisation adapted from (Paulsen et al., 2012). 14

Table 4.1. General Characteristics of Participants 71

Table 4.2. Frequency of NSAID use for training, competition, or recovery in ultra-endurance runners 73

Table 4.3. Themes in responses regarding NSAID intake during ultra-endurance running events. 74

Table 4.4. Considerations for avoiding NSAID use as determined by open-ended question responses. Raw data included illustrative extracts from open-ended question responses relevant to the theme. 77

Table 4.5. Attitudes toward NSAID use and impact on performance. 79

List of Figures

Figure 2.1. Schematic representation of exercise induced muscle damage, including the causes, physiological processes, and the effects on muscle. Unfamiliar exercise can cause mechanical injury to the muscle tissue, altering the homeostasis of the muscle tissue. A complex series of physiological processes are then initiated, both locally within the muscle and systemically, with a tight connection between the outlined responses. As a result, there is inflammation, delayed onset of muscle soreness (DOMS), and a decrease in muscle regeneration which in turn has a negative impact on athletic performance. Numerous factors influence an individual's response to EIMD, such as age, genetics, nutrition etc. Redrawn from Markus et al. (2021). 10

Figure 2.2. Typical magnitude and time course of EIMD symptoms, including maximal voluntary contraction (MVC), range of motion (ROM), DOMS (assessed by the visual analogue scale), swelling (measured by circumference) and plasma CK. Measurements taken before (Pre), immediately after (Post), and 1-5 days post exercise, and performed by healthy young men who were unaccustomed to exercise. Data taken from Damas et al. (2016) and re-drawn from Peake et al. (2017). 11

Figure 2.3. Schematic of the mechanism of action of NSAIDs. Arachidonic acid pathway showing production of prostaglandins from membrane phospholipids 25

Figure 2.4. Metabolism of PEA. (A) PEA is biosynthesized from a membrane phospholipid, N-palmitoyl-phosphatidyl-ethanolamine (NAPE), via several routes, the most investigated however is through the direct hydrolysis by N-acyl phosphatidylethanolamine-specific phospholipase D (NAPE-PLD).(**B**) PEA is then degraded to palmitic acid and ethanolamine by either fatty acid amide hydrolase (FAAH) or N-acylethanolamine-hydrolyzing acid amidase (NAAA) (Iannotti et al., 2016). 32

Figure 2.5. Molecular target and mechanisms of action of PEA. PEA directly activates GPR55 (pink arrow) and PPAR-a receptors (orange arrow). PEA further activates TRPV1 and increases the expression of CB_2 receptors (orange arrows) via direct activation of the PPAR-a receptors. PEA through the inhibition of the expression of FAAH (green arrow) or stimulation of the activity of DAGL (blue arrows), may increase the endogenous levels of AEA and 2-AF, which directly activate CB_1, CB_2 and TRPV1 receptors ("entourage effect"). PEA, potentially via an allosteric modulation of TRPV1 receptors, potentiates the activation of desensitization by AEA and 2-AG of TRPV1 receptors ("entourage effect"). The activation of mast cells is inhibited by PEA through an indirect CB_2-mediates mechanism. PEA also reduces the activation of microglia and astrocytes through a PPAR-a mediated mechanism. 34

Figure 3.1. C2C12 myoblasts at ~80% confluence. 42

Figure 3.2. Schematic representation of the MTT assay protocol for determining cell viability. (1) Cells are seeded into a 6-well plate and allowed to adhere. (2) The MTT reagent is added to each well, initiating the assay. (3) Plates are incubated for 3 hours to allow mitochondrial reductase in viable cells to reduce MTT into formazan crystals. (4) The reduction of MTT to

insoluble formazan is mediated by mitochondrial enzyme activity, serving as an indicator of metabolic activity and cell viability. (5) Absorbance of the dissolved formazan is measured to quantify cell viability. Higher absorbance indicates increased metabolic activity. 44

Figure 3.3. The basic layout of a flow cytometer apparatus, illustrating the fluidic, optical, and electronic systems. Cells in suspension flow in a single file through an illuminated volume where they scatter light and emit fluorescence. This is then detected by the detectors, which pick up a combination of scattered and fluorescent light. This data is then analysed by a computer that is attached to the flow cytometer using special software, where data such as the physical and chemical structure of the cells is generated. 46

Figure 3.4. Flow cytometry light scatter. Forward scatter (FSC), detected in line with the laser, correlates with cell size, while side scatter (SSC), detected perpendicular to the laser, reflects cellular granularity and internal complexity. 47

Figure 3.5. Gating strategy for C2C12 cells on the BD Accuri C6 flow cytometer. (a) Gating strategy for C2C12 myoblasts. Cells were first gated to include all events on the scatterplot. Debris in the lower left region of the FSC vs. SSC scatterplot was excluded. A secondary gate was applied to more precisely visualise the viable myoblast population. (b) Gating strategy for C2C12 myotubes. A similar approach to myoblast gating was used, with two separate gates applied to identify and visualise distinct myotube populations. 48

Figure 3.6. Propidium Iodide Staining for Differentiating Live and Dead Cells. Propidium iodide (PI) is a fluorescent dye used to distinguish between live and dead cells. PI is impermeable to live cells with intact membranes, but it penetrates and stains dead cells with compromised membranes, binding to DNA and resulting in a red fluorescence. This staining enables the identification of dead cells in a population when analysed using flow cytometry or fluorescence microscopy. 49

Figure 3.7. A schematic representation of antigen immunolabeling and fluorescent microscopy, demonstrating the binding of primary and secondary antibody to an antigen and the visualisation of fluorescence emitting cells through a fluorescent microscope. 51

Figure 4.1. Distribution of survey respondents across performance tiers. The bar chart illustrates the percentage and number (n) of athletes categorised by their self-assessed performance level, following the framework from McKay et al. (2021). 72

Figure 4.2. Distribution of NSAID intake across performance tiers. 74

Figure 4.3. Sources of NSAID information reports by participants. 75

Figure 4.4. (a) Awareness of adverse effects associated with NSAID use across performance calibre. (b) Themes related to awareness of adverse drug reactions to 76

Figure 4.5. Percentage of participants within performance tiers responding to the above statements: (a) "The benefit of using NSAIDs for my performance outweighs any negative effects", (b) "I believe I would be at a disadvantage to other competitors if I didn't use NSAIDs",

(c) "I believe I could perform just as well without NSAIDs as I could with using them", and (d) "I believe that NSAIDs improve competitive performance." 79

Figure 5.1. Experimental workflow for (**a**) the determination of dose tolerability. C2C12 myoblasts were differentiated in GM before 24 h treatment with PEA or vehicle (DMSO) control. MTT and PI exclusion assays were performed to determine the maximal tolerable dose of PEA. In workflow (**b**), C2C12 myoblasts were treated with PEA (10 µM) or vehicle control for 24 h. Myoblasts were then harvested and stained for DNA labelling with PI. Cell cycle phase distribution was then analysed using flow cytometry. In workflow (**c**), C2C12 myotubes were treated with PEA (10 µM) or vehicle control every 48 h throughout differentiation. On day 8, myotubes were fixed, stained with DAPI and MF-20, and imaged by immunofluorescence for morphological analysis. Image created using Biorender. Finally, in workflow (**d**), differentiated myotubes were exposed to PEA (10 µM) or vehicle control for 24 h before being lysed for column-based RNA extraction. Total RNA quantity and quality were determined prior to library preparation and next-generation sequencing. Pre-alignment QC was performed prior to quality trimming and STAR alignment, followed by quantification to the annotation model, counts were then normalised by median ratio, prior to DESeq2 statistical analysis. 99

Figure 5.2. Dose tolerability experiments on terminally differentiated myotubes. Metabolic activity (a) and cell viability (b) were determined by the MTT assay and propidium iodide (PI) exclusion in PEA-treated C2C12 myotubes over a range of concentrations (1-100µM). Data are presented as mean ± SD from n = 3 biological replicates for each dose. 100

Figure 5.3. Morphological analysis of myotubes treated throughout differentiation with PEA (10 µM) or vehicle control (CON). Measurements include (a) myotube area (μm^2), (b) myotube number and (c) nuclear fusion index (NFI,%). Analysis conducted using ImageJ. (d) Representative images of differentiated C2C12 myotubes stained for nuclei (DAPI, blue) and myosin heavy chain (MF-20, green). One independent image is presented per condition (CON and PEA). Scale bars = 250 µM. For morphological analyses, six images were acquired per well across three wells per condition. Quantification was performed on six randomly selected images per condition to ensure unbiased representation. Data are expressed as mean ± SD from n = 3 independent biological replicates for each dose. 102

Figure 5.4. (a) Cell cycle distribution of C2C12 myoblasts following 24 h treatment with PEA (10 µM) or vehicle control (CON), assessed by flow cytometry using propidium iodide (PI) staining. Cell cycle phases determined using appropriate gates based on PI fluorescence histograms, with G_0/G_1-phase cells identified by lower PI intensity, S-phase cells by intermediate intensity, and G_2/M -phase cells by higher intensity. (b) Representative PI fluorescence histogram (FL2-H, PE channel) illustrating DNA content profiles. Peaks correspond to G_0/G_1 (light blue), S-phase (orange), and G_2/M (red) cells. Analysis performed using FloJo software. Data are presented as mean ± SD from n = 3 biological replicates for each dose. 103

Figure 5.5. (a) Principal Component Analysis (PCA) of RNA-seq data, illustrating the variance in gene expression between PEA-treated and control samples. Each point represents an individual sample, with clustering patterns indicating transcriptomic differences between

conditions. Data are presented from n = 3 biological replicates for each dose. (b) Volcano plot depicting differentially expressed genes (DEGs), with -$\log_{10}$ FDR step-up on the y-axis and $\log_2$ fold-change on the x-axis. Grey points represent non-significant genes, blue points indicate downregulated genes, and red points indicate upregulated genes. (c) Clusters of uniquely downregulated genes and their associated Gene Ontologies. (d) Gene Ontology (GO) biological processes for all downregulated genes. (e) Clusters of uniquely upregulated genes and their associated Gene Ontologies. (f) GO biological processes for all upregulated genes. Single-node genes are excluded. Markov Clustering (MCL) was performed using the STRING app in Cytoscape (v10.3 for Mac). 104

Figure 5.6. DeSeq2 Normalised mRNA reads for (a) N acylethanolamine acid amidase (Naaa) and (b) fatty acid amide hydrolase (Faah). (c) Graphical representation of the role Naaa and Faah enzymes play in PEA metabolism. 105

Figure 6.1. Experimental design for assessing protein synthesis and abundance in C2C12 myotubes. (A) C2C12 myoblasts were cultured and differentiated over 7 days until mature myotubes were formed. (B) Myotubes were treated with PEA (10µM), IBU (100µM) or VC for 36hr. Simultaneously, cells were incubated with D2O (deuterium oxide) for isotopic labelling. Protein was harvested at 12 and 36hr post-treatment and analysed using liquid chromatography-mass spectrometry (LC-MS) to quantify both de novo protein synthesis and changes in relative protein abundance over time. Fractional synthesis rates (FSR) were calculated based on deuterium incorporation between 12–36hr, while changes in relative protein abundance (ABD) were determined from total protein levels at 36hr. 118

Figure 6.2. Global differences in fractional synthesis rates (FSR) across experimental conditions. Density plots illustrate the distribution of (log2-transformed FSR values; %/h) across each sample replicates (n = 3) for each condition: vehicle control (VC, grey), palmitoylethanolamide (PEA, blue), and ibuprofen (IBU, red). Boxplots represent condition-level summary of global protein synthesis rates, highlighting both PEA and IBU treatment show greater (stats reporting) global FSRs compared to VC. (B) Scatterplot visualising differences in the changes of protein-specific FSR between IBU and PEA conditions. Points reported as mean log2-fold change in FSR in IBU (IBU / VC) or PEA (PEA / VC). Pearson correlation revealed condition-specific changes in proteins between IBU and PEA. Overall highlighting whilst global patterns of changes in FSR may appear similar between conditions (A) the individual proteins responding in FSR are largely different between conditions (B). 124

Figure 6.3. Changes in muscle proteome dynamics in response to ibuprofen treatment**.** (A) Volcano plot showing protein-specific changes in fractional synthesis rate (FSR; $\log_2$ fold change IBU / VC, x-axis) and corresponding –$\log_{10}$ p-values (y-axis). Points represent individual proteins detected across conditions; colours denote significantly ($P<0.05$) upregulated (red) and downregulated (blue) proteins relative to vehicle control (VC). (B) Gene Ontology (GO) enrichment analysis of proteins with increased FSR following ibuprofen treatment. (C) Volcano plot showing protein abundance changes ($\log_2$ fold change IBU / VC). (D–E) GO enrichment analyses for proteins with increased (D) or decreased (E) abundance. Point size indicates the number of proteins in each GO term, and colour intensity reflects the adjusted p-value. 126

Figure 6.4. Changes in muscle proteome dynamics in response to PEA treatment. (A) Volcano plot showing protein-specific changes in fractional synthesis rate (FSR; $\log_2$ fold

change PEA / VC, x-axis) and corresponding $-\log_{10}$ p-values (y-axis). Points represent individual proteins detected across conditions; colours denote significantly ($P<0.05$) upregulated (purple) and downregulated (green) proteins relative to vehicle control (VC). (B) Gene Ontology (GO) enrichment analysis of proteins with increased FSR following PEA treatment. (C) Volcano plot showing protein abundance changes ($\log_2$ fold change PEA / VC). (D–E) GO enrichment analyses for proteins with increased (D) or decreased (E) abundance. Point size indicates the number of proteins in each GO term, and colour intensity reflects the adjusted p-value. 128
Figure 6.5. Effects of IBU and PEA treatment on ribosomal protein synthesis and abundance**.** (A) STRING-based network visualisation of cytosolic ribosomal proteins significantly changed in synthesis rate and /or abundance in response to different treatments. Each node represents a ribosomal protein from the large (60S) or small (40S) subunit, with border colour denoting proteins significantly altered in synthesis rate and fill colour denoting changes in abundance. Purple = PEA-specific, red = IBU-specific, orange = shared between PEA and IBU, grey = non-significant (NS). (B–C) Median ribosomal protein fractional synthesis rate (FSR, %/ h) for the 40S (B) and 60S (C) subunits. (D–E) Ribosomal protein abundance (fmol/ µg) for the 40S (D) and 60S (E) subunits. (B-E) Text annotations in panels represent Tukey-adjusted P-values for comparisons between each treatment and vehicle control-treated C2C12 cells. 130
Figure 6.6. Contribution of changes in synthesis to proteome remodelling. Scatterplots show the relationship between protein-specific changes in fractional synthesis rate (FSR; x-axis) and protein abundance (ABD; y-axis) following (A) ibuprofen (IBU) or (B) palmitoylethanolamide (PEA) treatment, expressed as $\log_2$ fold change relative to vehicle control (VC). Each point represents an individual protein detected in both datasets. Black lines denote linear regressions ± 95 % confidence intervals. The coefficient of determination (R^2) and associated p values are shown within each panel..... 131

Figure 7.1. Schematic overview of the downhill running (DR) training programme. Bars represent each separate DR training session, split into the four negative slopes (-5%, -10%, -15% and -17%; i.e. DR_5, DR_{10}. DR_{15} and $DR_{17,}$ respectively). Adapted from Bontemps et al. (2022). 147

Figure 7.2. Schematic overview of the experimental protocol. Participants began supplementation and D_2O enrichment three days prior to their final (10th) downhill running (DR) session. Pre-exercise physiological assessments were conducted before participants completed a 50-minute DR bout at a −17% gradient, performed at the highest speed reached during the training programme. The same assessments were repeated immediately post-exercise, with recovery monitored over the following seven days by conducting repeated physiological measurements. 149

Figure 7.3. Visual analogue scale (VAS) for rating perceived muscle pain (0-100 mm type). Schematic representation not to scale..... 152

Figure 7.4. Changes in maximal isometric voluntary torque (MIVT) normalised to pre-exercise values (%) over time. Black line**:** placebo (PLA); blue line: palmitoylethanolamide (PEA); red line**:** ibuprofen (Ibu).Data are presented as mean ± SEM. 154

Figure 7.5. Changes in control doublet force normalised to pre-exercise values (%) over time. Black line**:** placebo (PLA); blue line: palmitoylethanolamide (PEA); red line**:** ibuprofen (Ibu) Data are presented as mean ± SEM. 156

Figure 7.6. Torque–frequency relationship of placebo (PLA) group, all frequencies were normalised to torque at 100 Hz. Data are shown for each time point: Pre (black line), Post (blue line), 24h (purple line), 48h (red line), 5d (green line), and 7d (orange line). Frequencies tested were 1, 10, 15, 20, 30, and 50 Hz. Values are mean ± SD. 158

Figure 7.7. Torque–frequency relationship of palmitoylethanolamide (PEA) group, all frequencies were normalised to torque at 100 Hz. Data are shown for each time point: Pre (black line), Post (blue line), 24h (purple line), 48h (red line), 5d (green line), and 7d (orange line). Frequencies tested were 1, 10, 15, 20, 30, and 50 Hz. Values are mean ± SD. 159

Figure 7.8. Torque–frequency relationship of ibuprofen (Ibu) group, all frequencies were normalised to torque at 100 Hz. Data are shown for each time point: Pre (black line), Post (blue line), 24h (purple line), 48h (red line), 5d (green line), and 7d (orange line). Frequencies tested were 1, 10, 15, 20, 30, and 50 Hz. Values are mean ± SD. 160

Figure 7.9. Pain as assessed via the visual analogue scale (VAS) following the final DR session. (**a**) Peak pain scores across conditions. Bar chart showing mean (±SD) peak pain scores within each condition: placebo (PLA), palmitoylethanolamide (PEA), and ibuprofen (IBU). (**b**) Individual pain scores within condition across time. Heatmap displaying self-reported pain scores for each participant across all time points within conditions. Darker red indicates higher pain scores, whilst white represents no pain. 161

Figure 7.10. Changes in blood (a) sodium (mmol/L), (b) urea (mmol/L), (c) potassium (mmol/L), and (d) estimated glomerular filtration rate (eGFR) (mL/min/1.73m2) across time. Shaded areas represent average ranges for healthy adults (for context only). Data represented as mean ± SEM. 163

Publications Arising from this Thesis

Published

Cole, P.L., Bontemps, B., Pugh, J. and Owens, D.J., 2025. The prevalence and perceptions of non-steroidal anti-inflammatory drug use among ultra-endurance runners. *Research in Sports Medicine*, pp.1-19.

Cole, P.L., Gillham, S.H., Viggars, M.R., Close, G.L. and Owens, D.J., 2025. Palmitoylethanolamide (PEA) Regulates Cell Cyle Progression and Promotes an Anti-Inflammatory Transcriptomic Signature in C2C12 Skeletal Muscle Cells. *Physiological Reports*.

Under Review

Cole, P.L., Stead, C.A., Burniston, J.G., Owens, D.J., 2025. Comparative effects of palmitoylethanolamide and ibuprofen on the abundance profile and synthesis rate of proteins in C2C12 skeletal myotubes. *Proteomics.*

Conference Attendances

Women's Physiology and Nutrition Symposium: Liverpool, UK. July 2023.

European College of Sports Science: Rimini, Italy. June 2025.

Healthy Muscle Ageing Conference: Liverpool, UK. September 2023

Conference Presentations

Exploring the Efficacy of Palmitoylethanolamide (PEA) versus NSAIDs in Alleviating Exercise-Induced Muscle Damage: A Compartive Inveestigation in Downhill Running. European College of Sports Science: Rimini, Italy. June 2025.

Faculty of Science Research Festival – Best Oral Presentation: Liverpool, UK. February 2024.

Abbreviations

2-AG – 2 - arachidonoyl glycerol

AAF – Adverse analytical finding

ABD – Protein abundance

ADRV – Anti-doping rule violation

AEA – Anandamide

AKI – Acute kidney injury

ALIA – Autacoid local injury antagonism

BSA – Bovine serum albumin

CBD – Cannabidiol

CK – Creatine kinase

COX - Cyclooxygenase

CV – Cardiovascular

DAPI – 4',6-diamidino-2-phenylindole

DM – Differentiation media

DMEM – Dulbecco's modified eagles medium

DMSO – Dimethyl sulfoxide

DNA – Deoxyribonucleic acid

DOMS – Delayed onset muscle soreness

DR – Downhill running

D_2O – Deuterium oxide

E-C – Excitation-coupling

eGFR- Estimated glomerular filtration rate

EIMD – Exercise induced muscle damage

FAAH – Fatty acid amide hydrolase

FAE – Fatty acid ethanolamide

FBS – Fetal bovine serum

FSC – Forward side scatter

FSR – Fractional synthesis rate

GI – Gastrointestinal

GM – Growth media

GO – Gene ontology

GPR55 – G protein-coupled receptor 55

HS – Horse serum

Ibu – Ibuprofen

ICC/IF – Immunocytochemistry

IK – Isokinetic Dynamometer

IL – Interleukin

iNOS – Nitric oxide synthase

KE MVT – Knee extensor maximal voluntary activation

KF-κB – Nuclear factor kappa β

LC-MS – Liquid chromatography mass spectrometry

LN_2 – Liquid nitrogen

MCL – Markov clustering

MHC – Myosin heavy chain

MPS – Muscle protein synthesis

MRF – Myogenic regulatory factors

mRNA – Messenger ribonucleic acid

mTOR – Mammalian target of rapamycin

MTT – 3-[4,5-dimethylthiazol-2-yl]-2,5-diphenyl-2H-tetrazolium bromide

MVC – Maximal voluntary contraction

NAAA – N-acylethanolamine acid amidase

NAE – N-acylethanolamine

NAPE – N-acyl phosphatidylethanolamine

NAPE-PLD - N-acyl phosphatidylethanolamine – specific phospholipase D

NBCS – Newborn calf serum

NGF – Nerve growth factor

NSAID – Non-steroidal anti-inflammatory drug

OTC – Off the shelf

PAR-Q – Physical activity readiness questionnaire

PBS – Phosphate buffered saline

PCA - Principal component analysis

PEA – Palmitoylethanolamide

PFA – Paraformaldehyde

PGE_2 – Prostaglandin E_2

$PGF_2\alpha$ – Prostaglandin $F_2\alpha$

PI – Propidium iodide

PLA - Placebo

PMP – Perceived muscle pain

PPARα – Peroxisome proliferator activated receptor alpha

PS – Penicillin-streptomycin solution

PUFA – Polyunsaturated fatty acid

RBE – Repeated bout effect

RCT – Randomised control trial

RIPA – Radioimmunoprecipitation assay

RNA – Ribonucleic acid

ROM – Range of motion

ROS – Reactive oxygen species

RT-qPCR – Reverse transcriptase quantitative polymerase chain reaction

SC – Satellite cell

SSC - Side scatter

TF – Torque-frequency

TNF-α – Tumor necrosis factor alpha

TRPV1 – Transient receptor potential vanilloid 1

UTMB – Ultra trial du Mont Blanc

VA – Voluntary activation

VAS – Visual analogue scale

WADA – World anti-doping agency

Acknowledgments

There are far too many people to thank, without whom this PhD would not have been possible. However, I would first and foremost like to express my deepest gratitude to my supervisory team: Dr Daniel Owens, Professor Jatin Burniston, Dr Robert Erskine, and Professor Graeme Close. Graeme, it has been an honour to work under the guidance of someone so highly regarded in both elite sport and research. Rob, your expertise in muscle damage shaped what I consider my proudest piece of research to date, thank you for your constant encouragement and support throughout this journey. Jatin, I feel truly fortunate to have learned the world of proteomics from you; your patience, knowledge, and guidance have given me invaluable skills and insights. And finally, Dan, who would have thought that the undergraduate student who first completed their dissertation with you would still be working alongside you six years later? Words cannot fully capture my gratitude, not only for everything you have taught me about research, but also for the way you have helped me grow as a person, I'll forever be grateful for that.

I would also like to thank the wider community at RISES and LJMU. I feel truly privileged to have spent the past eight years at such a prestigious university, pursuing sports science research. Thank you for providing me the opportunity to contribute to this field and to be part of such an outstanding institution. I am especially grateful to Dr Neil Chester, Dr Jose Areta, Dr Julien Louis, Dr Theodoros Bampouras, Dean Morrey, Mark Doyle, and Jennifer Thomson, each of whom played an important role in different aspects of this thesis. I would also like to extend my sincere thanks to all the participants and students who volunteered their time (sometimes with gritted teeth) to take part in these studies. Your dedication and willingness to contribute made this work possible. To my fellow PhD students and colleagues, your support has been invaluable, and it has been a privilege to watch you all grow and succeed. Along the way, I have been fortunate to make lifelong friends. Loz, Rob, Chlo, Luke, Henry, Andy, and Scott—you're stuck with me now.

To my amazing family and friends. My wonderful best friends (you know who you are), I am so lucky to have you all. Thank you for always being my biggest supporters and making me laugh when I need it most. Ang and Mike, you're more than friends, you're family. Like my second parents, and I'm so grateful for all your love and support. To my beautiful family, I truly don't know where I'd be without you. Dad, you are my rock and my constant source of

support, always there when I need you. I could not have done this without your reliability and encouragement. Mum, whilst we joke and say I didn't get the "clever genes" from you, I like to think I see so much of you in myself – especially your kindness, your willingness to help others, and the positivity you bring to every situation. I hope I've made you both proud. To my sister (twinnie) Georgia, my lifelong best friend, your competitiveness, belief, and unwavering support have pushed me forward every single day. Sorry again to get one more up on you. Dan, as brother in laws go, you're not pretty bad. You're wittiness and sense of humour has helped brighten up those more difficult days. To my Nan and Taid, you can finally say your granddaughter is a Dr! I've always felt your pride and love, and it has carried me through this journey. Nan and Grandad, though you're no longer here, I feel your presence every day. That constant reminder gives me the strength and motivation to always make you proud. Finally, to my wonderful girlfriend Emma, your support has made this possible. You are the most caring, understanding, encouraging, and inspiring person I know. This achievement is as much yours as it is mine. I love you all more than anything, and I hope I've made you proud.

Dedication

This thesis is lovingly dedicated to my late grandparents, whose memory continues to guide and inspire me.

Arthur Frain and Doris Frain.

Everything I do in life is to make you both proud.

Chapter 1

General Introduction

This chapter provides a broad overview on exercise-induced muscle damage (EIMD), muscle repair processes, and strategies to reduce damage and soreness. It highlights current interventions and explores the potential of Palmitoylethanolamide (PEA) as a novel approach for aiding recovery.

1. General Introduction

Exercise-induced muscle damage (EIMD) is common amongst athletes and the general population, characterised by muscle soreness, localised swelling, reduced pressure pain threshold, and temporary declines in muscle strength, function and range of motion in the affected limb(s) (Clarkson and Hubal, 2002). EIMD typically occurs after unfamiliar muscle activity with a strong eccentric component or exercise with an unaccustomed increased intensity (Byrne et al., 2004). While skeletal muscle has an inherent capacity to repair itself, the nature and magnitude of the response depend on the severity of damage. Mild damage, characterised by a small reduction in force-generating capacity (< 20% reduction) and rapid recovery, may be resolved locally through cellular repair mechanisms with minimal inflammatory involvement (Paulsen et al., 2012). However, severe damage, characterised by a large reduction in force-generating capacity (≥ 50% reduction) and long-lasting recovery (> 1 week), triggers a more pronounced inflammatory and regenerative cascade involving satellite, inflammatory, vascular, and stromal cells (Paulsen et al., 2012, Tidball, 2005, Peake et al., 2017). Emerging evidence suggests that the initiation of a full regenerative response in skeletal muscle is contingent upon the severity of tissue disruption, rather than the mere presence of damage. Paulsen et al. (2012) highlight the tightly regulated nature of the leucocyte-mediated inflammatory response, noting that excessive or prolonged inflammation may hinder, rather than support, effective regeneration. Adding to this, Bernard et al. (2023) demonstrated in a murine model or electrically-evoked lengthening contractions, satellite cell proliferation occurs irrespective of damage severity. However, only severe damage characterised by myofiber necrosis results in a noticeable increase in terminal differentiation markers (Bernard et al., 2023). Therefore, while satellite cell activation is a consistent response to muscle damage, progression to complete myogenic differentiation depends on the presence of necrosis, identifying necrosis as a critical regulator of the later stages of muscle regeneration.

Whilst muscle possesses the intrinsic ability to repair itself, the associated symptoms of EIMD, most notably increased soreness and reductions in muscle function, are of particular concern to athletes. This is because their congested training and competition schedules necessitate frequent high-level performances, sometimes while symptoms of muscle damage persist (Carling et al., 2015). Recent work, applying machine learning models to recovery dynamics in

endurance athletes, has further emphasised the critical role of soreness, identifying it as one of the most influential predictors of daily recovery status and reinforcing its value as both a practical and physiological indicator of recovery (Rothschild et al., 2024). Consequently, optimising recovery strategies to reduce soreness and restore function is essential, as it enables athletes to return to training and competition more rapidly, supports increases in training intensity and volume, and ultimately contributes to improved performance outcomes.

Nonsteroidal anti-inflammatory drugs (NSAIDs) are commonly used for the treatment of muscle damage and delayed onset of muscle soreness (DOMS). NSAID's alleviate some of the symptoms associated with EIMD, by inhibiting the enzyme cyclooxygenase (COX), and thereby reducing the production of prostaglandins and attenuating the inflammatory response (Rainsford, 2009). The current evidence for the use of NSAID's in the prevention and/or reduction of the signs and symptoms associated with NSAID's is unclear. Yet for various reasons, athletes regularly take NSAID's to continue their athletic activities, despite acute traumatic or overload injuries. Research indicates that the prevalence of NSAID use in competitive sports ranges from 40 to 86% (Suzic Lazic et al., 2011, Taioli, 2007, Corrigan and Kazlauakaa, 2000). Due to athletes congested training periods, NSAID's are frequently used to accelerate recovery time. However, athletes are often unaware of the detrimental effects NSAID's may pose at higher doses. NSAID's are associated with several clinically meaningful adverse effects, including gastrointestinal (GI) issues, renal impairment, and cardiovascular diseases, which limits their long-term use (Ziltener et al., 2010, Lindhardsen et al., 2014). Moreover, inflammation constitutes the body's innate response to EIMD, and the application of NSAID's could potentially impede protein synthesis, thereby hindering the cycle of muscle damage, repair and adaptation following eccentric exercise (Southorn and Palmer, 1990). Most concerning for athletes, is that NSAID'S can suppress satellite cell or myoblast number after injury, which leads to a detrimental impact on recovery, especially in the later stages of repair from moderate to severe EIMD (Mikkelsen et al., 2009). Given the limited evidence on the acute effects of NSAID's, the lack of performance benefits and the negative long-term consequences of administration, alternative treatments are warranted.

Ultra-endurance sports are rapidly gaining popularity, as evidenced by an increase in the number of events and athlete participation. Among these, mountain ultramarathon events,

characterised by long distances (>42.195km), typically involve a large downhill running component, leading to EIMD. Due to the extreme nature of these events, there has been a significant increase in analgesic prophylactic use. Research conducted by Martínez et al. (2017) discovered that out of 238 mountain endurance athletes, 48.3% reported taking non-steroidal anti-inflammatory drugs (NSAIDs) either before, during and/or immediately after, with significantly higher numbers for the Ultra (60.3%) than for the Marathon (35.5%). Notably in this study, 87% of athletes reported using Ibuprofen for all the possible consumption time points (Martínez et al., 2017). Concerningly, athletes took NSAIDs mainly without a medical prescription (61.5%) (Martínez et al., 2017). Taking the above finding into consideration, together with the limited awareness of side effects, there's an increased risk that this could lead to athletes consuming more NSAIDs than the recommended dose. From an anti-doping perspective, use of NSAIDs is permitted by the World Antidoping Agency (WADA), however, due to recent findings surrounding their adverse effects, the Ultra Trail du Mont Blanc (UTMB), one of the world's leading ultra endurance race series, has banned their use across all UTMB events including UTMB-Mont Blanc world series final, due to 'negative health risks' (Pannone and Abbott, 2024).

Despite the high prevalence of NSAID use, individuals are also increasingly seeking natural alternatives to manage pain and inflammation. Treatment strategies often include both preventative and therapeutic measures. Currently, there is a heightened interest in natural compounds, such as dietary supplements and herbal remedies, which have a long history of use in reducing pain and inflammation (Reynolds et al., 1995). Researchers, coaches, and athletes have reported strategies that include the intake of plant-derived products such as ginseng, green tea, and spinach (Rojas-Valverde, 2021). Polyphenols, including flavonoids derived primarily from fruits and plants, have also become of great interest to athletes, due to their antioxidant and anti-inflammatory effects (Overdevest et al., 2018). Previous research suggests that polyphenols derived from blueberries and cherries mitigate muscle soreness and improve muscle strength following eccentric exercise (Overdevest et al., 2018). As a result, polyphenol supplementation is considered an effective adjunct approach to enhance exercise recovery although efficacy has not been demonstrated across all studies (Overdevest et al., 2018).

Of these natural compounds, cannabidiol (CBD) is an emerging substance being used due to its anti-inflammatory, antioxidative, analgesic and sleep-improving properties (Machado Bergamaschi et al., 2011, Mechoulam and Hanuš, 2002, Russo et al., 2007). Cannabinoids are now considered the second most commonly used substance among contact sports athletes, replacing nicotine (McDuff et al., 2019). This rise may stem from CBD's removal from the World's Anti-Doping Agency (WADA) prohibited substance list in 2018 (McCartney et al., 2020), but concerns around its use remain given that CBD is the only cannabinoid permitted and all other cannabinoids (of which there are ≥140) are prohibited. Most commercially available CBD products are broad spectrum and therefore often contain other cannabinoids than CBD. Recent studies show that commercially available products often contain significantly higher amounts of THC than stated on the label, often exceeding the legal threshold (≤ 1mg THC) and including other prohibited cannabinoids, risking ant-doping rule violations (ADRV) (Gurley et al., 2020). These risks and potential violations highlight the need for safer alternatives.

One potential alternative to CBD and NSAIDs is palmitoylethanolamide (PEA), an endocannabinoid (eCB)-like lipid mediator, belonging to the family of N-acyl-ethanolamine (NAE) fatty acid amides (Beggiato et al., 2019a). Numerous clinical trials have examined PEA as a treatment for pain management, with a recent systematic review identifying 10 studies which demonstrated PEA supplementation was associated with significantly greater pain reduction compared to inactive control conditions (Artukoglu et al., 2017). A triple-blinded randomized controlled trial (RCT) compared the efficacy of PEA to Ibuprofen in 24 patients with temporomandibular joint (TMJ) arthritis over a 2-week period (Marini et al., 2012). The results concluded that PEA was associated with a significantly greater reduction in pain compared to ibuprofen. Additionally, three patients in the ibuprofen group reported stomach aches as an adverse event, whereas no adverse events were reported in the PEA group (Marini et al., 2012). PEA's analgesic actions may be due to its agonism of peroxisome proliferator-activated receptor α (PPARα), as it's been demonstrated to have an essential role in the PEA pharmacodynamic pathways for pain management (Costa et al., 2002, Aloe et al., 1993). PEA also plays a crucial role in modulating the inflammatory response reducing the activity of the pro-inflammatory enzymes, including nitric oxide synthase (iNOS) and cyclooxygenase (COX-2) and by inhibiting mast cell degranulation (Petrosino and Di Marzo, 2017a).These potential

mechanisms of action may also alleviate painful symptoms of muscle damage induced by exercise, which is beneficial to individuals who require rapid recovery periods in between or indeed within bouts of acute successive exercise (Owens et al., 2019).

Building on this background, the central aim of this thesis is to comprehensively examine the prevalence and rationale behind NSAID use among athletes while exploring PEA as a potential alternative for mitigating the adverse effects of exercise-induced muscle damage and facilitating recovery, ultimately addressing critical gaps in current recovery strategies.

Chapter 2

Literature Review

This chapter critically evaluates the existing literature on the key topics explored in this thesis. It examines markers of exercise-induced muscle damage, strategies for symptom mitigation, and current concerns regarding NSAID use. Additionally, it reviews contemporary research on PEA as a potentially safer and equally effective alternative to NSAIDs, ultimately establishing the rationale for this thesis.

2.1 Skeletal Muscle Damage

Background: Human skeletal muscle constitutes about 40% of body mass and is composed of bundles of contractile multinucleated muscle fibers, which form during development through the fusion of muscle precursor cells called myoblasts. Unlike other cell types, mature muscle fibers are post-mitotic and therefore adaptation and repair rely on intracellular mechanisms and the fusion of myoblast to the damaged tissue rather than cell death and proliferation. A common cause of muscle damage and subsequent adaptation is contractile activity during exercise. In isometric exercise, the contracting muscle maintains its length while generating force. During concentric contractions, muscle shortens whilst producing force, whereas in eccentric exercise, muscle lengthens whilst contracting (Faulkner, 2003). It is contractile activity that is the key stimulus for favourable muscle adaptations (Hoppeler et al., 2011). All forms of exercise can cause damage and pain, especially if the individual is unaccustomed to the specific exercise or if performed with greater than normal intensity or duration. Mild damage caused by such contractions is efficiently repaired through the recruitment of intracellular vesicles (Steinhardt et al., 1994). However, since mature myofibers are terminally differentiated, severe damage necessitates the degeneration of muscle tissue and subsequent regeneration, which depends on the timely activation, proliferation, and differentiation of the resident muscle stem cells often termed ‘satellite cells’ (SCs). Upon differentiation, the activated satellite cells (myoblasts) develop into new myotubes or fuse with damaged myofibers, ultimately maturing into functional myofibers (Hindi and Millay, 2022). The restoration of the damaged muscle leads to the resolution of force and return to normal muscle function and movement.

2.1.1 Mechanisms of Exercise-Induced Muscle Damage

Skeletal muscle damage can be characterised as the loss of muscle function due to the physical disruption of muscle structures involved in force production or transmission. Such damage can stem from a variety of events, including direct trauma such as muscle lacerations and contusions, indirect insults such as strains and degenerative diseases such as muscular dystrophies and as a consequence of unaccustomed or eccentric exercise. (Huard et al., 2002, Crisco et al., 1994, Garrett Jr et al., 1984). Muscle soreness following unfamiliar strenuous exercise was first described by Theodore Hough in 1902 (Hough, 1902). Hough observed that

following exercise in untrained skeletal muscle, discomfort emerged 8-10 hours post-exercise, suggesting that this delayed response was not solely attributable to fatigue (Hough, 1902). Since then, it has become well established that performing unaccustomed exercise may cause damage to the structure of muscle cells. This type of exercise and the resulting symptoms are commonly referred to in the scientific literature as exercise-induced muscle damage (EIMD).

It is important to consider the type of muscle activity that most frequently induces EIMD and the mechanical factors that may account for this. Nowadays, it is well established that eccentric muscle contractions, which involve the active lengthening of muscle fascicles, produce greater forces than both isometric and concentration contractions, while requiring comparatively less metabolic energy expenditure (Hoppeler and Herzog, 2014). Eccentric muscle contractions occur when the force applied to the muscle exceeds the momentary force produced by the muscle itself, resulting in a lengthening action of the musculotendinous system (Lindstedt et al., 2001). For example, in modalities such as downhill running, the quadricep muscles lengthen to decelerate movement, with the gravitational force applied exceeding the muscle's capacity to generate a shortening contraction. Such contractions often lead to the weakening or rupture of one or more structural components of the myofibers, known as 'failing', resulting in reduced capacity for force generation. Muscle failure can occur if the tensile stress placed on the myofiber component surpasses its yield strength (Armstrong et al., 1991). Eccentric contractions can produce 150-200% of the maximal force of an isometric contraction, thus increasing the risk of muscle failure and damage (Woledge et al., 1985). McCully and Faulkner (1986) were the first to suggest that the greater force-generating capacity of eccentric contractions isn't the sole factor contributing to muscle damage. Their research showed that eccentric contractions producing 85% of maximal isometric force led to muscle damage, whereas concentric contractions at the same intensity did not (McCully and Faulkner, 1986). This suggests that the muscle length at which maximum force is produced, rather than the force itself, may be a key factor in determining the extent of damage. Similarly, Brooks et al. (1995) demonstrated that both peak tension and work done were strongly correlated with the extent of damage, but importantly, also highlighted that lengthening velocity and tension during lengthening were significant determinants of the degree of damage.

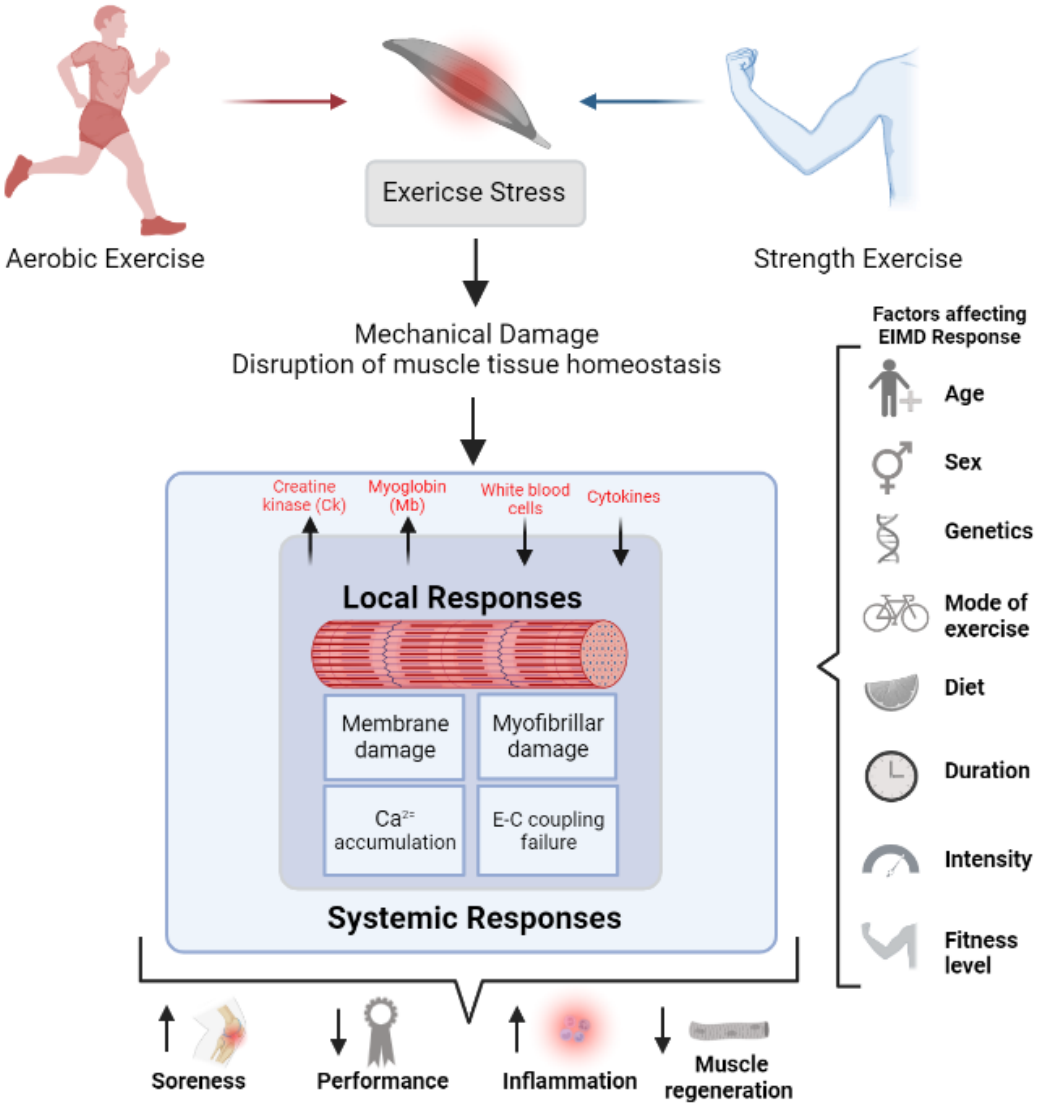

Figure 2.1. Schematic representation of exercise induced muscle damage, including the causes, physiological processes, and the effects on muscle. Unfamiliar exercise can cause mechanical injury to the muscle tissue, altering the homeostasis of the muscle tissue. A complex series of physiological processes are then initiated, both locally within the muscle and systemically, with a tight connection between the outlined responses. As a result, there is inflammation, delayed onset of muscle soreness (DOMS), and a decrease in muscle regeneration which in turn has a negative impact on athletic performance. Numerous factors influence an individual's response to EIMD, such as age, genetics, nutrition etc. Redrawn from Markus et al. (2021).

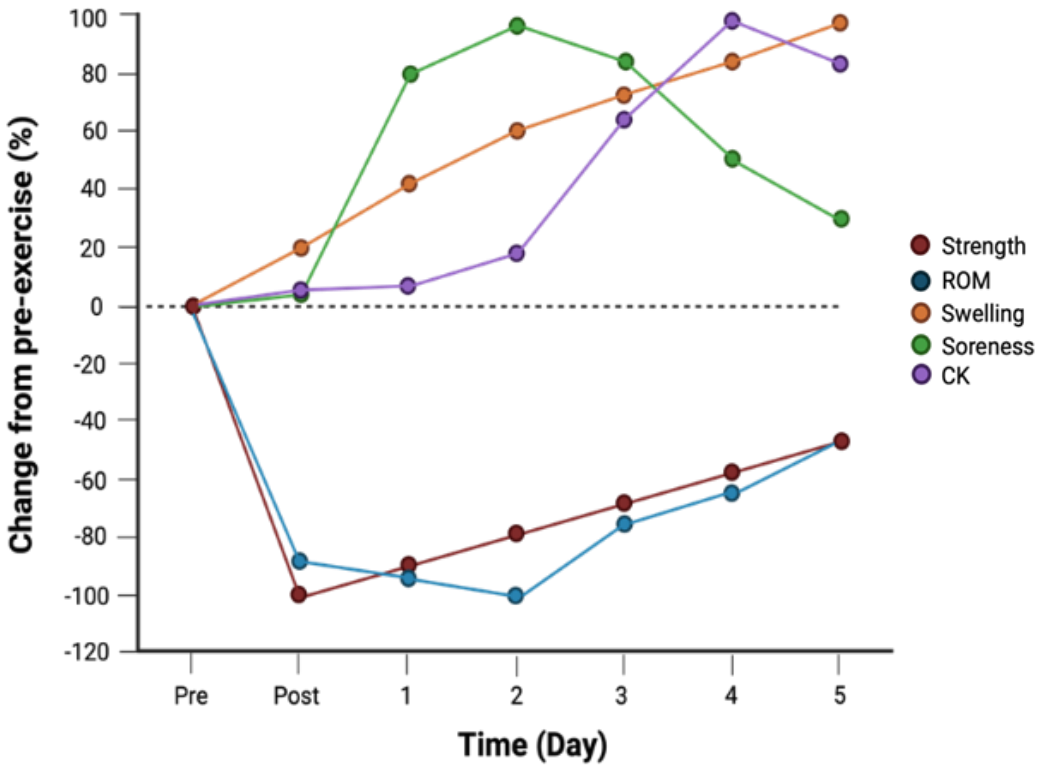

Figure 2.2. Typical magnitude and time course of EIMD symptoms, including maximal voluntary contraction (MVC), range of motion (ROM), DOMS (assessed by the visual analogue scale), swelling (measured by circumference) and plasma CK. Measurements taken before (Pre), immediately after (Post), and 1-5 days post exercise, and performed by healthy young men who were unaccustomed to exercise. Data taken from Damas et al. (2016) and re-drawn from Peake et al. (2017).

The complex mechanisms associated with muscle damage can be simplified into two main phases: (i) the initial phase, or primary damage, resulting from the mechanical stress of exercise; and (ii) secondary damage, which proliferates tissue damage through inflammatory processes.

2.1.2 Primary Damage

Immediately after a sequence of eccentric contractions, there are two prominent features of muscle damage. There is the presence of disrupted sarcomeres in myofibrils as well as

damage to the excitation-contraction (E-C) coupling system (Proske and Morgan, 2001). The damage process begins with the overstretch of sarcomeres. Fewer motor units are activated during eccentric contractions compared to concentric contractions for the same force, thus placing a large mechanical stress on a small number of muscle fibers, leading to some sarcomeres experiencing 'popping' during eccentric contractions (McHugh et al., 2000, Morgan and Allen, 1999, Proske and Morgan, 2001). Repeated eccentric contractions may place these passive structures under too much tension, which could lead to structural breakdown and impair the muscles' capacity to produce force (Howatson and Van Someren, 2008).

Excitation-contraction coupling, a fast signal transduction process in skeletal muscle, involves the depolarisation of sarcolemma membranes, activating the release of Ca^{2+} on the sarcoplasmic reticulum (Calderón et al., 2014). During eccentric contractions, mechanical stress is imposed upon muscle fibers, thus leading to disturbances in myocyte homeostasis and failure of the excitation-contraction coupling process (Clarkson and Hubal, 2002). E-C coupling failure attenuates sarcoplasmic reticulum (SR) release and reduces force production within the muscle immediately after eccentric exercise (Corona et al., 2010). Furthermore, mechanical damage to the SR can also cause an increase in the cytoplasm's Ca^{2+} levels, which is known to stimulate proteases that induce further damage to both contractile and non-contractile proteins (Verburg et al., 2005). Pro-inflammatory cytokines are released in response to the initial mechanical damage, which signals for a secondary damage event (Paulsen et al., 2012).

2.1.3 Secondary Damage

The disruption of intracellular Ca^{2+} homeostasis appears to be the catalyst for the events that occur after the primary phases of damage (Armstrong, 1984). An increase in the intracellular Ca^{2+} is believed to derive from extracellular sources, ultimately leading to further myofibrillar damage in skeletal muscle (Duncan, 1987). In rats, eccentric exercise has been demonstrated to result in a loss of sarcoplasmic reticulum membrane integrity and flux of Ca^{2+} into intracellular regions, which culminates in skeletal muscle damage (Yasuda et al., 1997). Additionally, recent research has demonstrated that changes to the sarcoplasmic reticulum

following lengthening contractions in humans triggers a disruption in calcium homeostasis (Nielsen et al., 2005). The influx of Ca^{2+} into the cytosol activates a chain of events that further damage the cell by inducing changes to the sarcoplasmic reticulum, mitochondria, cytoskeleton and myofilaments (Gissel and Clausen, 2001). Increased intracellular Ca^{2+} may also potentially produce uncontrolled muscular contractions, which could explain the increases in passive tension observed after EIMD (Proske and Morgan, 2001, Morgan and Allen, 1999).

The subsequent inflammatory response plays an important, though tightly regulated, role in clearing damaged tissue and facilitating the early stages of repair (Chazaud, 2016). Inflammation is characterised by the migration of fluid, plasma proteins and leucocytes into the tissue in response to infections, antigens, and injury (MacIntyre et al., 1995b). Various immune cell types infiltrate the damaged tissue, including neutrophils, mast cells, lymphocytes and eosinophils to carry out specific roles in a highly organised, temporal manner (Owens et al., 2019). Neutrophils are the first group of immune cells that infiltrate the injured tissue. Neutrophils contribute to the post-injury events in two ways: (i) they engage in phagocytosis, actively removing necrotic debris from the site of injury, and (ii) they magnify the inflammatory response by response by releasing pro-inflammatory cytokines such as IL-6 and TNF-α (Pizza et al., 2005, Rosenberg and Gallin, 1993, Cannon and St. Pierre, 1998). However, neutrophils also possess the ability to generate high quantities of cytolytic and cytotoxic substances via mechanisms dependent on NADPH oxidase derived superoxide anions. These mechanisms have the potential to exacerbate pre-existing damage and are consequently associated with the progression of secondary tissue injury (Nguyen and Tidball, 2003).

2.1.4 Markers of Muscle Damage

Several markers may be used to indicate muscle damage, which can be categorised into direct and indirect markers. Direct markers, such as MRI or muscle biopsies, are less feasible due to cost and invasiveness., thus, indirect markers are more commonly used. These markers include the temporal reduction in muscle strength and/or muscle soreness experienced several hours following exercise (i.e. 24-48h), increased production of myofibrillar proteins

such as creatine kinase (CK) and lactate dehydrogenase, and muscle swelling (Clarkson and Hubal, 2002). The most appropriate marker of EIMD is assessing muscle function after eccentric exercise (Warren et al., 1999, Paulsen et al., 2012). Depending on the initial damage, force losses can range from 15-60% and last up to 2 weeks ((Paulsen et al., 2012, Hyldahl et al., 2014). Delayed onset muscle soreness (DOMS) is frequently assessed, but its exact mechanisms remain unclear (Cheung et al., 2003). Muscle proteins like CK and myoglobin, which peak 2-6 days post-damage, leak into circulation due to increased membrane permeability after eccentric contractions (Byrne et al., 2004, Hyldahl and Hubal, 2014). However, these proteins do not indicate damage severity, therefore, all indirect markers of muscle damage should be considered and measured to understand the complex mechanisms associated with EIMD.

Table 2.1. Classification of exercise-induced muscle damage into mild, moderate and severe categories, based on structural changes, force loss and expected recovery time. Categorisation adapted from (Paulsen et al., 2012).

Severity	Structural Changes	Force Loss (% of baseline)	Expected Recovery Time
Mild	Minor sarcomere disruption; no clear membrane damage; intact cytoskeleton	≤ 20%	≤ 48 hours
Moderate	Sarcomere disruption with localised membrane damage; mild infiltration of inflammatory cells; Z-line streaming	20 – 50%	3-7 days
Severe	Extensive structural disruption; widespread sarcolemma damage; cytoskeletal breakdown; significant inflammatory response	≥ 50%	≥ 7 days

Note: Recovery time varies due to varying factors such as training status, nutrition, age and recovery strategies.

Muscle Function

Various measures of muscle function, such as limb flexibility, strength, countermovement jump, speed agility, and sport specific performance are used to assess muscle damage. However, a reduction in force-generating capacity is considered the most reliable indirect marker of EIMD and is measured by changes in maximal voluntary contraction (MVC) torque post-exercise (Szczyglowski et al., 2017). By definition, in mild EIMD the reduction of MVC is less than 20%, with minimal or no morphological changes and full-strength recovery within 48 hours. Moderate EIMD is characterized by a 20-50% reduction in MVC, accompanied by mild inflammation and some myofibrillar disruption, with a recovery period extending up to 7 days. The most prolonged and marked reductions in strength occur after high-load eccentric contractions, which can diminish muscle force-generating capacity by 50%, with significant tissue damage that may require several weeks to fully recover (Raastad et al., 2010). After eccentric exercise, an initial strength loss occurs immediately, with a second decline between 20-24 hours, likely due to inflammation or central inhibition from pain (Clarkson and Hubal, 2002, MacIntyre et al., 1995a). Only about 25% of early strength loss in EIMD is due to mechanical factors, with the remaining 75% attributed to impaired E-C coupling (Warren et al., 2002). Methodological issues, such as additional damage from testing and limitations in achieving true maximal strength, suggest other indirect markers of damage should also be assessed.

Blood Markers

One of the defining aspects of EIMD is the increased permeability of the cell membrane. As a result of this, intracellular muscle proteins, such as creatine kinase (CK), myoglobin, troponin, myosin heavy chain and lactate dehydrogenase may leak into systemic circulation (Brentano and Martins Kruel, 2011). While their concentrations in plasma or serum can indicate the extent of damage, they are significantly influenced by their clearance rates. CK is the most commonly measured marker, due to its relatively large increase in plasma concentration following EIMD and low cost to measure (Sorichter et al., 1995). Elevated circulating CK levels can be detected within 24 hours following resistance exercise, but peak levels (~2,00-10,000 IU) typically occur 3-7 days post-exercise and often take up to 10 days to return to baseline

(Nosaka et al., 2002, Clarkson and Hubal, 2002). There is great concentration variability in CK due to varying factors such as baseline CK concentrations, type of exercise, number of CK autoantibodies, sex and training status (Damas et al., 2016, Saxton and Donnelly, 1995). Therefore, CK concentrations should be interpreted with caution and ideally with other markers when used to assess the magnitude of EIMD.

Pro-inflammatory biomarkers are also analysed, indicating both local and systemic inflammatory responses. While exercise-induced inflammation is debated "good" or "bad", it plays a role in both muscle regeneration and repair. The post-exercise inflammatory response is characterised by a leukocyte-driven infiltration of pro-inflammatory cytokines, such as tumor necrosis factor (TNF)-a and various interleukins (IL-1b, IL-6, IL-8) that can often be detected in plasma within 0-4 hours after exercise (Paulsen et al., 2012). Konrad et al. (2011) reported that 2h of treadmill running immediately elevated plasma concentration of TNF-a and several ILs in endurance-trained males and females. The resistance exercise-induced infiltration of IL-6 has been associated with exercise intensity and contraction type in untrained males, however generally, systemic inflammation is often unrelated to the severity of EIMD (Peake et al., 2006, Mendham et al., 2011, Willoughby et al., 2003, Nosaka and Clarkson, 1996). It has been suggested that the increase in plasma IL-6 is primarily due to intramuscular IL-6 production following muscle contraction, independent of muscle damage *per se* (Steensberg et al., 2000). Supporting this, muscle biopsies have shown elevated mRNA expression of IL-6, IL-1b, IL-8, and TNF-a 24 hours following resistance exercise, although it should be noted that the biopsy procedure itself may induce some inflammation (Paulsen et al., 2012). Despite this, there is growing consensus that the initial inflammatory response plays a crucial role in muscle regeneration, as it involves a transition from pro-inflammatory to anti-inflammatory cytokines (Tidball, 2011).

DOMS

Delayed onset muscle soreness (DOMS) is a familiar experience for elite or novice athletes and is a further indirect measurement of EIMD (Cheung et al., 2003). DOMS is commonly characterised by muscle tenderness on palpation or during movement, accompanied by decreased flexibility and temporary loss of maximal voluntary force production (Gulick and Kimura, 1996). Symptoms usually present within 12-48 hours post-exercise, with tenderness

concentrated in the distal portion of the muscle peaking 24-72 hours thereafter (MacIntyre et al., 1995b). The localisation of tenderness can be attributed to the high concentration of pain receptors found in the connective tissue of the myotendinous region (Newham et al., 1982). The myotendinous junction is characterised by a continuous, extensively folded membrane that interdigitates with muscle cells (Newham et al., 1982). The oblique orientation of muscle fibers immediately before the myotendinous junction diminishes their capacity to withstand high tensile forces, therefore, the contractile sections of muscle fibers within the myotendinous junction of susceptible to microscopic damage (Noonan and Garrett Jr, 1992, Newham et al., 1982).

DOMS is predominantly associated with unfamiliar, high-force muscular activity and is most pronounced by eccentric actions (Schwane et al., 1983). The cascade of events linked to DOMS has been studied for more than a century. However, the underpinning mechanisms remain misunderstood. Numerous theories have been suggested to explain the sensations associated with DOMS, including lactate accumulation (Asmussen, 1953), muscle spasms (De Vries, 1967), inflammation (Smith, 1991) and connective tissue damage (Abraham, 1977). A widely accepted model proposes that eccentric loading causes damage to the muscle and connective tissue, initiating an acute inflammatory response involving oedema, immune cell filtration, and local sensitisation (Armstrong, 1990, Smith, 1991, Smith Jr and Jackson, 1990). In addition to muscle soreness, the structural damage to the muscle and connective tissues resulting from eccentric activity can lead to significant alterations in muscle function and joint mechanisms, ultimately reducing performance levels and training intensity for athletes.

Pain

While DOMS is often perceived as painful, it is important the differentiate this self-limiting post-exercise soreness from broader definitions of pain. In the context of EIMD, pain refers to a sensory and emotional experience resulting from actual or potential tissue damage and can extend beyond the transient soreness of DOMS. Muscle pain is often characterised by stiffness, muscle tenderness and localised pain (Lewis et al., 2012). It is believed to result from micro-trauma to the muscle due to the strain and disruption of the sarcomere, triggering an inflammatory response that sensitizes pain receptors, although the exact mechanisms are unclear (Lewis et al., 2012). DOMS may be one expression of this inflammatory response, but

pain can also occur independently of visible muscle damage or extend beyond the typical DOMS timeframe.

Noxious chemicals like histamines, bradykinins and prostaglandins are believed to contribute to the sensation of pain and soreness by activating type III and type IV nerve afferents that transmit pain signals from the muscle to the central nervous system (Friden and Lieber, 1992). In 2010, research by Murase et al. (2010) using a rodent model, demonstrated that bradykinin released during eccentric exercise increases nerve growth factor (NGF) levels via B2 receptors, contributing to mechanical hypersensitivity. In humans, nerve growth factor (NGF) has been shown to play a role in generating and potentiating pain following eccentric exercise (Nie et al., 2009). Another proposed pathway in the development of pain and soreness involves the activation of the COX-2-glial cell line-derived neurotrophic factor (GDNF) (Murase et al., 2013). Similar to the NGF pathway, GDNF likely induces muscle mechanical hyperalgesia by stimulating muscle nociceptors or binding to the extracellular receptors. Notably, some studies report signs of mechanical hyperalgesia in the absence of measurable muscle fiber damage, suggesting that extracellular matrix inflammation alone may drive pain responses (Peake et al., 2017).

2.2 Skeletal Muscle Repair

Background: Skeletal muscle, the most abundant tissue of the body, has the capacity to regenerate new muscle fibers in response to injury or following diseases such as muscular dystrophy (Carlson and Faulkner, 1983). Skeletal muscle repair is a highly synchronized process involving the activation of numerous cellular and molecular responses, where the coordination between inflammation and regeneration is essential for the beneficial outcome of the repair process following muscle damage (Chargé and Rudnicki, 2004). Minor damages caused by daily activity is repaired by the recruitment of intracellular vesicles, however more extensive muscle damage requires the migration and fusion of satellite cells (SC) (Grounds, 1991). The regeneration process follows three sequential yet overlapping stages: (1) an initial inflammatory response; (2) activation, migration, differentiation, and fusion of satellite cells (SCs); and (3) maturation and remodelling of newly formed myofibers (Yin et al., 2013).

2.2.1 Degeneration

Active muscle degeneration and inflammation occur within the first days after injury. Immediately following injury, damaged myofibers undergo necrosis, characterised by sarcolemma disruption and increased membrane permeability (Chargé and Rudnicki, 2004). This disruption in myofiber integrity results in the efflux of intracellular proteins, such as creatine kinase, into the circulation. Additionally, as cytosolic proteins do not necessarily provide an accurate representation of structural damage, structurally associated proteins such as myosin heavy chain (MHC) and troponin, have been proposed as more reliable markers of damage to the contractile apparatus (Sorichter et al., 1997, Sorichter et al., 1999). In particular, skeletal troponin I has been identified as an early and specific plasma biomarker of exercise-induced skeletal muscle damage (Sorichter et al., 1997). Furthermore, it has been hypothesized that damage to the sarcoplasmic reticulum and loss of calcium homeostasis contribute to calcium-dependent proteolysis activity, exacerbating tissue degeneration (Armstrong et al., 1991). For instance, calpain, which are calcium-activated proteases, play a central role in the degradation of myofibrillar and cytoskeletal proteins (Belcastro et al., 1998).

The early phase of muscle injury is typically accompanied by the activation of mononucleated cells, primarily inflammatory and myogenic cells which are regulated by factors released from the injured muscle(Tidball, 2005). Neutrophils are the first immune cells to infiltrate the injured site, appearing within 1-6 hours post-injury (Fielding et al., 1993, Orimo et al., 1991). Approximately 48 h after injury, macrophages become the predominant inflammatory cell type present, and transition through pro-inflammatory ($CD68^{+}/CD163^{-}$) to anti-inflammatory ($CD68^{-}/CD163^{+}$) phenotypes, migrating to the damaged area through the bloodstream (Orimo et al., 1991). Following infiltration, macrophages phagocytose necrotic debris and facilitate the resolution of inflammation, preparing for regeneration (Tidball and Villalta, 2010).

2.2.2 Regeneration

Following the clearance of damaged tissue, regeneration is initiated and can be identified by a series of morphological characteristics. An essential step during the regeneration phase is the activation and proliferation of satellite cells (SCs), the resident muscle stem cells. In response to regenerative cues, SCs exit quiescence and undergo asymmetric division to both

replenish the stem cell pool and provide committed myogenic progenitors. These progenitors proliferate, differentiate, and fuse either with existing damaged fibers or with one another to form new myofibers (Snow, 1977). Early regenerating fibers are characterised by the expression of embryonic isoforms of myosin heavy chain and basophilic staining, reflecting active protein synthesis (Whalen et al., 1990). A common morphological feature during regeneration is fiber splitting or branching, often resulting from incomplete fusion within a shared basal lamina (Blaivas and Carlson, 1991). Such features are more pronounced in pathological conditions and in aged or hypertrophic muscle (Bockhold et al., 1998, Schiaffino et al., 1979). Following myogenic cell fusion, the size of the newly formed myofibers is increased and myonuclei migrate to the periphery of the muscle fiber. Under normal conditions, the regenerated muscle is morphologically and functionally identical to undamaged muscle.

2.2.3 Satellite Cells

As introduce in Section 2.2.2, satellite cells (SCs) play a fundamental role in muscle regeneration. The regenerative capacity of terminally differentiated skeletal muscle relies primarily on SCs, a population of resident stem cells located between the basal lamina and sarcolemma of muscle fibers. Upon discovery, satellite cells were instantly postulated as a cell pool for muscle hypertrophy and repair, owed to the post mitotically quiescent nature of mature myofibers (Mauro, 1961). After further research, it was determined that satellite cells are vital for the regeneration process, as muscle does not regenerate when satellite cells are ablated (Relaix and Zammit, 2012). SCs remain in a quiescent state under homeostatic conditions, maintained by a specialized stem cell niche that tightly regulates their activation and self-renewal (Yin et al., 2013, Schultz et al., 1978).

Upon exposure to damaging stimuli, SCs are activated and leave quiescence where they enter the cell cycle, undergoing stochastic and asymmetric division. This process replenished the pool of satellite cells and prepares them to commit to becoming myoblasts (Fu et al., 2015). The myogenic commitment of activated SCs is governed by a tightly regulated network of myogenic regulatory factors (MRFs), including Myf5, MyoD, Myogenin, and MRF4 (Marsh et al., 1997). These transcription factors orchestrate the transition from proliferation to

differentiation and are dynamically regulated throughout the regenerative process (Braun and Gautel, 2011, Asfour et al., 2018). After exiting the cell cycle, myogenic cells fuse with one another to repair damaged myofibers or form nascent multinucleated myofibers (Karalaki et al., 2009). This occurs in two distinct phases: initial fusion to form nascent myotubes, followed by further fusion events that enlarge the fibers and restore contractile function (Yin et al., 2013). Remarkably, the SC pool is replenished during each regeneration cycle, enabling skeletal muscle to undergo complete regeneration and repair after repeated injuries.

2.3 Solutions to Reduce Damage and Soreness

With athletes often training or competing multiple times in a single day due to their demanding schedules, optimising and accelerating the recovery process is crucial to enhancing their performance. Various nutritional, physiotherapeutic, and pharmacological strategies have been examined for their effectiveness in restoring muscle function, alleviating soreness, and reducing intramuscular inflammation following exercise. Common therapeutic interventions that are used to treat the symptoms of EIMD include stretching, massage, cryotherapy, non-steroidal anti-inflammatory drugs (NSAIDS) as well as nutritional supplementation strategies (Peake et al., 2017). There is a greater interest in natural compounds, such as dietary supplements and herbal remedies, which have been used for centuries to reduce pain and inflammation (Reynolds et al., 1995). Preliminary research on cherry juice and polyphenols suggests they may mitigate indirect markers of muscle damage, though more studies are needed to confirm these findings (Bell et al., 2014, Myburgh, 2014). Studies on other physiotherapeutic interventions, such as vibration therapy and neuromuscular stimulation, have shown mixed or inconclusive results. As a result, it is not possible to draw definitive conclusions regarding their effectiveness in treating exercise-induced muscle damage.

2.3.1 Nutritional Supplementation

With training programmes becoming increasingly demanding, any potential support should be explored, and nutrition is a key area that can significantly impact performance. Since feeding is a fundamental physiological requirement, optimizing athletes' food intake is essential to maximize the benefits of their training. Faster and more efficient recovery allows athletes to train harder and respond better to training, ultimately improving performance. It

is widely recognised that optimal nutrition during post-exercise recovery is vital for facilitating muscle repair and regeneration (Beelen et al., 2010). Several nutritional interventions, discussed below, have been identified as potentially beneficial in aiding recovery after EIMD.

Protein

Protein supplements are one of the most popular dietary supplements used by athletes. Few studies have explored the role of protein supplementation in preventing or reducing symptoms related to EIMD. Evidence indicates, consuming protein or free amino acids around the time of exercise can alleviate markers of muscle damage and accelerate recovery of force (Howatson and Van Someren, 2008, Jackman et al., 2010, Nosaka, 2006). However, others have not found similar effects (Blacker et al., 2010, Wojcik et al., 2001). It is well established that maintaining a positive muscle protein balance is crucial for muscle repair and adaptation following EIMD. Early post-exercise protein consumption has been shown to promote muscle protein synthesis (MPS) and net protein accretion (Phillips, 2011). However, a recent systematic review by Pasiakos et al. (2014) concluded that protein supplementation had little effect on muscle damage and noted a large variation in both study designs and outcome measures in the pertinent literature. While protein is essential for the adaptive remodelling of skeletal muscle after exercise, it remains unclear whether supplementing with protein after EIMD accelerates recovery.

Polyphenols

Polyphenols, abundant in fruits and vegetables, are the biggest group of phytochemicals and are known for being strong antioxidants (Tsao, 2010). Flavonoids, such as quercetin and anthocyanins, have been examined for their ability to modulate inflammatory responses post-exercise (Nieman et al., 2007a, O'Fallon et al., 2012). Although some studies found no significant impact of quercetin on muscle recovery markers (Nieman et al., 2007b), others have demonstrated promising effects of polyphenol-rich foods. Tart Montmorency cherry juice, for example, has been shown to reduce muscle soreness and improve recovery of strength following eccentric exercise (Connolly et al., 2006, Sumners et al., 2011). These benefits are thought to result from attenuation of the secondary damage response, although the exact mechanisms remain unclear.

Omega-3

Much of the current literature suggests that the consumption of Omega-3 polyunsaturated fatty acids (n-3 PUFA) may improve the symptoms associated with EIMD. n-3 PUFAs such as eicosapentaenoic acid (EPA) and docosahexaenoic acid (DHA) possess anti-inflammatory properties and have been suggested to play a role in the regulation of skeletal muscle protein synthesis (Heaton et al., 2017). n-3 PUFAs are naturally abundant in foods such as nuts and oily fish, including salmon, mackerel, and tuna (Covington, 2004). Several studies have reported beneficial effects of prophylactic n-3 PUFA consumption on muscle function, inflammation and soreness following exercise (DiLorenzo et al., 2014, Tartibian et al., 2009, Philpott et al., Jouris et al., 2011). Tartibian et al. (2009) were the first to report that daily intake of 324mg EPA and 216mg DHA for 32 days alleviated perceived pain and range of motion decrements 48 hours post-exercise in healthy males. However, other studies show no effect of n-3 PUFA supplementation on muscle function, inflammation and DOMS following exercise (Gray et al., 2014, Tsuchiya et al., 2016). Overall, current research supports the potential of n-3 PUFA as an effective intervention for managing symptoms associated with EIMD.

Cannabidiol (CBD)

As outlined in the general introduction of this thesis, CBD is in an emerging compound of interest in the management of exercise-induced muscle damage (EIMD) due to it's anti-inflammatory and analgesic properties. However, research in the context of sports and performance is limited and first studies have shown a small effect on muscle soreness after CBD supplementation (Cochrane-Snyman et al., 2021, Hatchett et al., 2020). A significant concern surrounding CBD us relates to its legal status. Although removed from the WADA list in 2018, all other cannabinoinds remain prohibited in competetion. Specifcally, THC is considered an adverse analyticl finging (AAF) when its metabolites exceed a urinary threshold of ≥150 $ng \cdot ml^{-1}$, while no such thresholds are defined for other cannabinoids. This presents a concern for athletes, as many off-the-shelf (OTC) broad spectrum CBD products, have been found to contain trace amounts of these banned substances, posing a risk of unintentional anti-doping violations(Gurley et al., 2020, Johnson et al., 2022). Given the current lack of data and the complex legal status of CBD, athletes should approach its use with caution.

2.3.2 Pharmacological Interventions

Pharmacologial interventions are often consumed in doses exceeding recommendations, raising concerns about adverse efffects and in athletes, the risk of contaminated supplements. Non-steroidal anti-inflammatory drugs (NSAIDs), particularly ibuprofen and naproxen, are among the most commonly used substances to manage EIMD due to their anti-inflammatory, analgesic, anti-pyretic and antithrombotic effects (Tsitsimpikou et al., 2009, Schoenfeld, 2012). Elite athletes frequently use NSAIDs to reduce recovery time, continue training despite injury, or as a preventitive measure. These drugs are readily accessible over the counter and are not classified as performance-enhancing by WADA (Warden, 2009). Recent research indicates a significant prevalence of NSAID consumption among athletes, highlighting concerns about the limited awareness regarding the potential effects and side effects of these medications. A recent survey of 167 ultra-endurance runners reported that 53% used NSAIDs, most commonly ibuprofen, during both training and competition, despite 77% of participants acknowledging awareness of potential adverse effects.

When consumed immediatley before or after injury, NSAIDs can reduce musculoskeltal pain and support functional recovery (Warden, 2009). NSAIDs mediate their analgesic effects by inhibiting the cyclooxygenases COX-1 and COX-2, thus limiting the synthesis of prostanoids (Sisignano and Geisslinger, 2023). COX-1 enzymes are constitutively expressed in the body and involved in maintaining gastrointestinal mucosa, renal blood flow, and platelet aggregation, while COX-2 enzymes are induced by inflammatory stimuli (Tscholl Ph et al., 2017, Ghlichloo and Gerriets, 2019). Most NSAIDs are non-selective, inhibiting both isoforms, whereas COX-2 selective inhibitors like celecoxib aim to reduce inflammation with fewer gastrointestinal side effects (Chaiamnuay et al., 2006).

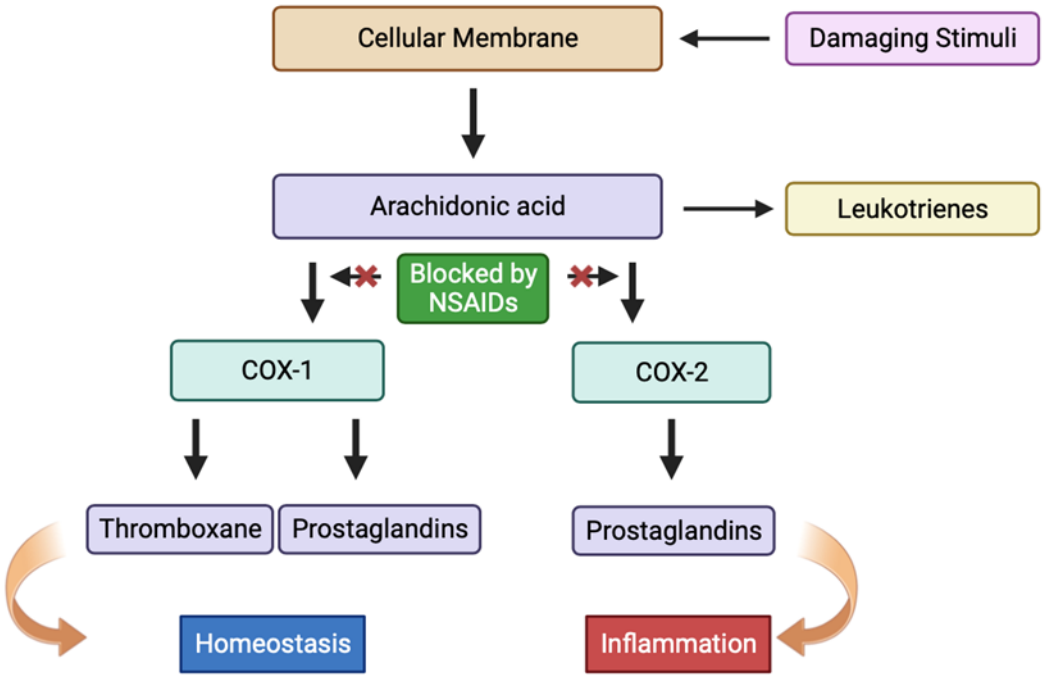

Figure 2.3. Schematic of the mechanism of action of NSAIDs. Arachidonic acid pathway showing production of prostaglandins from membrane phospholipids

NSAIDs are not benign agents, and like any substance introduced systemically, they have the potential to impact multiple bodily systems non-selectively, leading to adverse side effects. Engaging in prophylactic use can render athletes vulnerable to such adverse drug reactions, with one in five athletes reporting various side effects associated with NSAID usage (Suzic Lazic et al., 2011). Side effects can occur as a consequence of the broad application of NSAIDs, including general issues like gastrointestinal (GI) and cardiovascular (CV) effects, as well as athlete-specific concerns such as musculoskeletal and renal side effects (Warden, 2010). GI issues, such as ulcers and bleeding affect as many as 60% of all NSAID users, due to the inhibition of prostaglandins that protect the stomach lining (Jones et al., 2008). Moreover, NSAID use around exercise may increase GI permeability, though the impact remains unclear (Lambert et al., 2007). Concerningly for athletes, COX inhibition may impair muscle regeneration and collagen synthesis, key processes in tissue repair (Palmer, 1990, Warden, 2005). Studies have shown mixed results regarding the impact of NSAIDs on muscle protein

synthesis**.** Initial studies in animals suggested that NSAIDs impair protein metabolism by inhibiting COX enzymes, particularly affecting prostaglandin F2α (PGF2α), which is crucial for muscle protein synthesis (Palmer, 1990). Trappe et al. (2002) demonstrated that larger doses of ibuprofen (1200 mg) inhibit muscle protein synthesis rates in recreationally active males following intense eccentric exercise, with lower PGF2α levels in the treatment groups compared to placebo. However, one limitation of this study was that only mixed muscle protein synthesis was analysed, therefore, it's not clear what percentage of fractional synthesis rate (FSR) represents myofibrillar versus noncontractile proteins (i.e collagen). Given the equivocal acute effects of NSAIDs, the lack of performance benefits reported, and the possible negative long-term consequences of administration, the use of NSAIDs for the prevention and management of symptoms associated with EIMD is not advised.

2.4. Palmitoylethanolamide (PEA)

2.4.1 A novel alternative to NSAIDs

Palimitoylethanolamide (PEA) is emerging as a promising alternative to NSAIDs for the management of EIMD and supporting recovery. Unlike NSAIDs, which inhibit COX enzymes and reduce prostaglandin synthesis, PEA exerts its effects through its ability to affect multiple pathways at different receptor sites, including PPAR-a, G protein-coupled receptor 55 (GPR55), and indirectly on CBD receptors (CB_1 and CB_2) (Marini et al., 2012). Therefore, PE may offer anti-inflammatory and analgesic benefits without the GI, renal and cardiovascular risks associated with prolonged NSAID use (Gabrielsson et al., 2016). Multiple intervention studies have demonstrated that PEA (300-1200 mg/day) is effective in managing pain associated with osteoarthritis, with similar doses relieving headache pain with efficacy comparable to ibuprofen (Mallard et al., 2020, Lang-Illievich et al., 2022). Moreover, PEA has been shown to improve sleep quality and duration, factors crucial for muscle repair and athletic performance (Evangelista et al., 2018, Lamon et al., 2021).

PEA's application to an exercising population and it's potential for muscle recovery are not well understood. To date, only one study has examined the effects of PEA on recovery following muscle-damaging exercise. In this study by Mallard et al. (2020), liquid PEA (167.5mg Levagen+ with 832.5mg maltodextrin) or placebo (1g maltodextrin) was

administered to participants prior to performing an eccentric leg press protocol (4 sets at 80% 1-RM followed by a performance set at 70% 1 R-M). Their findings revealed a significant reduction in myoglobin and blood lactate concentrations in the PEA group compared to placebo. A significant increase in protein kinase B (PKB) phosphorylation was also observed before exercise in the PEA group, suggesting PEA may enhance skeletal muscle mass as activation of Akt/PKB stimulates muscle protein synthesis (Mallard et al., 2020), Although the mechanisms behind the reduced lactate response remains unclear, these findings suggest PEA may support higher exercise intensities between sessions, potentially enhancing training adaptations and performance in athletes with limited recovery time (Mallard et al., 2020).

More recently, Huschtscha et al. (2024) investigated the effects of daily PEA supplementation (2 x 175mg Levagen+) during an 8-week supervised resistance training programme (2 sessions a week) in 52 recreationally active adults. Their findings reveal that PEA significantly improved dynamic lower body power, assessed via countermovement jump, without impairing muscle hypertrophy or strength gains. The authors conclude that these novel findings suggest that moderate doses of PEA do not impair hypertrophy or power adaptations, unlike some NSAIDs have been shown to, and may enhance lower body power in recreationally active individuals (Huschtscha et al., 2024). While further research is warranted, PEA shows potential as a safe alternative to NSAIDs to manage muscular pain and may even exert some additional benefits.

2.4.2 Discovery of PEA

Naturally occurring fatty acid ethanolamides (FAEs) were first discovered in the early 1940's, when researchers noted that supplementing the diets of deprived children with dried chicken egg yolk, prevented recurrences of rheumatic fever (Coburn and Moore, 1943). In a continuation of this research, it was determined that lipid fractions, purified from egg yolk, in addition to peanut oil and soybean lecithin, exerted anti-allergic effects in guinea pigs (Coburn et al., 1954, Long and Martin, 1956). A seminal paper published in 1957 would later identify the agent responsible for these anti-inflammatory properties, whilst additionally clarifying its structure. The paper reported isolation of an anti-inflammatory component in the crystalline form derived from soybean lecithin as well as from a phospholipid fraction of egg yolk and hexane-extracted peanut meal (Kuehl Jr et al., 1957). The compound was tested after

conducting a local passive joint anaphylaxis assay in the guinea pig and determined as N-palmitoylethanolamine (PEA) (Kuehl Jr et al., 1957). With subsequent clinical studies indicating that PEA may have a beneficial function to play in the treatment of conditions ranging from pain to eczema, this research was driven by prior studies suggesting a component of egg yolk may have therapeutic benefits in treating rheumatoid arthritis (Rankin and Fowler, 2020) . This work eventually led to its discovery in mammalian tissues, as the presence of NAE's, including PEA, was reported in the lipid fraction of rat liver, brain, and skeletal muscle (Bachur et al., 1965). Since then, PEA has been identified in numerous regions; within the mouse brain and spinal cord, degenerating tissues, paw skin and canine heart extract (Lambert et al., 2002).

2.4.3 Pre-clinical investigations of PEA

Numerous preclinical studies support the view of PEA as an endogenous anti-inflammatory agent. In a granuloma-induced hyperalgesia model, PEA demonstrated anti-inflammatory and pain-relieving effects. When applied locally, it dose-dependently reduced NGF expression and release, inhibited mast cell degranulation, prevented nerve fiber formation and sprouting, alleviated mechanical allodynia, and normalized changes in sensory ganglia (De Filippis et al., 2011). In a mouse model of neuropathic pain, with chronic constrictive sciatic nerve injury, treatment with PEA (10 mg/kg) starting on the first day after the lesion, alleviated both thermal hyperalgesia and mechanical allodynia by targeting nociceptive pathway receptors (Costa et al., 2008). Di Cesare Mannelli et al. (2013a) observed comparable findings. Intravenous administration of 30 mg/kg PEA daily for 14 consecutive days, starting the day after surgery, reduced hypersensitivity to both noxious and non-noxious stimuli, preserved nerve morphology, and decreased endoneurial edema, immune cell infiltration, and pro-inflammatory mediators (Di Cesare Mannelli et al., 2013a). In a rat model of acute inflammation designed to induce paw edema using agents such as carrageenan and lipopolysaccharide (LPS) to simulate inflammatory conditions, PEA notably reduced paw edema when given intraperitoneally at doses of 10 mg/kg and 30 mg/kg (Petrosino et al., 2018). The results included decreased levels of pro-inflammatory cytokines such as TNF-a, IL-6 and IL-1b. Additionally, PEA-um suppressed the expression of enzyme like COX-2 and inducible nitric oxide synthase (iNOS), which are involved in the inflammatory response

(Petrosino et al., 2018). The same study also showed that PEA reduced nitrotyrosine formation, an indicator of oxidative stress, and inhibited mast cell infiltration in the inflamed paw tissues (Petrosino et al., 2018).

2.4.4 Clinical use of PEA

Following the discovery of PEA's anti-inflammatory properties, several interesting clinical studies were conducted and tested under the trade name 'Impulsin' by the Czech pharmaceutical company SPOFA (LoVerme et al., 2005). It was observed within these studies that PEA reduced the duration and severity of symptoms caused by the influenza virus in school children and soldiers (Mašek et al., 1974, Kahlich et al., 1979). The apparent success of the trials, in demonstrating and corroborating the beneficial effects of PEA on influenza symptoms, led to the clinical use of PEA in Czechoslovakia for acute respiratory diseases during the late 1970's. However, after numerous years on the market, PEA was withdrawn from clinical use due to an unelucidated mechanism of action, leading to a pause in research that lasted more than 20 years. In 1993, Italian Nobel Prize laureate Rita Levi Montalcini and co-workers discovered that some acylethanolamides, initially termed ALLIA-amides, are endogenously synthesized lipids exerting anti-inflammatory properties (Levi-Montalcini et al., 1996). This discovery attracted the scientific community's interest and provided a new understanding of the mechanism of action by which PEA exerts its anti-inflammatory and anti-analgesic properties (Keppel Hesselink, 2013). Since this research, there has been a continuous rise in interest in PEA, and a quick PubMed search using the term 'palmitoylethanolamide' reveals that since 2012, over 70-80 publications per year are focused on this lipid.

Current clinical studies on PEA primarily focus on pain and peripheral inflammatory conditions. The most extensive study of PEA for chronic pain involved patients with lumbosciatica, primarily due to nerve root compression (Guida et al., 2010). This multicentred, double-blind, randomized controlled trial tested two doses of micronized PEA (300 mg/day or 300 mg twice daily for 3 weeks) compared to a placebo. The 21-day treatment with micronized PEA (Normast) led to a dose-dependent reduction in pain intensity, as measured by the VAS scale (Guida et al., 2010). Additionally, PEA treatment was associated with a significant

decrease in the use of NSAIDs for managing chronic lumbosciatica. Gatti et al. (2012) conducted a similar study examining PEA's efficacy and safety in mitigating pain severity in patients with various pathological conditions. PEA was consumed at a dose of 600mg twice daily for 3-weeks, followed by a once-daily dose for 4-weeks to 610 patients. The main outcome measure was the assessment of pain using a numeric rating scale. PEA treatment resulted in a significant decrease in pain severity scores among all patients and notably, PEA's efficacy remained consistent across several pathological conditions contributing to pain (Gatti et al., 2012). Considerably, no adverse effects or safety issues were related to PEA administration. Additional studies investigating PEA across various pain models indicate its efficacy in reducing painful diabetic neuropathy, neuropathy from chemotherapy, pain from idiopathic axonal neuropathy and pain from sciatic and lumbosacral spine disease (Davis et al., 2019).

2.4.5 Pharmacokinetic Characteristics of PEA

Bioavailability & Distribution

Research available investigating the pharmacokinetic properties of PEA remains limited, partly due to its endogenous nature and complex metabolism. While PEA is endogenously produced, it can also be administered exogenously. However, due to its lipophilic nature, PEA has a low oral absorption in aqueous solvents meaning the dissolution rate is often the rate limiting step for its poor oral bioavailability (Impellizzeri et al., 2014a, Petrosino et al., 2018). Once absorbed, PEA is rapidly metabolised and excreted, with peak plasma concentrations reached within two hours, indicating a short half-life (Petrosino et al., 2016). There is a lack of extensive research surrounding the bioavailability of PEA, with no clear understanding of how the levels of this lipid can vary among individuals. A study conducted at Umeå University estimated pharmacokinetic parameters using in vitro data following oral administration of 100mg/kg PEA in corn oil to male Wistar rates (150-200g) (Vacondio et al., 2015, Gabrielsson et al., 2016). They determined that bioavailability was low, around 25%, but the volume of distribution exceeded the plasma volume, suggesting most of PEA was outside the blood after oral administration (Vacondio et al., 2015, Gabrielsson et al., 2016). Tissue distribution studies confirm the presence of PEA in multiple organs, including the adrenal glands, spleen, lungs, and heart, with lower concentrations in the brain and plasma (Gabrielsson et al., 2016, Petrosino and Di Marzo, 2017a).

To improve absorption, recent research has focused on micronisation, which involves reducing the particle size of PEA, thus increasing its surface area and absorption (Rankin and Fowler, 2020). In animal models, micronised and ultra-micronised PEA significantly reduced carrageenan-induced inflammation compared to non-micronised forms (Impellizzeri et al., 2014a). In human studies, Petrosino et al. (2016) reported that following administration of 300mg of micronized PEA at 0, 2, 4, and 6 hours, plasma concentrations doubled within 2 hours and returned to baseline levels after 4 hours. A recently developed formulation of PEA, LipiSperse™, improved bioavailability in healthy adults to 1.75 times that of standard PEA, surpassing baseline levels (Briskey et al., 2020).

Metabolism & Excretion of PEA

In the body, PEA is enzymatically hydrolysed to form palmitic acid and ethanolamine by two enzymes, endoplasmic reticulum localised fatty acid amide hydrolase (FAAH) and lysosomal N-acylethanolamine acid amidase (NAA) (Rankin and Fowler, 2020, Petrosino and Di Marzo, 2017a). The relative actions of these enzymes depend on their expression in different tissues, with FAAH potentially exhibiting higher expression in the liver and brain, whereas NAAA expression may be greater in the gut and macrophages (Rankin and Fowler, 2020, Alhouayek and Muccioli, 2014). Synthesis of PEA takes place in the membranes of several cell types and involves different steps and partly parallel pathways. The most investigated pathway goes via N-palmitoyl-phosphatidyl-ethanolamine, which belongs to the class of N-acyl phosphatidylethanolamines (NAPEs) (Keppel Hesselink et al., 2013) . The first step in this pathway involves the transfer of a fatty acid from phospholipids within the membrane to phosphatidylethanolamine (PE) (LoVerme et al., 2005). This process, catalysed by a calcium ion and cyclic-AMP regulated N-acyltransferase (NAT), leads to the formation of the FAE precursor NAPE (Ueda et al., 2001). The following step involves the cleavage of membrane-bound NAPE to release free PEA, which is mediated by a NAPE-specific phospholipase D (PLD).

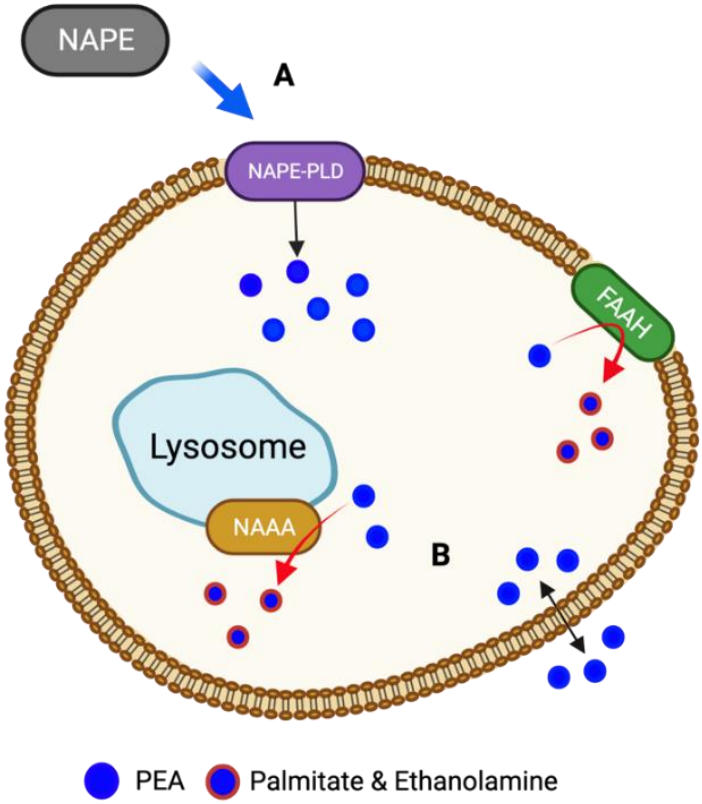

Figure 2.4. Metabolism of PEA. (A) PEA is biosynthesized from a membrane phospholipid, N-palmitoyl-phosphatidyl-ethanolamine (NAPE), via several routes, the most investigated however is through the direct hydrolysis by N-acyl phosphatidylethanolamine-specific phospholipase D (NAPE-PLD).(**B**) PEA is then degraded to palmitic acid and ethanolamine by either fatty acid amide hydrolase (FAAH) or N-acylethanolamine-hydrolyzing acid amidase (NAAA) (Iannotti et al., 2016).

While the metabolism of palmitic acid is well described, with evidence of the metabolic cascade of PEA into palmitic acid which is subsequently incorporated into phospholipids in intact cells, the extent and route of excretion of unmetabolized PEA is yet to be understood (Rankin and Fowler, 2020). To our knowledge, it is not known the extent to which orally or topically administered PEA is hydrolyzed to palmitic acid before its excretion from the body. Moreover, data surrounding the route of excretion of unmetabolized PEA is limited, therefore, further human studies of PEA pharmacokinetics in diverse populations are needed.

2.4.6 Mechanism of action

PEA's mechanism of action is multi-faceted, involving both direct and indirect molecular pathways. One of the earliest insights into its mechanism of action came the work of Professor Rita Levi-Montalcini, who discovered its ability to reduce the degranulation of mast cells *in vivo* in the ear pinna (Aloe et al., 1993). The authors observed a local antagonism in inflammation, termed "Autacoid Local Injury Antagonism" (ALIA), proposing a local autocrine/paracrine contribution to the control of negative feedback from mast cell responses to multiple activation signals (Keppel Hesselink, 2013). Another possible mechanism of action called "entourage effect" was proposed, in which PEA can act indirectly on cannabinoid receptors, in particular towards CB2 receptor explaining its activation, despite its low affinity (Petrosino et al., 2016). Due to its low affinity for binding to the CB2 receptor, a further mechanism mediated by PEA is proposed. This mechanism operates through the direct activation of two other receptor targets: PPAR-a, belonging to the nuclear receptor superfamily and the orphan GPR55 receptor (Verme et al., 2005). A pivotal question remains surrounding PEA, as to whether this multitude of effects can be attributed to a singular or multiple primary targets.

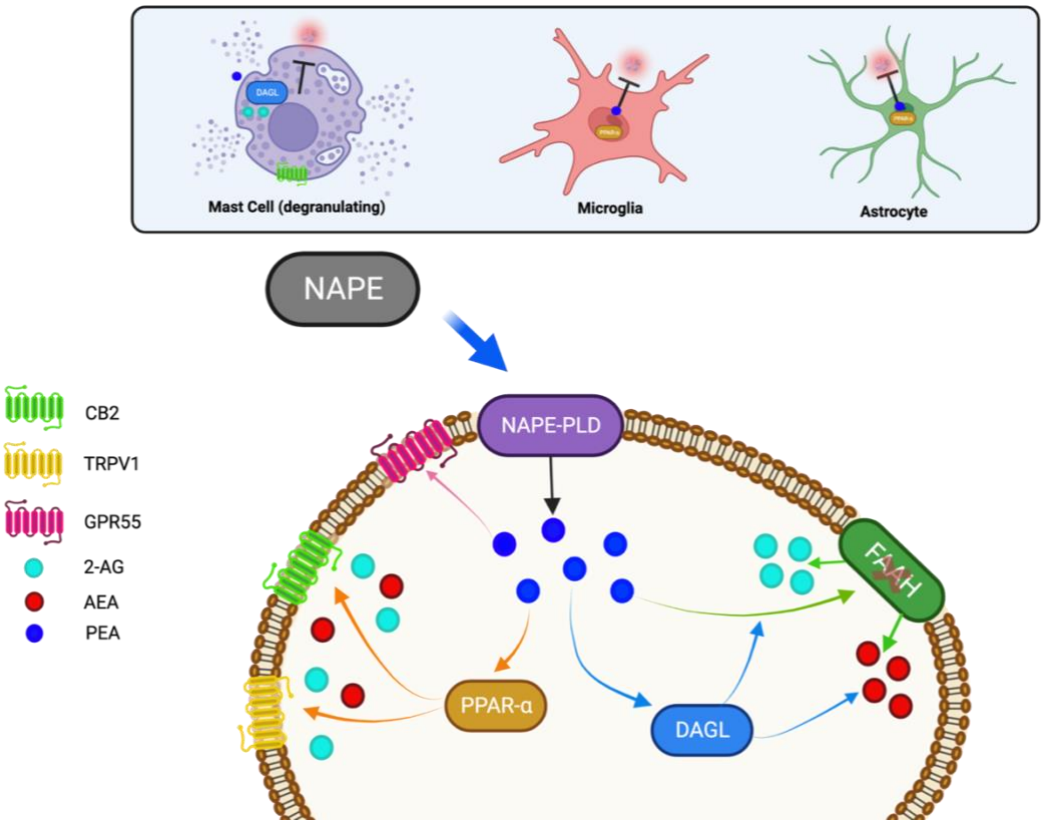

Figure 2.5. Molecular target and mechanisms of action of PEA. PEA directly activates GPR55 (pink arrow) and PPAR-a receptors (orange arrow). PEA further activates TRPV1 and increases the expression of CB_2 receptors (orange arrows) via direct activation of the PPAR-a receptors. PEA through the inhibition of the expression of FAAH (green arrow) or stimulation of the activity of DAGL (blue arrows), may increase the endogenous levels of AEA and 2-AF, which directly activate CB_1, CB_2 and TRPV1 receptors ("entourage effect"). PEA, potentially via an allosteric modulation of TRPV1 receptors, potentiates the activation of desensitization by AEA and 2-AG of TRPV1 receptors ("entourage effect"). The activation of mast cells is inhibited by PEA through an indirect CB_2-mediates mechanism. PEA also reduces the activation of microglia and astrocytes through a PPAR-a mediated mechanism.

2.4.7 Direct Molecular targets of PEA

PPAR-α

Peroxisome proliferator-activated receptor alpha (PPAR-a) is a nuclear receptor protein belonging to the family of PPARs and functions as a transcription factor regulating gene expression (Green and Wahli, 1994). PPAR-a is expressed in a variety of tissues and organs, including adipose tissue, kidney, heart, skeletal muscle, and several immune cells, with the highest levels of expression observed in the liver, which is notably the tissue demonstrating the greatest response to peroxisome proliferators (Issemann and Green, 1990, Nemali et al., 1988) (Braissant et al., 1996, Beck et al., 1992). A developing body of evidence has implicated PPAR-a in the control of inflammatory responses and these receptors are expressed in numerous cells of the immune system (Daynes and Jones, 2002). The first evidence of PEA as a potential agonist of PPAR-a was reported by LoVerme et al. (2005) who demonstrated that PEA activates the nuclear receptor PPAR-a with a potency comparable with that of the synthetic agonist Wy-14643, resulting in strong anti-inflammatory actions (Verme et al., 2005). Therefore, it was proposed, similar to all PPAR agonists, the binding of PEA to PPAR-a also produces a heterodimerization event with the retinoic acid receptor (RXR) (LoVerme et al., 2005). Thus, resulting in the formation of the activated receptor complex, which translocates the nucleus to bind to a peroxisome proliferator response element and decreases the transcription of pro-inflammatory genes (LoVerme et al., 2005).

GPR55

Since its initial cloning in 1999, the G-protein coupled receptor 55 (GPR55) has emerged as a potential new member of the endocannabinoid system (Sawzdargo et al., 1999). Despite

having a low homology with CB_1 and CB_2 receptors, it has been proposed that activation is initiated by the main psychoactive component of Cannabis sativa, Δ9-tetrahy-drocannabinol, and by the endocannabinoids, anandamide (AEA) and 2-arachidonoylgycerol (2-AG) (Sharir and Abood, 2010). At present, the relevance of the GPR55 receptor for the activation of anti-inflammatory/neuroprotective PEA-induced effects remains to be clarified. Current research suggests PEA may protect against atherosclerosis by promoting an anti-inflammatory and pro-resolving phenotype of macrophages, which involves the activation of the GPR55 receptor (Rinne et al., 2018). In a cellular model of Parkinson's disease, the presence of GPR55 expression demonstrated a protective effect against the insult exerted by MPP^+, but an agonist of GPR55 did not result in increased neuroprotection in cells expressing GPR55 (Martínez-Pinilla et al., 2019). Nevertheless, when administered chronically (over 5 weeks) to a murine model of Parkinson's disease, the GPR55 agonist abnormal cannabidiol (Abn-CBD), a synthetic cannabidiol isomer, demonstrated beneficial properties (Celorrio et al., 2017). Although its pharmacological properties are not fully elucidated, research suggests that GPR55 utilises various downstream signalling pathways, including the increase in calcium levels through interactions with Gq, G12, RhoA, actin, PLC and IP(3)R-gated stores (Lauckner et al., 2008). Taken together, these data suggest that the beneficial anti-neuroinflammatory effects of PEA might be potentially facilitated by GPR55 activation.

2.4.8 Indirect Molecular targets of PEA

CB_1 and CB_2 receptors

In addition to its direct action on PPAR-a and GPR55, convincing evidence suggests that PEA may elicit several indirect receptor-mediated actions, through the so-called entourage effect (Petrosino and Di Marzo, 2017a). The CB_1 and CB_2 receptors, similar to the orphan GPR55 receptor, also belong to the large family of G protein-coupled receptors, Class C (GPRCs) (Matsuda et al., 1990). Due to its weak affinity for CB_1 and CB_2 receptors, cannabinoid receptors are not considered direct targets of PEA, however, they can be indirectly activated by PEA via different mechanisms. Specifically, PEA might indirectly activate CB_1 and CB_2 receptors by functioning as a pseudo-substrate for FAAH, the enzyme responsible for the degradation of the endocannabinoid AEA, thus leading to a reduced degradation of AEA (Petrosino et al., 2016). This process results in elevated levels of AEA, subsequently leading to

increased activation of cannabinoid receptor-mediator signalling (Beggiato et al., 2019a). Moreover, recent research has demonstrated that PEA increased the levels of CB_2 receptor mRNA and protein through PPAR-a activation, and this effect is involved in PEA-induced alterations in microglial activity, including increased migration and phagocytic activity (Guida et al., 2017). Additionally, PEA inhibited mast cell (MC) activation and neo-angiogenesis, both of which were blocked by a CB_2 receptor antagonist, signifying the involvement of the CB_2 receptor (Vaia et al., 2016). The discovery that GRP55 can form receptor heteromers with either CB_1 and CB_2 receptors, raises the possibility that PEA could regulate the intracellular signalling mediated by CB_1 and/or CB_2, by interacting with the GPR55 protomer within these potential GRP55/CB_1 or GRP55/CB_2 heterodimers (Martínez-Pinilla et al., 2019, Balenga et al., 2014).

TRPV1

PEA has also been shown to indirectly activate the transient receptor potential vanilloid 1 (TRPV1) channel (Zygmunt et al., 2013). TRPV1 receptors are specialised receptors that respond to heat, as well as certain chemical compounds like capsaicin (found in chilli peppers and known for producing a burning sensation), and AEA. Two distinct mechanisms have been proposed for the effect of PEA at TRPV1 channels. The first mechanism suggests that PEA can indirectly activate TRPV1 through the 'entourage effect'. In particular, PEA-induced increase of endocannabinoid levels can modulate inflammation and other immune functions via TRPV1 channel (Ross, 2003). Additionally, supposed allosteric characteristics of PEA at TRPV1 channels have been proposed as a potential explanation for the compound's ability to increase the endocannabinoid-induced activation and desensitization of TRPV1 channels (Petrosino and Di Marzo, 2017a). As the existence of a direct biochemical interaction has been hypothesized, the second mechanism of action possibly involves the indirect activation of TRPV1 channels via PPAR-a (Ambrosino et al., 2013). Interestingly, recent reports have indicated that TRPV1 activation decreases central inflammation in multiple sclerosis, and there have been reports of neuroprotective effects of TRPV1 activation in animal models of Parkinson's and Alzheimer's diseases (Stampanoni Bassi et al., 2019, Zhao and Tsang, 2017, Nam et al., 2015).

2.5 Thesis Aims and Objectives

In summary, exercise-induced muscle damage (EIMD) is characterised by a distinct number of symptoms, most notably a temporary loss of muscle function, delayed-onset muscle soreness (DOMS), and localised pain. These symptoms typically reflect underlying structural disruption, inflammation, and the initiation of muscle regeneration processes. Although transient, they can impair performance and training consistently, making effective recovery strategies a priority for athletes. Non-steroidal anti-inflammatory drugs (NSAIDs) are commonly employed to manage pain and inflammation following EIMD. However, accumulating evidence indicates that repeated NSAID use may be associated with adverse effects, including gastrointestinal and renal complications, as well as potential interference with muscle protein synthesis, which could impair long-term muscle adaptation. In response to these concerns, several athletic governing bodies, such as the Ultra-Trail du Mont-Blanc (UTMB), have implemented bans on NSAID use during competition

These concerns and subsequent restrictions have prompted growing interest in novel, targeted interventions that can support recovery without attenuating the physiological adaptations associated with muscle damage. Palmitoylethanolamide (PEA), an endogenous fatty acid amide with well-documented anti-inflammatory and analgesic properties, has demonstrated therapeutic potential in both preclinical and clinical models of chronic pain and inflammation. However, despite its promise, investigations into the effects of PEA on skeletal muscle, particularly in the context of exercise-induced muscle damage, remain limited. A more comprehensive understanding of the role of PEA in muscle recovery may inform the development of therapeutic strategies that mitigate symptoms while preserving key mechanisms underpinning muscle repair and adaptation. Therefore, the overall aim of this thesis is to investigate the potential of PEA in alleviating symptoms associates with EIMD, and to characterise its effects on skeletal muscle at a functional, cellular and molecular level. To achieve this aim, the following objectives will be addressed:

1. Investigate the prevalence and perceptions of NSAID use among ultra-endurance runners to assess the need for safer alternatives in managing EIMD.
2. Characterise the effects of PEA on C2C12 skeletal muscle myogenesis and gene expression in vitro.

3. Compare the effects of PEA and the NSAID Ibuprofen on protein synthesis and protein abundance in C2C12 skeletal muscle myotubes in vitro.
4. Evaluate the potential of PEA as an alternative to NSAIDs for alleviating symptoms of EIMD using an in vivo downhill running model.

Chapter 3

General Methodology

This chapter outlines the general methodologies, and the theoretical foundations of the approaches used in the investigations conducted for this thesis. Assays specific to a methodology performed in one chapter are described within that chapter.

3. General Methodology

3.1 Cell Model of Myogenesis

A 2D *in vitro* study design was employed for the cellular experiments in this thesis, where C2C12 myoblasts were differentiated in a two-dimensional culture system. The advantages of 2D cell models include simplicity, low-cost maintenance, and the ability to conduct functional tests. Additionally, 2D cultures offer high replicability and straightforward analysis for experiments. The differentiation of skeletal muscle cells *in vitro* serves as a valuable model for examining various stages of myogenesis, including cell proliferation, fusion, and myotube maturation. Detailed descriptions of growth conditions, reagents, and cell treatments are provided in the following sections.

3.2 Cell Culture

All cell culture experiments were performed in a Kojair Biowizard Silverline class II hood under aseptic conditions (Kojair, Vippular, Finland). All cells were sub-cultured and incubated at 37°C and 5% CO_2 in a Binder incubator (Binder, NY, USA) and were routinely monitored using an inverted light microscope (Olympus, CKX31, Japan). All liquids and waste media were removed via aspiration (Charles Austen Pumps Ltd, Surrey, UK).

3.2.1 Cell Culture Reagents

Dulbecco's modified Eagle's medium (DMEM) with ultraglutamine 1 and high ($4x10^4$ $mg{\cdot}L^{-1}$) glucose was purchased from Gibco (Life Technologies, California, US) and was used for murine C2C12 cells. All serum was purchased from Gibco (Life Technologies, California, US) and included: horse serum (HS), newborn calf serum (NBCS) and fetal bovine serum (FBS). The antibiotics penicillin and streptomycin (PS) were added to all media (1%: 50 U/mL penicillin and 50 ug/mL streptomycin). Phosphate buffered Saline (PBS) was used to wash cell monolayers and was prepared by placing 10 PBS tablets (Sigma-Aldrich, Sigma Life Sciences, St Louis, MO, USA) into 1000ml of dH_20. For cell adherence, gelatin type A from porcine skin was used (Sigma-Aldrich Company Ltd. Dorset, UK) and reconstituted to create a working stock of 0.2% gelatin.

Growth media (GM) for C2C12 cells comprised: DMEM, 10% FBS, 10% NBCS and 1% syringe filtered PS. Differentiation media (DM) included: DMEM, 2% HS and 1% PS. GM was used to promote cell proliferation and DM was used to induce cell differentiation. Palmitoylethanolamide (PEA) (molecular mass 299.5 g/mol) was provided by Gencor Pacific Ltd, Hong Kong in powdered from and reconstituted in Ethanol. Ibuprofen (molecular mass 206.28 g/mol) was provided by Sigma-Aldrich Company Ltd, UK in powdered form and reconstituted in Ethanol.

3.2.3 Plasticware

All cell populations were sub-cultured on T75 culture flasks (Corning, NY, USA) and experiments conducted on 6 and 12-well plates (Corning, NY, USA). Eppendorf's (Eppendorf, Hamburg, Germany) and cryogenic vials (Simport Scientific, Saint-Mathieu-de-Beloeil, Canada) were used throughout cell culture experiments.

3.2.4 C_2C_{12} Skeletal Muscle Cells

Murine C2C12 skeletal muscle myoblasts were obtained from the American Tissue Culture Collection (ATCC; Rockville, USA) and were passaged to increase cell yield and stored in liquid nitrogen (LN_2) until needed for experiments. C2C12 cells are the C12 sub-clone of the C2 parental cell line, originally derived from the injured leg of the C3H mouse (Yaffe and Saxel, 1977). The C12 sub-clone was chosen for its differentiation capability, hence the extensive use of this cell line for *in vitro* research.

3.2.5 Passaging C_2C_{12} myoblasts

C2C12 skeletal muscle myoblasts were sub-cultured in T75 flasks (Thermo Fisher Scientific, Waltham, MA, USA) containing 15ml GM. The T75 flask was then placed in the incubator at 37°C, 5% CO_2 to proliferate until ~80% confluency was attained. Once this confluency was achieved, remaining GM was aspirated, and cells washed twice with 1X PBS. To detach the cells from the flask surface, 1ml of trypsin EDTA was added to the culture flask, ensuring full coverage, and incubated for 5 minutes (37°C, 5% CO_2). Following the detachment of cells, 4ml

of GM was added to the flask to neutralise trypsin activity, and the cells were subsequently counted.

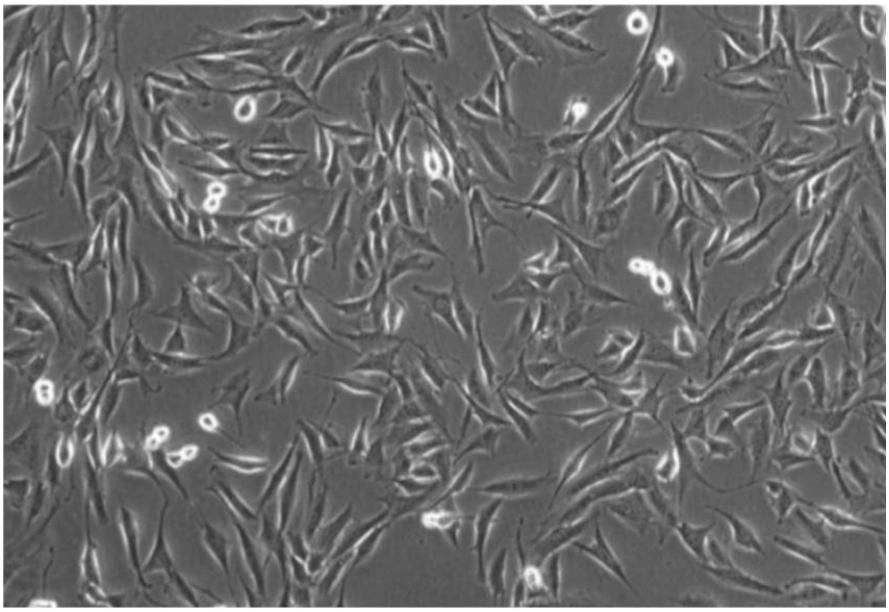

Figure 3.1. C2C12 myoblasts at ~80% confluence.

3.2.6 Cell Counting by Trypan Blue Exclusion

Cells were manually counted on a Neubauer haemocytometer (BLAUBRAND® Neubauer, Sigma-Aldrich, Poole, UK) using the trypan blue exclusion method, whereby 20uL of cell suspension was homogenised with 20uL 0.4% trypan blue stain (Sigma-Aldrich, Poole, UK) in a 1:1 ratio. The solution was then pipetted onto either end of the haemocytometer, flooding both chambers via capillary action. Cells in the four corner grids were counted under a microscope (Olympus CKX31 Microscope) at ^{X} 10 magnification. Viable cells were recognised as small, round, and clearly visible, while non-viable cells were misshapen, slightly larger and had lost their membrane integrity, hence were trypan blue positive and excluded from cell counts. The resultant mean of 4 grids was calculated, which represented average cell numbers per 0.1 mm^3 grid. This value was then multiplied by 2, to account for the trypan blue dilution factor or 1:1. A further multiplication by 10^4 was undertaken to extrapolate the number of cells in the 0.1 mm^3 to 1 cm^3 (equivalent to 1ml of cell suspension). The total number of cells present within the cell suspension could be calculated by simply multiplying the total volume of cell suspension (mL).

Required mL trypsinized cells = Required seed (no.cells/mL) / cell count (no.cells/mL) x Required mL of media

3.2.7 Cell Cryopreservation and Resuscitation

Once counted (see section 3.2.6), GM was added to existing cell suspension to ensure a concentration of 1 x 10^6 cells/mL. Dimethyl sulfoxide (DMSO) (Sigma-Aldrich, Poole, UK), a cryoprotectant that prevents ice crystal formation, was added at 10% of the total cell suspension volume, before distributing the cell suspension into labelled (name, cell line, passage number, concentration and date) 2 mL cryovials (Simport Scientific, Fisher Scientific, UK). Cryovials were then transferred to a cryopreservation container ('Mr Frosty', Thermo Fisher Scientific, Waltham, MA, USA) containing isopropanol (Sigma-Aldrich, Poole, UK) before being placed in a -80°C freezer for 24 hours to ensure a gradually freezing rate (-1°C/min^{-1}). Following 24 hours, cryovials were submerged in liquid nitrogen (LN_2). When resuscitating cells from LN_2, cryovials were sprayed with 70% ethanol and placed under the hood to thaw at room temperature. Cell suspension was then pipetted onto a pre-gelatinised T75 flask (10 mL of 0.2% gelatin (Sigma-Aldrich, Poole, UK) and incubated at 37°C, 5% CO_2 for 15 minutes) containing 15 mL of preheated (37°C) GM and incubated at 37°C, 5% CO_2 to enable cell attachment. The time to reach ~80% confluency for 1 x 10^6 cells was approximately 48 hours.

3.2.8 Microscopy and Live Imaging

Live images of cell monolayers were captured using a Leica DMII6000B Live Imaging Microscope (Leica Biosystems, Wetzlar, Germany). Images of cell monolayers were taken using the 10x objective and 0.5 magnification c-mount fitted to the camera. Image inspection and processing was conducted using Leica Application Suite for Windows (Leica Biosystems, Wetzlar, Germany) and Image J (1.53a, National Institutes of Health, USA).

3.4 MTT Cell Viability Assay

3.4.1 General Principle

The MTT (diphenyl tetrazolium bromide) assay is a colorimetric assay used to assess cell metabolic activity. This assay relies on the ability of NADPH-dependent cellular

oxidoreductase enzymes to reduce the tetrazolium dye, MTT, into an insoluble formazan product, which appears purple in colour. The absorbance of the purple solution can be quantified by measuring it at a specific wavelength (570 nm). Thus, this assay provides a measure of cell viability based on the reductive activity within cells, as the enzymatic conversion of MTT to formazan crystals occurs in the mitochondria of living cells.

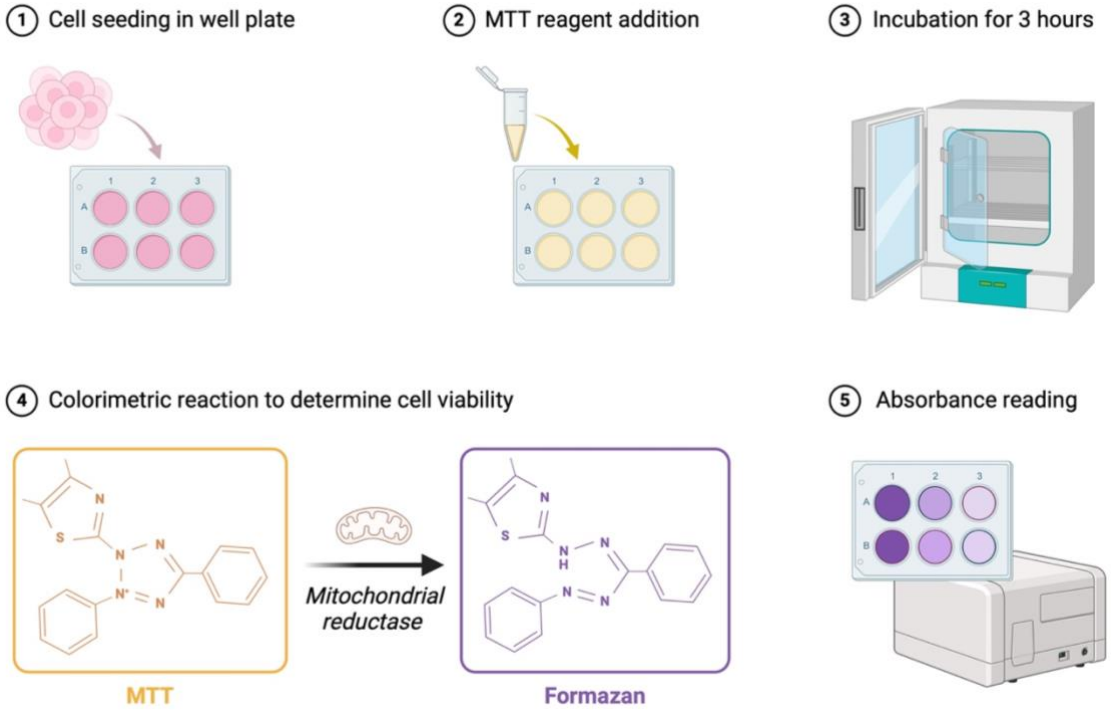

Figure 3.2. Schematic representation of the MTT assay protocol for determining cell viability. (1) Cells are seeded into a 6-well plate and allowed to adhere. (2) The MTT reagent is added to each well, initiating the assay. (3) Plates are incubated for 3 hours to allow mitochondrial reductase in viable cells to reduce MTT into formazan crystals. (4) The reduction of MTT to insoluble formazan is mediated by mitochondrial enzyme activity, serving as an indicator of metabolic activity and cell viability. (5) Absorbance of the dissolved formazan is measured to quantify cell viability. Higher absorbance indicates increased metabolic activity.

3.4.2 General Protocol

Tetrazolium dye was added to PBS at a concentration of 5mg.ml-1 to generate an MTT solution. MTT solution (5mg/ml) was added to each well (amount of MTT solution was equal to 10% of total media). Plates were then incubated for 180-minutes, during this time the MTT should interact with NADPH-dependant cellular oxidoreductase enzymes to form visible purple formazan crystals at the bottom of the well. Following this incubation period, existing

media was aspirated before a second incubation period lasting 6-minutes, with the lid of the plate removed. Thereafter, DMSO (500 µL) was added to cell monolayers resulting in a purple-coloured solution. Plates were then placed on a plate rocker for 2-minutes at 120 rpm until all cells were lifted from the base of the well. Plates were then positioned into a Spark multimode microplate reader (Tecan, Mannedorf, Switzerland) and measured at a wavelength of 570 nm. All data were presented as a relative % of vehicle control (DMOS; 100% Viable). Cell viability data was generated and analysed in Microsoft Edexcel (Version 16.61.1).

3.5 Flow Cytometry

3.5.1 General Principle

Flow cytometry is a fast and reliable technique for quantifying viable cells. Assessing cell viability is crucial when evaluating a cells response to specific supplements or other environmental factors. The quantification of single cell characteristics is possible via a liquid passing through a (or multiple) light streams. Flow cytometry can quantify the granularity and fluorescent aspects of cells (Adan et al., 2017). The quantification of different properties of a molecule can be assessed by measuring how the molecule scatters and/or emits light as it passes through a known light source. This emitted or scattered light is then detected by an array of sensors.

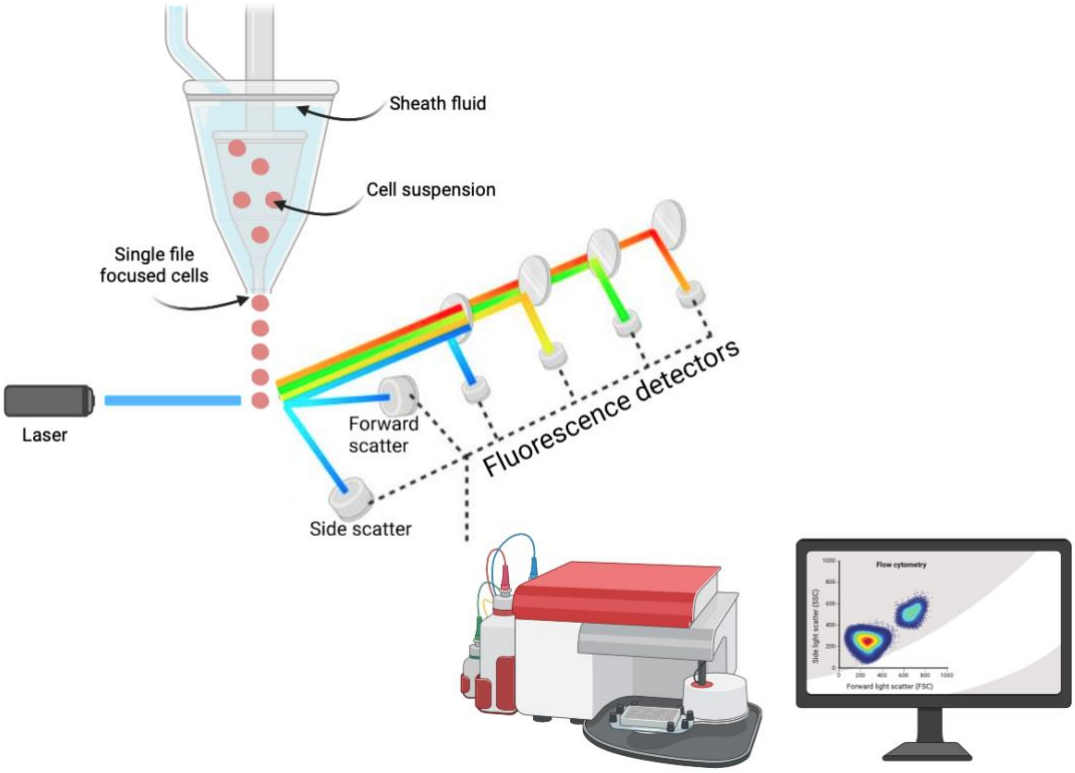

Figure 3.3. The basic layout of a flow cytometer apparatus, illustrating the fluidic, optical, and electronic systems. Cells in suspension flow in a single file through an illuminated volume where they scatter light and emit fluorescence. This is then detected by the detectors, which pick up a combination of scattered and fluorescent light. This data is then analysed by a computer that is attached to the flow cytometer using special software, where data such as the physical and chemical structure of the cells is generated.

To accurately determine the properties of individual cells, the cell suspension is first passed through a stream of sheath fluid, which hydrodynamically aligns the cells into a single file as they move through the laser beam. Prior to any fluorescent probe analysis, the flow cytometer initially measures two aspects of the light: forward scatter (FSC) and side scatter (SSC). The FSC detector is positioned in line with the laser beam, and as cells pass through, they deflect the light, casting a 'shadow' on the detector. This information is then used to estimate cell size, with larger cells casting larger shadows. The SSC detector, positioned perpendicular to the laser beam, captures light that is scattered by internal cellular components as it enters the cell. The amount of scattered light correlates with the complexity of the cell; more scattered light indicates greater cellular complexity. The FSC and SSC data are combined in a dot plot, where populations of similarly sized and complex cells group together. From the plot created,

the nature of the cellular population can be determined; healthy cells cluster in specific region, while cells undergoing apoptosis, which tend to shrink and become more complex, shift to a different region on the graph. Each flow cytometer can be equipped with a range of different detectors, with some having up to sixteen different channels. The flow cytometer used within the current study was a BD accuri C6 with four channels of fluorescence intensity: FL-1,FL-2, FL-3, FL-4.

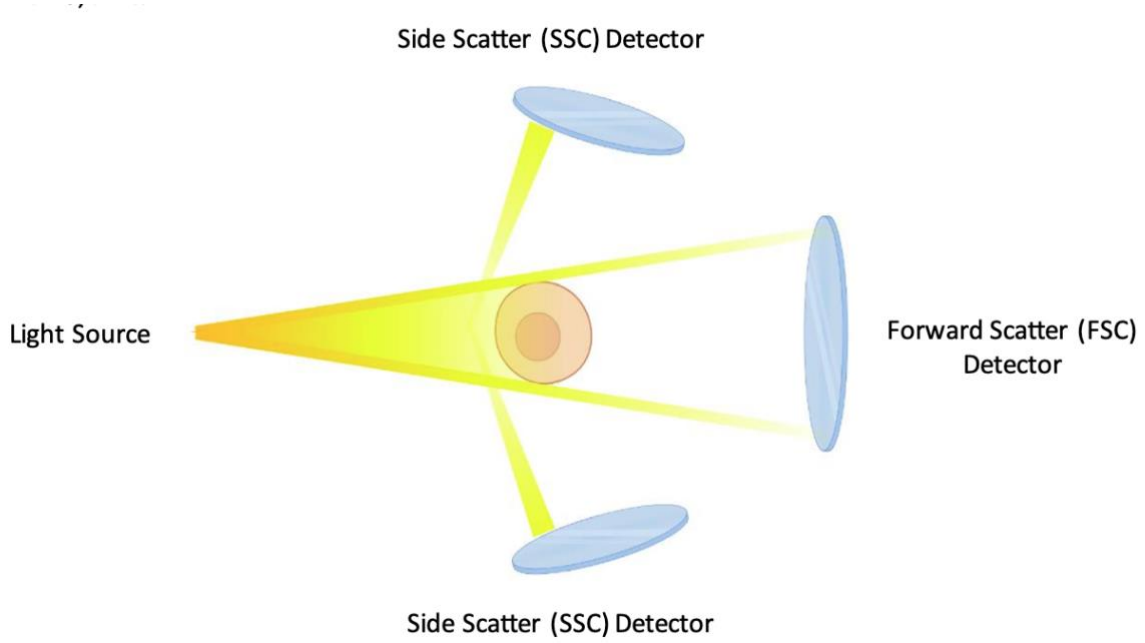

Figure 3.4. Flow cytometry light scatter. Forward scatter (FSC), detected in line with the laser, correlates with cell size, while side scatter (SSC), detected perpendicular to the laser, reflects cellular granularity and internal complexity.

3.5.2 General Protocol

Before completion of experimental procedures, a control population of cells was first analysed via flow cytometry to establish forward scatter (FSC) and side scatter (SSC) gating parameters and quantify background fluorescence. For this, 200 µl of a cell suspension was loaded into the flow cytometer, and the cell population was gated based on the densest region, representing viable cells (Figure 3.5). Once defined, these gating parameters were kept consistent across all subsequent experiments using the same cell type.

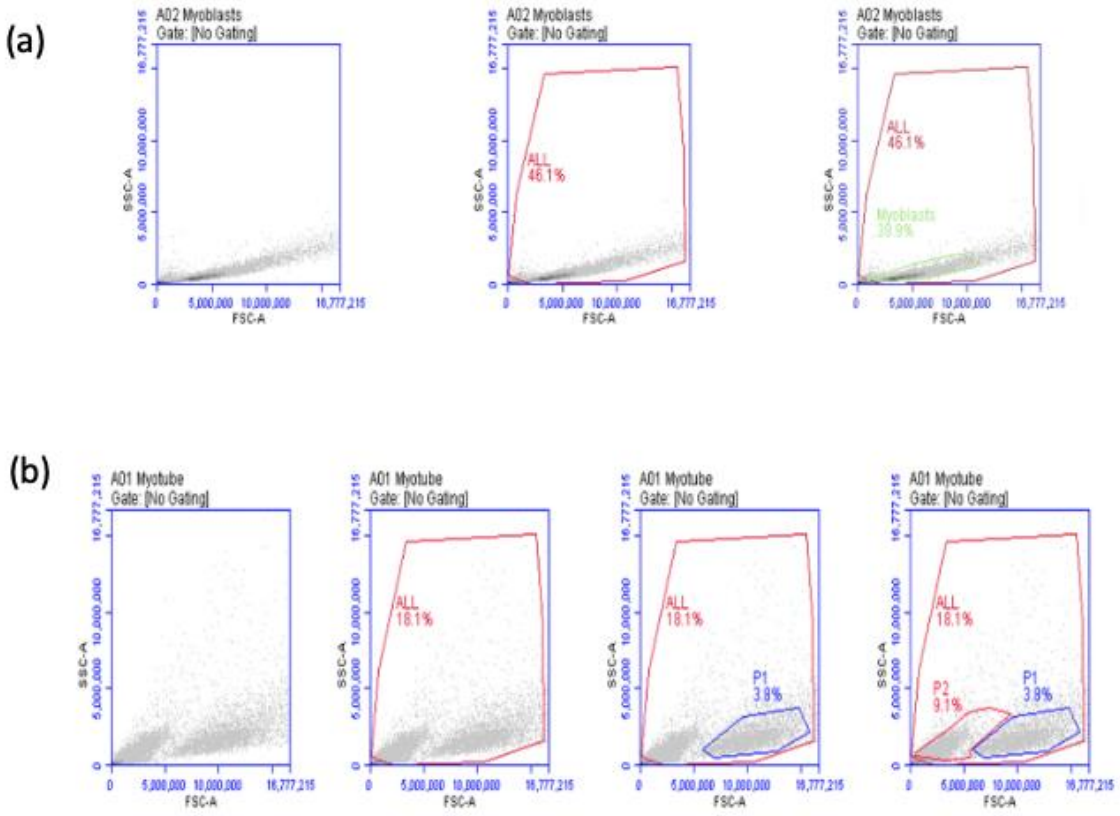

Figure 3.5. Gating strategy for C2C12 cells on the BD Accuri C6 flow cytometer. (a) Gating strategy for C2C12 myoblasts. Cells were first gated to include all events on the scatterplot. Debris in the lower left region of the FSC vs. SSC scatterplot was excluded. A secondary gate was applied to more precisely visualise the viable myoblast population. (b) Gating strategy for C2C12 myotubes. A similar approach to myoblast gating was used, with two separate gates applied to identify and visualise distinct myotube populations.

3.6 Propidium Iodide (PI) Assay

3.6.1 General Principle

Propidium Iodide (PI) is a red-fluorescent dye which penetrates only damaged cellular membranes. Upon entry, PI binds to double-stranded DNA. PI is not membrane-permeable, meaning it cannot enter intact plasma membrane and therefore will only be present in the DNA of cells where the plasma membrane has been compromised/permeabilized. This makes it a useful method to differentiate between necrotic, apoptotic, and healthy cells based on membrane integrity. PI is used more often than other nuclear stains as it is reasonable, stable

and a suitable indicator of cell viability, based on its capacity to exclude dye in living cells (Rieger and Barreda, 2016).

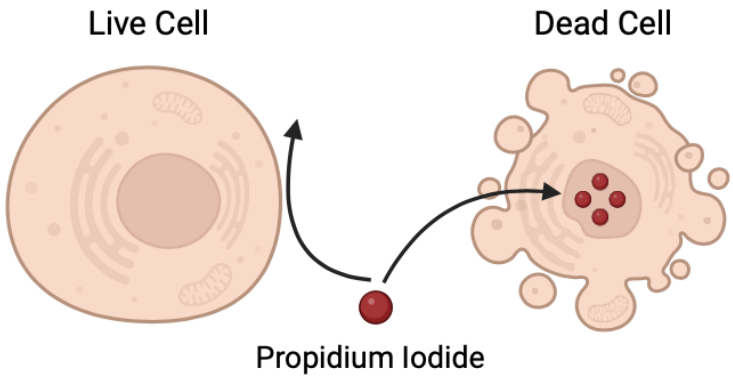

Figure 3.6. Propidium Iodide Staining for Differentiating Live and Dead Cells. Propidium iodide (PI) is a fluorescent dye used to distinguish between live and dead cells. PI is impermeable to live cells with intact membranes, but it penetrates and stains dead cells with compromised membranes, binding to DNA and resulting in a red fluorescence. This staining enables the identification of dead cells in a population when analysed using flow cytometry or fluorescence microscopy.

3.6.2 General Protocol

Existing media was pipetted into corresponding labelled Eppendorf's, i.e., media from cell monolayers dosed with 1µM PEA, was pipetted into an Eppendorf labelled 1µM PEA. Monolayers were then washed twice with PBS, before 200µL of trypsin was added and incubated for 5 minutes. The media collected in the first step was then used to neutralize the trypsin, ensuring the corresponding Eppendorf was used for each well. The solution of trypsin and media was homogenized before being pipetted back into the Eppendorf. Eppendorf's were then centrifuged for 5 minutes at 3000 rcf. Remaining media was aspirated, and a small white pellet of cells was present at the bottom of the Eppendorf. Fresh DM (200µL) was then added to each Eppendorf and vortexed fully until the pellet dissolved. Samples were then prepared to be analysed via the flow cytometer. 20µL of PI solution (ThermoFisher Scientific) was added to each sample and vortexed. Analysis of samples needed to be done quickly, as longer incubation periods can lead to increased cellular death. The dye has an

excitation/emission maximum of 493/636 nm, however upon binding, that excitation/emission maxima increase to 535/617 nm. All PI assays were normalised to cell events (count) on the BD Accuri C6 with each assay ending once 20,000 events had been recorded.

3.7 Immunofluorescence (IF) Imaging

3.7.1 General Principle

Immunocytochemistry (ICC/IF) is a technique used to detect the presence of a specific protein or antigen within cells by use of a specific antibody that binds to it. This antibody binding allows the protein to be visualized under a microscope. ICC/IF is a powerful method for studying the sub-cellular localization of proteins. The typical ICC/IF protocol includes steps for fixation (preserving cellular structures while rendering the cells non-viable), blocking, primary antibody incubation, and secondary antibody incubation.

3.7.2 General Protocol

Existing media was aspirated, and cell monolayers were washed 3 times with PBS. To fix the cells, paraformaldehyde (PFA 4%) solution was added to monolayers and incubated at room temperature for 10 minutes. Thereafter, the fixative solution was removed, and wells were washed 3 times with PBS. The fixed sample can be stored for several days at 5°C. Existing PBS was aspirated and permeabilization buffer (PBS + 0.1% Triton X-100) was added to each well and incubated at room temperature for 15 minutes. The permeabilization buffer was removed, and the monolayers were washed twice with cold PBS. Blocking buffer (10% Goat Serum in PBS, diluted 1:500) was then added and incubated at room temperature for 30 minutes. Afterward, the monolayers were washed once with PBS, and the primary antibody (MF-20 in BSA, diluted 1:300) was added to each well, ensuring the lights were dimmed due to the light sensitivity of MF-20. The plates were then wrapped in parafilm and placed in the fridge at 5°C overnight.

After the overnight incubation, the primary antibody was removed, and the wells were washed three times with cold PBS, allowing each wash to sit for 5 minutes. Next, the

secondary antibody (Alexa-Fluor goat anti-mouse 488 in BSA, diluted 1:400) was added, and the plates were covered with foil and left at room temperature for 60 minutes. Following this, the secondary antibody was removed, and the cell monolayers were washed twice with PBS. The final step involved nuclear counterstaining with DAPI, a blue-fluorescent DNA stain, diluted in H2O (1:100). This was added to the monolayers and incubated at room temperature for 15 minutes, protected from light. The DAPI solution was then aspirated, a small amount of PBS was added to the wells, and the plates were wrapped in foil before being stored in the fridge (5°C) until ready for imaging.

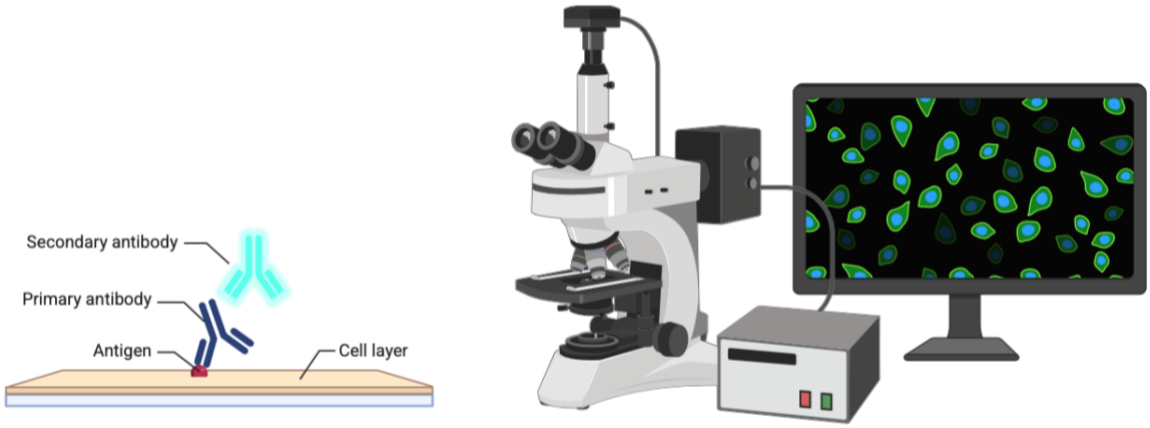

Figure 3.7. A schematic representation of antigen immunolabeling and fluorescent microscopy, demonstrating the binding of primary and secondary antibody to an antigen and the visualisation of fluorescence emitting cells through a fluorescent microscope.

All stained monolayers were captured under a Leica DM116000B Microscope (Leica Biosystems, Wetzlar, Germany) at 10x objective. Blue colour channels (wavelength ~490-450mn) were used as an indicator of DAPI and green colour channels (wavelength ~560-520nm) were used as an indicator for MyHC (Myosin Heavy Chain). Twelve images were taken per condition

3.7.3 Measuring Myotube Number and Area

Myotube counting is a fundamental part of analysis as it allows for the quantification of myotubes formed during culture. Pre-stained images were uploaded into ImageJ for Macintosh (Rasban, W.S., ImageJ, U.S. National Institutes of Health, Bethesda, Maryland,

USA). Images were prepared for analysis first by setting the image scale. Thereafter, each image was edited (brightness & contrast) to ensure differentiation of myotubes was possible. All images were scaled appropriately according to the level of magnification used during imaging, set to 8-bit and displayed a binary state. The freehand selection tool was used to remove any areas of the monolayer which could interfere with myotube identification. Myotubes were classified as multi-nucleic structures with an observable outer membrane.

3.7.4 Measuring Number of Nuclei

The number of nuclei was counter per image as this was later used to calculate nuclear fusion index (NFI). In the present study, nuclei number was measured in ImageJ. Images were inverted, the appropriate threshold set (majority of nuclei highlighted) and the watershed setting applied. The smallest nuclei within the image was identified and the mean value was calculated. The image was then analysed, and all nuclei equal to or greater than the mean size of the smallest nuclei outputted.

3.7.5 Measuring Number of Nuclei Per Myotube

To accurately calculate the average number of nuclei per myotube, the multi-point tool in ImageJ was used. Individua blue DAPI channel images were overlayed onto the corresponding green MyHC channel images and the number of nuclei within each myotube counted. To calculate the average number of nuclei per myotube, the number of nuclei within myotubes was divided by the number of myotubes.

3.8 Cell Cycle Analysis with PI

3.8.1 General Principle

Cell cycle analysis using propidium iodide (PI) is a widely employed method for assessing the distribution of cells across different phases of the cell cycle (G0/G1, S and G2/M). The cell cycle analysis and DNA content measurement of cells can be assessed by flow cytometry using nucleic acid staining dyes like PI. PI enters the cells and binds to the DNA. However, a critical step is required to prevent misinterpretations, such as interference from RNA staining. To avoid this, the solution must include RNase treatment before the experiment is conducted.

The principle is that the fluorescent dye (PI), specifically binds to double-stranded DNA in the cell suspension of permeabilised cells or isolated nuclei. The fluorescence intensity of PI incorporated into the cells is directly proportional to the DNA content within the cells (Nunez, 2001). Flow cytometry analysis enables the possibility to understand various parameters cumulatively, such as proliferation, apoptosis, or other cell-cycle related processes, making it a valuable tool for the screening of possible toxic treatments such as drugs

3.8.2 General Protocol

Existing media was aspirated, and cell monolayers were washed 2 times with PBS. To harvest cells, 200 µL of trypsin was added to each well and incubated for 5 minutes. Once detached, cells were pipetted into a single cell suspension in buffer (e.g PBS + 2% FBS; PBS + 0.1% BSA). Cells were then washed with PBS and centrifuged at 3000 rfc for 5 minutes, this step was repeated twice. Cells were then resuspended at 3-6 x 10^6 cells/mL. Next, 500 µL of cells were aliquoted into a 15 mL polypropylene, V-bottomed tube, and 5 mL of cold 70% ethanol was added dropwise while gently vortexing. Vortexing is essential to ensure the cells don't fix to one another in clumps when adding the ethanol. Cells were then fixed for at least 1 hour at 4°C on ice (cells can be stored in 70% ethanol at -20°C for several weeks prior to PI staining and flow cytometric analysis). After fixation, cells were washed and centrifuged as described above again. To ensure only DNA is stained, cells were treated with Ribonuclease A to remove RNA. 50 µL of RNase A solution (final concentration 0.5ug/ml) was added directly to the cell pellet. Then, 1 mL of PI solution was added and cells vortexed and incubated overnight (or at least 4 hours) at 4°C. Samples were stored at 4°C until analysed by flow cytometry (analysed at a low flow rate under 400 events/second).

3.9 Gene Expression Analysis

For the analysis of gene expression, Next-generation RNA sequencing (RNA-Seq) was employed.

3.9.1 RNA-Seq General Principle

The transcriptome encompasses the complete set of transcripts in a cell, along with their abundance, at a specific developmental stage or physiological condition. Studying the

transcriptome is essential for interpreting the functional elements of the genome, identifying the molecular components of cells and tissues, and also for understanding development and disease. Transcriptomics aims to achieve several key objectives: to catalog all transcript species, including mRNAs, non-coding RNAs, and small RNAs; to define the transcriptional structure of genes (i.e. start sites, 5' and 3' ends, splicing patterns and other post-transcriptional modifications); and to measure dynamic changes in transcript expression levels during development or in repones to various conditions (Wang et al., 2009).

Next-generation RNA sequencing is quickly becoming the method of choice for transcriptional profiling experiments. Unlike, microarray technology, high throughput sequencing enables the identification of novel transcripts, without needing a sequenced genome and removes background noise commonly associated with fluorescence-based quantification. Additionally, RNA-seq provides genome-wide analysis of transcription at a single nucleotide resolution, including the detection of alternative splicing events and post-transcriptional editing events. All RNA-seq experiments follow a similar protocol. First, RNA is converted to a library of cDNA fragments with adaptors attached to one or both ends. Each molecule, regardless of amplification, is subsequently sequenced in a high-throughput manner to generate short sequences from one end (single-end sequencing) or two ends separated by an unsequenced fragment (paired-end sequencing). After sequencing, the resultant reads are either mapped to a reference genome or reference transcripts, or assembled de novo without a reference genome, to generate a genome-scale transcription map that includes both the transcriptional structure and the expression levels of each gene.

3.9.2 RNA Isolation

RNA extraction from cell lysates was performed using the Qiagen RNeasy mini extraction kit (Qiagen, Switzerland) according to the manufacturer's instructions. Terminally differentiated C2C12 monolayers were lysed with buffer RLT from the Qiagen RNeasy kit. RNA was then extracted from cell lysates using the RNeasy kit with proteinase K digestion, as per the manufacturer's guidelines. Eluted RNA was stored at -80°C until required for determination of total RNA and library processing.

3.9.3 RNA Quantification

Total RNA was quantified using a Nanodrop 8000 and RNA quality was assessed using an Agilent® Bioanalyser (average RIN score=7, 260/280=2.1, 260/230=1.6). RNA samples were then diluted to 20 ng·µL-^{1} using RNase-free water.

3.9.4 RNA Library Preparation and Sequencing

Libraries were constructed from 100ng of total RNA with Poly-A tail enrichment of mRNA using NEBNext® Ultra™ II RNA Library Prep Kit for Illumina® (Cat. ID. E7770L. New England Biolabs UK. Hitchin, Herts) with Agencourt AMPureXP Sample Purification Beads (Cat. ID. A63880. Beckman Coulter. Wycombe, UK) as per manufactures guidelines, by Bart's and the London Genome Centre at Queen Mary, University of London. The resultant barcoded libraries were sequenced on an Illumina NextSeq 2000 using 2X50 bp paired-end sequencing. An average of 22 million paired-end reads was achieved per sample.

3.10 Proteomic Analysis

For the analysis of protein abundance and synthesis rates, liquid chromatography coupled with mass spectrometry (LC-MS/MS) was employed.

3.10.1 LC-MS General Principle

Unlike the genome, which is the same in every cell of an individual, the proteome differs between cell types and conditions. This enables the classification of cells based on their protein expression patterns and the identification of changes in specific contexts, such as exercise. Information at the protein level cannot be uncovered or accurately predicted solely from gene sequences or mRNA expression levels, therefore, methods for direct analysis of proteins are required for proteome characterisation (Griffin et al., 2002). Whilst no single technology can completely characterise all aspects of proteomes, mass spectrometry (MS) is the most powerful and adaptable method for proteomic analysis.

MS-based proteomics enables the large-scale, high-resolution analysis of proteins by measuring the mass-to-charge ratio of ionised peptide fragments. Typically, proteins are enzymatically digested (e.g., with trypsin) into smaller peptides, which are then separated by

liquid chromatography (LC) before entering the mass spectrometer. Within the mass spectrometer, peptides are ionised, detected, and fragmented to generate unique spectral fingerprints that allow for both identification and quantification. Tandem MS (MS/MS) adds an additional layer of precision by selecting and further fragmenting specific peptide ions, improving confidence in protein identification. The combination of LC with MS therefore allows for sensitive, unbiased detection of a wide range of proteins, even in complex biological samples. In addition to steady-state protein abundance, advanced approaches such as isotope labelling (e.g., with deuterium) permit dynamic measurements of protein turnover, offering insights into the synthesis and degradation rates of individual proteins.

3.10.2 Protein Extraction and Digestion

Protein was extracted from cell monolayers using ice-cold RIPA buffer (0.5 M Tris-HCl pH 7.4, 1.5 M NaCl, 2.5% deoxycholic acid, 10% NP-40, 10 mM EDTA) including complete protease inhibitors (Roche, Switzerland). Following a 5-minute incubation on ice, lysates were harvested using a cell scraper and stored at –80 °C. Protein concentration was determined using the Bradford assay (Sigma-Aldrich, UK) against a BSA standard curve prepared in RIPA buffer.

Protein samples (100 µ) were precipitated in five volumes of ice-cold acetone (–20 °C, 1 hr), centrifuged (5,000 × g, 5 min), air-dried, and resuspended in UA buffer (8 M urea, 100 mM Tris, pH 8.5). Samples were reduced with 100 mM DTT (37 °C, 15 min), followed by alkylation with 50 mM iodoacetamide (4 °C, 20 min, protected from light). After washing, samples were exchanged into 50 mM ammonium bicarbonate and digested overnight at 37 °C with sequencing-grade trypsin (1:50 enzyme: protein; Promega, Madison, WI, USA). Digestion was stopped with 0.2% trifluoroacetic acid (TFA), and 4 µg peptide aliquots were desalted using C18 ZipTips (Millipore, Billerica, MA, USA). Peptides were resuspended in 0.1% formic acid with 10 fmol/µL yeast alcohol dehydrogenase (ADH1; Waters Corp., Milford, MA) as internal standard for LC-MS/MS analysis.

3.10.3 Protein Identification and Quantification

Peptides were analysed by LC-MS/MS using an Ultimate 3000 RSLC nano LC system coupled to a Q-Exactive Orbitrap mass spectrometer (Thermo Scientific). Peptides were separated using a C18 analytical column with a linear acetonitrile gradient (0.1% formic acid) at 300 nL/min. MS data were acquired in data-dependent mode with full scans at 70,000 resolution (m/z 300–1600), followed by MS/MS of the top 10 precursors using HCD at 17,500 resolution. Raw data were processed using Progenesis QI for Proteomics (Nonlinear Dynamics, Waters Corp., UK) for label-free quantification. MS/MS spectra were exported in Mascot generic format and searched against the *Rattus norvegicus* Swiss-Prot database (release 2022_08) using Mascot Server v2.8. Search parameters included trypsin specificity (2 missed cleavages), carbamidomethylation of cysteine (fixed), and methionine oxidation (variable). Mass tolerances were 10 ppm for precursor ions and 20 ppm for fragments. Protein abundance was calculated using unique peptides with identification scores corresponding to <1% FDR.

3.10.4 Dynamic Proteome Profiling

Mass isotopomer abundance data were extracted from MS spectra using Progenesis QI for Proteomics. Deuterium incorporation into newly synthesised proteins was quantified by calculating the relative isotopomer abundance (RIA) of the first isotopomer (m_1) relative to the sum of m_0 and m_1 across the chromatographic peak for each peptide. RIA values were modelled using rise-to-plateau kinetics, with plateau enrichment ($RIA_{plateau}$) estimated based on the number of exchangeable C–H bonds per peptide and the deuterium enrichment in the precursor pool. Kinetic modelling was performed using in-house Python scripts (v3.12.4) following published methods (Sadygov, 2020a, Ilchenko et al., 2019). Protein degradation rate constants ($k_{ne}g$) were calculated from the change in RIA between the beginning and end of labelling periods, adjusted for changes in protein abundance. Fractional synthesis rates (FSR) were derived by multiplying $k_{ne}g$ by 100, and protein-level FSR values were reported as the median of unique constituent peptides.

3.11 Location of Testing and Ethical Approval

Exercise tests, biochemical and molecular analysis were completed within the laboratories of the Research Institute for Sport & Exercise Sciences. Analyses of C2C12 gene expression for study two was performed at the London Genome Centre at Queen Mary, University of London and analysis of kidney function markers for study four was performed at the University of Liverpool. Ethical approval for studies one (Chapter 4) and four (Chapter 7), respectively was granted by the Liverpool John Moores University Research Ethics and Governance Committee. All samples and data were collected and stored according to the Declaration of Helsinki.

3.12 General Screening and Inclusion Criteria

Participants who volunteered to take part in the human investigations within this thesis (Chapter 7) were required to provide written informed consent prior to any experimental procedures. In the first instance, participants were provided with a participant information sheet which outlined the study's procedures and thereafter they completed a physical activity readiness questionnaire (PAR-Q). The inclusion criteria is outlined below:

- Recreationally active males and females
- Aged 18-35
- No reported use of PEA or other sports supplements within the past month including NSAID's
- Agree to maintain their normal training regime throughout the study
- No uncontrolled physical or mental health problems
- Not currently taking prescribed medication
- No history of allergic reaction (e.g., rhinitis, urticaria, contact dermatitis, anaphylaxis) or significant adverse responses to NSAID's or painkillers
- None smoker
- No medical prescribed diet (i.e., low carbohydrate or ketogenic diets)
- No recent musculoskeletal injury
- Free from chronic illness (e.g., cancer, diabetes, stomach issues)
- No current or previous stomach ulcers
- At the standard of readiness to exercise as indicated by PAR-Q

3.13 Blood Sampling

For the analysis of kidney function markers (Creatinine, Potassium, Sodium and Urea) and D_2O enrichment, participants provided venous blood samples at various time points, drawn from the antecubital vein into an ethylenediaminetetraacetic acid (EDTA) and serum separator tube (SST) vacutainer. Briefly, the phlebotomist explained the procedure to the participant, palpated the area to locate an appropriate vein, and then cleaned the site with an alcohol wipe. A single-use tourniquet was applied to the upper arm, and a 21G x ¾" x 12" blood collection kit (BD Vacutainer, NJ, USA) was inserted into the vein. Once a flashback was observed, indicating successful vein entry, a 10 mL EDTA/SST vacutainer was attached to the butterfly needle to begin sampling. The tourniquet was released during the filling process, and once the vacutainer was full, the needle was removed from the arm, and a clean gauze was applied to the site with pressure. All sharps were disposed of according to health and safety guidelines. Participants were then given a plaster to cover the wound after sampling. The filled vacutainers were inverted 6–8 times to ensure proper mixing of the anticoagulant. Samples were centrifuged for 15 minutes at 2500 RCF and 4°C. Following centrifugation, approximately 1 mL of plasma and serum supernatant was aliquoted into three 1.5 mL Eppendorf tubes and stored at −80°C.

3.14 Muscle Biopsy Procedure

On arrival (~8.30 am) to the muscle biopsy suite at Liverpool John Moores University, participants were asked to relax on a hospital bed whilst the biopsy site was prepared. Muscle biopsies were performed on the left leg of participants. First, the incision site (*Vastus Lateralis*) was shaved to ensure maximal sterility and washed with an alcohol swab and Hydrex surgical scrub (ECOLAB Ltd. Leeds, UK) following which, a sterile sheet was placed around the sterile site. To anaesthetise the biopsy site, bupivacaine hydrochloride (Astra Zenica. Luton, UK) was administered at a concentration of 5 $mg.mg^{-1}$ (approximately 1.5 ml administered). A disposable sterile scalpel was used to penetrate the skin and underlying muscle fascia, followed by the use of a Weil-Blakesley conchotome, a specialized instrument designed for extracting small tissue samples, to obtain the muscle biopsy.

3.15 Assessment of Peak Oxygen Uptake ($VO2_{peak}$)

Following calibration of the apparatus used for gas analysis as per manufacturer's guidelines, participants completed a health screening and readiness to exercise questionnaire. Upon completion of both questionnaires, participants performed a maximal running test to exhaustion on a motorised, bidirectional treadmill (H/P/Cosmos® Pulsar 3P, Traunstein, Germany). The test started with the slope and speed set to +1% and 9 km/h, respectively. Speed was then increased by 1km/h per min up to 16km/h, at which point the slope was increased by 1% per min until exhaustion. Breath-by-breath gas exchange values were recorded and averaged every 30s by Cortex Metalyzer 3B (Leipzig, Germany). The criteria for determining VO_{2peak} previously set were: (i) attainment of a VO_2 plateau despite increasing exercise intensity, (ii) a respiratory quotient exceeding 1.10, and (iii) a heart rate within 10 bpm of the age-predicted maximum. The measured VO_{2peak} was defined as the final and highest VO_2 plateau, which was clearly identifiable at the conclusion of the exercise test.

3.16 Muscular Function Tests

3.16.1 KE Isometric MVT

KE isometric MVT was assessed on a Human Norm isokinetic dynamometer (IKD) (Human Norm, CSMI, Massachusetts, USA) and analysed using AcqKnowledge data acquisition software (Biopac Systems Inc., Goleta, CA, USA). Participants were seated as per the manufacturer's guidelines, with the hip joint set at 85° (supine=180°) and non-extendable straps crossing the chest, waist and quadriceps to maximise the isolation of the target muscle group (include figure). The dynamometer's rotational axis was aligned with each participant's lateral femoral epicondyle by adjusting the seat height and length. The lever arm was securely fastened to the lower leg, positioning the bottom of the padded section 2 cm above the lateral malleolus and the knee angle was set to 90° using goniometry. Additionally, during all contractions, participants were instructed to fold their arms across their chest to avoid extraneous movement.

The warm-up comprised 10 submaximal isokinetic extensions ($60°\cdot s^{-1}$) performed with increasing intensity, i.e ~10% to ~80% of perceived maximal effort, followed by two repetitions at ~80% MVIC. Thereafter, participants performed three KE isometric MVT's with 60 s rests

between each contraction. During all MVT, participants were given visual feedback on a projector screen that showed the force-time trace. Participants received a 3 s verbal countdown before extending their knee as “fast and as hard as possible” on each contraction and consistent verbal encouragement was provided. Peak torque (Nm) was calculated for each trial by taking the maximum value during the 3 s contraction. The peak force of the three KE isometric MVT recorded was used for subsequent analysis.

3.16.2 Voluntary Activation (VA)

To measure quadriceps femoris muscle voluntary activation via the ITT, stimulation electrodes (95x9cm rectangle self-adhesive electrodes (Dura-Stick, Hannover, Germany) were used. The general procedure has been described elsewhere (Erskine et al., 2009, Erskine et al., 2010, Marshall et al., 2014). Briefly, participants were positioned on the IKD as described above (section 3.16.1). Electrodes were placed approximately 5cm above the knee joint across the *vastus medialis* (VM) and proximal to the acetabulofemoral joint across the *vastus lateralis* (VL). Participants were required to fully extend and contract the quadriceps to make the muscle body more apparent prior to electrode placement. To obtain the maximal twitch torque, electrical stimulation was applied to the VM and VL with a constant current stimulator (DS7AH, Digitimer, UK). The amplitude started with 50 mA to familiarise the participants to the stimulation and was gradually increased in 50 mA increments until a plateau in double torque was achieved. The stimulus was then increased an additional ~10% to achieve supramaximal stimulation. That setting was applied during all maximal contractions in the experimental session. The maximal doublet stimulation was then used following a 2-minute rest, to elicit resting maximal doublet torque in the resting state (control doublet). Participants then received a 3-s verbal countdown and performed a KE isometric MVT, during which a second (superimposed) doublet was applied at the point of maximal voluntary torque, which was visually determined as the point of torque plateau. This procedure was repeated 3 times with 2-minute rest between trials. A standard equation was then used to calculate voluntary activation: (*VA (%) = [1 – (superimposed doublet torque/control doublet torque)] x 100*.

3.16.3 Torque-Frequency Relationship

Participants were positioned on the IKD as described above (section 3.16.1) and electrodes were placed as described above (see section 3.16.2). The torque-frequency relationship was determined by percutaneous electrical stimulation of the quadriceps femoris muscle group at 1 Hz and 10, 15, 20, 30, 50 and 100 Hz for 1 s each in a random order and with 15 s rest between each stimulation. The stimulus intensity for 100 Hz stimulation was the amplitude necessary to elicit ~30% MVC KE torque at BV, and the same amplitude was used for the same test at all other time points. The absolute torque at each frequency was normalised to the torque at 100Hz for each time point.

Chapter 4

The Prevalence and Perceptions of Non-Steroidal Anti-Inflammatory Drug Use Among Ultra-Endurance Runners

This chapter investigates the prevalence and perceptions of non-steroidal anti-inflammatory drug (NSAID) use among ultra-endurance runners of varying performance levels. It details the study's aims, design, methodology, and key findings, offering insight into how and why these athletes use NSAIDs, their awareness of associated risks, and their openness to safer and potentially effective alternatives.

4.1 Abstract

Introduction: Ultra-endurance running imposes extreme physical demands often resulting in exercise-induced muscle damage (EIMD), pain, and inflammation. Many athletes use non-steroidal anti-inflammatory drugs (NSAIDs) despite safety concerns, questionable efficacy, and recent bans in some events. However, the prevalence, patterns, and cultural drivers of NSAID use across performance levels remain underexplored. **Methods:** This mixed-methods, cross-sectional survey included 166 ultra-endurance runners across five self-reported performance tiers. The survey, developed iteratively with expert input, captured NSAID usage during training and competition, motivations, perceived risks/benefits, information sources, and openness to alternatives. Quantitative data were analysed descriptively; qualitative responses underwent inductive thematic analysis. **Results:** Over half (53%) reported NSAID use, with ibuprofen most common. Usage patterns varied by calibre; Tier 5 (World-class) athletes described strategic use, while lower tiers reported more reactive use. Despite 77% being aware of potential harms, most often renal and gastrointestinal (GI), usage remained high due to perceived benefits. Female participants reported use often linked to menstrual or menopause-related discomfort. Information sources were largely informal, reflecting entrenched norms around pain management. **Conclusion:** Findings highlight the need for targeted behaviour change strategies, sex-informed approaches, and development of safer, evidence-based pain management alternatives in ultra-endurance sport.

4.2 Introduction

Ultra-endurance running events, commonly referred to as ultramarathons, encompass any race exceeding the traditional marathon distance of 42.195 km (26.2 miles), ranging from 50 km races to multi-day events covering hundreds of kilometres (Scheer et al., 2020). These races are conducted on diverse terrains, including trails, mountains, deserts, and roads. Popular worldwide ultra-endurance events include the Ultra-Trail du Mont-Blanc (UTMB), Comrades Marathon, Marathon des Sables, and Western States Endurance Run. Over the past decade, participation in ultramarathons has exponentially risen, accompanied by growing research interest in understanding the psychophysiological and biomechanical factors that dictate performance in these events (Berger et al., 2024).

Performance in ultramarathons is influenced by a complex interplay of psychophysiological and environmental factors, which may partly differ from those governing shorter endurance events. For example, aerobic capacity ($\dot{V}O_{2max}$) explains a fair component of endurance performance over distances up to marathon (Billat et al., 2001, Maughan and Leiper, 1983, Hagan et al., 1981) and fractional utilisation of $\dot{V}O_{2max}$ is an even stronger predicter performance in races up to marathon distance (Sjodin and Svedenhag, 1985). However, this predictive power declines as race length increases (Coates et al., 2021). In ultramarathons under 100 km, $\dot{V}O_{2max}$ retains moderate relevance but for races exceeding this distance, factors such as peripheral muscle fatigue, body composition, and running economy become increasingly important (Pastor et al., 2022). Moreover, the influence of aerobic capacity appears to vary by athlete calibre, with greater predictive value in faster competitors (Martinez-Navarro et al., 2022). These findings suggest that ultramarathon performance is constrained by the relative contribution of aerobic metabolism but also by musculoskeletal resilience and race-specific strategies and psychology.

Exercise-induced muscle damage (EIMD) is widely recognized as another primary factor mitigating performance in ultramarathons, particularly in events exceeding 100 km. Unlike gastrointestinal distress, which affects up to 80% of competitors (Tiller et al., 2019) but can often be managed mid-race, some markers of EIMD (e.g. ultra-structural disruption, inflammation, oedema) accumulate progressively and cannot be reversed over the course of a race. In ultra- endurance events with a significant downhill running component, grade-

specific biomechanical and structural alterations occur (reviewed in Bontemps et al. (2020)), which leads to acute and delayed neuromuscular alterations (reviewed in Owens et al. (2019)) and EIMD characterised by (i) structural alterations, such as Z-line disruption and sarcomere length non-uniformity; (ii) functional declines, including reduced strength and impaired running economy; (iii) symptomatic responses like delayed-onset muscle soreness; and (iv) systemic markers, such as elevated creatine kinase levels in the bloodstream (Giandolini et al., 2016, Malm et al., 2004). Surveys of ultramarathon runners highlight that EIMD (including neuromuscular fatigue) are the most frequently cited physiological barriers to performance (Tiller and Millet, 2025), surpassing both gastrointestinal issues and respiratory limitations. Given the prolonged recovery time required following extensive EIMD, understanding strategies to mitigate this process is crucial for improving both performance and post-race recovery.

To manage muscle soreness and nociceptive discomfort due to EIMD, many marathon and ultramarathon runners turn to pharmacological interventions, including nonsteroidal anti-inflammatory drugs (NSAIDs). Despite reports of use, the efficacy and safety of NSAIDs in this context remain contentious, particularly given recent bans in high-profile events such as UTMB, which has banned the use of ibuprofen in all events due to purported 'negative' health risks. Some authors suggest that acute kidney injury (AKI) associated with ultra-endurance performance correlates with NSAID use and therefore NSAIDs act as a significant risk factor for AKI (Hodgson et al., 2017). Indeed, NSAIDs may affect renal function in athletes by increasing water retention by arginine vasopressin in kidneys and reducing glomerular filtration rate (Baker et al., 2005). However, the subsequent effect on core temperature regulation and sweat loss in athletes is less clear (Emerson et al., 2021). Moreover, ibuprofen aggravates exercise-induced small intestinal injury and induces gut barrier dysfunction in healthy individuals (Van Wijck et al., 2012). The reliance on NSAIDs over alternative analgesics suggests a gap in both knowledge and available strategies for pain management in endurance athletes.

Athlete calibre may be an important factor influencing NSAID use in ultra-endurance running. Performance level can shape not only physiological demands but also competition strategies, recovery practices, and the perceived trade-offs between potential benefits and health risks

of pharmacological aids. Higher-calibre athletes may face greater performance pressures, competitive anxiety, and a "win at all costs" mentality, which have been linked to increased use of ergogenic substances despite known risks (Melzer et al., 2022). In this context, elite athletes may be more inclined to incorporate NSAIDs in a planned and strategic way to maintain performance, whereas recreational athletes may use them more reactively in response to discomfort. While NSAID prevalence has been reported in general endurance-running populations, no study to date has examined how usage patterns and motivations vary systematically by athlete calibre. Addressing this gap is important for developing targeted education and intervention strategies that reflect the differing pressures, beliefs, and practices across the performance spectrum.

Therefore, the primary aim of this study was to investigate the prevalence of NSAID use among ultra-endurance runners across five performance calibres from Recreationally Active to World-class, while also exploring perceptions of effectiveness, reasons for use, and openness to potentially safer alternatives through a combination of closed- and open-ended questions. Additionally, the study aimed to gain insight into the underlying beliefs and influences shaping NSAID use within the ultra-endurance running community.

4.3 Methods

4.3.1 Ethical Approval

This study was granted ethical approval by Liverpool John Moores University Research Ethics Committee (UREC reference: 24/SPS/063). Informed consent was provided by survey participants prior to beginning the survey. Potential participants could withdraw at any time without reason, and their data was removed and deleted.

4.3.2 Survey Design

A cross-sectional, mixed-methods survey, combining closed and open-ended questions was employed. The survey (Supplemental material 1) was designed through an iterative process by experts, to capture the performance calibre and training history of participants, prevalence and details of NSAID use, reasons for use, perceptions and practical insights surrounding NSAID use during training and competition, sources of education used for NSAID use and openness to alternatives to NSAIDs. Defining who is 'an expert' is subject to debate and there

are several methods for doing so (Mauksch et al., 2020) . We acknowledge suggestions by Kuchinke (1997), which state that part of being an expert is high commitment to the domain of expertise, which is in line with the general emphasis on deliberate practice in expert learning (Ericsson et al., 1993). To define how close the experts are to the topic, we propose objective closeness i.e. familiarity with the topic as a result of exploration by research (as proposed by Needham and de Loë (1990). The authors have demonstrable published research experience in endurance and ultra-endurance performance and as practitioners providing nutrition and physiological support to amateur and elite ultra-endurance athletes. The survey also underwent iterative piloting with a small group of ultra-endurance athletes to ensure face validity, clarity, and comprehension. Feedback was used to refine wording, improve logical flow, and minimise ambiguity. Internal consistency was not assessed statistically, as the survey did not employ multi-item scales intended to measure a single latent construct.

4.3.3 Participants

Participant recruitment took place between November 2024 to February 2025. Participants were eligible if they were aged 18 or older, had trained for or completed at least one ultra-running event (>42.195 km) in the past 12 months, and could describe their training and performance calibre using a provided framework. To define training and performance calibre of the athlete(s) supported by the survey respondents, a modified version of the participant classification framework proposed by McKay et al. (2021) was employed. In brief, this system uses training volume and performance metrics to classify a participant to one of the following:

- Tier 5: World Class • World medallists. • World and within 2% of • Top 3-20 in world rankings.
- Tier 4: International/Elite • Competing at the international level. • Top 4-300 in world rankings, with this on size and depth of competition in the event. • Achievement of within ~7% of world-record performance and/or world-leading performance. • Maximal, or within the given with intention to compete at
- Tier 3: Level • Competing at the national level. • Competing in national and/or state leagues/tournaments. • Achievement of within ~20% of world- record performance and/or world-leading performance. • Completing structured and periodized training

and developing towards (within ~20%) of maximal or nearly maximal norms within the given sport. • Developing proficiency in skills required to perform sport.

- Tier 2: Trained/Developmental • Local-level representation. • Regularly training ~3 times per week. • Identify with a specific sport. • Training with a purpose to compete. • Limited skill development.
- Tier 1: Recreationally Active • Meet World Health Organisation minimum activity aged 18-64 years old completing at least 150 to 300 min moderate-intensity activity or 75-150 min of vigorous intensity activity a week, plus muscle- strengthening activities 2 or more days a week. • May participate in multiple sports/forms of activity.

The sample size was determined based on the principle of information power, which suggests that the adequacy of a sample is dependent on the richness of the data and its relevance to the study aims rather than a predetermined number (Braun and Clarke, 2016). Data collection ceased when the research team determined that sufficient responses had been gathered to meaningfully address the research questions. This decision was informed by ongoing assessment of data saturation, ensuring that additional responses were not yielding new insights relevant to the study's objectives.

For the quantitative component of our investigation, no *a priori* sample size calculation was conducted due to the exploratory nature of the study, the absence of prior data on NSAID use by performance tier, and the very small global population of athletes in the highest tier. Instead, recruitment aimed to maximise response rates across all tiers to permit meaningful descriptive comparisons.

4.3.4 Data Collection and Handling

Prospective respondents were invited to participate in the current survey via social media platforms (X, Instagram and LinkedIn) and contacted by email, where this information was publicly available. Invitations also encouraged prospective respondents to share the invitation to participate within their network or institution to maximise recruitment coverage. Information about the study was also shared through podcasts that targeted the ultra-endurance community, particularly those with guest speakers with a wide-reaching network of listeners. Survey responses were collected via Jisc Online Surveys tool (Jisc v.3, Bristol, UK)

and data exported to Microsoft Excel (v.16.7) for analysis. The survey was conducted and distributed in English, with data obtained from participants across multiple countries. Figures were produced in GraphPad prism (v.9 GraphPad Software, Boston, Massachusetts USA). Due to the sensitive nature of the survey, respondents were not required to complete all questions of the survey. As such, the number of respondents per questions is explicitly stated in the results section.

4.3.5 Thematic Analysis

We conducted an inductive thematic analysis of open-ended survey responses following the six-step approach outlined by Braun and Clarke (2006). First, we familiarized ourselves with the data through repeated reading and initial note-taking. Next, we generated codes across the dataset, capturing key features of the data relevant to the research question. These codes were then collated into potential themes, which were refined and reviewed to ensure they accurately reflected the dataset. Themes were defined and named to best represent the patterns identified, and a final analysis was conducted to produce a coherent narrative supported by illustrative data extracts.

4.4 Results

4.4.1 Participant Characteristics

A total of 166 participants completed the survey, with nationality distribution as follows: UK (39%), USA (27%), Canada (6%), Ireland (5%), Hungary (4%), Australia (3%), Germany (2%), Italy (2%), France (2%), and the Netherlands (2%). Additionally, 0.6 % of participants were from Argentina, Croatia, Finland, Bulgaria, Latvia, Malta, Norway, Poland, Portugal, South Africa, Switzerland, and Ecuador. Table 1 displays the general characteristics of participants, as well as self-reported years competing in ultra-endurance racing, races per year and training volume in the 3 months leading up to 'A' race (priority race in the athlete's annual race calendar).

Table 4.1. General Characteristics of Participants

	Participants (*n* = 166)
Sex: Male *(n, %)*	101 (61%)
Female *(n, %)*	65 (39%)
Age (Years)	41.1 ± 9.3
Weight (kg)	71.5 ± 13.4
Height (cm)	175.1 ± 9.3
Years in Ultra-Endurance Racing	6.5 ± 4.9
Races per Year (50km+)	3.1 ± 1.6
Training Volume (h/week) *	12.8 ± 6.4

*Note: The values are the mean ± S.D * Training volume in the 3 months leading up to 'A' race.*

Previous research highlights the widespread use of analgesics and NSAIDs in professional and elite sports, as well as among high-performance amateur athletes (Leyk et al., 2023). However, NSAID consumption across different performance levels has yet to be specifically categorised in ultra- endurance running. Therefore, to characterise NSAID use in the context of performance calibre, participants were asked to self-select which tier best describes their performance calibre. The participant classification framework outlined by McKay et al. (2021) and as described in Methods was adopted (data presented in Figure 4.1).

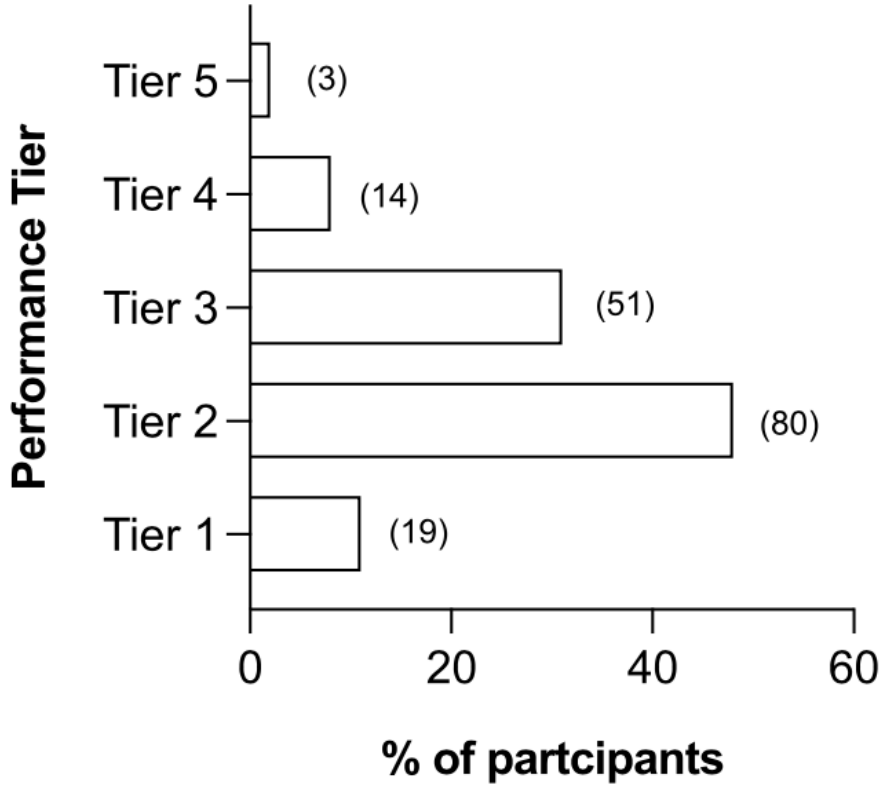

Figure 4.1. Distribution of survey respondents across performance tiers. The bar chart illustrates the percentage and number (n) of athletes categorised by their self-assessed performance level, following the framework from McKay et al. (2021).

4.4.2 NSAID Consumption

Participants were first informed that questions regarding NSAID use specifically referred to oral forms (e.g., pills, capsules, soft gel capsules) and events where the use of NSAIDs is permitted. A non-exhaustive reference list and guidance for identifying NSAIDs were provided to participants to assist in identifying NSAID use during training and/or competition. Of the 166 participants in the study, 53% (n = 89) reported taking NSAIDs in training, competition or both. Among participants who reported NSAID use, 85 chose to provide further context for their use; 78% (n = 66) reported using them to 'mask an existing injury', while 56% (n = 48) reported using them to 'prevent performance deterioration' during training or competition. Participants were allowed to select either or both responses. Among NSAID users whose primary reason for use was alleviating discomfort rather than masking injury, 45% (n = 38) reported using NSAIDs during training, 61% (n = 52) during recovery and 59% (n = 50) during

competition. Participants were allowed to select multiple responses. Subsequently, participants were offered to describe the regularity of their NSAID use in training, recovery or competition to alleviate discomfort. Responses (n = 88) are summarised in Table 4.2.

Table 4.2. *Frequency of NSAID use for training, competition, or recovery in ult*ra-endurance runners.

Note: *This refers to NSAID use intended to alleviate discomfort associated with the session or event, reduce perceived performance deterioration, or improve performance, and specifically excludes use for masking existing injuries.*

	Training (n = 89)	**Recovery (n = 89)**	**Competition (n = 89)**
***Always** % (n)*	0 % (0)	0 % (0)	5 % (4)
***Very often** % (n)*	1 % (1)	6 % (5)	7 % (6)
***Often** % (n)*	5 % (4)	8 % (7)	6 % (5)
***Sometimes** % (n)*	27 % (24)	33 % (29)	29 % (25)
***Rarely** % (n)*	67 % (59)	-3 % (47)	54 % (47)

Participants were asked to name NSAIDs consumed during training, recovery and competition to alleviate discomfort, reduce performance deterioration, or enhance performance, excluding use for masking existing injuries. Ibuprofen was the most popular NSAID consumed, with 84% (n = 71) participants reporting use, followed by 11% (n = 9) for naproxen, 8% (n = 7) for diclofenac, 4% (n = 3) for aspirin, 1% (n = 1) for celecoxib and 8% (n = 7) for other. When asked whether their NSAID intake during training and/or competition was planned (similar to event nutrition), or unplanned (taken only when deemed necessary), 14% (n = 9) of participants reported planned use, whereas 71% (n = 48) of participants reported unplanned use and 15% (n = 10) reported both. When examining NSAID usage across performance tiers, Tiers 1 through to 4 reported the highest percentage of unplanned use. In contrast, all participants in Tier 5 reported both planned and unplanned NSAID intake, with planned consumption at specific time points and additional consumption as the need arose. Figure 4. 2 shows the distribution of NSAID intake across performance tiers. Participants who reported planned NSAID use were asked about its distribution during an event.

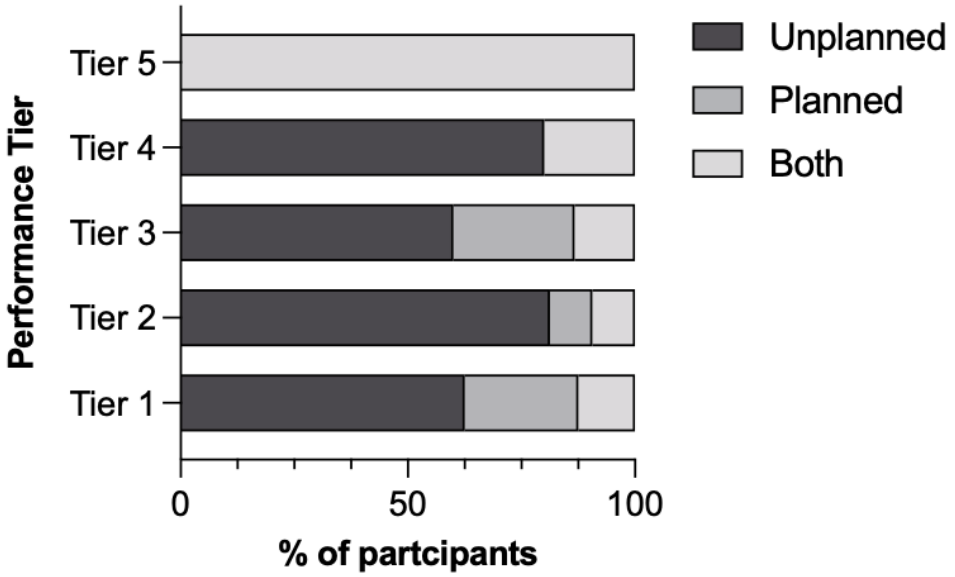

Figure 4.2. Distribution of NSAID intake across performance tiers.

Twenty-five participants who used NSAIDs during competition were able to articulate whether they had a strategy towards their NSAID use. Twenty-four percent (n = 6) of participants who used NSAIDs during ultra-endurance running events reported intake both before or at the start of the event. In addition, another twenty-four percent (n = 6) reported intake at specific time points during the race. An additional 16% (n = 4) indicated NSAID use towards the latter half/end of the event. A further twelve percent (n = 3) reported using them as needed due to acute injury, 8% (n = 2) of participants used them halfway through the event, and 16% (n = 4) of participants reported other varying reasons. Responses are reported in Table 4.3.

Table 4.3. Themes in responses regarding NSAID intake during ultra-endurance running events.

	Participants (n=25)
Only before/at the start of event *% (n)*	24% (6)
Only at specific time points *% (n)*	24% (6)
Only halfway through the event *% (n)*	8% (2)
Only towards the end/finish of event *% (n)*	16% (4)
Only if the need arises (acute injury) during event *% (n)*	12% (3)
Other *% (n)*	16% (4)

Note: *The sample size (n = 25) reflects the number of respondents to this specific question*.

4.4.3 NSAID Information and Awareness of Adverse Drug Reactions

When asked about sources of information regarding NSAIDs, 41% (n = 64 of 155 respondents) of participants cited websites as their primary source. This was followed by a similar proportion of participants citing podcasts (33%, n = 51) and doctors (31%, n = 48) as their source of information. Interestingly, only 5% (n = 8) of participants reported obtaining NSAID information from a nutritionist/dietician. The remaining responses are reported in Figure 4.3. Tier 1 participants identified doctors as their primary source of information regarding NSAIDs (19%), while Tier 4 participants reported both doctors and coaches (27%) as their main sources. In Tier 2, websites were cited as their primary source of information, whereas in Tier 3, participants (18%) favoured podcasts. Finally, Tier 5 participants evenly distributed their sources of information across doctors, academic literature, academic consultations, and websites, with each source accounting for 25%.

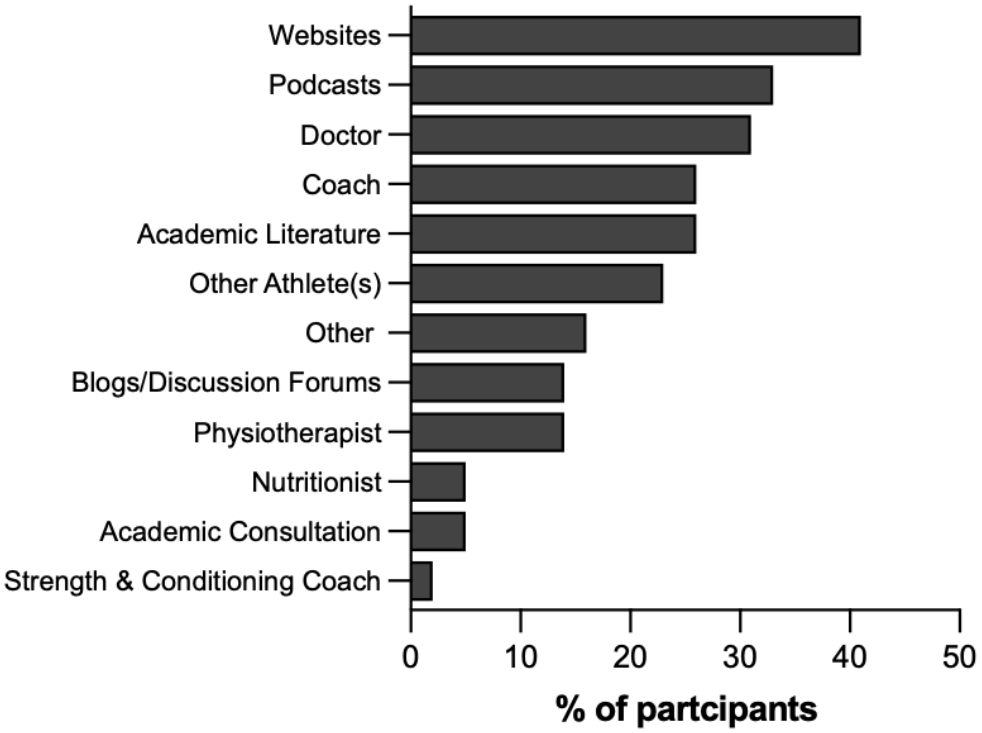

Figure 4.3. Sources of NSAID information reports by participants.

Participants were asked if they were aware of the potential adverse effects associated with the use of NSAIDs. A total of 77% (n = 127) of participants stated they were aware, while 6% (n = 10) of participants were not aware, and 17% (n = 29) were unsure. Awareness of the

potential adverse effects of NSAIDs exceeded 50% across all performance tiers, indicating a generally high level of awareness regardless of performance calibre. Notably, Tier 1 had the highest proportion of participants who were either unaware (15%) or unsure (25%), while participants in Tier 5 were the only group to report 100% awareness (see Figure 4.4 a). However, the small sample size in Tier 5 should be considered when interpreting these results. Among participants aware of the potential side effects, the most reported side effect was renal (kidney) issues, with 80% (n = 101) of participants reporting awareness of it. Gastrointestinal issues were reported by 31% (n = 39) of participants and 7% (n = 9) mentioned rhabdomyolysis as a possible adverse effect. Responses are reported in Figure 4.4 b).

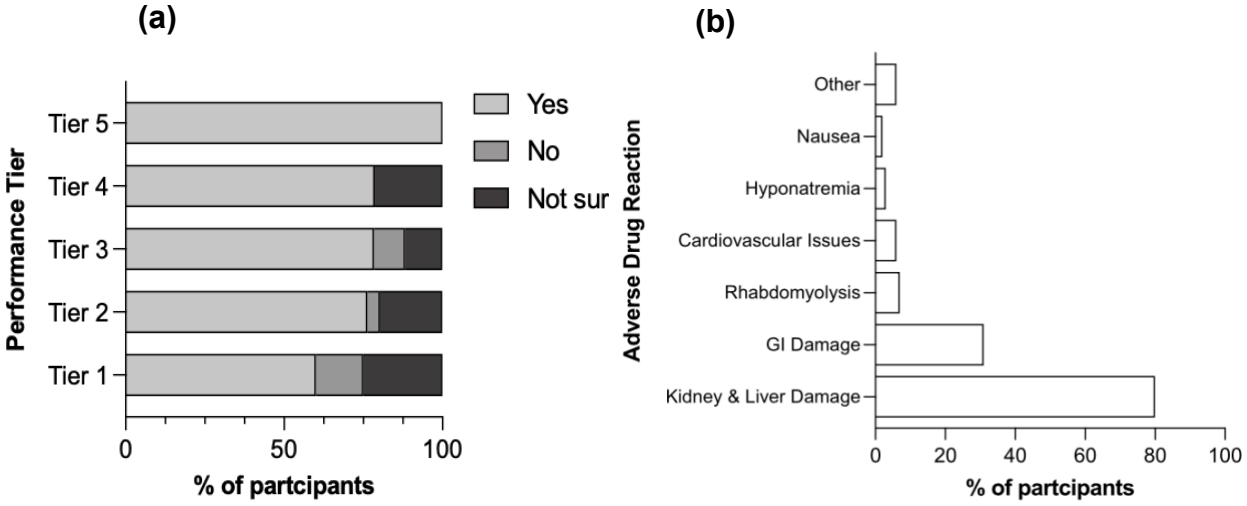

Figure 4.4. (a) Awareness of adverse effects associated with NSAID use across performance calibre. (b) Themes related to awareness of adverse drug reactions to NSAIDs.

4.4.4 Considerations and Attitudes Towards NSAID Use

The closed-ended questions in this survey provided valuable data on performance level, NSAID consumption, and awareness of adverse effects. However, to gain richer insights into participants' considerations, perceptions, and attitudes towards NSAID use, we also included open-ended questions in this section. Participants were asked about their reasons for considering NSAID use (n = 164 responses). The most common reasons reported were to reduce “muscle pain” or “damage” (37%, n = 60) and to reduce “inflammation” (32%, n = 52). Other reasons cited were to reduce “soft tissue pain” (20%, n = 33), to reduce “perception of effort” (8%, n = 13) and to reduce “performance deterioration” (10%, n = 17). Additionally,

45% (n = 73) of participants reported they would not consider using NSAIDs, similar to when asked about NSAID use during training or competition. Participants who selected "Other" (10%, n = 17) and those who indicated they would not consider using NSAIDs were asked to provide reasons for their responses. Similarly, some participants that would not consider using NSAIDs also provided open ended text responses regarding their considerations for avoiding NSAID use. Illustrative extracts and emergent themes are presented in Table 4.4.

Table 4.4. Considerations for avoiding NSAID use as determined by open-ended question responses. Raw data included illustrative extracts from open-ended question responses relevant to the theme.

Illustrative Extracts	Emergent Theme
"Too dangerous for my heart and kidneys." *"I would not want to delay my recovery, or have GI distress, or kidney issues."*	Health Risks and Side Effects
"I prefer to do things naturally if at all possible. Sleep, hydration, nutrition." *"I don't eat any chemicals unless it's unavoidable."*	Preference for Natural or Alternative Approaches
"Using them creates an expectation of less discomfort/reduces my tolerance for discomfort". *"I also don't want to develop a tolerance to reduce my body's ability to adapt to exercise."*	Concerns About Pain Tolerance and Adaptation
"Studies show no positive performance impact on endurance due to NSAIDs during runs with high risk of negative effects" *"I'm not aware of any benefits of using NSAIDs so I wouldn't use them"*	Lack of Perceived Benefit
"I prefer to avoid medications in general and feel that the risks do not outweigh the benefits." *"If I were to use medication to mask pain, I would choose a med that acts only on pain signalling/perception rather than inflammatory pathways."*	General Avoidance of Medications
"Because the point of running ultra-endurance events is to "endure". That means any sort of drug taken to reduce the amount of pain is against the idea of why you test yourself in an endurance race. I run to test my limits. I don't race to win" *"View their use as dangerous, and their systemic use as cheating"*	Violation of Sporting Culture and Values

To gain a deeper understanding of athlete's attitudes towards NSAID use, participants were provided with several statements and asked to choose the response that most accurately reflected their views (n = 165 responses). A substantial proportion (39%, n = 63) of participants strongly disagreed that the benefits of NSAID use outweigh any negative effects, while 14% (n = 22) agreed. Regarding perceived competitive disadvantage, the majority of participants (35%, n = 56) disagreed that not using NSAIDs would put them at a disadvantage compared to competitors, while 33% (n = 52) were neutral, and only 11% (n = 17) agreed. Conversely, 30% (n = 48) of participants agreed that they could perform just as well without NSAIDs as with them, while 16% (n = 26) disagreed. When asked whether NSAIDs improve competitive performance, 40% (n = 64) of participants were neutral, while 24% (n = 39) of participants agreed, and 19% (n = 31) disagreed. All statements and corresponding responses are reported in Table 4.5. A similar proportion of participants across performance tiers responded consistently to each statement. Notably, the highest percentage of participants in Tier 5 believed that the benefits of using NSAIDs outweigh the negative effects and that NSAIDs enhance competitive performance. Across Tiers 1 to 4, more than 50% of participants disagreed with the statements that they would be at a competitive disadvantage if they did not use NSAIDs and that NSAIDs enhance competitive performance. Thirty percent or more of participants across performance Tiers 1 to 4 remained neutral on the statement that the benefits of using NSAIDs for performance outweigh any negative effects, suggesting uncertainty regarding the overall impact of NSAIDs on performance. This may reflect mixed perceptions of their effectiveness or concerns about potential side effects. Lastly, participants were asked if they would consider using scientifically proven alternative methods to manage discomfort and pain during training and racing, regardless of their current or past NSAID use, provided these methods had minimal side effects. In response, 82% (n = 136) of participants stated they would be open to alternative methods, 5% (n = 8) reported they would not, and 13% (n = 21) were uncertain.

.

Table 4.5. Attitudes toward NSAID use and impact on performance.

	Strongly Disagree *% (n)*	**Disagree** *% (n)*	**Neutral** *% (n)*	**Agree** *% (n)*	**Strongly Agree** *% (n)*
'The benefit of using NSIADs for my performance outweighs any negative effects'	39% (65)	20% (33)	23% (38)	14% (23)	4% (6)
'I believe that I would be at a disadvantage to other competitors If I didn't use NSAIDs'	20% (33)	36% (59)	32% (53)	10% (17)	2% (4)
'I believe I could perform just as well without using NSAIDs as I could with using them'	2% (3)	16% (26)	29% (48)	32% (52)	22% (36)
'I believe that NSAIDs improve competitive performance'	12% (19)	20% (33)	39% (65)	25% (41)	4% (7)

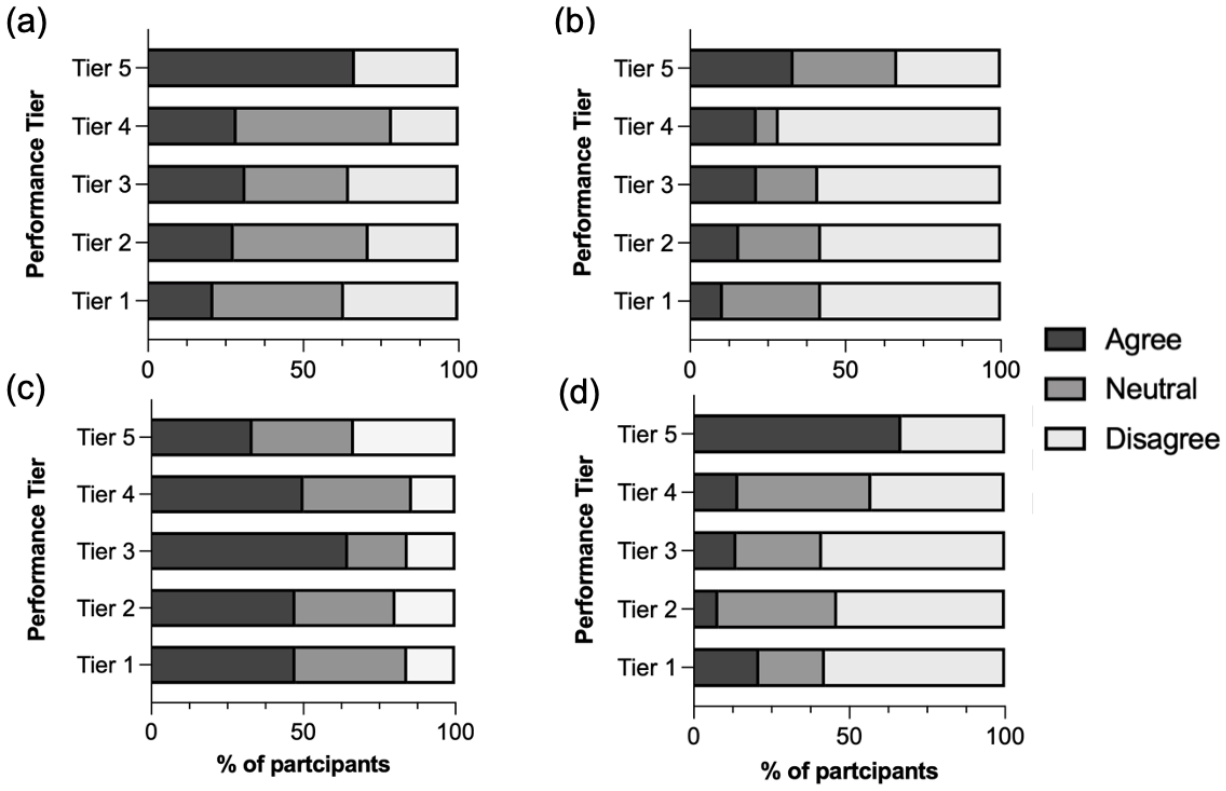

Figure 4.5. Percentage of participants within performance tiers responding to the above statements: (a) "The benefit of using NSAIDs for my performance outweighs any negative

effects", (b) "I believe I would be at a disadvantage to other competitors if I didn't use NSAIDs", (c) "I believe I could perform just as well without NSAIDs as I could with using them", and (d) "I believe that NSAIDs improve competitive performance."

4.4.5 Consideration of NSAID Use Amongst Female Athletes

Whilst sex-specific differences in NSAID use was not a primary aim of this survey, our results revealed themes that are noteworthy. Among male participants, 52% (n = 53) reported using NSAIDs, with 56% (n = 36) of females reporting NSAID use. Participants were invited to share any additional information regarding their own NSAID use that might be relevant for future research. A large proportion of participants reported using NSAIDs exclusively for menstrual pain:

"My NSAID use is purely related to severe period pain. I will only take NSAIDs if I have severe period pain which would otherwise impair my performance"

Another female-specific reason for NSAID use reported by participants was to alleviate discomfort related to menopause:

"Through peri-menopause NSAIDs have helped me with joint and hip discomfort, not injury related but it does help my performance".

These findings suggest that NSAID use among female participants may be influenced not only by exercise-related factors but also by menstrual and menopause-related discomfort, highlighting the need for further research into sex-specific reasons for NSAID use and targeted interventions for women.

4.5 Discussion

The primary aim of this study was to investigate the prevalence of NSAID use among ultra-endurance runners across five performance calibres from recreational to World-class, while also exploring perceptions of effectiveness, reasons for use, and openness to potentially safer alternatives through a combination of closed- and open-ended questions. Additionally, the study aimed to gain insight into the underlying beliefs and influences shaping NSAID use within the ultra-endurance running community.

To our knowledge, this is the first study to comprehensively examine NSAID use in ultra-endurance runners across defined performance levels, offering new insights into usage patterns, motivations, and beliefs that have been largely overlooked in previous research (Joslin et al., 2013, Pannone and Abbott, 2024, Gorski et al., 2011). The high prevalence of NSAID use reported here (53%) aligns with previous studies reporting rates between 48-61% in endurance runners and ultramarathon participants (Martínez et al., 2017, Hoffman and Fogard, 2011). Ibuprofen was the most frequently consumed NSAID (84%), followed by naproxen (11%), possibly reflecting their over-the-counter availability in countries such as the UK and USA, which accounted for most participants in this survey. A novel aspect of our findings is that while all participants in Tier 5 (World-class) report both planned and unplanned NSAID use, consuming them at specific time points and as needed for acute injuries, NSAID consumption in the lower tiers was predominantly unplanned. Whilst the sample of Tier 5 athletes was small due to the very small number of athletes in this category worldwide, the results may suggest that higher tier competitive athletes incorporate NSAIDs into their competition strategies in a more structured manner, akin to nutrition planning, whereas lower-calibre athletes tend to use NSAIDs more reactively in response to emerging discomfort. Within the constraints of small subgroup sizes and our descriptive design, a greater proportion of Tier 5 respondents endorsed statements that the benefits of NSAID use outweigh potential adverse effects and that NSAIDs enhance competitive performance relative to lower tiers. However, these comparisons are descriptive only and should be interpreted with caution. This finding may reflect a “win at all costs” mentality and the performance-driven beliefs often observed in elite sport (Watson and White, 2007). NSAID use was similar between male and female participants (52% and 56%, respectively), with many females reporting menstrual and menopause-related pain as primary reasons for use in open-ended survey responses. These novel insights highlight the importance of considering sex-specific factors when evaluating NSAID consumption in ultra-endurance sports and opens new avenues for research in female ultra-endurance athletes.

It could be speculated that a lack of knowledge of possible side effects of NSAIDs during exercise could account for the high frequency of use by athletes. However, our data suggest this not to be the case since 77% of participants acknowledged associated risks, which represents a substantial increase in awareness compared with other reports (Gorski et al.,

2011, Warner et al., 2002, Thorpe et al., 2022). The high prevalence of NSAID use in the face of knowing the associated risks suggests that perceived benefits, particularly in reducing muscle pain or damage (37%) and inflammation (32%), may outweigh concerns for many ultra-endurance runners. These findings are supported by previous research, in which 62% of professional triathletes who took NSAIDs immediately before or during a race, expected the drug to prevent pain during the race (Gorski et al., 2011). Holgado and colleagues' suggestion that NSAID use may be driven by the perceived ergogenic benefits, despite an awareness of the risks involved, also supports our perspective (Holgado et al., 2018). The most frequently reported reason for NSAID use in the present study was to mask an existing injury (78%), followed by preventing performance deterioration (56%). The tendency of athletes with minor injuries to continue training and competing rather than allowing for full recovery has been identified as a key factor contributing to the high prevalence of NSAID use in other reports and may lend further support to our data (Warden, 2009, Corrigan and Kazlauskas, 2003).

A possible explanation for more than half of the athletes in our survey reporting NSAID use could be the absence of well-documented alternatives to manage nociceptive discomfort (such as muscle soreness), or the potential concerns associated with alternative options. As an example, cannabidiol (CBD) is permitted for use by WADA and has demonstrated anti-inflammatory and analgesic properties, suggesting its potential as an alternative to NSAIDs (Machado Bergamaschi et al., 2011, Mechoulam and Hanuš, 2002). Within elite sport, CBD use has increased since its removal from the World Anti-Doping Agency (WADA) prohibited list (Kasper et al., 2020), but concerns remain given that CBD is the only cannabinoid permitted for use and all other cannabinoids (of which there are ≥140) are prohibited. Most commercially available CBD products are broad spectrum and therefore often contain other cannabinoids than CBD with some studies suggesting that commercially available products often contain significantly higher amounts of THC than stated on the label, often exceeding the legal threshold and including other prohibited cannabinoids (Gurley et al., 2020). Therefore, the present study highlights an innovation gap in the management of discomfort and pain in sport, underscoring the need for validated alternative methods with no adverse effects, an area of high interest, as 82% of participants in our study expressed a willingness to try such approaches.

A further theme which arose from our data as a factor influencing NSAID use is the reliance on fellow athletes for information, with 23% of participants reporting this as their primary source of information, consistent with previous research (Overbye, 2021). This may reflect broader cultural norms within sport, where performance, self-management, and peer advice shape attitudes toward analgesic and NSAID use (Read et al., 2023). Risk-sharing cultures often reinforce such behaviours, where self-administration and knowledge exchange among peers foster a sense of autonomy and expertise (Malcolm, 2009). In this context, athletes often act as 'mini experts', relying on personal experience and anecdotal advice to make independent decisions about NSAID use (Roderick, 2006). The self-administration of these substances poses risks and may be influenced by the subcultural norms and traditions within the specific sporting environment (Overbye, 2021).

Building on this, understanding and addressing the cultural, behavioural and psychological factors that influence athlete's decision-making is essential if safer alternatives to pain management are to be implemented. Although NSAID use does not constitute a violation of anti-doping regulations in many competitions (with exceptions such as UTMB regulations), athletes frequently report using these substances for performance reasons, as demonstrated in the present study. Melzer et al. (2022) have shown that athlete's attitudes towards ergogenic substances are often influenced by their desire to minimise pain and maintain performance, particularly in high pressure or competitive environments. Athletes experiencing elevated levels of competitive anxiety or adhering to a "win at all costs" mentality may be more inclined to use NSAIDs, viewing them as a means to maintain or enhance performance despite the known associated risks (Melzer et al., 2022). The tendency for athletes to use NSAIDs when the perceived benefits are high and the risk of detection is low (Melzer et al., 2022) is reflected in our findings, where over 60% of participants across all performance levels agreed or remained neutral about the benefits of NSAIDs outweighing any negative effects (Figure 5a). Our observations may be explained by the Low-Cost Hypothesis and Rational Choice Theory (Clarke and Cornish, 2017, Diekmann and Preisendörfer, 2003). According to the Low-Cost Hypothesis, individuals are more likely to engage in a given behaviour when the perceived cost or risk is minimal. The Rational Choice Theory further posits that an athlete's decision-making involves weighing potential benefits against associated costs. In this context, the perceived benefits of pain relief and performance

enhancement likely outweigh the perceived risks. Consequently, interventions aimed at reducing NSAID use should extend beyond knowledge-based approaches and incorporate targeted behaviour change strategies that address risk perception, decision-making processes, and the cultural acceptance of NSAID use in sports.

4.6 Limitations

This study provides novel and important insights into NSAID use among ultra-endurance runners, however several limitations should be acknowledged. Firstly, the cross-sectional survey design limits causal inference. While associations between NSAID use and factors such as performance tier, sex, and perceived benefits were observed, we cannot determine directionality or causality from this data.

Second, the survey relied on self-reported data, which may be subject to recall bias or social desirability bias. For instance, underreporting or overreporting of NSAID use, particularly in relation to competition rules or health concerns, cannot be excluded. Whilst the anonymous nature of the survey may reduce this bias, it must be acknowledged.

Third, the distribution of participants across performance tiers was uneven, with fewer in Tier 5 (World-class) and 4 (International/Elite). Whilst it could be argued that this limits generalisability to all elite and world class athletes it should be acknowledged that such athletes represent a considerably smaller population to sample. For example, Tier 5 athletes are World medallists, World record holders and athletes achieving within 2% of world-record performance and/or world-leading performance and those in Top 3-20 in world rankings. As we report data for 3 athletes in this category, it represents approximately 15% of the athletes who meet these criteria. Likewise, while the sample was international, there was higher representation from English-speaking countries, which may reflect regional attitudes, regulations, and access to NSAIDs that are not globally representative.

Fourth, although we explored reasons for NSAID use, the survey did not capture data on specific dosages, chronicity of use, or co-ingestion with other substances (e.g., caffeine, supplements), which may influence outcomes and health risks. Additionally, menstrual and menopause-related NSAID use emerged as a significant theme, but the survey was not designed to comprehensively explore sex-specific motivations or hormonal influences on pain

management. Future studies should also consider incorporating pharmacokinetic assessments and wearable monitoring technologies to better understand the physiological impact of NSAID use in ultra-endurance settings.

Fifth, while thematic analysis enriched the findings, qualitative responses were brief and context-limited, and further qualitative studies involving semi-structured interviews and focus groups may better capture the nuanced beliefs, behaviours, and cultural drivers surrounding NSAID use in ultra-endurance sport. Due to the sensitive nature of the survey and guidance from the authors local ethics committee, respondents were not obliged to answer all questions. Taken together, interpretations of these cultural and contextual factors in the present study should be viewed as speculative and theoretically informed, drawing on existing literature rather than derived from in-depth ethnographic or cultural analysis.

Finally, as the recruitment materials referenced NSAID use in the study title, there is a possibility of self-selection bias, whereby individuals with experience or strong views on NSAID use may have been more likely to participate. This may have influenced the prevalence estimates reported, although the inclusion criteria explicitly invited participants irrespective of prior NSAID use.

4.7 Conclusion

Taken together, this study highlights the high prevalence of NSAID use among ultra-endurance runners across performance levels, driven by pain management, injury masking, and perceived performance benefits, despite widespread awareness of associated risks. Patterns of use varied by calibre, with elite athletes employing more strategic use and lower-tier athletes using NSAIDs reactively. The influence of peer advice, sex-specific factors, and cultural norms underscores the complexity of decision-making around NSAID use. Critically, our findings reveal an innovation gap in safe, evidence-based alternatives with 82% of participants expressing openness to such options. Addressing this gap will require more than education alone and should incorporate targeted behaviour change strategies that consider risk perception, cultural influences, and athlete motivations are essential to support healthier and more sustainable approaches to pain management in sport

Transition to Chapter 5

A growing reliance on NSAIDs among ultra-endurance runners, despite widespread awareness of their risks, underscores a clear gap in safe and effective strategies for managing pain, inflammation, and muscle stress. The behavioural patterns identified in this chapter highlight not only the cultural normalisation of NSAID use but also the strong demand for alternatives that can support recovery without compromising athlete health. To address this need, the next chapter shifts from athlete behaviour to mechanistic investigation, exploring the biological actions of palmitoylethanolamide (PEA) in skeletal muscle. By examining how PEA influences myogenesis and inflammatory signalling at the cellular level, Chapter 5 provides foundational evidence that may inform the development of safer, targeted interventions for muscle recovery and performance

Chapter 5

Palmitoylethanolamide (PEA) Regulates Cell Cyle Progression and Promotes an Anti-Inflammatory Transcriptomic Signature in C2C12 Skeletal Muscle Cells

This chapter explores the effects of PEA on terminally differentiated C2C12 skeletal muscle myotubes. As the direct impact of PEA on skeletal muscle remains largely unknown, this study aims to investigate its influence on myogenesis and employs transcriptomic analysis to investigate changes in gene expression following PEA treatment. The findings provide initial insight into the potential mechanisms through which PEA may act in skeletal muscle.

5.1 Abstract

Introduction: Palmitoylethanolamide (PEA) is an endogenous lipid mediator with immunomodulatory actions, yet its effects in skeletal muscle remain poorly defined. We examined whether PEA influences myogenesis and profiled the acute transcriptomic response of differentiated C2C12 myotubes to 10 µM PEA. **Methods:** C2C12 murine myoblasts were cultured and differentiated into myotubes to investigate the effects of PEA. Dose-tolerability was established using metabolic activity (MTT) and propidium iodide (PI) exclusion assays across concentrations from 1–100 µM. Based on these results, 10 µM PEA was selected for subsequent experiments. On day 7 of differentiation, myotubes were treated with PEA or vehicle control (VC) for 24hr, followed by RNA extraction and quality assessment prior to library preparation and next-generation sequencing on an Illumina platform. Differential expression analysis was conducted using DESeq2, with gene ontology and protein–protein interaction networks assessed via STRING and Cytoscape. Complementary analyses included immunofluorescence staining of myotube morphology, cell cycle progression via PI staining and flow cytometry, and imaging with fluorescence microscopy. Statistical analyses were performed in GraphPad Prism, with significance set at $\alpha \leq 0.05$. **Results:** PEA decreased myotube number (90.3 ± 10.6 vs 112.6 ± 10.1 control) while increasing nuclear fusion index (37.8 ± 5.7% vs 30.7 ± 3.2%); myotube area was unchanged. In myoblasts, 24 h PEA increased G_0/G_1 (48.2 ± 1.2% vs 42.3 ± 1.9%) and reduced S-phase (21.7 ± 1.2% vs 25.5 ± 1.2%), consistent with G_1 arrest. RNA sequencing identified 1,952 differentially expressed genes enriched for cytokine–receptor interactions and inflammatory signalling. PEA downregulated NF-κB target cytokines while upregulating interferon-related and chemokine genes, indicating an anti-inflammatory/immune-priming profile. N-acylethanolamine acid amidase was highly expressed and induced, whereas fatty acid amide hydrolase remained low and unchanged, suggesting muscle-specific reliance on NAAA metabolism. **Conclusion:** These data show that PEA biases skeletal muscle toward a less proliferative but more fused and inflammation-resolving phenotype, with transcriptional reprogramming of immune pathways and preferential NAAA engagement. These findings motivate *in vivo* studies to test whether such actions benefit muscle regeneration, adaptation, or anti-atrophy interventions.

5.2 Introduction

Palmitoylethanolamide (PEA) is an endogenous fatty acid amide with well-documented anti-inflammatory, analgesic, and neuroprotective properties (Skaper et al., 2015, Petrosino and Di Marzo, 2017b). Endogenous PEA is biosynthesized from the membrane phospholipid N-palmitoyl-phosphatidylethanolamine (NAPE), most prominently via hydrolysis by N-acyl phosphatidylethanolamine-specific phospholipase D (NAPE-PLD) in neuronal, glial, and immune cells (Iannotti et al., 2016). Following synthesis, PEA is degraded by fatty acid amide hydrolase (FAAH) or N-acylethanolamine-hydrolysing acid amidase (NAAA). PEA acts through multiple signalling pathways, including direct activation of GPR55 and PPAR-α, and indirect modulation of TRPV1 channels and CB2 receptors via PPAR-α-dependent mechanisms (Di Cesare Mannelli et al., 2013b). PEA may also enhance endocannabinoid signalling by elevating anandamide (AEA) and 2-arachidonoylglycerol (2-AG), contributing to the so-called “entourage effect” (De Petrocellis et al., 2001). While these mechanisms are well described in neural and immune cells, their presence and relevance in other tissues remain unclear.

Through activation of these signalling networks, PEA has been shown to modulate inflammatory and nociceptive pathways, making it a promising candidate for conditions characterised by pain, inflammation, and neurodegeneration. Given the close interplay between inflammation and skeletal muscle function, PEA has attracted attention for its potential role in muscle health, particularly in the context of pain, inflammation, degeneration, and exercise-induced muscle damage (EIMD). Preclinical models demonstrate that PEA supplementation accelerates muscle repair by reducing pro-inflammatory cytokine expression and promoting tissue regeneration (Lo Verme et al., 2005). PEA’s interaction with PPAR-α has been identified as a central mechanism driving these anti-inflammatory and pro-resolving effects (D'Agostino et al., 2012). Micronized PEA formulations have further been shown to reduce nitrosative stress in peripheral tissues, such as carrageenan-induced paw oedema, by decreasing nitrotyrosine formation and myeloperoxidase activity (Impellizzeri et al., 2014b). To our knowledge, similar antioxidant effects of PEA have not yet been investigated in skeletal muscle tissue, where oxidative stress also plays a key role in damage, recovery and adaptation. Clinical investigations provide further support for PEA's role in pain management and muscle health. A meta-analysis by Paladini et al. (2016) highlighted significant pain relief

in patients with chronic pain conditions, including musculoskeletal disorders, with PEA supplementation improving quality of life and functional outcomes, while an exploratory study in elderly individuals with sarcopenia suggested improvements in muscle strength and performance following PEA supplementation (Gatti et al., 2012)

Beyond its anti-inflammatory and analgesic actions, PEA may also influence energy metabolism. Through PPAR-α activation, PEA regulates fatty acid oxidation and mitochondrial function in metabolically active tissues (Lo Verme et al., 2005). In non-muscle models, PEA has been associated with improved mitochondrial respiration and reduced oxidative damage. For example, in diet-induced obese mice, oral PEA enhanced hepatic mitochondrial oxidative capacity, improved energy efficiency, and reduced lipid accumulation via PPAR-α and AMPK pathways (Annunziata et al., 2020). Ultramicronized PEA has also been shown to preserve respiratory complex I and FoF1 ATPase activity under inflammatory stress in neural models (Bellanti et al., 2022). Whether these PPAR-α-mediated effects of PEA extend to skeletal muscle, a tissue with high metabolic and mitochondrial demands, remains unknown. In addition, PEA's neuroprotective effects, including modulation of mast cell activity and neuroinflammation (Gabrielsson et al., 2016), could indirectly benefit muscle function by alleviating neuropathic pain often associated with muscle disorders. Nonetheless, the direct impact of PEA on mitochondrial pathways and energy metabolism in skeletal muscle has not yet been elucidated.

Taken together, the direct effects of PEA on skeletal muscle remain poorly understood. Specifically, little is known about its role in skeletal muscle myogenesis or the transcriptional response of muscle cells to PEA exposure. These fundamental insights could improve the quality of PEA research in muscle and pave the way to future work. Therefore, the specific aims of this study were to (i) investigate if PEA impacts skeletal muscle myogenesis and (ii) explore the acute transcriptional response of skeletal myotubes following PEA treatment, thereby providing new insights into the molecular mechanisms underlying PEA's effects on muscle tissue.

5.3 Materials and Methods

5.3.1 Chemicals, Reagents and Plasticware

PEA was purchased from Sigma-Merck and reconstituted in DMSO as per manufacturer guidelines. Reconstituted PEA was stored at -20°C and used within 3 weeks of reconstitution. When required, PEA stock solution was diluted further in culture media for the experiments outlined herein.

Dulbecco's modified eagle medium (DMEM), fetal bovine serum (FBS), new-born calf serum (NBCS), penicillin-streptomycin (pen-strep), trypsin-EDTA and horse serum (HS) were purchased from Thermo Fisher Scientific (Oxford, UK). Phosphate buffered saline (PBS) tablets, DMSO and gelatin from porcine skin were purchased from Sigma Aldrich (Gillingham, UK). T75 culture flasks and 6 well culture plates were purchased from Nunc (Thermo Fisher Scientific. Oxford, UK).

C2C12 myoblasts were purchased from ATCC (LGC Standards, Middlesex, UK). All experiments detailed in this manuscript were performed on C2C12s between passage 5 and 10. For the isolation of high-quality RNA, RNeasy isolation kits were purchased from Qiagen (Qiagen Ltd. Manchester, UK).

5.3.2 Cell Culture

C2C12 murine myoblasts were cultured on gelatin (0.2%) coated 6-well culture plates in humidified 5% CO_2 at 37°C in growth media comprising DMEM, 10% FBS, 10% NBCS and 1% of a pen-strep solution. Upon reaching ~80% confluence, monolayers were washed twice with pre-warmed PBS and switched to low serum differentiation media (DM), DMEM, 2% HS and 1% pen-strep. Every 48h thereafter, DM was removed from monolayers via aspiration and was replaced with fresh media. Cells were terminally differentiated by day-8 of low serum DM exposure.

5.3.3 Dose Tolerability Experiments

To ascertain an appropriate dose that would maximise the signal but minimize toxicity to the terminally differentiated C2C12 myotubes used in this study, we relied on previous literature to develop our own dose tolerance experiments. Given the lack of research regarding the

effects of PEA on the viability of C2C12 skeletal muscle cells, we determined our dosage selections on those used within general cell culture studies across multiple studies. Previous studies have examined the effects of 0.1, 0.5, 1, 10µM PEA on RBL-2H3 cells, a basophilic leukaemia cell line, and discovered no detrimental effects on viability and cytoxicity at the maximum concentration of 10µm (Petrosino et al., 2019). Additionally, another study identified 100µM as the optimal dose for reducing the effects of lipopolysaccharide (LPS) on N9 microglia cells (D'Aloia et al., 2021). While these studies were conducted on different cell lines, considering these findings collectively, we investigated 1, 10 and 100µM of PEA. We utilized a metabolic activity assay and propidium iodide exclusion assay to determine cytotoxicity of PEA.

5.3.4 Metabolic Activity Assay (MTT)

C2C12 myoblasts were seeded at 6 x 10^4 cells.mL^{-1} in pregelatinized 6-well plates in GM and cultured to 80% confluence. Thereafter, cells were induced to terminally differentiate as described under the cell culture section above. After 8days of differentiation, existing DM was removed from monolayers. Following three PBS washes, monolayers were treated with either DM containing vehicle solution DMSO (CON) or DM+PEA at doses from 1-100 µM (Figure 2). Following 24h treatment, MTT solution was added to each well at 10% of total well volume and incubated for 180min. Thereafter, existing media was removed from monolayers before another, short incubation of 6min, which was completed with plate lids removed. Five hundred microlitres of DMSO was then added to each well, and plates were agitated on a plate rocker at 120 rpm for 2 min to ensure all cells had detached from the plate. Plates were then positioned into a Spark multi-mode microplate reader (Tecan, Mannedorf, Switzerland) and measured at a wavelength of 570 nm to detect the change in absorbance.

5.3.5 Cell Viability assay (Propidium iodide exclusion)

In a separate experiment, myoblasts were seeded at 6 x 10^4 cells·mL^{-1} in pregelatinized 6-well plates in GM and cultured to 80% confluence. Thereafter, cells were induced to terminally differentiate as described under the cell culture section above. On day 8 of differentiation, existing media was removed from monolayers, which were subsequently treated with either DM containing vehicle solution DMSO (CON) or DM+PEA at doses from 1-

100µM (Figure 5.1). Following 24 h treatment, existing media was pipetted into 1.5 mL Eppendorf tubes and monolayers were washed twice with prewarmed PBS. Thereafter, trypsin– EDTA 0.025% was added to each well and plates were incubated for 5min (37°C degrees, 5% CO_2). The removed media was then placed back onto its corresponding well to allow serum to neutralize the activity of trypsin. This solution was then pipetted into a 1.5mL Eppendorf and centrifuged for 5 min at 300 × *g*. Following centrifugation, the existing media was aspirated from each Eppendorf, leaving a small pellet of cells. Two hundred microlitres of fresh DM was then added to each Eppendorf, and cell pellets were fully resuspended by pipetting to create a solution of cells and DM. Propidium Iodide (5mg·mL^{-1} in ddH_2O) was then added to each Eppendorf at a concentration of 1:100 and these were vortexed for 20 s before a 5-min incubation (37°C degrees, 5% CO_2). PI fluorescence was then analysed via flow cytometry using the FL-3 channel on a BD AccuriTM C6 Plus Flow Cytometer (BD Biosciences, Berkshire, UK). First, negative and positive controls were established whereby PI-free cells were analysed for background fluorescence alongside cells treated with 50% *v/v* H_2O_2. PI-free cells had no increase in fluorescence, whilst H_2O_2 increased fluorescence (Data not shown). The excitation/emission maximum of the dye is typically 493/636; upon binding to DNA, excitation/emission maxima increased to 535/617 nm.

5.3.6 Next Generation RNA Sequencing

5.3.6.1 Cell Treatments

After assessing the tolerability of C2C12 myotubes to different doses of PEA, we noted a significant decrease in metabolic activity and cell viability at 100 µM PEA, as indicated by the MTT and PI assays. Therefore, we selected 10 µM PEA for subsequent experiments. To determine the transcriptional response to 10 µM PEA, we terminally differentiated C2C12 myotubes as described above. On day 8 of differentiation, the differentiation medium (DM) was removed and replaced with DM containing either vehicle (DMSO), PEA (10 µM). Myotubes were then cultured in the respective treatment for 24 hours before being harvested for RNA extraction. Duplicate wells (technical replicates) were used for each treatment, and the experiment was repeated three times (experimental replicates), generating n=6 samples per treatment.

5.3.6.2 RNA Isolation

Following a 24-hour treatment with PEA or vehicle control, terminally differentiated C2C12 monolayers were lysed with buffer RLT from the Qiagen RNeasy kit (Qiagen Ltd). RNA was then extracted from cell lysates using the RNeasy kit with proteinase K digestion, as per the manufacturer's guidelines. Eluted RNA was stored at -80^{O}C until required for determination of total RNA and library processing.

5.3.6.3 Determination of RNA Quantity and Quality

Total RNA was quantified using a Nanodrop 8000 and RNA quality was assessed using an Agilent® Bioanalyser (average RIN score = 7, 260/280 = 2.1, 260/230 = 1.7). RNA samples were then diluted to 20 ng·µL^{-1} using RNase-free water.

5.3.6.4 RNA Library Preparation and Sequencing

Libraries were constructed from 100 ng of total RNA with Poly-A tail enrichment of mRNA using NEBNext® UltraTM II RNA Library Prep Kit for Illumina® with Agencourt AMPureXP Sample Purification Beads (Beckman Coulter. Wycombe, UK) as per manufacturers guidelines, by Bart's and the London Genome Centre at Queen Mary, University of London. The resultant-barcoded libraries were sequenced on an Illumina NextSeq 2000 using 2x50 bp paired-end sequencing. An average of 25 million paired- end reads was achieved per sample.

5.3.6.5 RNA Sequencing

FastQ files were imported to Partek® Flow® Genomic Analysis Software Partek Inc. (Missouri, USA) for pipeline processing. Pre-alignment QA/QC was performed on all reads prior to read trimming (Reads with Phred score <20 removed). STAR alignment 4.4.1d was used to align trimmed reads to the *Mus musculus* genome, mm39. Aligned reads were then quantified to the Ensembl transcriptome annotation model v.100. Post alignment QC reports are provided in Supplementary Table 1. Filtered raw counts were used for normalisation and differential analysis with DESeq2 (Love et al., 2014) through Partek® Flow®. Gene transcripts were considered significantly different between groups when the q-value <0.05. Volcano plots and annotation charts were generated in R studio (version 2023.06.1+524), Principal Component Analysis (PCA) plots were generated in Partek® Flow® and bar charts were constructed in

GraphPad Prism version 10.0.0 for Windows (GraphPad Software, Boston, Massachusetts USA). To facilitate further discovery and reproducibility, all RNA-seq data from this study are openly available via the Gene Expression Omnibus (GEO accession number GSE307376).

5.3.7 Immunofluorescence (IF) Staining

C2C12 myoblasts were seeded at 6 x 10^4 cells.mL^{-1} in pregelatinized 6-well plates in GM and cultured to 80% confluence. Existing GM was then aspirated, and cell monolayers were washed twice with PBS. Monolayers were then treated with DM containing either vehicle solution DMSO (CON) or DM+PEA (10 µM). Every 48 h, existing media was removed, monolayers washed once with PBS and fresh DM (including treatment) was introduced to monolayers up until day 8 of differentiation. On day 8 of differentiation, existing media was aspirated, and monolayers were washed three times with PBS. To fix the cells, paraformaldehyde (PFA 4%) solution was added and incubated at room temperature for 10 minutes. Thereafter, the fixative solution was removed, and monolayers were washed 3 times with PBS. The fixed sample can be stored for several days at 5°C. Remaining PBS was aspirated and permeabilization buffer (PBS + 0.1% Triton X-100) was added to each well and incubated at room temperature for 15 minutes. The permeabilization buffer was removed, and monolayers were washed twice with cold PBS. Blocking buffer (10% Goat Serum in PBS, diluted 1:500) was then added and incubated at room temperature for 30 minutes. Monolayers were then washed once with PBS, and the primary antibody (Myosin heavy chain [MF-20]; Mouse, 1:300, 1% BSA) (Developmental Studies Hybridoma, Bank, Iowa, USA) added to each well, ensuring dimmed lights due to the light sensitivity of MF-20. Plates were then wrapped in parafilm and placed in the fridge at 5°C overnight.

Following overnight incubation, the primary antibody was removed, and monolayers were washed three times with cold PBS, allowing each wash to sit for 5 minutes. The secondary antibody (Alexa-Fluor 488; Goat anti-mouse, 1:500, 1% BSA) (Thermo Scientific Inc; Massachusetts, USA) was then added, and plates were covered with foil and left at room temperature for 60 minutes. Following this, the secondary antibody was removed, and monolayers were washed twice with PBS. The final step involved nuclear counterstaining with 4’,6-diamidino-2-phenylindole, DAPI, a blue-fluorescent DNA stain, diluted in H2O (1:100).

This was added to the monolayers and incubated at room temperature for 15 minutes, protected from light. DAPI solution was then aspirated and PBS (200 µl) added to wells.

5.3.8 Image Acquisition

A Leica DMII6000b Microscope (Leica Biosystems; Wetzlar, Germany) was used to capture fluorescently labelled monolayers as it allows for co-visualization of MF-20 with DAPI (Thermo Scientific Inc; Massachusetts, USA). Images of cell monolayers were taken using the 10× objective and 0.5 magnification c-mount fitted to the camera. Blue colour channels were used as an indicator of DAPI with the wavelength measured at 358/461 nm (Fluorescent filter; EX: 340–380, DC: 400, EM: 450–490). Green colour channels were used as an indicator for MF-20, with the wavelength measured at

499/520 nm (Fluorescent filter; EX: 460–500, DC: 505, EM: 512–542). Image inspection and processing was conducted using Leica Application Suite for Windows 7, (Leica Biosystems; Wetzlar, Germany) and Image J 1.53a (National Institutes of Health; Maryland, USA).

5.3.9 Cell Cycle Analysis with Propidium Iodide

C2C12 myoblasts were seeded at 6 x 10^4 cells.mL^{-1} in pre gelatinized 6-well plates and treated with GM containing either vehicle solution DMSO (CON) or DM+PEA (10 µM). Following 24h treatment, existing media was aspirated, and monolayers were washed twice with PBS. To harvest cells, 200 µL of trypsin was added to each well and incubated for 5 minutes. Once detached, cells were pipetted into a single cell suspension in buffer (PBS + 2% FBS; PBS + 0.1% BSA). Cells were then washed with PBS and centrifuged at 3000 × *g* for 5 minutes, this step was repeated twice, and cells resuspended at 3-6 x 10^6 cells.mL^{-1}. Next, 500 µL of cells were aliquoted into a 15 mL polypropylene, V-bottomed tube, and 5 mL of cold 70% ethanol was added dropwise while gently vortexing. Cells were then fixed for at least 1 hour at 4°C on ice. After fixation, cells were washed once with PBS and centrifuged as described above again. To ensure only DNA was stained, cells were treated with Ribonuclease A to remove RNA. Fifty microlitres of RNase A solution (final concentration 0.5 µg.mL^{-1}) was added directly to the cell pellet. Then, 1 mL of PI solution was added, and cells vortexed and incubated overnight (or at least 4 hours) at 4°C. Samples were then analysed using a BD Accuri C6 flow cytometer (BD Biosciences, San Jose, CA, USA) equipped with four fluorescence

channels (FL-1, FL-2, FL-3, FL-4). PI dye exhibits an excitation/emission maximum of 493/636 nm, which shifts to 535/617 nm upon binding, and was detected in the FL-3 channel. Samples were acquired at a low flow rate (<400 events·s^{-1}), and data collection was complete once 20,000 events had been recorded. Gating was first performed on forward and side scatter to exclude debris and aggregates, followed by fluorescence intensity gating in FL-3 to identify positive from negative cell populations. All assays were normalised to total event counts.

5.3.10 Statistical Analysis

5.3.10.1 Dose Tolerability

All statistical analysis and figures regarding dose tolerability experiments were conducted using GraphPad Prism™ for Macintosh (Version 9.3.1). All data were normally distributed, and as such were assessed with a one-way ANOVA. Significance was assumed if α reached ≤0.05. All data are presented as mean ± standard deviation (SD).

5.3.10.2 Myotube Morphology

All statistical analysis and figures regarding myotube morphology experiments were conducted using GraphPad Prism™ for Macintosh (Version 9.3.1). Myotube number and NFI (%) data were normally distributed, and as such were assessed with an unpaired t-test. Myotube area (µm2) data were not normally distributed, so were assessed with a Mann-Whitney U test. For all data, significance was assumed when α ≤0.05. All data are presented as mean ± standard deviation (SD).

5.3.10.3 Cell Cyle Analysis

All statistical analyses and figures regarding cell cycle progression experiments were conducted using GraphPad Prism™ for Macintosh (Version 9.3.1). All data were normally distributed, and as such were assessed with a two-way ANOVA. Post hoc comparisons were conducted using Bonferroni's multiple comparisons test to determine differences between conditions at each cell cycle phase. For all data, significance was assumed if α reached ≤0.05. All data are presented as mean ± standard deviation (SD).

5.3.11 Bioinformatics

To visualise gene interactions and clusters of proteins that they encode with known physical interactions, STRING (string.db.org) was deployed on commonly up regulated and down regulated DEGs. Networks were exported to Cytoscape (v10.3 for Mac) to generate figures shown in results section. Protein-protein interaction (PPI) networks were constructed using known interaction data and analysed using the Markov Clustering (MCL) algorithm to identify functionally related gene clusters. MCL was applied by simulating random walks through the network, with iterative expansion and inflation steps to enhance the separation of densely connected regions. Clustering was performed using an inflation parameter of 0.2 to control cluster granularity. Gene Ontology (GO) term enrichment was assessed for each cluster to determine functional associations. Single-node genes with no known interactions were excluded from visualization.

Circos plots were made using RStudio (v2014.12.0) using the following packages; circlize v0.4.16, dplyr v1.1.4, readr v2.1.5, tidyr v1.3.1, complexheatmap v2.24.1, grid v4.5.0, and tibble v3.3.0.

Experimental workflows are presented schematically in Figure 5.1.

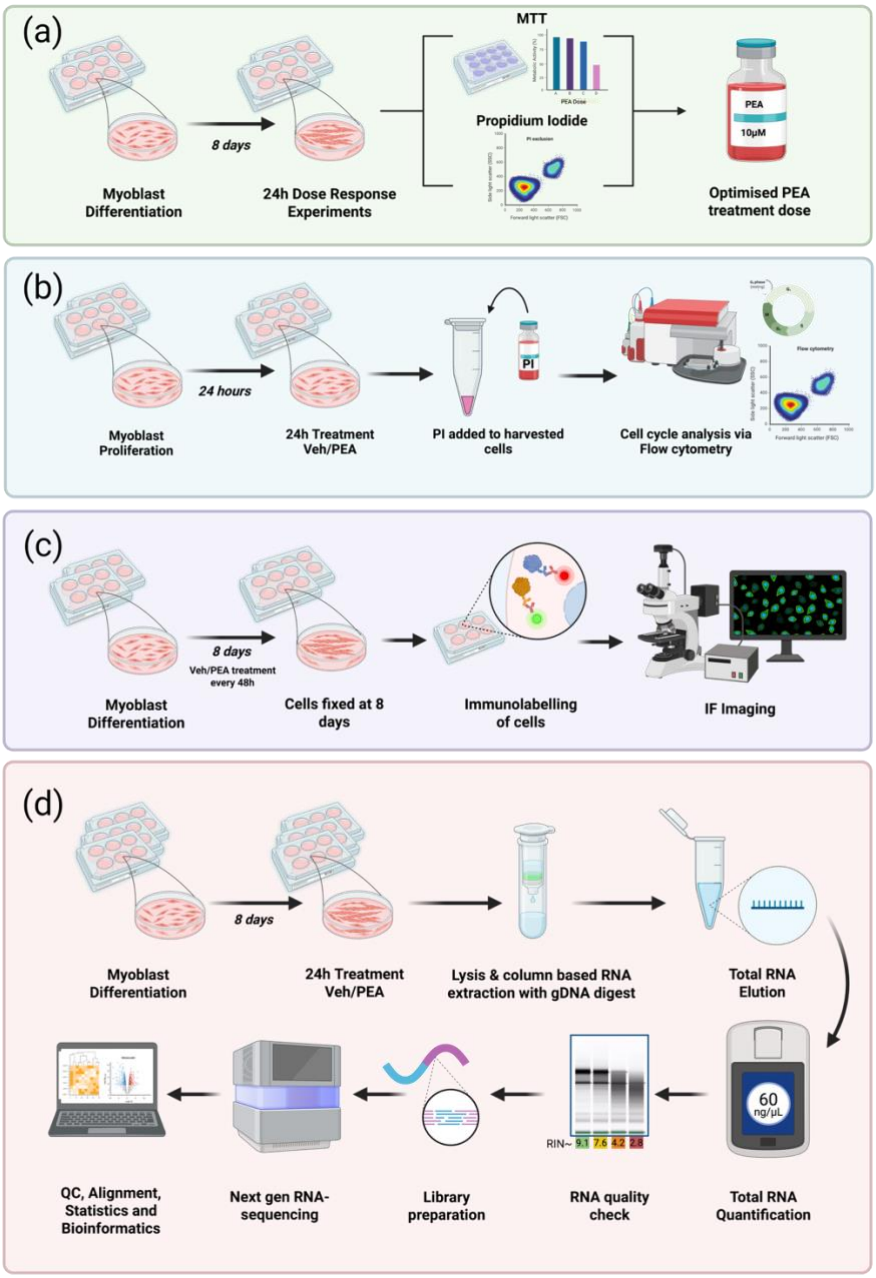

Figure 5.1. Experimental workflow for (**a**) the determination of dose tolerability. C2C12 myoblasts were differentiated in GM before 24 h treatment with PEA or vehicle (DMSO) control. MTT and PI exclusion assays were performed to determine the maximal tolerable dose of PEA. In workflow (**b**), C2C12 myoblasts were treated with PEA (10 µM) or vehicle control for 24 h. Myoblasts were then harvested and stained for DNA labelling with PI. Cell cycle phase distribution was then analysed using flow cytometry. In workflow (**c**), C2C12 myotubes were treated with PEA (10 µM) or vehicle control every 48 h throughout differentiation. On day 8, myotubes were fixed, stained with DAPI and MF-20, and imaged by immunofluorescence for morphological analysis. Image created using Biorender. Finally, in workflow (**d**), differentiated myotubes were exposed to PEA (10 µM) or vehicle control for 24 h before being lysed for column-based RNA extraction. Total RNA quantity and quality were

determined prior to library preparation and next-generation sequencing. Pre-alignment QC was performed prior to quality trimming and STAR alignment, followed by quantification to the annotation model, counts were then normalised by median ratio, prior to DESeq2 statistical analysis.

5.4 Results

5.4.1 Dose Tolerability

Following 24 h of PEA exposure, metabolic activity, as determined by the MTT assay, was significantly reduced following 100µM compared to control ($p<0.0001$; Figure 5.2a). Additionally, there was a significant reduction in the percentage of live cells, as determined by the PI assay, at 100µM PEA compared to control ($p = 0.02$; Figure 5.2b). Based on these observations, we selected the maximum 10µM PEA to evaluate its potential effects on skeletal muscle myogenesis and the transcriptome of terminally differentiated myotubes.

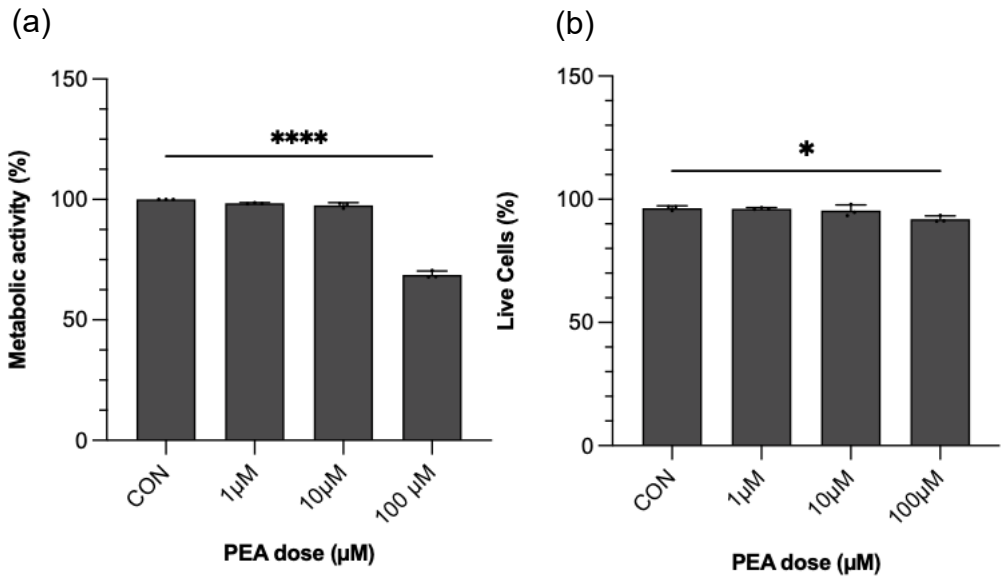

Figure 5.2. Dose tolerability experiments on terminally differentiated myotubes. Metabolic activity (a) and cell viability (b) were determined by the MTT assay and propidium iodide (PI) exclusion in PEA-treated C2C12 myotubes over a range of concentrations (1-100µM). Data are presented as mean ± SD from n = 3 biological replicates for each dose.

5.4.2 Myotube Morphology

The morphology of C2C12 myotubes treated with either control (CON) or PEA (10 µM) throughout differentiation (every 48 h), was assessed using immunofluorescence staining for myosin heavy chain (MF-20) and nuclear counterstaining with DAPI. Morphological analysis

included quantification of myotube number, myotube area (µm²), and the nuclear fusion index (NFI, %). There was no significant difference in myotube area (µm²) between CON (296.6 ± 441.4) and PEA (284.5 ± 383) (p = 0.44; Figure 5.3a). However, there was a significant decrease in myotube number following PEA treatment (90.3 ± 10.6) compared to CON (112.6 ± 10.1) (p <0.0001; Figure 5.3b). Nuclear fusion index (NFI, %) was significantly increased following PEA treatment (37.8 ± 5.7) compared to CON (30.7 ± 3.2) (p = 0.02; Figure 5.3c).

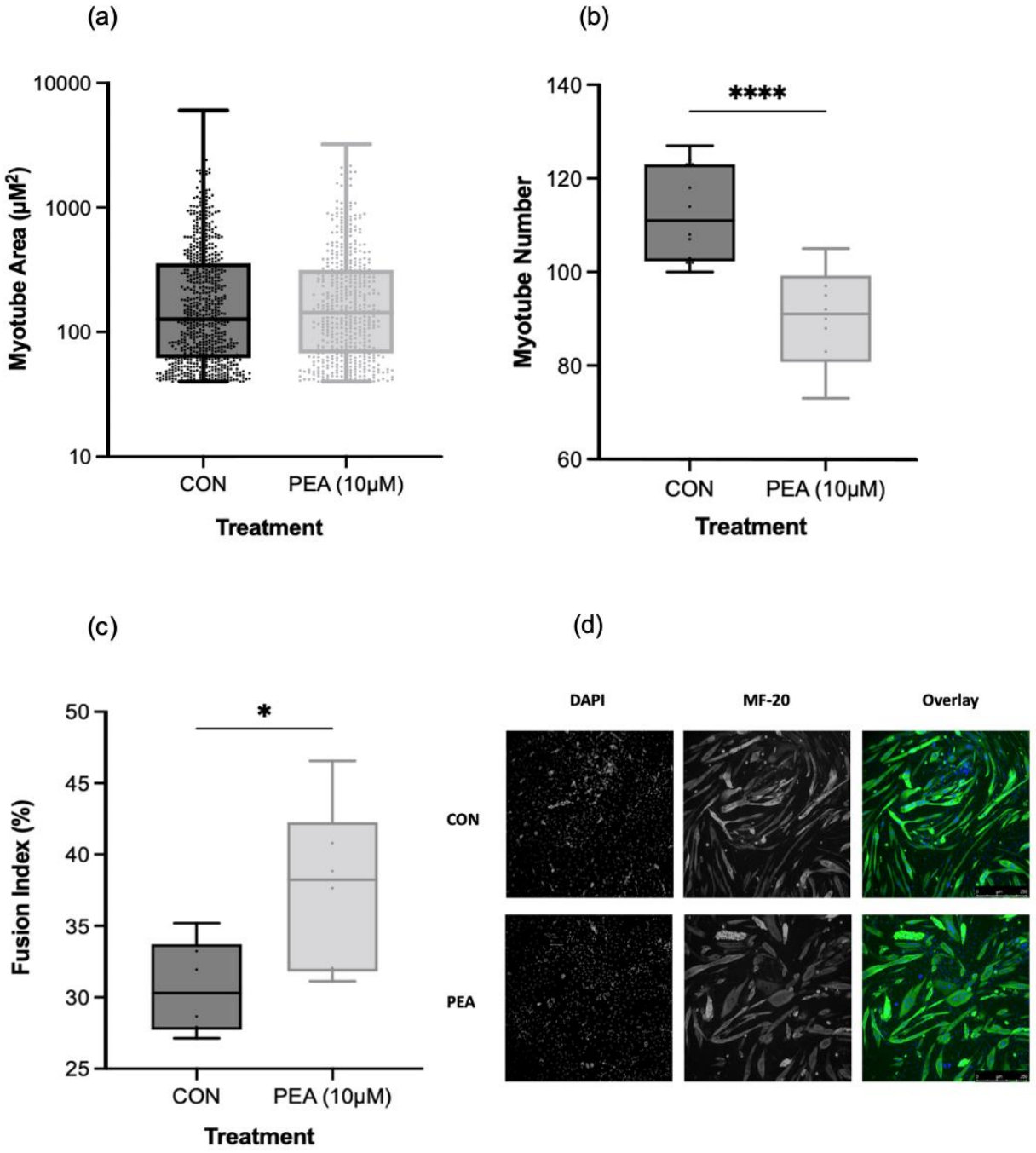

Figure 5.3. Morphological analysis of myotubes treated throughout differentiation with PEA (10 µM) or vehicle control (CON). Measurements include (a) myotube area (µm^2), (b) myotube number and (c) nuclear fusion index (NFI,%). Analysis conducted using ImageJ. (d) Representative images of differentiated C2C12 myotubes stained for nuclei (DAPI, blue) and myosin heavy chain (MF-20, green). One independent image is presented per condition (CON and PEA). Scale bars = 250 µM. For morphological analyses, six images were acquired per well across three wells per condition. Quantification was performed on six randomly selected images per condition to ensure unbiased representation. Data are expressed as mean ± SD from n = 3 independent biological replicates for each dose.

5.4.3 Myoblast Cell Cycle Phase Analysis

To further investigate the effects of PEA on C2C12 skeletal muscle cells, we assessed its impact on cell cycle progression using propidium iodide (PI) staining. There was a significant main effect of cell cycle phase ($p < 0.0001$), with a significant interaction between condition and phase also observed ($p < 0.0001$). Bonferroni's multiple comparisons test revealed that PEA treatment (10 µM for 24h) led to a significant accumulation of cells harbouring in the G0/G1 phase (48.2 ± 1.2 %) compared to CON (42.3 ± 1.9 %) ($p = 0.0002$), with a concomitant significant reduction in the proportion of cells in the S-phase (21.7 ± 1.2 %) compared to CON (25.5 ± 1.2 %) ($p = 0.008$).

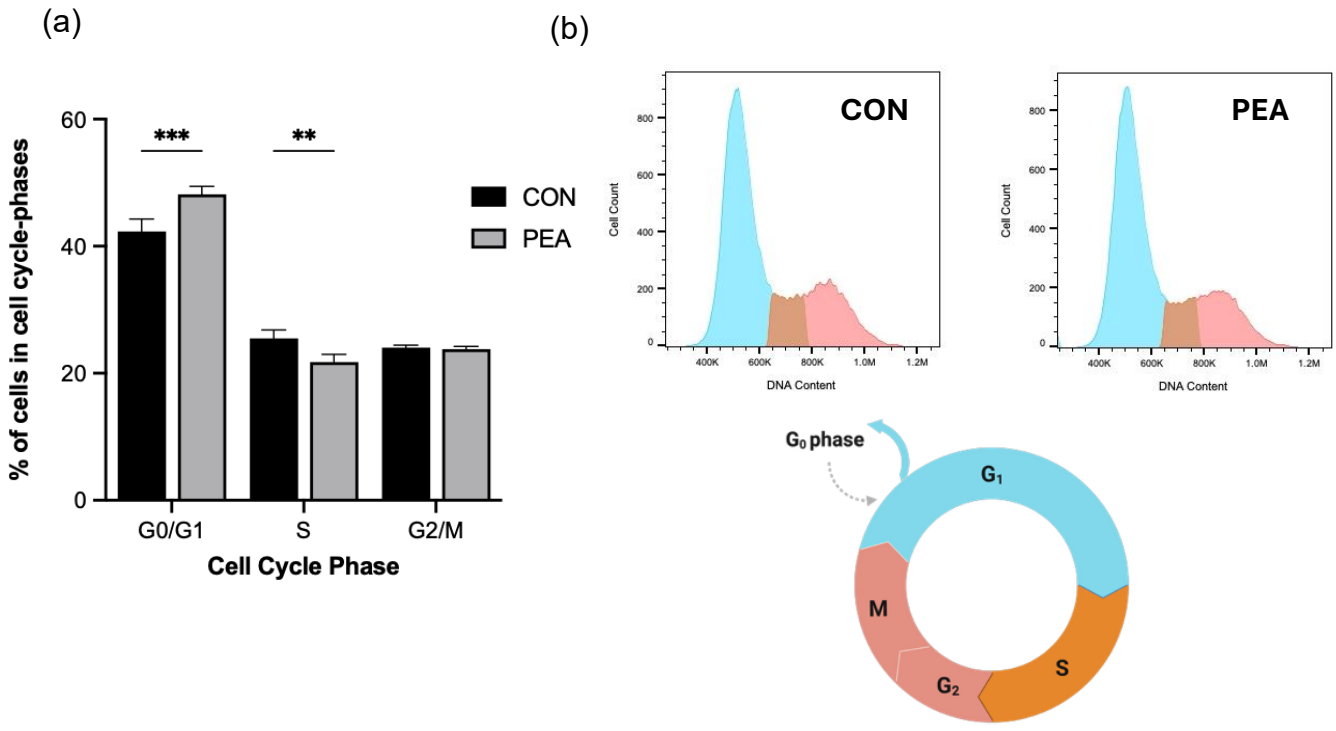

Figure 5.4. (a) Cell cycle distribution of C2C12 myoblasts following 24 h treatment with PEA (10 µM) or vehicle control (CON), assessed by flow cytometry using propidium iodide (PI) staining. Cell cycle phases determined using appropriate gates based on PI fluorescence histograms, with G_o/G_1-phase cells identified by lower PI intensity, S-phase cells by intermediate intensity, and G_2/M -phase cells by higher intensity. (b) Representative PI fluorescence histogram (FL2-H, PE channel) illustrating DNA content profiles. Peaks correspond to G_o/G_1 (light blue), S-phase (orange), and G_2/M (red) cells. Analysis performed using FloJo software. Data are presented as mean ± SD from n = 3 biological replicates for each dose.

5.4.4 Acute Transcriptomic Response to PEA in C2C12 Myotubes

The PCA plot (Figure 5.5 a) visualises the multidimensional relationships among the gene expression profiles of CON and PEA treated cells. The plot reveals distinct clusters of gene expression profiles between conditions. Using $q < 0.05$, we found that 1952 genes were differentially expressed in PEA compared to CON. Of these genes, 1028 were significantly upregulated, and 924 were significantly downregulated.

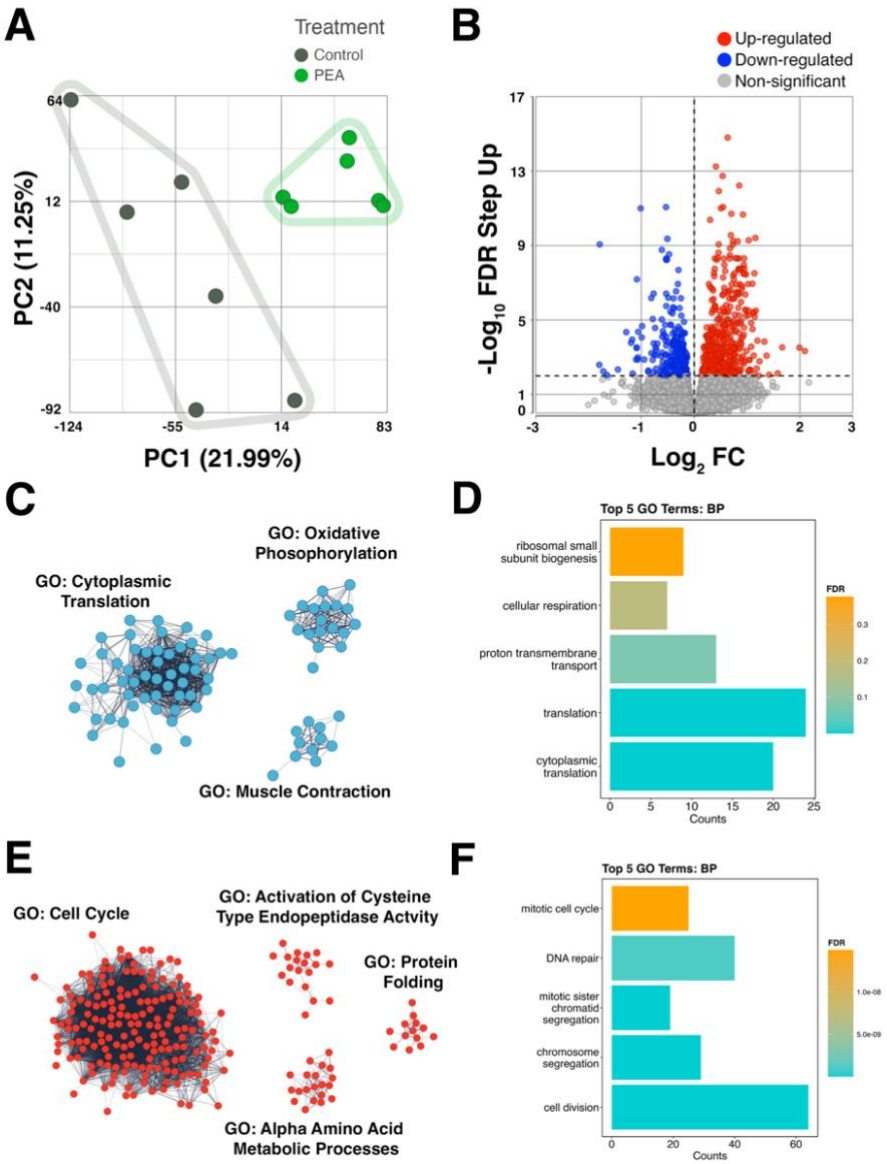

Figure 5.5. (a) Principal Component Analysis (PCA) of RNA-seq data, illustrating the variance in gene expression between PEA-treated and control samples. Each point represents an individual sample, with clustering patterns indicating transcriptomic differences between conditions. Data are presented from n = 3 biological replicates for each dose. (b) Volcano plot depicting differentially expressed genes (DEGs), with -$\log_{10}$ FDR step-up on the y-axis and $\log_2$ fold-change on the x-axis. Grey points represent non-significant genes, blue points indicate downregulated genes, and red points indicate upregulated genes. (c) Clusters of uniquely downregulated genes and their associated Gene Ontologies. (d) Gene Ontology (GO) biological processes for all downregulated genes. (e) Clusters of uniquely upregulated genes and their associated Gene Ontologies. (f) GO biological processes for all upregulated genes. Single-node genes are excluded. Markov Clustering (MCL) was performed using the STRING app in Cytoscape (v10.3 for Mac).

5.4.5 Transcriptional Response of PEA Metabolising Enzymes in Skeletal Muscle

Two enzymes are reported to be responsible for PEA hydrolysis to palmitic acid and ethanolamine; N-acylethanolamine acid amidase (*Naaa*) and fatty acid amide hydrolase (*Faah*). Following stimulation of myotubes with 10 mM the expression of *Naaa* was significantly upregulated vs control, whereas *Faah* expression was unaltered (Figure 5.6). Notably, *Naaa* reads were ~20 fold higher than *Faah* suggesting that *Naaa* dependent PEA metabolism may be more abundant in C2C12 myotubes.

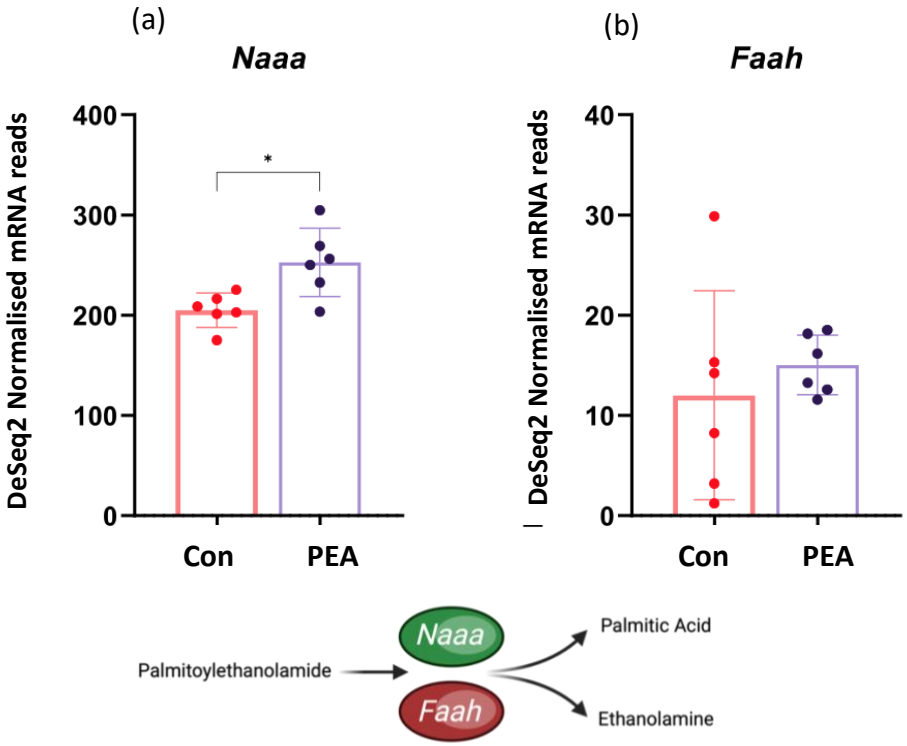

Figure 5.6. DeSeq2 Normalised mRNA reads for (a) N acylethanolamine acid amidase (Naaa) and (b) fatty acid amide hydrolase (Faah). (c) Graphical representation of the role Naaa and Faah enzymes play in PEA metabolism.

5.4.6 PEA modulates the expression of interleukin genes, their receptors and inflammatory pathways

Given the established role of palmitoylethanolamide (PEA) in modulating immune function, and emerging evidence suggesting potential actions in skeletal muscle, we investigated its role in modulating the transcriptome in C2C12 myotubes. We queried interleukins, their receptors and established inflammatory pathways (KEGG) to assess how PEA alters their expression. RNA-seq analysis performed 24-hours following exposure to 10mm PEA treatment revealed

many genes relating to ‘Cytokine-receptor-interactions', ‘Chemokine signalling’, ‘JAK-STAT signalling’ ‘NF-κB signalling’, ‘NOD-like receptor signalling’ and ‘Toll-like receptor signalling’ were differentially expressed, summarised in the Circos plot which clusters genes by their associated pathway and ranks them by Log^2 fold change, (Figure 5.7).

Our data supports the notion that C2C12 myotubes exposed to PEA promotes an anti-inflammatory transcriptional profile and suppresses TNF signalling associated genes. Genes encoding pro-inflammatory cytokines *Il1a, Il1b, Il33*, *Il12a* and *Tnfrsf19* were downregulated suggesting suppression of pro-inflammatory signalling. These cytokines are also Nuclear Factor kappa B (NF-κB) targets suggesting reduced NF-κB transcriptional activity which is further supported by the downregulation of *Nfkbia*. *Socs1*, the gene encoding Suppressor of Cytokine Signalling 1 was also downregulated and is a negative regulator of the NF-κB signalling pathway. We also observed upregulation of interferon-related genes *Stat2*, *Oas1b*, *Gbp7* and chemokines *Cxcl14*, *Ccl5* suggesting immune priming while attenuating NF-κB-driven inflammation.

These findings and prior literature would be supportive of the hypothesis that PEA, directly or indirectly activates PPARα as reported in neural and immune cells. However, we found that PPARα was expressed at extremely low levels in C2C12 myotubes, <10 normalised counts and unaffected by PEA treatment. While we did not assess PPARα activity or protein abundance directly, our data suggest that PEA’s effects may not be wholly through modulation of PPARα activity, but through PPARα independent mechanisms, potentially involving alternative immune modulatory pathways.

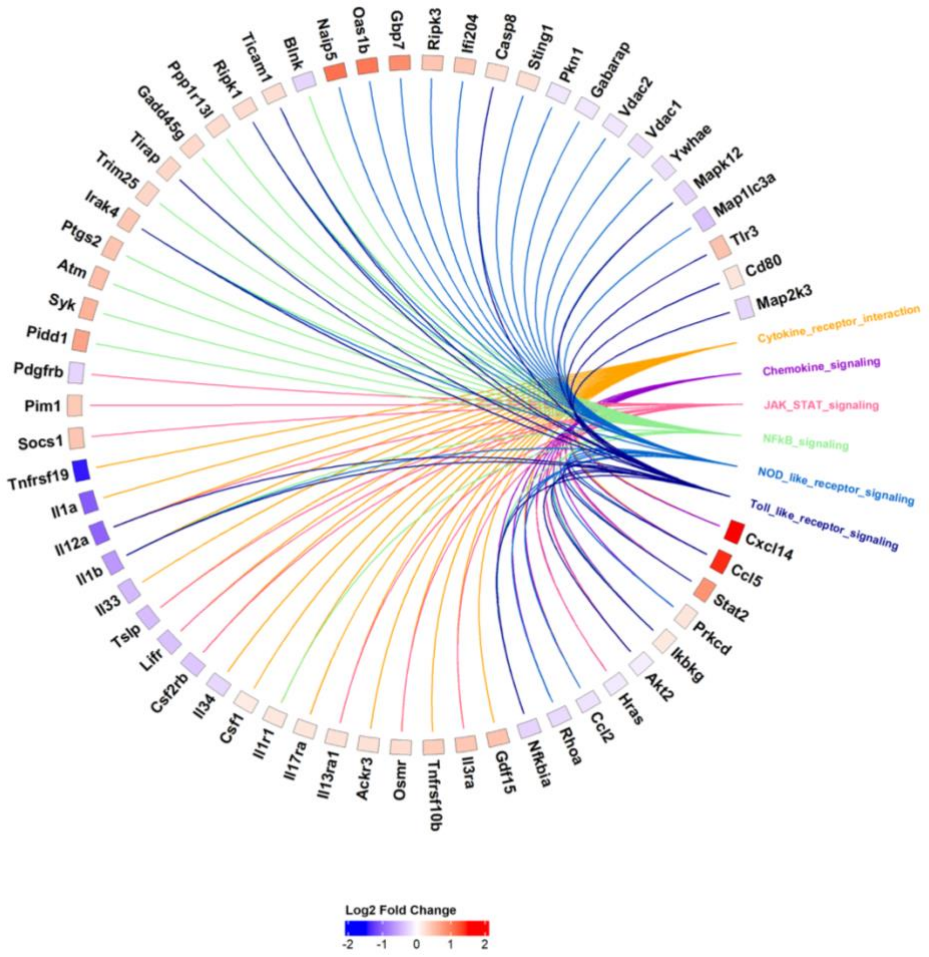

Figure 5.7. Differential gene expression in C2C12 myotubes following palmitoylethanolamide (PEA) treatment (10 µM) compared with control. Data are presented as log_2 fold change. Circos plot of differentially expressed inflammatory genes mapped to key inflammatory related signalling pathways. Genes are clustered into pathways and ranked by log_2 fold change. Gemes present in multiple pathways are connected by multiple-coloured nodes.

5.5 Discussion

The aims of this study were to (i) determine whether palmitoylethanolamide (PEA) influences skeletal muscle myogenesis and (**ii**) characterise the acute transcriptional response of differentiated myotubes to PEA treatment. We observed that PEA exposure accelerated cell cycle exit and elicited a distinct transcriptomic profile, with 1,952 genes differentially expressed ($q < 0.05$, fold change > 1) compared with controls (1,028 upregulated and 924 downregulated). Notably, expression of *N-acylethanolamine acid amidase* (*Naaa*) was markedly higher and significantly upregulated, whereas *fatty acid amide hydrolase* (*Faah*) exhibited low expression and no significant change, suggesting *Naaa* may be the dominant

enzyme for PEA hydrolysis in muscle. The transcriptional landscape also featured upregulation of cytokine receptors and apoptosis-related genes, indicative of heightened immune readiness, alongside downregulation of pro-inflammatory cytokines and NF-κB inhibitors, consistent with dampened inflammatory signalling potentially via alternative pathways. Strikingly, *peroxisome proliferator-activated receptor alpha* (*PPARα*), often considered the primary mediator of PEA's effects, was expressed at low levels in C2C12 myotubes and remained unchanged with treatment, challenging the view that PPARα is the dominant signalling route in muscle. Taken together, these findings not only support an inflammation-resolving role for PEA in skeletal muscle but also provide, to our knowledge, the first comprehensive transcriptomic evidence in myotubes revealing immune-modulatory and metabolic signatures that occur independently of canonical PPARα signalling.

Cell cycle analysis via flow cytometry revealed that 24-hour exposure to 10μM significantly increased the proportion of cells in the G0/G1 phase, with a corresponding decrease in the S-phase. This accumulation of cells in the G0/G1 phase is indicative of G1-phase arrest and suggests that PEA may impede cell cycle progression. This aligns with previous studies in other cell types where PPARα activation has been shown to induce G0/G1 cell cycle arrest through downregulation of G1/S transition regulators such as cyclin D1, CDK4 and CDK2 (Lien et al., 2013, Gizard et al., 2005). These effects are specifically mediated by selective PPARα agonists, including WY-14,643 and GW7647, indicating a direct ligand-dependent role of PPARα in cell cycle regulation (Lien et al., 2013, Gizard et al., 2005). Such G1 arrest is a common feature of anti-proliferative signalling and may explain the reduced number of myotubes observed following PEA treatment. Interestingly, although PPARα is typically considered the principal mediator of PEA's effects, it was expressed at low levels and remained unchanged following PEA treatment in our transcriptomic dataset. This suggests that PEA may exert similar anti-proliferative effects via alternative signalling pathways. Supporting this, Pagano et al. (2021) demonstrated that ultra-micronized PEA (um-PEA) exerted anti-proliferative effects on two different colon adenocarcinoma cell lines via PPARα and GPR55 antagonists. Collectively, these findings provide further evidence that PEA may regulate cell cycle progression in C2C12 skeletal muscle, contributing to the suppression of myoblast proliferation in the present study and influencing subsequent myotube formation.

A novel finding In the current study relates to the PEA hydrolysing enzymes N-acylethanolamine acid amidase (*Naaa*) and fatty acid amide hydrolase (*Faah*), which hydrolyse PEA to palmitic acid and ethanolamine. *Naaa* catalyses the hydrolysis of PEA primarily in lysosomes at acidic pH using a cysteine-based mechanism and exhibits high substrate selectivity for saturated N-acylethanolamines (NAEs) such as PEA (Scalvini et al., 2020, Tsuboi et al., 2005, Ueda et al., 2010). In contrast, *Faah* catalyses PEA hydrolysis less efficiently in the endoplasmic reticulum at neutral pH using a serine hydrolase mechanism and preferentially hydrolyses unsaturated NAEs such as anandamide (Cravatt et al., 1996, Ahn et al., 2008). Our data indicate that exposure of skeletal muscle myotubes to 10 mM PEA led to significant induction of *Naaa* gene expression vs control. In contrast, *Faah* expression was unaltered. Notably, *Naaa* reads were ~20 fold higher than *Faah* suggesting that *Naaa* dependent PEA hydrolysis may be the dominant mechanism of metabolism in muscle cells and requires further targeted experiments to confirm this.

Finally, PEA is known for its anti-inflammatory and neuroprotective properties. Our data support this in skeletal muscle cells, as PEA-treated muscle cells exhibited a distinct transcriptional profile characterised by the downregulation of NF-κB target genes including *Il1a*, *Il1b*, Il12a, *Il33*, and *Tnfrsf19.* This transcriptional shift is particularly relevant as NF-κB activity has been widely implicated in skeletal muscle wasting and impaired regeneration (Glass, 2005, Li et al., 2008). Suppression of NF-κB target cytokines by PEA therefore suggests a potential role In promoting a pro-regenerative and anti-catabolic environment. Coupled with increased fusion index, these data raise the possibility that PEA modulates muscle differentiation by reducing inflammatory signalling while permitting enhanced myonuclear accretion. However, whether this translates into functional benefits such as improved regeneration following injury or attenuation of muscle atrophy in chronic disease remains to be established.

5.6 Limitations

A major challenge in cell culture experiments is the translation of findings to in vivo conditions, particularly regarding the concentrations of compounds under investigation. Briskey et al. (2020) reported that following the consumption of 300 mg of PEA, peak plasma concentrations reached ~ 19.08 pmol·mL^{-1} at 125 minutes, equivalent to about 0.019 µM. To

enhance absorption, they also examined Levagen+**,** a PEA formulation utilizing dispersion technology. Peak plasma concentrations of Levagen+ were elevated to ~ 27.1 pmol·mL^{-1} at 105 minutes post-consumption, equivalent to about 0.027 µM (Briskey et al., 2020). It is important to note that both endogenous PEA levels and exogenously administered PEA have been reported to result in low plasma concentrations due to poor absorption (Hauer et al., 2013, Beggiato et al., 2019b). Whilst plasma concentration and what the muscle is exposed to in the extracellular fluid may differ, it is important to recognise that we used a considerably higher concentration of PEA in our in vitro studies (10 µM).

While our transcriptomics experiment investigated the effects of PEA on mature myofibers, it's important to acknowledge that our in vitro model contains a subpopulation of unfused myoblasts. During differentiation, not all C2C12 myoblasts successfully fuse into multinucleated myotubes, and previous studies have documented the presence of unfused myoblasts remaining in the culture (Veliça and Bunce, 2011). These residual myoblasts could contribute to the observed expression of cell-cycle related transcription factors/genes, as they may still be actively proliferating or transitioning into a differentiated state. This variability within the cell population should be considered when interpreting our results.

A final limitation to be considered Is that messenger RNA provides a valuable molecular snapshot of the cellular response to perturbations in homeostasis and typically precedes changes in protein synthesis. However, the extent to which transcript abundance reflects alterations in peptide production remains uncertain, and we cannot exclude the possibility of a "first exposure" effect, whereby an initial challenge may not reliably reproduce the transcriptomic shifts observed here.

5.7 Conclusion

Taken together, this study provides the first comprehensive transcriptomic characterisation of skeletal muscle myotubes exposed to PEA, revealing coordinated immune-modulatory, metabolic, and cell cycle‑regulatory responses that occur independently of canonical PPAR α gene activation. The marked induction of *Naaa* relative to *Faah* suggests a muscle-specific bias towards lysosomal PEA hydrolysis, representing a novel aspect of PEA metabolism in this tissue. These findings expand current understanding of PEA's molecular actions beyond

neural and immune systems, pointing to previously unrecognised pathways through which PEA may influence muscle inflammation, regeneration, and adaptation. To facilitate further discovery and reproducibility, all RNA-seq data from this study are openly available via the Gene Expression Omnibus (GEO accession number GSE307376). Further work should now establish whether PEA's dual actions, restricting proliferation while enhancing fusion and dampening inflammatory signalling, translate into functional benefits for muscle growth, recovery from injury, or adaptation to exercise *in vivo.*

Transition to Chapter 6

The findings presented in this chapter demonstrate that PEA promotes an anti-inflammatory, immune-modulating, and fusion-oriented phenotype in skeletal muscle cells, suggesting a mechanistic profile distinct from that typically associated with NSAID exposure. These results raise important questions about how such molecular signatures translate to broader aspects of muscle proteostasis, particularly in comparison with ibuprofen, which remains widely used despite concerns regarding its impact on muscle adaptation. To address this gap, the next chapter extends the investigation from gene expression to protein-level regulation, directly comparing the effects of PEA and ibuprofen on protein synthesis and abundance in differentiated C2C12 myotubes. This transition enables a more comprehensive evaluation of how these compounds influence muscle remodelling and provides critical insight into whether PEA may represent a safer, more targeted alternative for supporting muscle repair.

Chapter 6

Comparative Effects of Palmitoylethanolamide (PEA) and Ibuprofen on Protein Abundance and Synthesis in C2C12 Skeletal Myotubes

This chapter examines the direct effects of PEA and Ibu on protein synthesis and protein abundance in C2C12 skeletal muscle myotubes. Given the conflicting evidence regarding the impact of NSAIDs on muscle protein synthesis, often attributed to variations in study design and methodology, this study adopts a controlled, in vitro model. By integrating measures of both synthesis and abundance, the aim is to provide a clearer understanding of how these compounds influence muscle cell proteostasis and to explore their potential implications for adaptive muscle remodelling.

6.1 Abstract

Introduction: Palmitoylethanolamide (PEA) is an endogenous fatty acid amide with analgesic and anti-inflammatory properties, but its effects on skeletal muscle proteostasis remain unclear. This study aimed to determine how PEA and Ibu influence skeletal muscle proteome remodelling by profiling protein synthesis and abundance in differentiated C2C12 myotubes on a protein-by-protein basis. **Methodd**: Differentiated C2C12 myotubes were treated for 36hr with vehicle control (VC), PEA (10 μM), or Ibu (100 μM). Dynamic proteome profiling was performed using deuterium oxide labelling and high-resolution mass spectrometry to quantify protein-specific fractional synthesis rates (FSR) and relative protein abundance. **Results:** We quantified the fractional synthesis rates (FSR) and relative abundance for 1,541 and 3085 proteins, respectively. On average mixed-protein FSR was similarly increased across Ibu and PEA treatments (+55% and +44 %, respectively; $P > 0.05$) but protein-specific resolution of changes in synthesis rates revealed that PEA significantly ($P < 0.05$) regulated the synthesis rates of 103 proteins (101 upregulated), while Ibu altered 172 proteins (165 upregulated). Furthermore, both PEA and Ibu induced clear differences in muscle proteome remodelling. Whereby, Ibu stimulated the synthesis and accumulation of proteins associated with muscle contraction and extracellular matrix (ECM) organisation alongside reorganisation of metabolic pathways via downregulation of abundance for proteins associated with carbohydrate metabolism and increased abundance of those associated with lipid metabolic pathways. Whereas PEA elicited a more specific response targeted towards expansion of the ribo-proteome. Further analysis of the ribosomal protein pool revealed both PEA and Ibu induced significant ($P < 0.05$) increases in total ribosomal protein synthesis (~ 80 %) and the abundance of the 40S small ribosomal subunit (~ 18 %). **Conclusion:** Overall, these data Implicate enhanced ribosomal capacity to be an adaptive feature conserved between both PEA and Ibu treatment which may aid in repair and regeneration of muscle following acute exercise. However, Ibu also induced broader proteome adaptation associated with ECM remodelling and enhanced lipid metabolism. These findings provide the first proteome wide analysis of PEA and Ibu in muscle cells. Whereby, PEA is identified as a mechanistically distinct and more targeted alternative to NSAIDs with potential to support muscle repair and adaptation.

6.2 Introduction

Palmitoylethanolamide (PEA), a naturally occurring fatty acid amide, has recently been identified as a promising alternative to non-steroidal anti-inflammatory drugs (NSAIDS) due to its analgesic and anti-inflammatory properties (Petrosino and Di Marzo, 2017a, Hesselink and Hekker, 2012). PEA acts through mechanisms distinct from NSAIDs, notably by modulating proliferator-activated receptor alpha (PPARα) and G protein-coupled receptor 55 (GPR55) (LoVerme et al., 2005). In addition, PEA has been reported to indirectly target transient receptor potential vanilloid receptor 1 (TRPV1) (Paterniti et al., 2013) and CB_1 and CB_2 receptors (Petrosino et al., 2016). Unlike NSAIDS, PEA does not inhibit cyclooxygenase or prostaglandin synthesis, suggesting it may attenuate inflammation and pain without interfering with pathways involved in muscle protein synthesis (MPS). PEA has beneficial effects in models of neuropathic pain (Gabrielsson et al., 2016), neuroinflammation (Petrosino and Schiano Moriello, 2020), and tissue injury (Verme et al., 2005), yet its influence on skeletal muscle recovery and adaptive signalling pathways following exercise-induced muscle damage (EIMD) is unexplored.

Whilst PEA has not been explored in the context of EIMD, NSAIDs such as ibuprofen (Ibu) are routinely used in both recreational and elite sports, primarily to manage pain and inflammation associated with EIMD. Surveys conducted on ultra-endurance runners indicate that NSAID use is high and is often used without medical supervision The adverse effects of chronic NSAID use are well-established, including heightened risk of upper gastrointestinal issues (Bhala et al., 2013), shorter-term NSAID use during training and competition to alleviate EIMD-related symptoms is prevalent amongst endurance sports. Despite widespread use and growing awareness of potential adverse effects, few studies have evaluated how NSAIDs may influence muscle adaptive responses and cellular processes at the molecular level.

The effects of NSAIDs on human muscle adaptation may be context dependent. In older individuals, daily consumption of Ibu (1,200 $mg.day^{-1}$) or acetaminophen (ACET; 4,000 $mg.day^{-1}$) during a 12-week programme of progressive resistance training did not impair muscle mass gains, and in some individuals, potentiated muscle hypertrophy and gains in strength (Trappe et al., 2011). Similarly, a moderate dose of Ibu (400 $mg.day^{-1}$) had no detrimental effect on hypertrophy in young individuals (Krentz et al., 2008), whereas a high dose of Ibu (1,200

mg.day^{-1}) attenuated muscle growth and strength gains (Lilja et al., 2018). The effects of local infusion of NSAIDs on human muscle adaptation are also unclear. In one study, NSAID infusion inhibited satellite cell responses to resistance exercise (Mikkelsen et al., 2009), whereas a separate study using an identical infusion protocol found no impact on muscle protein synthesis or gene expression following eccentric exercise (Mikkelsen et al., 2011). These discrepancies across prior studies may reflect underlying differences in age-related inflammatory profiles and training status, highlighting the complexity of interactions between NSAIDs and muscle responses to exercise.

Acute studies have provided further mechanistic insight by demonstrating that NSAID consumption can blunt the exercise-induced increase in muscle protein synthesis following resistance exercise, possibly through reduced prostaglandin signalling. Trappe et al. (2011) reported that skeletal muscle fractional synthesis rate (FSR), measured 24h post-exercise, was significantly increased in the placebo group but remained unchanged in the Ibu and ACET group. This may be partly explained by the observation that NSAID administration attenuates the exercise-induced increase in prostaglandin $F_2\alpha$ ($PGF_2\alpha$) and prostaglandin E_2 (PGE_2) protein levels, lipid mediators known to regulate protein turnover (Shen et al., 2006, Trappe et al., 2001). Earlier in vitro and animal studies showed that prostaglandins released from contracting muscle exert complex effects on protein turnover, stimulating synthesis via $PGF_2\alpha$ and influencing degradation pathways via PGE_2 (Rodemann and Goldberg, 1982, Palmer, 1990, Vandenburgh et al., 1990). However, these studies relied on radioisotope labelling and measured mixed-protein synthesis, limiting the resolution of protein-specific responses. As a result, the exact mechanism of action of NSAIDs on anabolic and catabolic pathways remains unclear. Dynamic proteome profiling offers a more powerful approach by combining stable isotope labelling with peptide mass spectrometry to quantify protein turnover and abundance at the individual level (Camera et al., 2017). We have previously used dynamic proteome profiling to illustrate how specific proteins and pathways are remodelled during C2C12 differentiation (Stansfield et al., 2021). Such resolution is critical for determining whether NSAID treatment impairs or selectively alters these processes.

To address this, the aims of this work were twofold: first, to evaluate the muscle protein synthetic responses to Ibu and PEA treatment using dynamic proteome profiling, assessing

both **bulk fractional synthesis rates (FSR)** and **protein-specific FSR** in response to treatment. Second, to assess proteome remodelling by integrating protein-specific FSR with protein abundance. By intergrating the measurement of protein-specific abundance and synthesis rates the effects of Ibu and PEA on muscle proteome dynamics can be captured in an unbiased manner. Through direct application of these treatments to differentiated myotubes in vitro, this study aimed to provide the first comprehensive analysis of the effects of Ibu and/ or PEA treatment on the synthesis of muscle proteins assessed on a protein-by-protein basis. Furthermore, we provide the first direct comparison of Ibu and PEA on muscle cells to understand as to whether PEA represents a potential, mechanistically distinct alternative to NSAIDs, capable of attenuating inflammation without compromising anabolic signalling or protein synthesis pathways involved in muscle adaptation and recovery.

6.3 Methods

6.3.1 Chemicals, Reagents and Plasticware

Palmitoylethanolamide (PEA; molecular mass 299.5 g/mol) was obtained from Gencor Pacific Ltd (Hong Kong) in powdered form and reconstituted in ethanol to 50 mg/mL (≈167 mM). Stocks were stored at −20 °C and used within 3 weeks, and were diluted in culture media as required for experiments.

Ibuprofen (Ibu; molecular mass 206.29 g/mol) was purchased from Sigma Aldrich (Gillingham, UK) in powdered form and reconstituted in ethanol to 50 mg/mL (≈243 mM). Stocks were stored at −20 °C and used within 3 weeks, and were diluted in culture media as required for experiments.

Dulbecco's modified eagle medium (DMEM), fetal bovine serum (FBS), new-born calf serum (NBCS), penicillin-streptomycin (pen-strep), trypsin-EDTA and horse serum (HS) were purchased from Thermo Fisher Scientific (Oxford, UK). Phosphate buffered saline (PBS) tablets, DMSO and gelatin from porcine skin were purchased from Sigma Aldrich (Gillingham, UK). T75 culture flasks and 6-well culture plates were purchased from Nunc (Thermo Fisher Scientific. Oxford, UK). C2C12 myoblasts were purchased from ATCC (LGC Standards,

Middlesex, UK). All experiments detailed in this manuscript were performed on C2C12s between passage 5 and 10.

6.3.2 Cell Culture

C2C12 murine myoblasts were cultured in gelatin (0.2%) coated 6-well culture plates in humidified 5% CO_2 at 37°C in growth media comprising DMEM, 10% FBS, 10% NBCS and 1% pen-strep solution. Upon reaching ~80% confluence, monolayers were washed twice with pre-warmed PBS and cultured in low serum differentiation media (DM), DMEM, 2% HS and 1% pen-strep. Every 48hr thereafter, DM was removed from monolayers via aspiration and was replaced with fresh media for 7 days. Isotopic labelling of newly synthesised proteins was achieved by supplementing media with 4% deuterium oxide (D_2O). To investigate protein abundance and FSR during late differentiation, separate cell cultures were incubated in DM containing either H_2O or D_2O during 7-10 days of differentiation. Proteins extracted from control cells (DM+H_2O) were used to measure the natural isotopic abundance of proteins in the absence of D_2O.

6.3.3 Cell treatments

Pilot experiments (data not reported) investigated C2C12 myotube viability across a range of PEA (1, 10 and 100µM) and Ibu (1, 10 and 100µM) concentrations, identifying 10µM PEA and 100µM Ibu as optimal doses for subsequent experiments. On day 7 of differentiation, DM was aspirated, monolayers were washed twice with PBS and treated with fresh DM containing either vehicle control (DMSO), PEA (10µM) or Ibu (100µM). Myotubes were then cultured in the respective treatments for 36hr, with protein collected at two different time points (12hr and 36hr) for the analysis of FSR and protein abundance, see Figure 6.1.

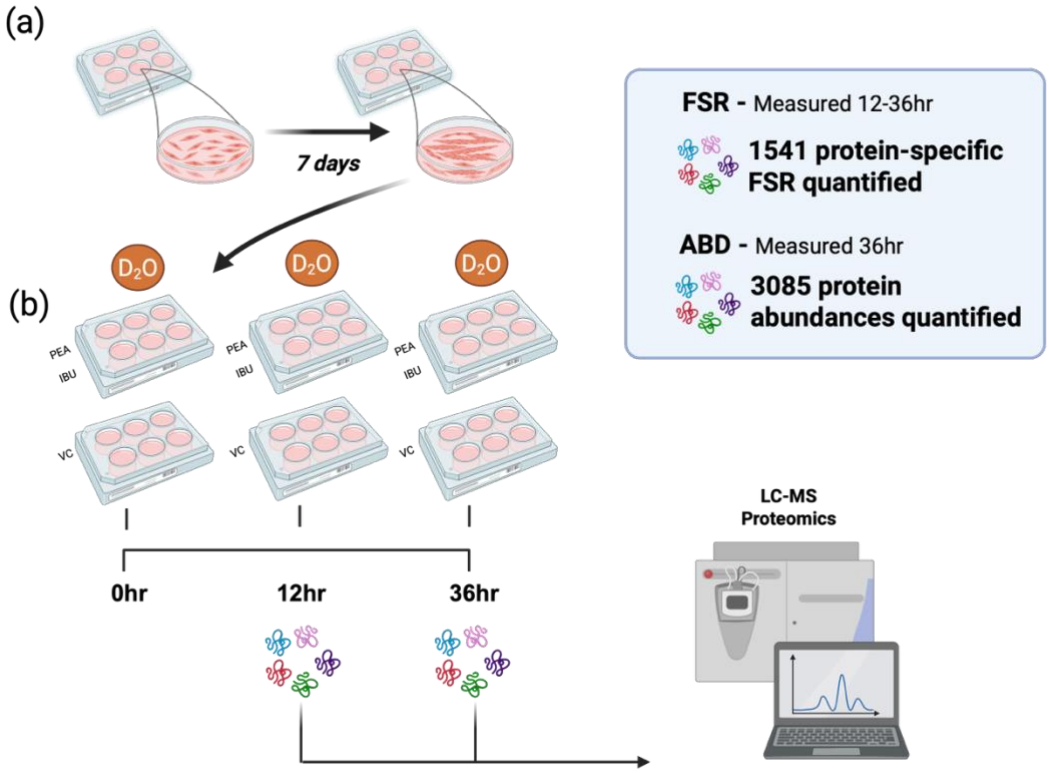

Figure 6.1. Experimental design for assessing protein synthesis and abundance in C2C12 myotubes. (A) C2C12 myoblasts were cultured and differentiated over 7 days until mature myotubes were formed. (B) Myotubes were treated with PEA (10µM), IBU (100µM) or VC for 36hr. Simultaneously, cells were incubated with D2O (deuterium oxide) for isotopic labelling. Protein was harvested at 12 and 36hr post-treatment and analysed using liquid chromatography-mass spectrometry (LC-MS) to quantify both de novo protein synthesis and changes in relative protein abundance over time. Fractional synthesis rates (FSR) were calculated based on deuterium incorporation between 12–36hr, while changes in relative protein abundance (ABD) were determined from total protein levels at 36hr.

6.3.4 Proteomic Analysis

Cells were washed twice with ice-cold PBS, prior to incubation on ice in 250µL/well RIPA buffer (0.5 M Tris-HCL , pH 7.4, 1.5 M NaCl, 2.5% deoxycholic acid, 10% NP-40, 10 mM EDTA) including complete protease inhibitors (Roche; Basel, Switzerland) for 5 min. Thereafter, cells were harvested using a cell scraper and stored at -80°C. Protein concentrations of each protein sample were measured using the Bradford assay (Sigma-Aldrich, Poole, Dorest,

United Kingdom against bovine serum albumin (BSA) standards (0-2 mg mL^{-1}) prepared in RIPA buffer.

Muscle proteins were processed for mass spectrometry by tryptic digestion according to the filter aided sample preparation (FASP) method (Wiśniewski et al., 2009). Lysates containing 100 µg protein were precipitated in 5 volumes acetone at -20 °C for 1 h. After centrifugation (5,000 x g, 5 min), acetone was decanted and the protein pellets were air dried and then resuspended in 200 µl of UA buffer (8 M urea, 100 mM tris, pH 8.5). Samples were incubated at 37 °C for 15 min in UA buffer with 100 mM dithiothreitol (DTT) followed by 20 min at 4 °C in UA buffer containing 50 mM iodoacetamide (protected from light). Samples were washed twice with 100 µl UA buffer and transferred to 50 mM ammonium hydrogen bicarbonate (Ambic). Sequencing grade trypsin (Promega; Madison, WI, USA) in 50 mM Ambic was added at an enzyme to protein ratio of 1:50 and the samples were digested overnight at 37 °C. To terminate digestion, peptides were collected in 50 mM Ambic and trifluoracetic acid (TFA) was added to a final concentration of 0.2 % (v/v). Aliquots, containing 4 µg peptides, were desalted using C_{18} Zip-tips (Millipore, Billercia, MA, USA) and resuspended in 0.1% formic acid spiked with 10 fmol μL^{-1} yeast alcohol dehydrogenase (ADH1) (Waters Corp. Milford, MA) in preparation for liquid chromatography-mass spectrometry (LC-MS/MS) analysis.

6.3.5 Liquid chromatography-tandem mass spectrometry

Peptide mixtures were analysed using an Ultimate 3000 RSLC nano liquid chromatography system (Thermo Scientific) coupled to Q-Exactive orbitrap mass spectrometer (Thermo Scientific). Samples were loaded on to the trapping column (Thermo Scientific, PepMap™ Neo, 5 µm C18, 300 µm X 5 mm), using ulPickUp injection, for 1 minute at a flow rate of 25 µl/min with 0.1 % (v/v) TFA and 2% (v/v) ACN. Samples were resolved on a 110 cm analytical column (µPAC Neo; Thermo Fisher) using a gradient of 97.5 % A (0.1 % formic acid) 2.5 % B (79.9 % ACN, 20 % water, 0.1 % formic acid) to 50 % A: 50 % B over 150 min at a flow rate of 300 nl/min. Data-dependent selection of the top-10 precursors selected from a mass range of m/z 300-1600 was used for data acquisition, which consisted of a 70,000-resolution full-scan MS scan at m/z 200 (AGC set to 3e6 ions with a maximum fill time of 240 ms). MS/MS data were acquired using quadrupole ion selection with a 3.0 m/z window, HCD fragmentation with a normalized collision energy of 30 and in the orbitrap analyzer at 17,500-

resolution at m/z 200 (AGC target 5e4 ion with a maximum fill time of 80 ms). To avoid repeated selection of peptides for MS/MS, the program used a 30 s dynamic exclusion window.

6.3.6 Label-Free Quantification of Protein Abundance

Progenesis Quantitative Informatics for Proteomics (QI-P; Nonlinear Dynamics, Waters Corp., Newcastle, UK) was used for label-free quantitation (LFQ), consistent with previous studies (Stansfield et al., 2021, Brown et al., 2022). MS data were normalized by inter-sample abundance ratio, and relative protein abundances were calculated using nonconflicting peptides only. MS/MS spectra were exported in Mascot generic format and searched against the Swiss-Prot database (2022_08) restricted to 'Rattus' (8,071 sequences) using locally implemented Mascot server (v.2.8 www.matrixscience.com) with automatic target-decoy search. The enzyme specificity was trypsin with 2 allowed missed cleavages, carbamidomethylation of cysteine (fixed modification) and oxidation of methionine (variable modification). M/Z error tolerances of 10 ppm for peptide ions and 20 ppm for fragment ion spectra were used. The Mascot output (xml format), restricted to non-homologous protein identifications was recombined with MS profile data in Progenesis. Protein abundance data was calculated using only unique peptides with identification scores of <1 % false-discovery rate (FDR).

6.3.7 Dynamic proteome profiling

Mass isotopomer abundance data were extracted from MS spectra using Progenesis Quantitative Informatics (Non-Linear Dynamics, Newcastle, UK). Consistent with previous work (Stansfield et al., 2021, Brown et al., 2022), the abundances of peptide mass isotopomers were collected over the entire chromatographic peak for each proteotypic peptide that was used for label-free quantitation of protein abundances. Mass isotopomer information was processed using in-house scripts written in Python (version 3.12.4). The incorporation of deuterium into newly synthesised protein was assessed by measuring the increase in the relative isotopomer abundance (RIA) of the m_1 mass isotopomer relative to the sum of the m_0 and m_1 mass isotopomers that exhibits rise-to-plateau kinetics of an exponential regression (Sadygov, 2020b) as a consequence of biosynthetic labelling of proteins *in vivo*.

$$RIA = \frac{m_1}{m_0 + m_1}$$

Equation 1

The plateau in RIA ($RIA_{plateau}$) of each peptide was derived from the total number (N) of ^2H exchangeable H—C bonds in each peptide, which was referenced from standard tables (Holmes et al., 2015), and the difference in the D:H ratio ($^2H/^1H$) between the natural environment (DH_{nat}) and the experimental environment (DH_{exp}) based on the molar percent enrichment of deuterium in the precursor pool, according to (Ilchenko et al., 2019).

$$RIA_{plateau} = 1 - \left(\frac{1}{\left(\frac{1}{1 - RIA(t_0)} \right) + N(DH_{exp} - DH_{nat})} \right)$$

Equation 2

The rate constant of protein degradation (k_{deg}) was calculated between the beginning (t_0) and end (t_1) of each 10-day labelling period. Calculations for exponential regression (rise-to-plateau) kinetics reported in (Ilchenko et al., 2019) were used and *Kdeg* data were adjusted for differences in protein abundance (P) between the beginning (t_0) and end (t_1) of each labelling period.

$$k_{deg} = -\frac{1}{t - t_0} \bullet \ln\left(1 - \frac{RIA(t_1) - RIA(t_0)}{RIA_{plateau} - RIA(t_0)}\right) \bullet \frac{P(t)}{P(t_0)}$$

Equation 3

Fractional synthesis rates (FSR) for individual peptides were derived by multiplying peptide K_{deg} by 100. Individual protein FSR were calculated as the median FSR of unique peptides comprising the parent protein.

3.6.8 Statistical and Bioinformatic Analysis

Unless stated otherwise, data are presented as mean ± standard deviation (SD) and statistical analyses were conducted in R (version 4.5.1). All proteomic data were filtered to exclude proteins that were not quantified across all conditions (VC, Ibu, and PEA) at all in all replicates (n = 3, in each group) to avoid reliance of data imputation. All data were analysed using one-way analysis of the variance (ANOVA) to assess effects of treatment (Ibuprofen or PEA vs

vehicle control). For individual protein abundance and synthesis data, Type I error was assessed following the computation of P values in proteomic and dynamic proteomic data by calculating false-discovery rates (q values) using the 'qvalue' package (R/Bioconductor) (Storey and Tibshirani, 2003). Proteins that exhibited statistically significant ($P < 0.05$) effects of condition on changes in synthesis rates or abundance were included for downstream bioinformatic analysis.

To assess global changes in protein synthesis rates the median fractional synthesis rate was calculated in each replicate and compared between conditions. The similarity between protein-specific synthesis responses to ibuprofen (IBU) and PEA treatment was assessed by Pearson's correlation, comparing $\log_2$ fold changes (treatment/ control) in fractional synthesis rate between conditions. Correlation analysis was conducted using Pearson's correlation to assess the association between protein-specific $\log_2$ fold changes in fractional synthesis rate and abundance within each treatment, to provide an estimate of the relationship between changes in synthesis and proteome remodelling.

Functional enrichment of significantly up- and downregulated proteins was performed using the clusterProfiler package (Yu et al., 2012) with the org.Mm.eg.db database. Gene Ontology biological process (BP), molecular function (MF), and cellular component (CC) terms were tested using the enrichGO function, with adjusted p-values calculated using the Benjamini–Hochberg method. The top 10 most significantly enriched terms were reported and visualised.

For specific analysis of ribosomal proteome responses proteins containing the term "ribosome" in their description were extracted from the full dataset and classified as cytosolic or mitochondrial based on subunit annotation (40S/60S or 28S/39S, respectively). Within the cytosolic subset, proteins were further grouped by subunit (40S or 60S), and median fractional synthesis rate (FSR) and total abundance were calculated per replicate and treatment condition to provide representative subunit-level measures of ribosomal protein dynamics. Data were analysed using one-way analysis of variance (ANOVA) to assess the effect of treatment (ibuprofen and PEA vs. vehicle control). Where a significant main effect of treatment was identified ($P < 0.05$), pairwise comparisons were performed using Tukey's post hoc test to determine differences between treatment and control conditions.

To visualise networks of proteins of interest, bibliometric mining in the Search Tool for the Retrieval of INteracting Genes/proteins using the evidence of interaction sources, experimental verified protein-protein interaction data, gene onology databases, and co-expression data with the minimum required interaction score set at 0.4 (medium confidence) were used (STRING, Version 12). Protein-Protein interaction networks were visualised using the STRINGdb package in R (version 2.12.1) (Szklarczyk et al., 2023). Protein-protein interaction networks were transferred via the RCy4 R packaged (Version 1) and visualised using Cytoscape version 3.9.1 (Shannon et al., 2003).

To assess the relationship between changes in protein synthesis and steady-state abundance, log_2 fold changes (treatment vs. vehicle control) were calculated for each protein. Pearson's correlation analysis was then performed to determine the degree of association between synthesis rate and abundance responses within each treatment condition offering insight into the role of changes in degradation on proteome remodelling.

6.4 Results

6.4.1 Dynamic proteome profiling of C2C12 myotubes

Dynamic proteome profiling was conducted on proteins that had high-quality peptide mass isotopomer profiles. In total, we quantified the fractional synthesis rates (FSR; %/h) and abundance (femtomole/ μg protein; fmol/μg) of 2513 and 3328 proteins, respectively. Prior to statistical analyses, all data were stringently filtered to exclude proteins that were not quantified in all conditions (VC, Ibu, and PEA) across all replicates (n = 3 in each group) following 36 h of treatment. After filtering, 1541 protein-specific FSR were quantified across the 12 – 36h measurement period in all conditions and replicates. Furthermore, 3085 protein abundances, quantified after 36 h of VC, Ibu, or PEA treatments, were submitted for statistical analysis.

6.4.2 Mixed Protein Fractional Synthesis Rates (FSR)

Global changes in protein synthesis rates were assessed by calculating mixed-protein FSR for each sample (median FSR of 1541 individual protein FSRs). One-way ANOVA revealed no significant difference ($p = 0.184$) in the mixed protein FSR between VC (0.88 ± 0.25 %/h), Ibu (1.37 ± 0..38 %/h), and PEA (1.27 ± 0.24 %/h) (Figure 6.2A). Differences in protein synthetic responses (log_2 fold change treatment/ control) showed limited concordance between Ibu and PEA treatments ($R^2 = 0.34$, $P < 0.001$), indicating that while the overall direction of response was similar, each treatment induced distinct protein-specific alterations (Figure 6.2B).

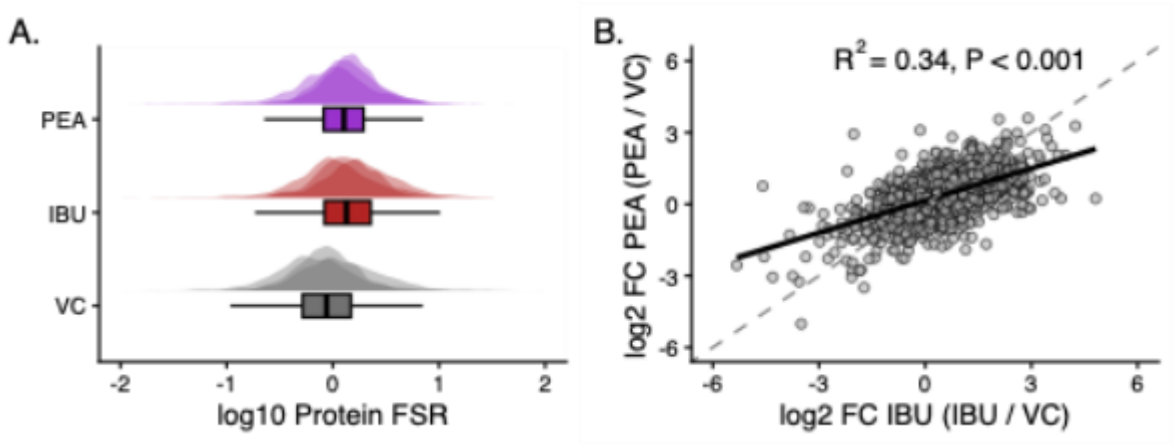

Figure 6.2. Global differences in fractional synthesis rates (FSR) across experimental conditions. Density plots illustrate the distribution of (log2-transformed FSR values; %/h) across each sample replicates (n = 3) for each condition: vehicle control (VC, grey), palmitoylethanolamide (PEA, blue), and ibuprofen (IBU, red). Boxplots represent condition-level summary of global protein synthesis rates, highlighting both PEA and IBU treatment show greater (stats reporting) global FSRs compared to VC. (B) Scatterplot visualising differences in the changes of protein-specific FSR between IBU and PEA conditions. Points reported as mean log2-fold change in FSR in IBU (IBU / VC) or PEA (PEA / VC). Pearson correlation revealed condition-specific changes in proteins between IBU and PEA. Overall highlighting whilst global patterns of changes in FSR may appear similar between conditions (A) the individual proteins responding in FSR are largely different between conditions (B).

6.4.3 Alterations in proteome dynamics in response to Ibuprofen

Protein-specific FSR were quantified across the 12-36 h treatment period and compared using a one-way ANOVA to assess changes in FSR between Ibu and VC conditions on a protein-by-

protein basis. A total of 172 proteins exhibited significant ($p \leq 0.05$, $q < 0.18$) differences in FSR. Among the 172 proteins exhibiting significant differences, > 95 % (165) of proteins increased in synthesis rate in Ibu treated cells. Functional enrichment analysis revealed no clear over-representation of specific gene onotology (GO) terms to be specifically upregulated in synthesis rate following Ibu treatment. Rather, the most enriched terms (adjusted P = 0.79) were associated with generic terms attributed to muscle cell development such as 'supramolecular complex' (39 proteins), 'ribosomal subunit' (14 proteins; Rpl19, Rpl22, Rpl28, Rpl3, Rpl35, Rpl35a, Rpl38, Rplp2, Rps14, Rps19, Rps20, Rps21, Rps27a, and Fau), 'striated muscle thin filament' (4 proteins; Actn3, Tnnt2, Tpm1, and Tpm2) (see Figure 6.3B). Therefore, indicating Ibu to induce a global increase in protein synthesis rates across numerous subclasses of proteins.

To assess the extent of proteome remodelling following Ibu treatment, a separate one-way ANOVA was performed to evaluate differences in protein abundance between Ibu and VC conditions following 36h treatment. A total of 561 proteins exhibited significance ($p \leq 0.05$, $q < 0.16$). In contrast to the global anabolic protein synthetic response, 352 and 209 proteins were upregulated and downregulated in abundance, respectively, following Ibu treatment.

Among the 561 proteins exhibiting significance, 352 were upregulated and 209 were downregulated in response to Ibu treatment. Proteins increased in abundance following Ibu treatment were enriched for GO terms associated with extracellular matrix remodelling (e.g. extracellular matrix; 21 proteins and collagen-containin extracellular matrix; 20 proteins) alongside GO terms 'calcium ion binding' (31 proteins; adjusted P = 0.03), amide binding (18 proteins, adjusted P = 0.03), monocarboxylic acid binding (9 proteins; adjusted P = 0.03), and fatty acid binding (8 proteins; adjusted P = 0.03). Large networks of proteins associated with the GO term 'Myofibril' (26 proteins; adjusted P = 0.17) and ribosome (19 proteins; adjusted P = 0.23) were also increased in response to Ibu treatment (see Figure 6.3D).

From the 208 proteins decreased in abundance following Ibu treatment, functional enrichment analysis identified enrichment of GO terms associated with ribonucleotide binding (50 proteins; adjusted P = 0.03) and carbohydrate metabolic processes (21 proteins; adjusted P = 0.07), including the regulatory subunit (gamma-1) of 5'-AMP-activated protein

kinase (AMPK), hexokinase-2, the pyruvate dehydrogenase (PHD) inhibitor - PDH kinase isozyme 2 and 3 isoenzymes of phosphofructokinase (PFKAL and PFKAP, respectively) (see Figure 6.3E). Thus, indicating Ibu treatment to increase the abundance of proteins associated with muscle growth and structural development alongside re-wiring of metabolic pathways through increased abundance of proteins associated with lipid metabolism and decreased abundance of proteins associated with carbohydrate metabolism.

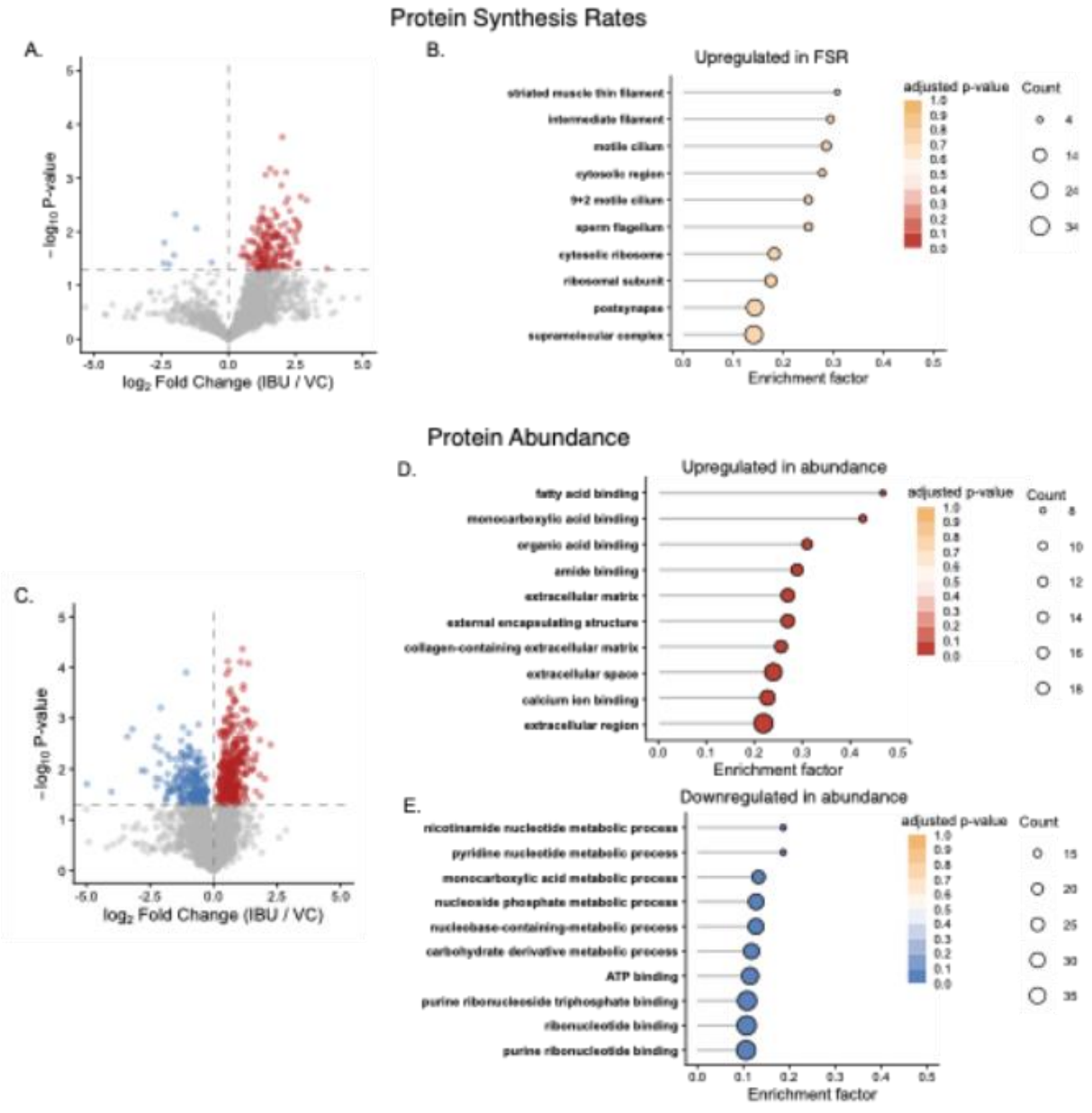

Figure 6.3. Changes in muscle proteome dynamics in response to ibuprofen treatment**.** (A) Volcano plot showing protein-specific changes in fractional synthesis rate (FSR; $\log_2$ fold change IBU / VC, x-axis) and corresponding $-\log_{10}$ p-values (y-axis). Points represent individual proteins detected across conditions; colours denote significantly (P<0.05) upregulated (red)

and downregulated (blue) proteins relative to vehicle control (VC). (B) Gene Ontology (GO) enrichment analysis of proteins with increased FSR following ibuprofen treatment. (C) Volcano plot showing protein abundance changes (log_2 fold change IBU / VC). (D–E) GO enrichment analyses for proteins with increased (D) or decreased (E) abundance. Point size indicates the number of proteins in each GO term, and colour intensity reflects the adjusted p-value.

6.4.4 Alterations in proteome dynamics in response to Palmitoylethanolamide

Protein-specific FSR were quantified across the 12-36 h treatment period and compared using a one-way ANOVA to assess changes in FSR between PEA and VC conditions on a protein-by-protein basis. A total of 103 proteins exhibited significant ($p \leq 0.05$, $q < 0.43$) differences in FSR. In line with the response to Ibu, 101/103 proteins were increased in synthesis rate in response to PEA treatment. A number of the top 10 enriched GO terms were comprised of terms associated with the ribosome and in particular a network of 8 proteins associated with the 40S small ribosomal subunit (Npm1, Rps14, Rps16, Rps2, Rps20, Rps27l, Rps3, Rps8) were significantly increased in synthesis rate in response to PEA treatment (see Figure 6.4B). Furthermore, from a total of 75 proteins significantly ($p \leq 0.05$, $q < 0.99$) changed in protein abundance following PEA treatment, GO terms associated with translation and the ribosome were significantly enriched (adjusted $P < 0.001$) within the 39 proteins upregulated in PEA treated cells. These included 14 proteins comprising the ribosome (Rpl10, Rpl13a, R pl22, Rpl28, Rpl3, Rpl35, Rpl35a, Rpl36, Rpl7, Mrpl28, Rps14, Rps20, Rps27, Rps3) (see Figure 6.4D). Therefore, highlighting PEA results in similar global increases in protein synthetic responses, however, results in much more targeted and coordinated proteome remodelling primarily focussed on upregulation of ribosomal proteins.

In contrast GO terms associated with the 36 proteins decreased in abundance following PEA treatment highlighted a downregulation of proteins associated with regulation of the immune response (Abcd3, Slc12a2, Slc15a4, Slc27a4, Septin2) (see Figure 6.4E).

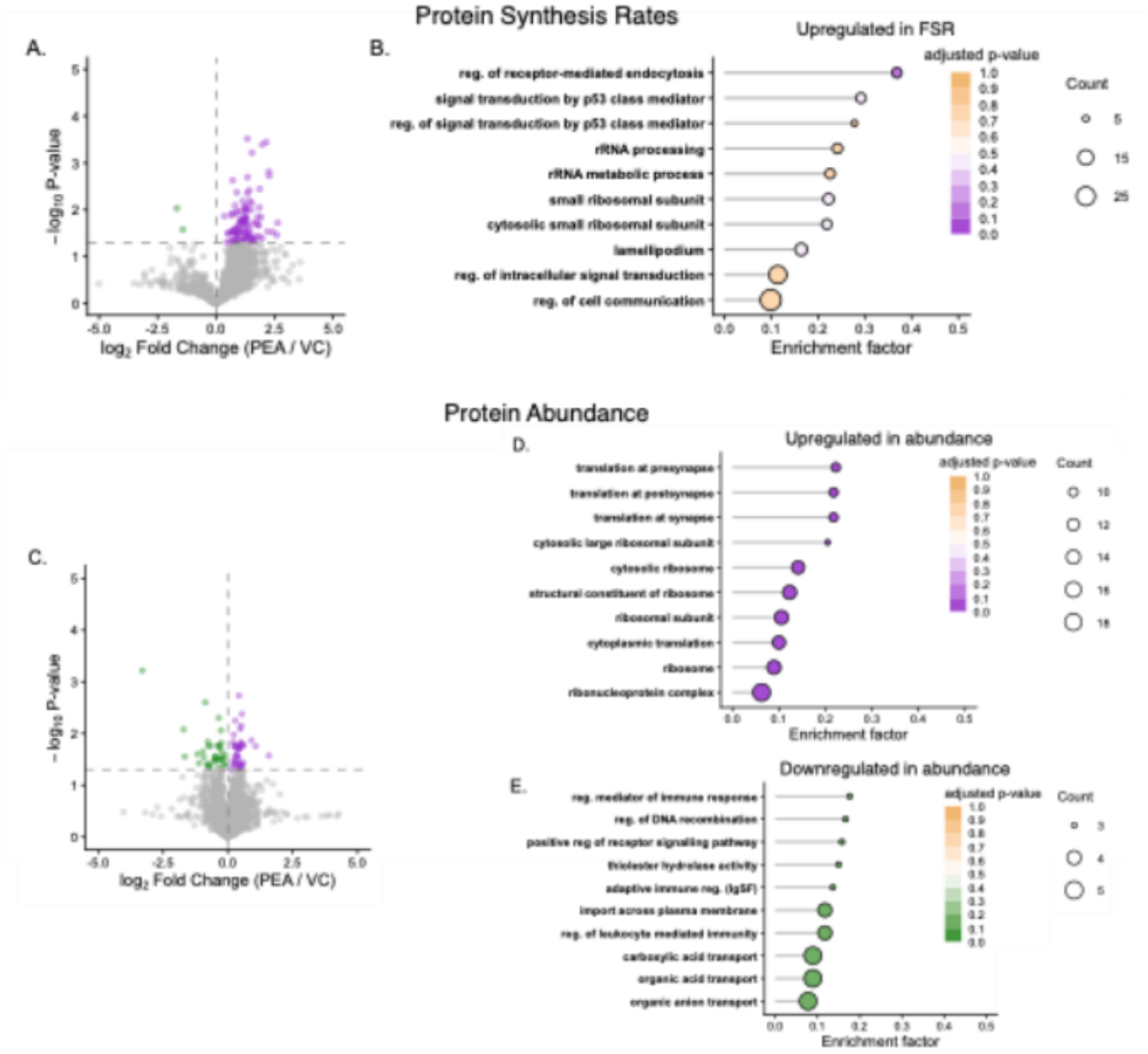

Figure 6.4. Changes in muscle proteome dynamics in response to PEA treatment. (A) Volcano plot showing protein-specific changes in fractional synthesis rate (FSR; log_2 fold change PEA / VC, x-axis) and corresponding $–log_{10}$ p-values (y-axis). Points represent individual proteins detected across conditions; colours denote significantly (P<0.05) upregulated (purple) and downregulated (green) proteins relative to vehicle control (VC). (B) Gene Ontology (GO) enrichment analysis of proteins with increased FSR following PEA treatment. (C) Volcano plot showing protein abundance changes (log_2 fold change PEA / VC). (D–E) GO enrichment analyses for proteins with increased (D) or decreased (E) abundance. Point size indicates the number of proteins in each GO term, and colour intensity reflects the adjusted p-value.

6.4.5 Ibuprofen and PEA increase ribosomal protein abundance and turnover

Following the observation of changes in networks of ribosomal proteins being a core component of the response to PEA and IBU, we aimed to assess changes in mixed-ribosomal synthesis rate and total ribosome abundance following different treatments. Both PEA and Ibu induced significant increases in ribosomal protein synthesis rate, across both the 40S and 60S ribosomal subunit. The 40S subunit showed a significant treatment effect (P = 0.032), with IBU (+67 %; P = 0.06) and PEA (+80 %; P = 0.04) both increased relative to control (0.61 ± 0.09 %/h) (see Figure 6.5B). Similarly, 60S subunit synthesis rates were higher following IBU (+90 % ; P = 0.012) and PEA (+79 %; P = 0.021) compared with control (0.65 ± 0.13 %/h) (see Figure 6.5C). Indicating similar increases in ribosomal protein synthesis in response to both PEA and Ibu.

Both treatments induced a coordinated upregulation of ribosomal protein abundance across subunits. The 40S subunit increased by +17 % with ibuprofen (53.5 ± 2.83; P = 0.056) and +18 % with PEA (55.9 ± 2.98; P = 0.014) relative to control (47.3 ± 1.60) (see Figure 6.5D). The 60S subunit showed a comparable pattern, rising by +15 % with ibuprofen (76.9 ± 9.8) and +20 % with PEA (80.3 ± 5.8) versus control (66.8 ± 2.7; P = 0.11 (see Figure 6.5E). Indicating, both treatments induced concordant increases in ribosomal protein abundance and synthesis, indicating stimulation of ribosome biogenesis and enhanced ribosomal protein turnover.

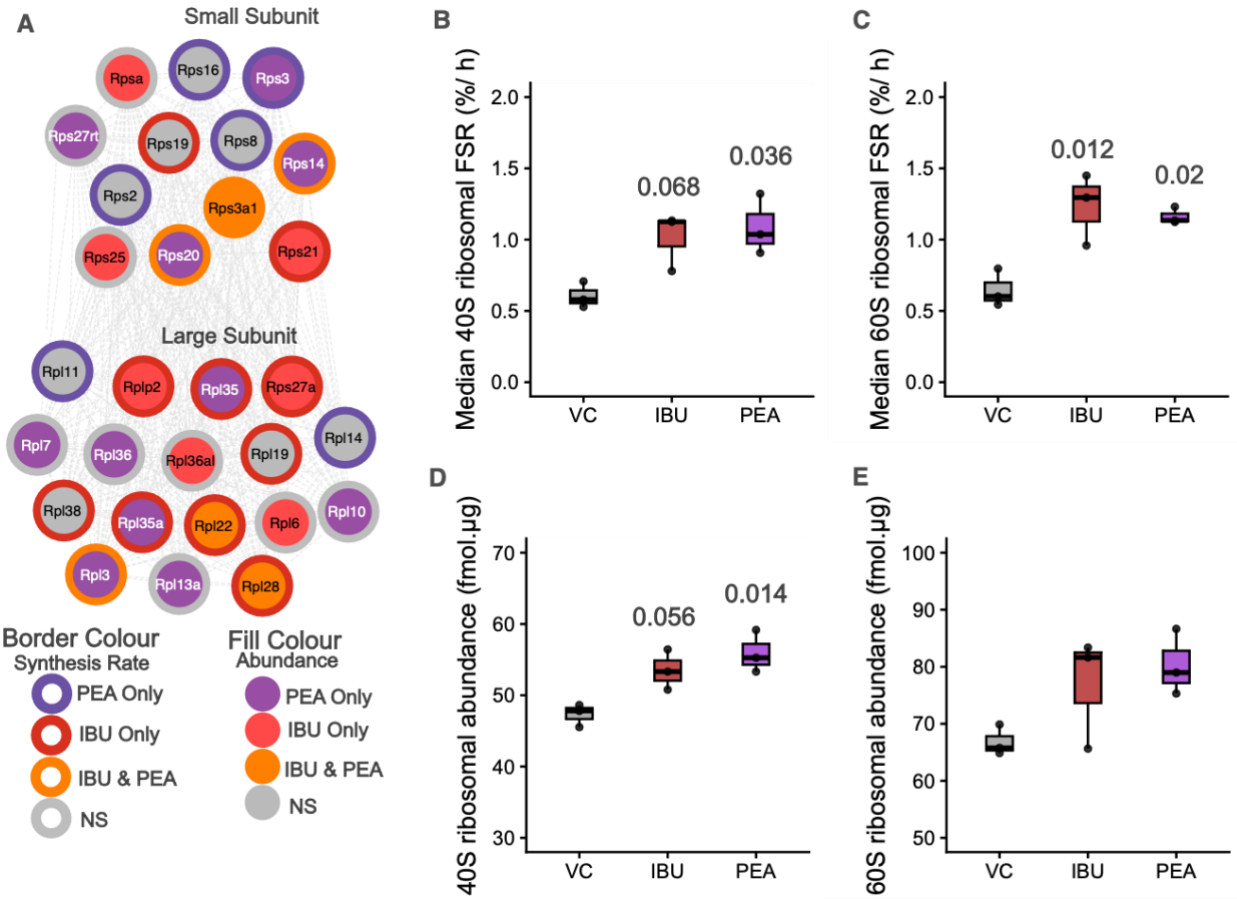

Figure 6.5. Effects of IBU and PEA treatment on ribosomal protein synthesis and abundance**.** (A) STRING-based network visualisation of cytosolic ribosomal proteins significantly changed in synthesis rate and /or abundance in response to different treatments. Each node represents a ribosomal protein from the large (60S) or small (40S) subunit, with border colour denoting proteins significantly altered in synthesis rate and fill colour denoting changes in abundance. Purple = PEA-specific, red = IBU-specific, orange = shared between PEA and IBU, grey = non-significant (NS). (B–C) Median ribosomal protein fractional synthesis rate (FSR, %/ h) for the 40S (B) and 60S (C) subunits. (D–E) Ribosomal protein abundance (fmol/ µg) for the 40S (D) and 60S (E) subunits. (B-E) Text annotations in panels represent Tukey-adjusted P-values for comparisons between each treatment and vehicle control-treated C2C12 cells.

6.4.6 Relationship between changes in protein synthesis and proteome remodelling

To assess the relationship between changes in protein synthesis and abundance, correlation analyses were performed across all quantified proteins for both IBU and PEA treatments (Figure 6). For IBU, changes in fractional synthesis rate (FSR) were moderately correlated with changes in abundance (R^2 = 0.36, P < 0.001), indicating that approximately one-third of the variation in protein abundance could be explained by alterations in synthesis rate (Figure 6.6A). In contrast, the relationship was markedly weaker following PEA treatment (R^2 = 0.08, P < 0.001), suggesting a more transient co-regulation of changes in abundance and synthtesis rate (Figure 6.6B). Together, these findings indicate that IBU-induced proteome remodelling more strongly reflects sustained changes in protein synthesis, whereas PEA elicits a comparatively decoupled response between synthesis and accumulation indicating a coordinated increase in protein degragradtion alongside synthesis resulted in relatively little protein abundance accumulation.

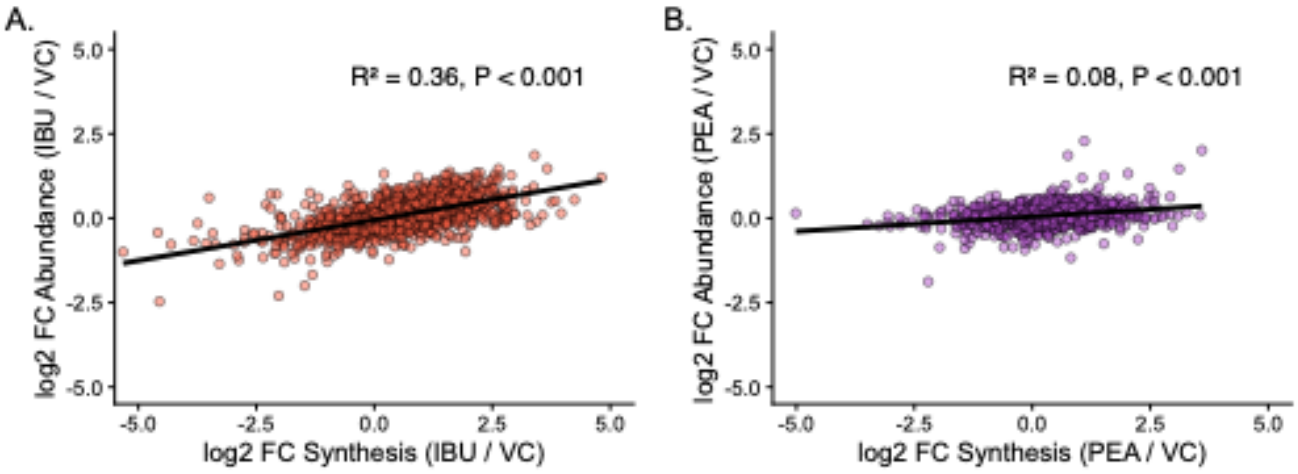

Figure 6.6. Contribution of changes in synthesis to proteome remodelling. Scatterplots show the relationship between protein-specific changes in fractional synthesis rate (FSR; x-axis) and protein abundance (ABD; y-axis) following (A) ibuprofen (IBU) or (B) palmitoylethanolamide (PEA) treatment, expressed as log_2 fold change relative to vehicle control (VC). Each point represents an individual protein detected in both datasets. Black lines denote linear regressions ± 95 % confidence intervals. The coefficient of determination (R^2) and associated p values are shown within each panel

6.5 Discussion

This study provides the first proteome-wide analysis of the effects of ibuprofen (Ibu) and palmitoylethanolamide (PEA) on proteome dynamics in skeletal muscle cells. Using high-resolution mass spectrometry-based proteomics combined with deuterium oxide labelling, we resolved the abundance and synthesis rates of 3328 and 2513 proteins, respectively, across vehicle control (VC), Ibu, and PEA-treated C2C12 cells. Our findings demonstrate that both Ibu and PEA enhance the synthesis and abundance of ribosomal proteins. However, Ibu induced a broader spectrum of remodelling associated with increased abundance of extracellular matrix and contractile proteins alongside increased abundance of enzymes associated with lipid metabolism and concomitant decreases in the abundance of proteins associated with carbohydrate metabolism. Whereas PEA-induced proteome remodelling was more specific resulting in increased synthesis and abundance of predominantly only ribosomal proteins.

Previous studies have suggested that NSAIDs can suppress aspects of translational regulation and ribosomal biogenesis and are therefore, inhibitory to the acute remodelling process following exercise. For example, ibuprofen and indomethacin have been shown to inhibit insulin-stimulated rRNA synthesis in myoblasts (Palmer et al., 1989), while acute ibuprofen ingestion blunts post-exercise increases in the phosphorylation of p70S6K and ribosomal protein S6 in human skeletal muscle (Markworth et al., 2014). However, these acute effects contrast with findings from prolonged NSAID administration. Recent work reports chronic administration during resistance training does not impair ribosomal biogenesis or hypertrophy (Lilja et al., 2023 and Roberts et al., 2024b). In our current work, Ibu treatment increased both the synthesis rate and abundance of ribosomal proteins, consistent with enhanced ribosome biogenesis (see Figure 6.5). Ribosomal FSR increased by approximately +80–90 % relative to VC, and total ribosomal protein abundance increased by ~15 %. When compared directly, both Ibu and PEA produced concordant increases in ribosomal protein synthesis and abundance, indicating a shared upregulation of translational machinery in response to both treatments. Ribosomal proteome expansion have been highlighted as an early molecular feature of hypertrophic adaptation to resistance training (Stead et al., 2025, Jessen et al., 2024). Therefore, this PEA and Ibu induced increase in ribosomal proteins may suggest a potentially beneficial role in these compounds being used alongside resistance training interventions.

Whilst no interference effect of NSAIDs/ COX inhibitors on resistance exercise outcomes have been reported following chronic training in younger participants (Trappe and Liu, 2013). Studies in older participants reported greater increases in muscle volume and strength in the resistance training plus NSAID group (Trappe et al., 2011). Follow up analysis revealed COX inhibitor consumption during resistance exercise in older individuals enhanced myocellular growth, particularly in Type I muscle fibers (Trappe et al., 2016). Therefore, these data suggest under cicumstances where sufficient muscle protein synthetic responses occur (e.g. in young, healthy individuals following resistance exercise), there may be no further benefit of Ibu/ PEA supplementation combined with training. However, the ageing-specific potentiation of resistance training outcomes may suggest that in contexts where there is impaired protein turnover, there may be a beneficial effect of these treatments as an adjunct supplemement to training. This raises the possibility that modulation of ribosome abundance and turnover via administration of Ibu or PEA may facilitate recovery and adaptation, particularly in the context of exercise-induced muscle damage or recovery or where basal protein turnover is impaired. Interestingly, while both compounds elicited convergent increases in ribosomal protein synthesis and abundance, PEA's effects appeared more molecularly targeted, eliciting predominantly ribosomal remodelling, compared with the broader metabolic and structural remodelling induced by Ibu. This distinction raises an important question as to whether PEA could represent a pharmacological means of selectively enhancing translational capacity without the wider metabolic interference associated with NSAIDs/ COX inhibitors. Therefore, future studies should aim to clarify whether PEA's action on ribosomal pathways contributes to a more specific, adaptive mode of proteome regulation in muscle.

The increase in ribosomal proteins coincided with a broader proteome remodelling characterised by increased abundance of proteins associated with extracellular matrix (ECM) remodelling and muscle contraction. Although ECM remodelling during muscle regeneration and hypertrophy are similar, each processes are distinct with different satellite cell requirements (McCarthy et al., 2011). Previous work investigating the effect of NSAIDs on muscle cells in vitro report high doses, similar to those used in the current work, augments myogenic cell proliferation but have no measurable effect on myotube size (Roberts et al., 2024a). Therefore, highlighting NSAIDS may influence cell cycle progression and myogenic differentiation within skeletal muscle cells, rather than inducing hypertrophy of myotubes.

Organisation and expansion of the ECM is essential for myogenesis (Melo et al., 1996) and proteomic profiling identified the induction of the dystrophin complex, such as dystroglycan and sarcoglycan, was associated with later stage myogenesis (Kislinger et al., 2005). Our current word identified significant enrichment of proteins associated with extracellular matrix proteins (e.g. Thrombospondin-1, Nidogen-2, Dystroglycan 1, and Cathepsins B, L, Z) to be increased in abundance following Ibu treatment. Furthermore, the development and maturation of the contractile apparatus during myogenesis requires a parallel increase in calcium-dependent cycling proteins to handle the rapid fluxes in Ca2+ associated with muscle contractility (MacLennan and Kranias, 2003). Untargetted proteomic profiling during C2C12 myoblast differentiation reported late stage differentiating cells was associated with increased abundance of calcium transporters and proteins linked to skeletal muscle excitation/contraction (such as actin, myosin, troponin, nebulin, titin, desmin, and α-actinin) (Kislinger et al., 2005). In line with these works we identified significant enrichment of calcium handling proteins to be increased in abundance following 36 h of Ibu treatement. Our abundance profiling reports increased abundance of numerous proteins associated with muscle contractile apparatus, including tropopinins (Tnnc1,Tnnt2, and Tnnt3), Tropomyosins (Tpm1 and Tpm2) and myosin light chain proteins (Myl1, Myl4, and Myl9), as well as alpha-actinin-3 (Actn3). Taken together, these data indicate that Ibu promotes a transition of muscle cells toward a pro-myogenic state characterised by ribosomal expansion, ECM remodelling, and maturation of the contractile apparatus. This profile reflects activation of anabolic and structural programmes typical of differentiating or regenerating myotubes, suggesting that NSAID exposure at this stage may increase cellular processes underpinning muscle repair and adaptation.

Beyond its effects on structural remodelling, Ibu treatment also induced coordinated changes in metabolic proteins, suggesting wider metabolic remodelling. In particular, Ibu increased the abundance of proteins involved in lipid and fatty acid binding (e.g., fatty acid translocase CD36 and fatty acid-binding protein 3). CD36 is a key regulator of long-chain fatty acid uptake and oxidation in skeletal muscle, and muscle-specific ablation of CD36 impairs exercise-induced increases in fatty-acid oxidation despite normal mitochondrial biogenesis (McFarlan et al., 2012). Furthermore, Ibu decreased the abundance of proteins associated with carbohydrate metabolism, including key glycolytic enzymes like hexokinase-2, phosphofructokinase (PFKAP;

platelet type and PFKAL; liver type) and pyruvate dehydrogenase kinase isozyme 3 (PDK3). Notably, PFKAP also plays an important role in linking macrophage activation to glycolytic control and NADPH metabolism (O'Neill and Pearce, 2016, Kelly and O'neill, 2015). Under normal conditions, transient macrophage activation promotes glycolysis to generate NADPH that supports antioxidant defence and tissue-repair signalling. However, chronic suppression of these pathways, such as repeated or high-dose NSAID exposure, as applied in the current work, could attenuate glycolytic metabolism, resulting in a re-organisation of metabolic pathways towards enhanced lipid utilisation. While the present study involved acute exposure of Ibu directly to muscle cells in vitro, a reduced interaction of macrophages and muscle cells might be expected in vivo where greater macrophage–muscle cross-talk occurs. Therefore, Ibu-induced decreases in prostaglandin-mediated signalling may alter metabolic phenotype in vivo. Because previous NSAID-muscle studies were largely hypothesis-driven (e.g., focusing on ribosomal biogenesis or cell cycle status) such metabolic adaptations induced by NSAIDs have been likely overlook, which could have important implications for exercise-induced adaptation where NSAIDs are used alongside training. Furthermore, during myogenic differentiation, muscle metabolism traditionally transitions from glycolytic to more oxidative, with mitochondrial biogenesis and fatty-acid oxidation pathways up-regulated (Hughes et al., 1999). This metabolic switch further supports structural protein responses, highlighting a change in cell status toward a more mature, oxidative, contractile phenotype. Taken together, the metabolic signature we observe aligns with the pro-myogenic programme evidenced by ECM/contractile enrichment in Ibu treated muscle cells reinforcing the concept that Ibu promotes a shift in cell cycle characteristics towards that of later stage myogenic differentiation.

The connection between changes in protein synthesis rate and abundance differed between Ibu and PEA treatments. In response to Ibu treatment, there was a moderate positive correlation between FSR and protein abundance ($R^2 = 0.36$) (see Figure 6.6A), suggesting that increases in synthesis was associated with protein accumulation. This coordinated pattern suggests an anabolic profile of proteome remodelling, comparable to that observed following resistance exercise (Camera et al., 2017, Stead et al., 2025), where elevated synthesis drives net accretion of structural and contractile proteins. In contrast, the relationship between protein synthesis and abundance following PEA treatment was weak ($R^2 = 0.08$; Figure 6.6B),

despite a marked increase in synthesis rates across 101 proteins. Furthermore, statistical analysis identified 75 of 3085 proteins with nominally significant changes in abundance ($P \leq 0.05$). However, the uniformly high q-values (all = 0.99) indicate that although PEA stimulated changes in protein synthesis rates, this was not accompanied by measurable accumulation of proteins within the 36 h treatment window. Therefore, suggesting enhanced synthesis without net proteome remodelling. This decoupling between synthesis and accumulation indicates an elevation in global protein turnover, reflecting a equal balance between protein synthesis and degradation. Increased turnover is a key component of muscle protein homeostasis and is recognised as essential for maintaining protein quality in skeletal muscle (Sandri, 2013, Brown et al., 2022, Srisawat et al., 2024). PEA may therefore facilitate improvements in proteome quality control within muscle, thus aiding recovery processes following acute exercise or damage through increased degradation and recycling of damaged/ dysfunctional proteins. Collectively, these data suggest PEA enhances turnover, which in turn may lead to improvement in muscle proteostasis.

In the present study, no significant differences were observed in mixed-protein FSR between treatments (see Figure 6.2A). However, such measures represent the average synthesis of thousands of proteins, each of which may respond differently to a given intervention. As a result, bulk mixed-protein estimates can mask important, protein-specific effects. Consistent with this, while global FSR appeared similar between treatments, Ibu significantly altered the synthesis of 172 proteins and PEA altered 103 proteins relative to vehicle control (Figures 6.3–6.4). Moreover, the moderate correlation between protein-specific responses to Ibu and PEA (Figure 6.2B) suggests both shared and treatment-specific regulation of synthetic processes. These findings underscore the value of dynamic proteome profiling in revealing selective pharmacological effects on muscle protein metabolism that are invisible to conventional mixed-protein or abundance-based approaches. By resolving individual protein turnover rates, this approach enables identification of subtle yet coordinated shifts in synthesis within distinct molecular networks, providing mechanistic insight into how pharmacological agents, such as NSAIDs or lipid amides, influence the muscle proteome beyond their classical anti-inflammatory actions.

6.6 Limitations

Several limitations should be acknowledged. First, the use of an in vitro C2C12 model allows for the controlled investigation of cellular responses, but it does not capture the systemic complexity of muscle tissue in vivo, including immune, vascular, and neural interactions that may influence drug responses. Moreover, C2C12 cultures contain a subpopulation of unfused myoblasts as identified in previous studies (Veliça and Bunce, 2011), which therefore may introduce variability in protein expression patterns.

This study provides novel mechanistic insight into the direct actions of PEA and Ibu on skeletal muscle, but the pharmacokinetics and metabolism of PEA and Ibu in vivo are not replicated in cellculture studies. Ibu undergoes extensive hepatic metabolism, primarily in the liver, via cytochrome P450 enzymes (mainly CYP2C9) and subsequent glucuronidation, which influences its half-life, tissue distribution, and local concentration (Rainsford, 2009). PEA, on the other hand, is primarily metabolised locally within tissues, including the liver, intestine, immune cells and skeletal muscle, by the hydrolytic enzymes fatty acid amide hydrolase (FAAH) and N-acylethanolamine-hydrolysing acid amidase (NAAA) (Petrosino and Di Marzo, 2017a). Importantly, the relative contribution of FAAH versus NAAA to PEA metabolism is tissue-dependent and may vary with cell type, pathological state, or whether PEA is endogenously produced or exogenously applied (Petrosino and Di Marzo, 2017a). These enzyme expression patterns and invidual variability introduce significant complexity when translating in vitro results to in vivo, as such, the effects observed in this C2C12 model may differ under physiological conditions where PEA metabolism and distribution are regulated.

Finally, the concentrations used in this study were selected based on prior dose-response experiments and existing literature (Roberts et al., 2024a). One key issue is the use of supratherapeutic concentrations of Ibu in vitro. A review by Graham and Scott (2021) highlights that many of the cellular effects attributed to NSAIDs, including Ibu, are observed only at concentrations that far exceed those attainable in vivo. This is particularly important when considering the high degree of plasma protein binding that limits the free, pharmacologically active fraction of Ibu in circulation (Lin et al., 1987). As a result, in vitro studies using micromolar or even millimolar concentrations may not reflect the true biological activity of Ibu iunder physiological conditions. These discrepancies raise important concerns

regarding the relevance and translatability of such findings to in vivo contexts, where drug metabolism, distribution, and systemic interactions are tightly regulated.

6.7 Conclusion

Acute treatment with ibuprofen (Ibu) and palmitoylethanolamide (PEA) induced largely distinct dynamic proteomic responses in C2C12 myotubes. Interestingly, in response to both treatments we observed a conserved increase in ribosomal protein synthesis and abundance, consistent with enhanced translational capacity in muscle. However, Ibu exerted broader effects on protein-specific remodelling increasing networks of proteins associated with a pro-myogenic phenotype. Potentially highlighting the ability of Ibu to support adaptation and regeneration following exercise and injury. Whereas the response to PEA was mostly specific to only changes in ribosomal protein abundance and induced increases in global rates of protein turnover. Therefore PEA may offer the potential to improve muscle protein homeostasis and quality control pathways without overt proteome reorganisation. These findings demonstrate the value of dynamic proteomics in resolving mechanistic differences between interventions that are not apparent from bulk/ static measures alone and provide mechanistic insight into how Ibu and PEA may influence muscle adaptation and support recovery to acute exercise or injury.

Associated data: All data supporting the findings of this study are available from public repositories. Raw LC–MS/MS data files have been deposited in the PRIDE repository under accession number [**xxxxxx**]. Processed and analysis-ready datasets, along with the full R analysis pipelines used to generate all figures and statistical outputs, are available via GitHub at: https://github.com/cstead27/C2C12_PEA_IBU_Dynamic_Proteomics

Transition to Chapter 7

The data presented in this chapter demonstrates that PEA and Ibu exert distinct yet partially overlapping influences on skeletal muscle proteostasis, with PEA emerging as a more targeted modulator of ribosomal capacity and Ibu eliciting broader remodelling of metabolic and structural pathways. These mechanistic insights raise important questions about how such cellular signatures translate to functional outcomes in vivo, particularly in the context of

exercise-induced muscle damage where NSAIDs are frequently used despite ongoing concerns regarding their safety and efficacy. To bridge this gap, the next chapter moves from controlled cell-based experimentation to a translational human model, evaluating whether the differential molecular actions of PEA and Ibu observed in vitro correspond to meaningful differences in pain, neuromuscular function, and recovery following downhill running. This progression enables a comprehensive assessment of PEA's potential as a safer alternative to NSAIDs using an ecologically valid exercise model.

Chapter 7

Exploring the efficacy of Palmitoylethanolamide (PEA) versus NSAIDs in Alleviating Exercise-Induced Muscle Damage: A Comparative Investigation in Downhill Running

This chapter investigates the effects of PEA and Ibu on symptoms associated with EIMD induced by downhill running. Given the widespread reliance on NSAIDs among endurance athletes, despite concerns regarding their efficacy and safety, this study sought to evaluate whether PEA could serve as a safer alternative. Using a controlled, double-blind, randomised design, the chapter examines neuromuscular function, perceived pain, and renal markers across recovery to provide a translational assessment of PEA's efficacy and safety in an ecologically relevant model of EIMD.

7.1 Abstract

Introduction: Ultra-endurance running (>42.195km), often involves extensive downhill running (DR), leading to exercise-induced muscle damage (EIMD), of which pain and loss of function are key markers. Consequently, anti-inflammatory and pain medication use is common in athletes during competition and training. NSAID use in athletes is controversial, may not have ergogenic benefits and may be associated with adverse effects, including gastrointestinal and renal dysfunction. Palmitoylethanolamide (PEA), an endogenous fatty acid with anti-inflammatory and analgesic properties, offers a potentially safer alternative with no known side effects. This study investigates the efficacy of PEA and Ibuprofen (IBU), compared to Placebo (PLA), in alleviating symptoms of EIMD. **Methods:** Twelve healthy individuals were acclimated to DR during a 4-week training programme, consisting of 9 (15-30min) sessions on a motorised treadmill at different negative gradients (-5/-10/-15%) and a running speed equivalent to 60-65% VO_2max. After session 9, participants were randomised in a double-blind manner to receive: PLA (1000mg/day), PEA (600mg/day), or IBU (800mg/day) along with 4% deuterium oxide (D_2O) for 10 days for muscle protein synthesis measurement. At day 3 of supplementation, participants performed a 50-minute DR (-15-17%) to induce muscle damage. Blood for the analysis of kidney function and maximal isometric voluntary torque (MIVT), voluntary activation (VA) and torque frequency (TF) was measure**d** pre- and immediately post-DR and at 24h, 48h, 5d and 7d post-exercise. A Visual Analog Scale (VAS) was used daily during the 7d recovery to assess pain. A two-way mixed ANOVA was used to detect changes between time and condition, with significance set at $p \leq 0.05$. All data are expressed as mean±SD. **Results:** The DR protocol induced moderate muscle damage, evidenced by a ~20% reduction in MIVT immediately post-exercise that persisted for 48 h across all groups ($p < 0.001$, $\eta_p^2 = 0.64$). VA decreased significantly post-exercise ($p < 0.001$, $\eta_p^2 = 0.82$), with a significant time × condition interaction ($p = 0.009$, $\eta_p^2 = 0.38$); VA was lower in PEA compared to Ibu immediately post-exercise ($p = 0.027$). Control doublet force declined post-exercise across all conditions ($p < 0.001$, $\eta_p^2 = 0.61$), with a time × condition interaction ($p = 0.043$, $\eta_p^2 = 0.32$). Torque-frequency analysis revealed significant main effects of time and frequency (both $p < 0.001$), with low-frequency fatigue evident post-exercise, but no condition effects. PMP decreased over time ($p < 0.001$, $\eta_p^2 = 0.86$), with complete pain resolution by day 7 in both PEA and Ibu groups compared to persistent pain in PLA ($p < 0.001$). Estimated glomerular filtration rate (eGFR) decreased immediately post-exercise ($p < 0.001$) but returned to baseline by 24 h, with no differences between conditions. Other kidney function markers (sodium, potassium, urea) remained within normal ranges throughout. **Conclusion:** Daily PEA supplementation (600 mg/day for 10 days) did not significantly enhance recovery of muscle function following moderate EIMD induced by downhill running. However, complete resolution of perceived muscle pain by day 7 in both PEA and Ibu groups compared to placebo suggests a potential delayed analgesic effect. Neither intervention adversely affected kidney function. Given the established safety profile of PEA and known risks associated with chronic NSAID use, PEA may represent a promising alternative for pain management in endurance athletes, though larger studies are needed to confirm these findings.

7.2 Introduction

Exercise-induced muscle damage (EIMD) often occurs following unaccustomed or high-intensity eccentric exercise, particularly in modalities such as downhill running (DR) (Giandolini et al., 2016, Bontemps et al., 2019). Symptoms typically present within several hours to days post-exercise and include reductions in muscle strength and power, increased perceived muscle pain (PMP), and elevated circulating levels of muscle-specific proteins and inflammatory markers (e.g., creatine kinase, TNF-α) (Ebbeling and Clarkson, 1989, Hyldahl and Hubal, 2014, Douglas et al., 2017). In addition to systemic responses, EIMD, particularly following prolonged and DR, has been shown to impair neuromuscular function through both central and peripheral mechanisms (Millet et al., 2003, Garnier et al., 2018). Central fatigue arises from impaired neural drive or motor unit recruitment within the central nervous system, while peripheral fatigue reflects dysfunction at or beyond the neuromuscular junction, including impairments in muscle excitation and contraction processes (Kirkendall, 1990). Neuromuscular impairments, together with elevated pain perception and sustained inflammatory responses, may hinder subsequent performance and delay return to training or competition for athletes. Accordingly, there is a growing interest in alternative nutritional and pharmacological strategies that aim to mitigate EIMD and accelerate recovery.

In ultra-endurance events, where performance is influenced by a complex interplay of psychophysiological and environmental factors, certain markers of EIMD can be exacerbated and accumulate over time. While the grade-specific biomechanical and structural alterations associated with the downhill running component in ultra-endurance events have been identified as a key factor limiting performance (Bontemps et al., 2020), a growing body of research suggests that pain is also a major performance limiter in ultra-endurance athletes (Tiller and Millet, 2025). The mechanical trauma associated with muscle damage elicits a local inflammatory response, presenting as swelling, pain, and soreness. Heightened perceptions of pain and soreness frequently arise mid-race and often lead to a decline in running velocity, ultimately impairing performance (Tiller and Millet, 2025). Therefore, strategies that can effectively alleviate pain and preserve muscle function are highly relevant to both athletic performance and recovery.

Nonsteroidal anti-inflammatory drugs (NSAIDs), such as ibuprofen, remain among the most frequently used pharmacological interventions for managing EIMD symptoms due to their proven efficacy in reducing inflammation and pain management. Research highlights widespread use among both recreational and elite athletes, particularly during endurance events where pain management is prioritised. However, regular NSAID use is not without risk. Gastrointestinal bleeding, renal stress, and cardiovascular complications are well-documented, particularly during endurance exercise where blood flow to visceral organs is reduced (Warden, 2009, Pannone and Abbott, 2024). Furthermore, inflammation constitutes the body's innate response to EIMD, and suppression of this response may interfere with adaptive signalling pathways, potentially impairing muscle adaptation following damage (review in Schoenfeld (2012). Indeed, some studies have demonstrated that NSAIDs may blunt satellite cell activity, inhibit muscle protein synthesis, and impair anabolic responses to training (Trappe et al., 2002, Mikkelsen et al., 2009), though others have shown that these effects may be context- and dose-dependent.

Palmitoylethanolamide (PEA) has emerged as a potential alternative to NSAIDs. PEA is an endogenous lipid amide with analgesic and anti-inflammatory properties, primarily mediated through the activation of peroxisome proliferator-activated receptor-alpha (PPARα) and transient receptor potential vallinoid 1 (TRPV1) (Marini et al., 2012, Ambrosino et al., 2013). Supplementation with PEA, at doses ranging from 300 to 1200 mg, has been shown to reduce pain in various clinical conditions, including osteoarthritis, carpal tunnel syndrome, and severe headaches, with efficacy comparable to that of ibuprofen (Lang-Illievich et al., 2023, Briskey et al., 2021, Briskey et al., 2022). In contrast to NSAIDs, PEA does not appear to disrupt muscle anabolic signalling, as a recent training study demonstrated that daily PEA supplementation (300mg) over 8 weeks of resistance training did not impair skeletal muscle hypertrophy or functional gains (Huschtscha et al., 2024). However, evidence supporting PEA's role in muscle recovery remains limited, with only two studies to date examining its effects, both reporting no significant benefits of acute supplementation on muscle soreness or strength recovery following eccentric exercise in healthy males (Mallard et al., 2020, Schouten et al., 2024). Notably, both studies focused exclusively on acute dosing strategies and assessed recovery in the days following isolated resistance-based protocols, potentially limiting generalisability to

prolonged or metabolically demanding exercise. Moreover, neither study evaluated physiological safety markers nor directly compared PEA to NSAIDs.

Therefore, the aim of the present study was to evaluate the efficacy of daily PEA supplementation (600mg/day for 10 days) compared to ibuprofen (Ibu) (800mg/day for 10 days) in alleviating symptoms of EIMD, specifically impairments in muscle function and perceived muscle pain following downhill running. Additionally, this study sought to assess the renal safety profile of both interventions. Hypothesis to be tested?

7.3 Methods

7.3.1 Ethical Approval

This study was granted ethical approval by Liverpool John Moores University Research Ethics and Governance Committee (UREC reference: 23/SPS/064). All samples and data were collected and stored according to the Sixth Declaration of Helsinki. All participants were informed of the experimental procedures and gave their written informed consent before any testing was conducted.

7.3.2 Participants

Thirteen healthy individuals volunteered to take part in the study but one withdrew during the study for personal reasons. A total of 12 adults (10 males and 2 females; age: 25.15±2.09 years; maximal oxygen uptake: 52.8±8.5 mL/min/kg) completed the study. An a priori power analysis was conducted using G*Power software (v3.1.9.6, Heinrich-Heine-Universitat Dusseldorf, Dusseldorf, Germany) based on the data from Bontemps et al. (2022) for muscle function changes over time (effect size f: 0.5; α: 0.05; Power (1-β):0.80), 12 participants were necessary for the present study. This sample size allowed for the allocation of 4 participants to each independent experimental group, ensuring balanced group distribution in line with the study design. Subjects were recruited broadly from the student population of Liverpool John Moores University (LJMU, Liverpool, UK). All participants were screened for inclusion as described in the General Methods chapter (Chapter 3) of this thesis.

7.3.3 Study Design

Participants were required to visit the LJMU research laboratory on 15 separate occasions: (i) familiarisation (1st visit), (ii) downhill running training programme (9 visits), (iii) EIMD trial and recovery (5 visits). The study employed a parallel-group, double-blind, randomised controlled design consisting of three independent groups, each receiving a different supplement condition. During the first visit, participants arrived ~8am following an overnight fast and restricted caffeine intake. Bioelectrical impedance analysis was performed to assess body composition, along with the collection of baseline blood, urine and muscle samples. Participants were also familiarised with the three different tests used to assess force, function and fatigue on an isokinetic dynamometer (IKD) (Humac Norm, CSMI, Massachusetts, USA). Following this, participants were asked to perform a maximal exercise test on a motorized bi-directional treadmill (H/P Cosmos ® Pulsar 3P, Traunstein Germany) to determine each subject's VO_{2peak} (see section 3.15*).* After a 15-minute recovery period, participants were familiarised with the DR at three different declines (-5%, -10% and -15%; DR5, DR10, DR15, respectively) at speeds associated with 60-65% VO_{2peak} for each decline (familiarization duration: 10-15-minutes). Subsequently, subjects were familiarized with the other experimental procedures. Participants were then randomized in a double-blind manner by an independent researcher, who assigned each individual to group A, B, or C using a pre-determined randomisation list. These group codes corresponded to one of three supplement conditions (PLA, PEA, or IBU), with the identity of each condition concealed from both participants and investigators until data collection was complete**.** Subsequent visits were dedicated to DR training sessions and D20 enrichment and experimental visits. The 11th visit was the EIMD trial, which involved a 50-minute downhill run (-17%) and measurements collected pre and post exercise. The remaining visits were time-stamped (24 hours, 48 hours, 5 days and 7 days) to assess recovery.

7.3.4 Training Programme Overview

The DR training programme consisted of 9 supervised sessions conducted in the research laboratory, under the constant supervision of the primary investigator, for a total duration of four consecutive weeks (Figure 7.1). This structured training phase was implemented to

minimise inter-individual variability in responsiveness to eccentric exercise, to control for the repeated-bout effect by standardising prior exposure to downhill running, and to replicate the progressive conditioning period typically undertaken by athletes before competition or heavy training blocks. The training sessions were scheduled at the same time of day (±1.5 hours) and spaced at least 48 hours apart for passive rest. All DR training sessions involved running on a motorized treadmill secured using a dedicated chest harness, at three consecutive and continuous declines (-5%, -10%, and -15%), at a metabolic intensity corresponding to the speed associated with 60-65% of peak oxygen uptake (VO_{2peak}) for each slope, respectively. These speeds were estimated during a familiarisation session and adjusted if necessary, during the first training session using the same respiratory gas exchange analyser, then kept constant throughout the experimental intervention. The average speeds associated with 60-65% VO_{2peak} were as follows: -5% 10.9±0.9, -10% 11.8±1.1, -15% 12.7±1.2. The total effective running time (ranging from 15 to 30 minutes) and workload (i.e., increasing the effective running time at the different declines) were gradually increased during the training protocol. The final (10th) DR session consisted of a 50-minute run at a -17% decline, performed at the highest speed achieved by the participant during the training programme, with the objective of inducing muscle damage. Before each treadmill running session, subjects performed a warm-up comprising 5 minutes of running at +1% incline and 3 minutes at -10%, at a metabolic intensity corresponding to the speed associated with 60-65% VO_{2peak}.

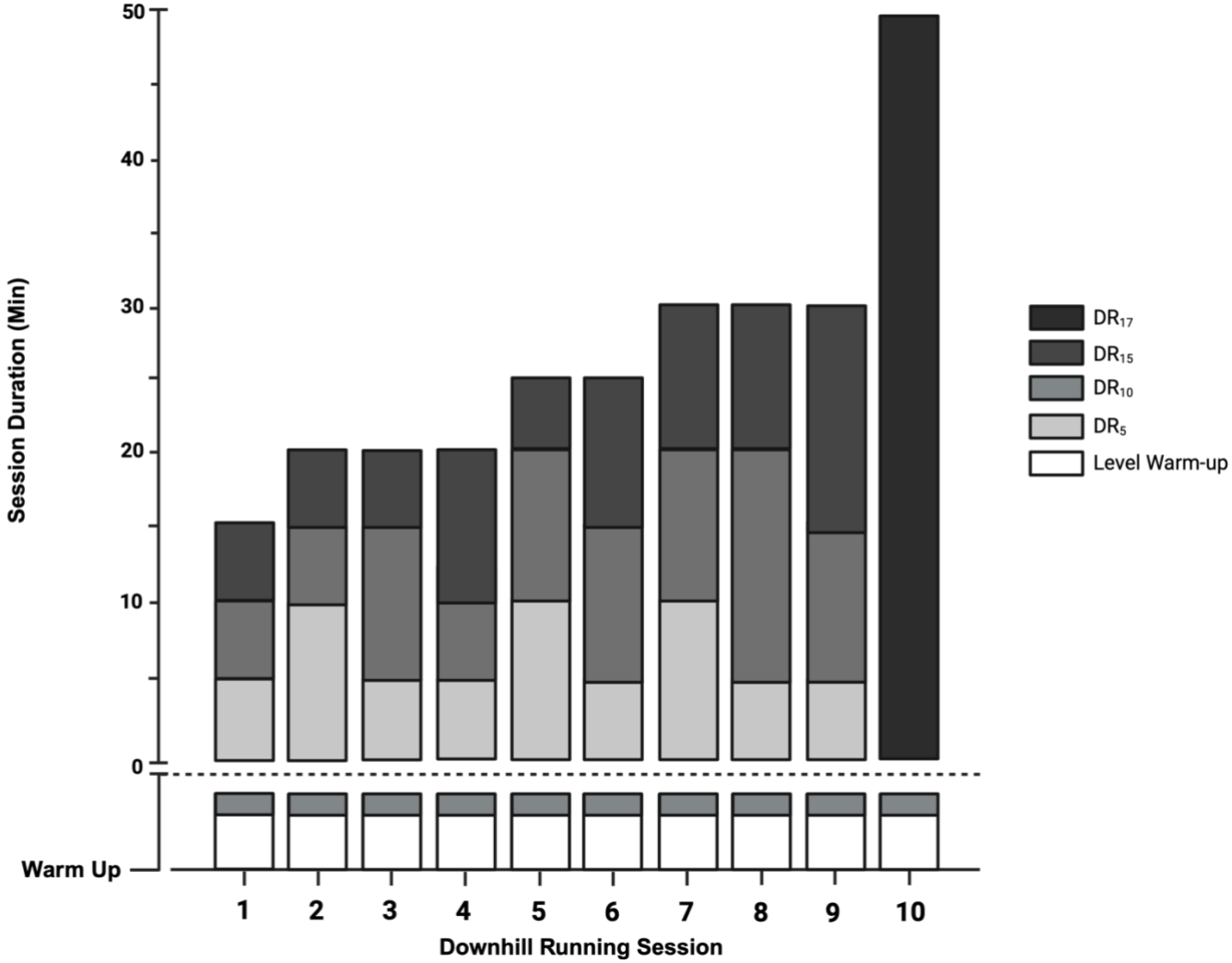

Figure 7.1. Schematic overview of the downhill running (DR) training programme. Bars represent each separate DR training session, split into the four negative slopes (-5%, -10%, -15% and -17%; i.e. DR_5, DR_{10}. DR_{15} and DR_{17}, respectively). Adapted from Bontemps et al. (2022).

7.3.5 Experimental Protocol

Participants received their assigned supplement and D_2O (see Section 7.3.6 - 7.3.7) upon completing their ninth DR session and were instructed to begin consumption five days later. Supplementation commenced three days prior to participants returning to the laboratory to complete the final (10th) DR session. Prior to exercise, a series of physiological assessments were conducted, including blood and urine sampling, a muscle biopsy from the vastus lateralis of the left leg, and neuromuscular function tests of the right leg, specifically measuring knee-extensor (KE) isometric maximal voluntary torque (MVT), voluntary activation (VA), and the torque-frequency (TF) relationship. Participants then completed a 50-minute DR session at a -17% decline, performed at the highest speed reached during the training programme. Immediately post-exercise, the same physiological measurements were repeated. To assess perceived muscle pain, participants were provided with a visual analogue scale (VAS), which they were required to complete daily for seven days. Follow-up laboratory visits occurred at 24 hours, 48 hours, 5 days, and 7 days post-exercise, during which the same physiological measurements were performed, with muscle biopsies collected only at the 24-hour and 7-day time points.

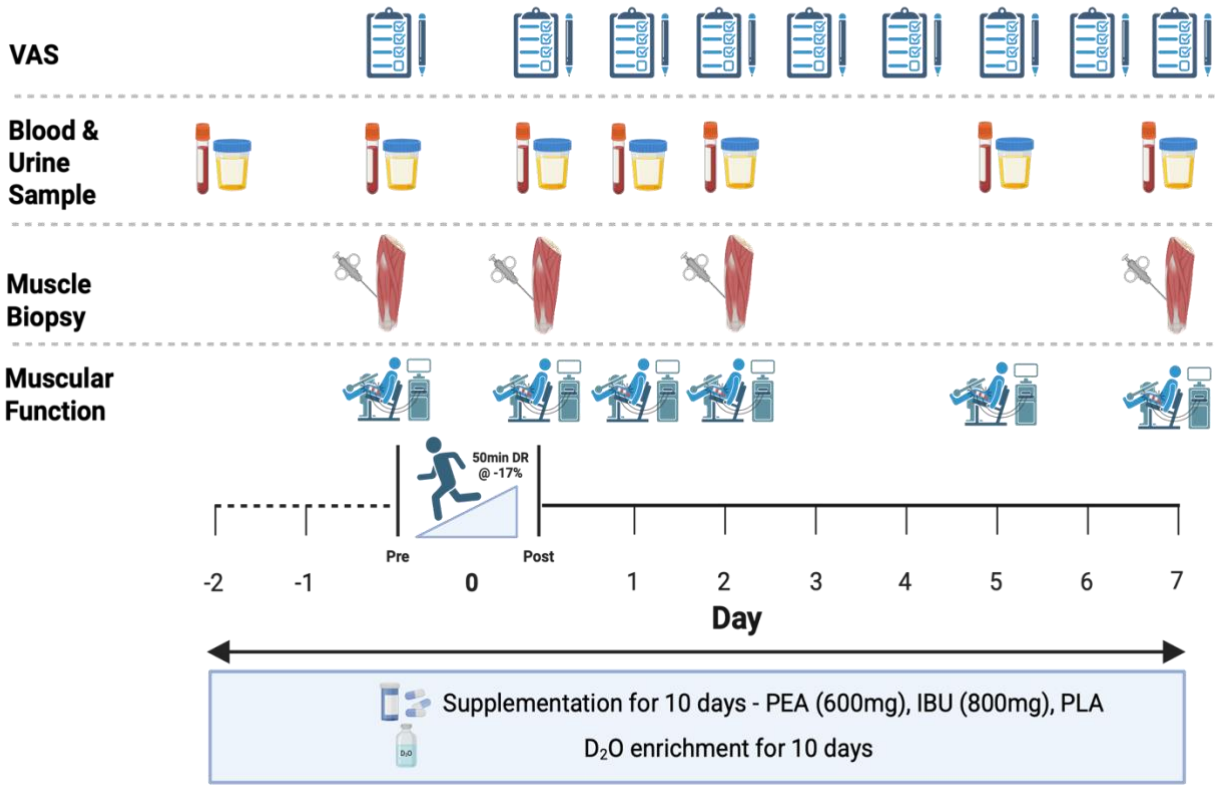

Figure 7.2. Schematic overview of the experimental protocol. Participants began supplementation and D_2O enrichment three days prior to their final (10th) downhill running (DR) session. Pre-exercise physiological assessments were conducted before participants completed a 50-minute DR bout at a −17% gradient, performed at the highest speed reached during the training programme. The same assessments were repeated immediately post-exercise, with recovery monitored over the following seven days by conducting repeated physiological measurements.

7.3.6 Treatments

Participants were randomly assigned in a double-blind manner (see section 7.3.3) to one of three supplementation groups: Palmitoylethanolamide (PEA), Ibuprofen (IBU), or Placebo (PLA). PEA was provided in the form of Levagen+ at a dosage of 600 mg/day (2 x 150mg tablets taken twice daily) and IBU at 800 mg/day (2 x 200mg tablets taken twice daily). PLA was provided as maltodextrin (2 x 250mg tablets taken twice daily). Participants were instructed to consume their assigned supplement twice in the morning (8:00 AM ± 1 hour) and twice in the evening (6:00 PM ± 1 hour). Compliance was monitored by supervising morning doses where possible, sending reminders for evening doses, and requesting that participants return their supplement containers at the end of the study to verify adherence.

7.3.7 Stable Isotope Labelling

Deuterium oxide (D_2O) dosing consisted of a 'loading phase' followed by a 'maintenance phase'. Labelling commenced on day -2 of each measurement period. During the loading phase (days -2 and -1), participants consumed ten doses of 0.66 $mL \cdot kg^{-1}$ body mass of 99.8 atom % D_2O (Sigma-Aldrich) approximately one hour apart each day, resulting in a total loading dose of 13.2 $mL \cdot kg^{-1}$ body mass. To maintain D_2O enrichment, participants consumed a single daily dose of 0.66 $mL \cdot kg^{-1}$ body mass D_2O throughout the measurement period (8 days).

7.3.8 Food Provision

On days where participants completed a DR session and during the 10 days of supplementation, participants were required to follow a standardised diet to control macronutrient intake (i.e. 1g/kg fat, 1.5 g/kg protein and 3-5 g/kg carbohydrates).

Individualised meal plans were provided, ensuring macronutrient distribution was tailored to each participant's body weight. As food was not provided to participants, they were informed of the most affordable supermarkets to purchase their food. Prior to the start of the study, all participants were screened for dietary requirements and food allergies. Any necessary adjustments were incorporated into their individualised meal plans to accommodate specific needs.

After each DR session, participants were required to consume a recovery shake (MRM Muscle Recovery Drink Powder, NutritionX, Gloucester, UK) formulated with a 2:1 carbohydrate-to-protein ratio, providing 30 g of protein and 60 g of carbohydrates per serving. The serving size was adjusted based on body weight to align with the standardised dietary intake outlined above. The provision of recovery shakes aimed to minimise the risk of injury, support adequate recovery before subsequent DR sessions, and standardise post-exercise nutritional intake. Participants were instructed to refrain from using any additional nutritional supplements (e.g. protein powders, creatine, or anti-inflammatory supplements) throughout the study period, to reduce potential confounding effects.

7.3.9 KE Isometric MVT

KE isometric MVT was assessed using a Human Norm isokinetic dynamometer (IKD) (Human Norm, CSMI, Massachusetts, USA) and analysed using AcqKnowledge software (Biopac Systems Inc., Goleta, CA, USA). Participants were seated and secured according to the standardised positioning described in Section 3.16.1 of this thesis. Following a standardised warm-up (10 submaximal isokinetic extensions at $60°\cdot s^{-1}$), participants performed three maximal voluntary isometric contractions (3 s each) with 60 s rest between each contraction. Real-time visual feedback and verbal encouragement were provided. Peak torque (Nm) was calculated for each trial, with the highest value used for further analysis.

7.3.10 Voluntary Activation (VA)

Voluntary activation was assessed using the interpolated twitch technique (ITT), as previously described elsewhere (Erskine et al., 2009, Erskine et al., 2010, Marshall et al., 2014). Briefly, participants were positioned on the IKD (see Section 3.16.1) and stimulation electrodes were

placed on the skin distally and proximally over the vastus medialis and lateralis (see Section 3.16.2). Supramaximal stimulation (DS7AH, Digitimer, UK) was delivered to elicit a resting doublet torque by increasing the amplitude in 50 mA increments until an involuntary torque plateau was observed, with a further ~10% increase to ensure supramaximal stimulation. After a 2-minute rest, participants performed a 3-second maximal voluntary contraction (MVC), during which a superimposed doublet was delivered at the torque plateau and at rest prior to the MVC. This procedure was repeated 3 times with 2-minute rest between trials and the highest MVC was used for subsequent analysis. A standard equation was then used to calculate voluntary activation: (*VA (%) = [1 – (superimposed doublet torque/control doublet torque)] x 100*.

7.3.11 Torque-Frequency Relationship

The torque-frequency relationship was assessed using percutaneous electrical stimulation of the quadriceps, with electrode placement and participant positioning as described in Sections 3.16.1 and 3.16.2 of this thesis. Stimulation was delivered at 1, 10, 15, 20, 30, 50, and 100 Hz (1 s per pulse, random order) with 15 s rest between stimuli. The amplitude was set to evoke ~30% MVC torque at 100 Hz at baseline and was used consistently at all time points (PRE, POST, 24h, 48h, 5d, and 7d). The absolute torque at each frequency was normalised to the torque at 100Hz for each time point.

7.3.12 Perceived Muscle Pain

Perceived muscle pain (PMP) was evaluated daily for 7 days following the EIMD trial using an ungraded visual analogue scale (VAS). Participants were asked, "How severe is your pain today? (localized to the quadriceps)." The scale was anchored at two points: 'No Pain' at score 0 and 'Pain as bad as it could be' at score 100 (Haefeli and Elfering, 2006). Participants completed the VAS twice daily, once in the morning (~8 AM ± 1 hour) and once in the evening (~6 PM ± 1 hour). For both sessions, they were instructed to complete the VAS after sitting sedentary for 5 minutes and again after performing 5 slow squats, emphasizing the eccentric phase of the movement.

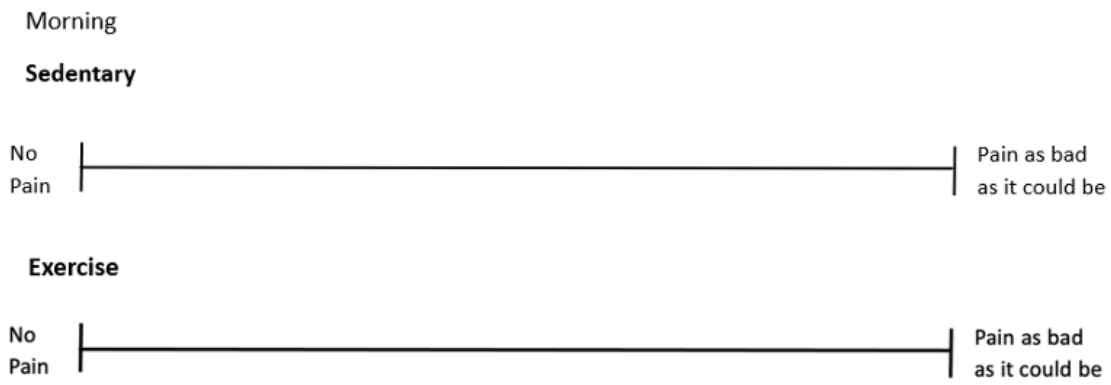

Figure 7.3. Visual analogue scale (VAS) for rating perceived muscle pain (0-100 mm type). Schematic representation not to scale.

7.3.13 Kidney Function Tests

Venous blood samples were collected from participants via standard phlebotomy procedures (see section 3.14) in serum separator tube (SST) vacutainers and centrifuged at 2500 RCF for 15 minutes at 4°C. Serum aliquots were transported and analysed at the University of Liverpool for biochemical analysis. Quantification of serum potassium, sodium, urea, and creatinine was performed using standard clinical chemistry assays. Estimated glomerular filtration rate (eGFR) was calculated based on serum creatinine concentrations using the Chronic Kidney Disease Epidemiology Collaboration (CKD-EPI) equation (Inker et al., 2021). Venous blood samples were collected at seven time points: baseline, immediately before and after the 10th DR session, and at 24 hours, 48 hours, 5 days, and 7 days post-exercise.

7.3.14 Muscle Biopsy

A detailed description of the muscle biopsy procedure is provided in Section 3.15 of this thesis. Briefly, participants arrived at the muscle biopsy suite at Liverpool John Moores University (~8.30 am) and rested while the biopsy site (left vastus lateralis) was prepared under sterile conditions. Local anaesthetic (bupivacaine hydrochloride) was administered, and a small incision was made to extract the tissue sample using a Weil-Blakesley conchotome. Muscle biopsies were collected at six time points: baseline, after DR session 4, immediately before and after the 10th DR session, and at 48 hours and 7 days post-exercise. All samples were prepared for subsequent analysis. A portion of each biopsy was mounted and processed for

immunohistochemical analysis to assess ultrastructural muscle alterations via electron microscopy. The remaining tissue was snap-frozen in liquid nitrogen for later analysis of protein abundance and synthesis rates, quantified using LC-MS. Analysis of these samples was not completed within the project timeframe due to unforeseen equipment issues and time constraints, and consequently, the data are not included in this thesis.

7.3.15 Statistical analysis

All statistical analyses were conducted in SPSS (version 29.0.2.0) and figures produced in Prism (version 10.2.3). A two-way mixed analysis of variance (ANOVA) was conducted to examine the interaction between experiment condition (PLA, PEA, IBU) and time (Pre, Post, 24h, 48h, 5d and 7d) for outcome measures including maximal isometric voluntary torque, voluntary activation, resting control doublet force, kidney function markers and average pain scores across time. For torque-frequency, a three-way mixed ANOVA was first performed to examine the effects of condition, time and frequency (1 Hz, 10 Hz, 15 Hz, 20 Hz, 30 Hz, 50 Hz) on evoked torque. To further explore within-condition patterns, separate two-way repeated-measures ANOVAs (time x frequency) were conducted for each experimental condition. Where Mauchly's test of sphericity had been violated, Greenhouse-Geisser ($\varepsilon < 0.75$) or Huynh-Feldt ($\varepsilon > 0.75$) corrections were applied. Where appropriate, significant main effects or interactions ($p < 0.05$) were followed up with Fisher's LSD post-hoc pairwise comparisons. Partial eta squared (η_p^2) effect sizes were reported for each statistical model, and the thresholds for η_p^2 are defined as small ($\eta_p^2 = 0.01$), medium ($\eta_p^2 = 0.06$), and large ($\eta_p^2 = 0.14$) (Cohen, 2013).

7.4 Results

7.4.1 Maximal Isometric Voluntary Contraction

A two-way mixed ANOVA revealed a significant main effect of time on maximal isometric voluntary torque (MIVT) ($p < 0.001$, $\eta_p^2 = 0.64$) (Figure 7.4). Pairwise comparisons (Fisher's LSD) indicated a significant reduction in MIVT immediately post-exercise ($p < 0.001$), as well as at 24 h ($p < 0.001$) and 48 h ($p = 0.004$) compared to pre-exercise values. Furthermore, MIVT at 24 h and 48 h was significantly lower than at 5 d and 7 d post-exercise ($p < 0.005$), and values at 5 d remained significantly lower than at 7 d ($p = 0.046$). No significant interaction between time and condition was detected ($p = 0.83$, $\eta_p^2 = 0.11$), nor was there a significant main effect of condition on MIVT ($p = 0.92$, $\eta_p^2 = 0.02$).

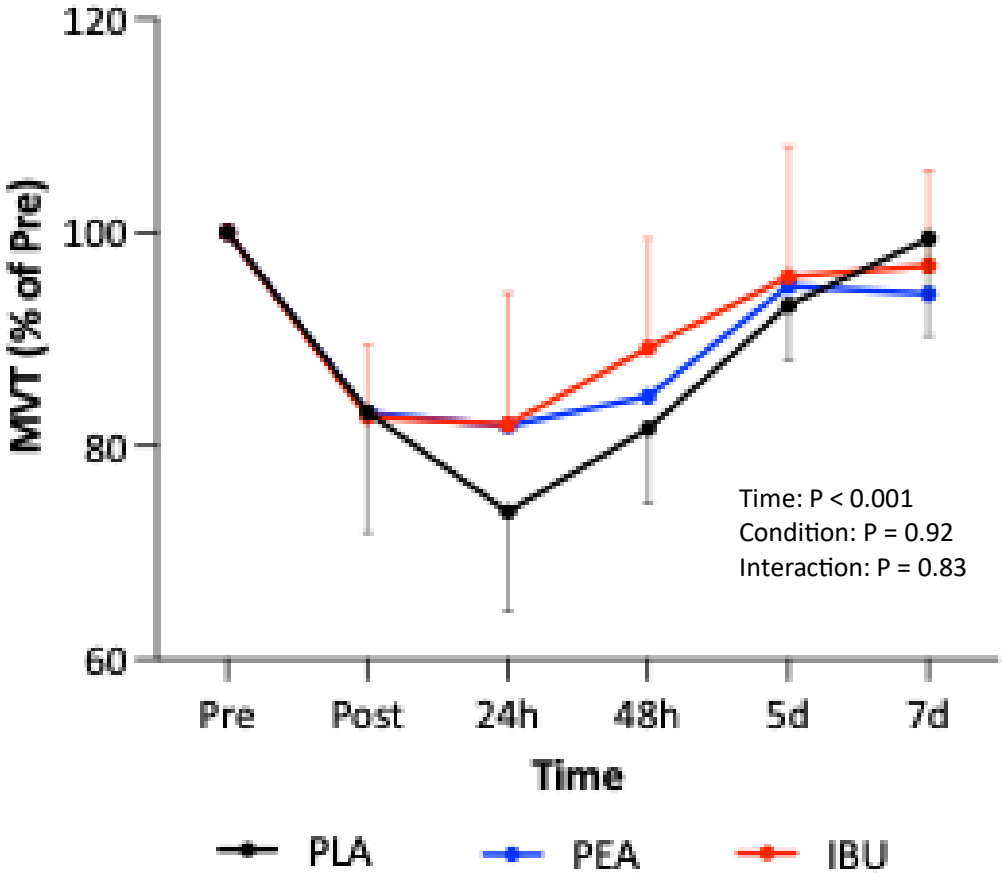

Figure 7.4. Changes in maximal isometric voluntary torque (MIVT) normalised to pre-exercise values (%) over time. Black line**:** placebo (PLA); blue line: palmitoylethanolamide (PEA); red line**:** ibuprofen (Ibu).Data are presented as mean ± SEM.

7.4.2 Voluntary Muscle Activation

A two-way mixed ANOVA revealed a significant main effect of time on voluntary activation (VA, %) ($p < 0.001$, $\eta_p^2 = 0.82$) (Figure 7.5). Pairwise comparisons (Fisher's LSD) indicated that VA (%) was significantly reduced immediately post-exercise ($p < 0.001$), as well as at 24 h ($p = 0.002$) and 48 h ($p < 0.001$) compared to pre-exercise. Additionally, VA (%) at 24 h was significantly lower than at 5 d ($p = 0.035$) and 7 d ($p = 0.003$), and VA (%) at 48 h remained significantly reduced compared to 5 d ($p = 0.027$) and 7 d ($p = 0.002$). There was a significant time × condition interaction ($p = 0.009$, $\eta_p^2 = 0.38$). Pairwise comparisons (Fisher's LSD) revealed immediately post-exercise, VA (%) was significantly lower in the PEA group compared to the Ibu group ($p = 0.027$). No significant main effect of condition on VA (%) was observed ($p = 0.761$, $\eta_p^2 = 0.05$).

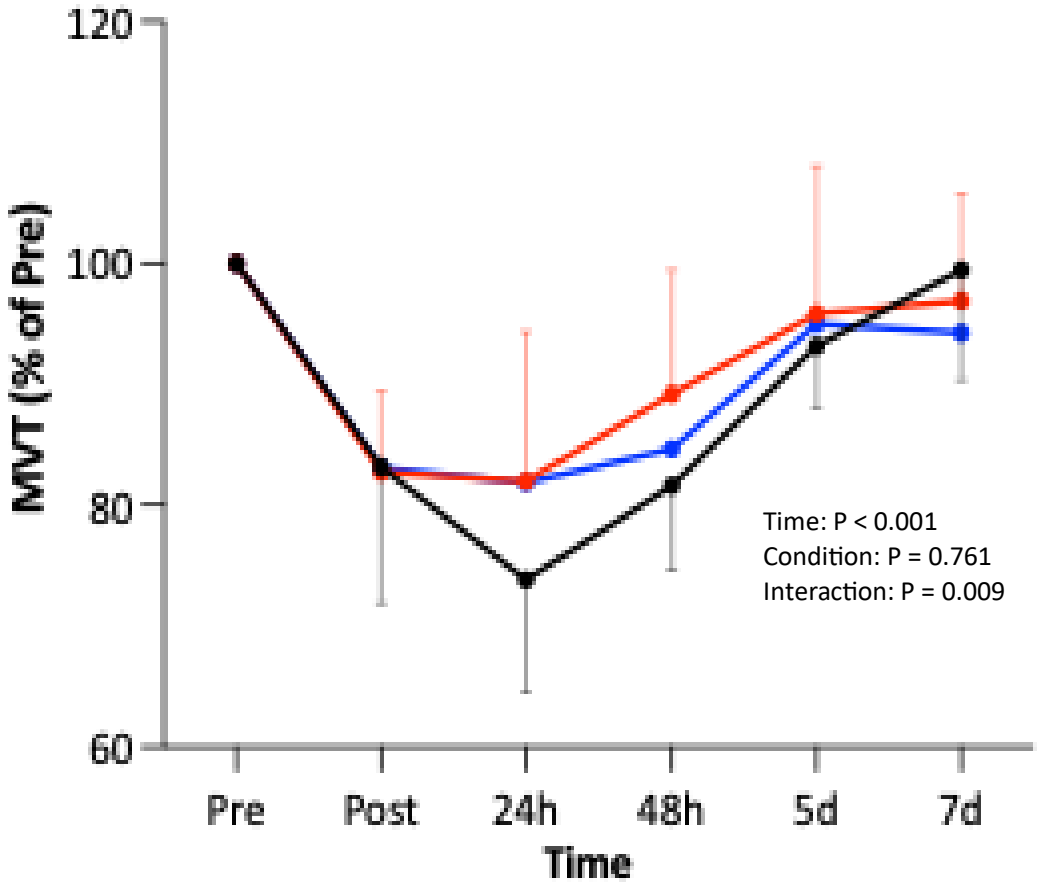

Figure 7.5. Changes in voluntary activation (%) over time. Black line**:** placebo (PLA); blue line: palmitoylethanolamide (PEA); red line**:** ibuprofen (Ibu). Data are presented as mean ± SEM.

7.4.3 Resting Control Doublet Force

A two-way mixed ANOVA revealed a significant main effect of time on resting control doublet force (% Pre) ($p < 0.001$, $\eta_p^2 = 0.61$) (Figure 7.6). Pairwise comparisons (Fisher's LSD) revealed a significant reduction in control doublet force immediately post-exercise ($p < 0.001$), as well as at 24 h ($p = 0.002$) and 48 h ($p = 0.016$) compared to pre-exercise. Additionally, control doublet force post-exercise was significantly reduced compared to 5 d and 7 d ($p < 0.001$, respectively), as was resting evoked torque at 24 h compared to 5 d ($p = 0.002$) and 7 d ($p < 0.001$). Resting control doublet force remained significantly reduced at 48 h compared to 5 d ($p = 0.029$) and 7 d ($p = 0.016$). There was a significant time × condition interaction ($p = 0.043$, $\eta_p^2 = 0.32$). Pairwise comparisons (Fisher's LSD) revealed that at 5 d, control doublet force was significantly reduced in the PLA group compared to the PEA group ($p = 0.017$). No significant main effect of condition on control doublet force was observed ($p = 0.717$, $\eta_p^2 = 0.06$).

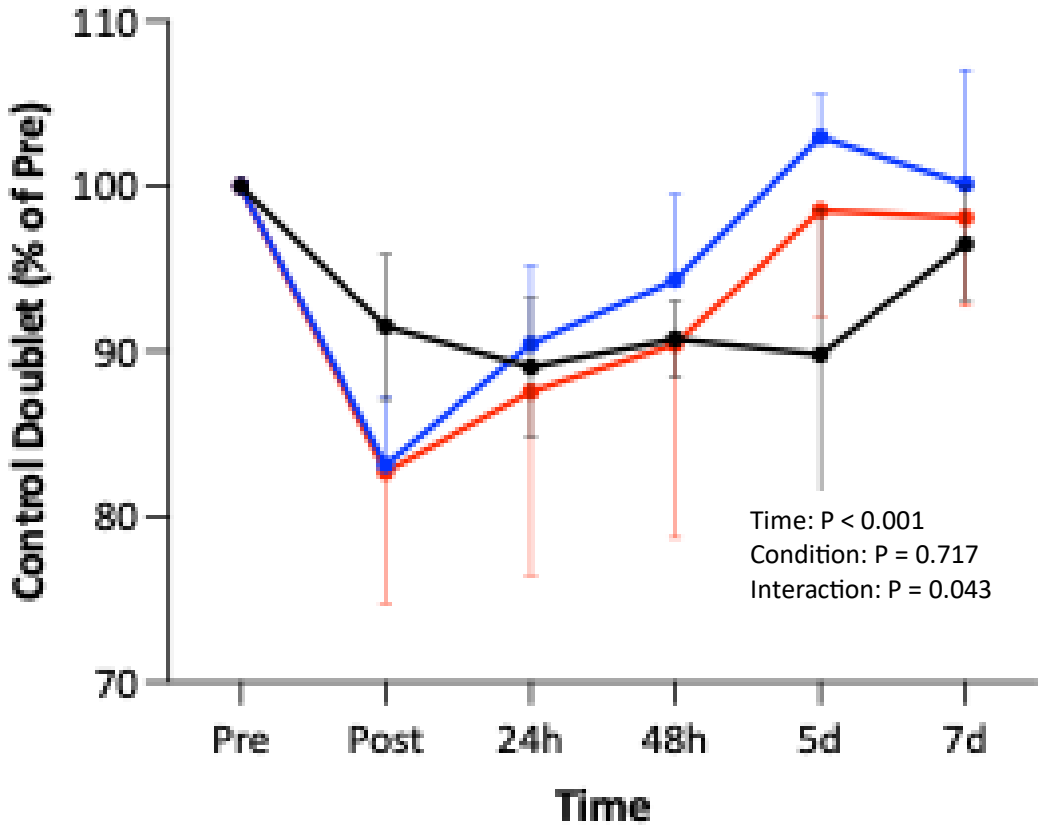

Figure 7.5. Changes in control doublet force normalised to pre-exercise values (%) over time. Black line**:** placebo (PLA); blue line: palmitoylethanolamide (PEA); red line**:** ibuprofen (Ibu) Data are presented as mean ± SEM.

7.4.4 Torque Frequency Relationship

The torque-frequency relationship was assessed via electrical stimulation to indicate peripheral muscle fatigue. A three-way mixed repeated-measures ANOVA (condition x time x frequency) was first conducted to examine overall group differences in the torque-frequency response. This analysis revealed a significant main effect of time ($p < 0.001$, $\eta_p^2 = 0.98$) and frequency ($p < 0.001$, $\eta_p^2 = 0.97$), as well as a significant time x frequency interaction time ($p < 0.001$, $\eta_p^2 = 0.87$). However, no significant main or interaction effect of condition (PLA, PEA, IBU; all $p > 0.05$) was observed, suggesting that recovery patterns in torque did not alter between conditions. On this basis, separate two-way repeated-measures ANOVAs (time x frequency) were performed within each condition to further characterise changes in torque across the recovery period.

PLA

In the PLA group, a significant main effect of time on torque–frequency ($p = 0.013$, $\eta_p^2 = 0.81$), a significant main effect of frequency ($p < 0.001$, $\eta_p^2 = 0.99$), but no significant time × frequency interaction ($p = 0.078$, $\eta_p^2 = 0.57$) was observed. Post-hoc paired *t*-tests revealed significant reductions in torque from Pre to Post at all frequencies ($p < 0.05$), with the magnitude and duration of recovery differing by frequency. At lower frequencies (1–15 Hz) torque values demonstrated partial recovery by 48 h ($p > 0.05$ vs. Pre). At higher frequencies (20-50 Hz), torque remained significantly lower than Pre at 48 h ($p < 0.05$), although values increased significantly from 24 h to 48 h ($p < 0.05$). Recovery of torque to baseline values was evident by 5 and 7 d across all frequencies (Figure 7.6).

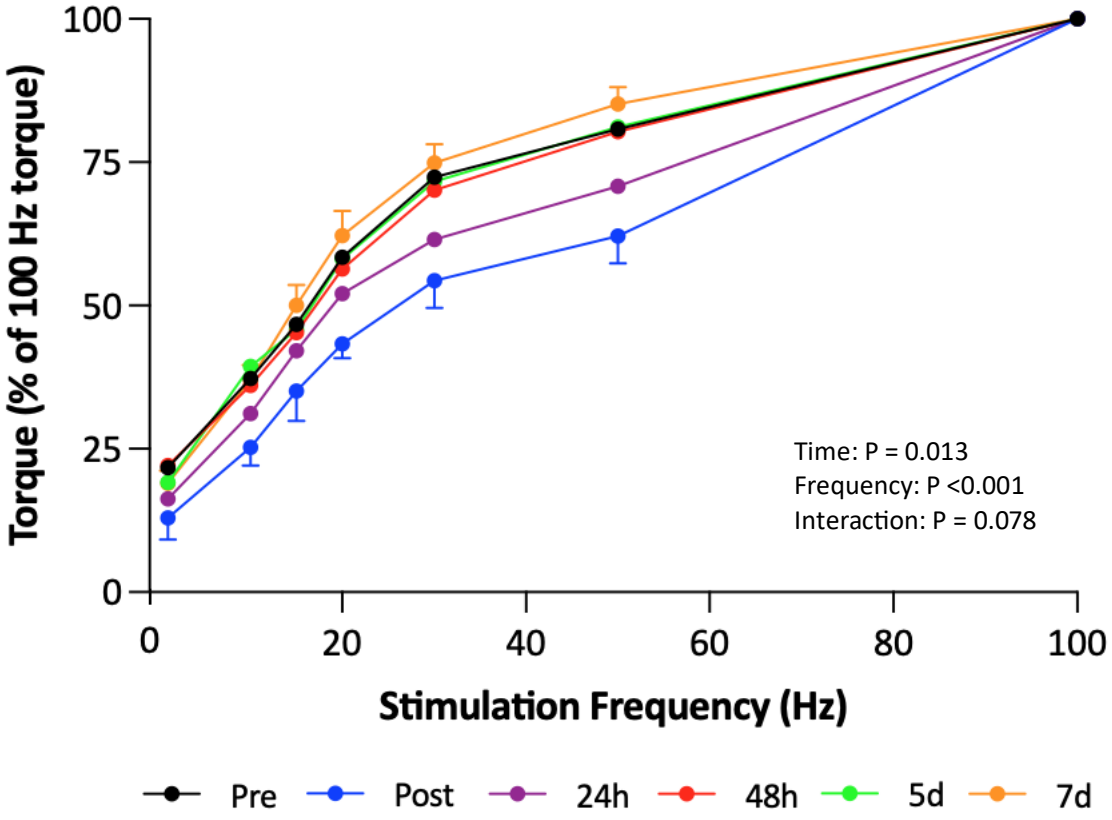

Figure 7.6. Torque–frequency relationship of placebo (PLA) group, all frequencies were normalised to torque at 100 Hz. Data are shown for each time point: Pre (black line), Post (blue line), 24h (purple line), 48h (red line), 5d (green line), and 7d (orange line). Frequencies tested were 1, 10, 15, 20, 30, and 50 Hz. Values are mean ± SD.

PEA

In the PEA group, a two-way repeated-measures ANOVA revealed a significant main effect of time torque–frequency ($p = 0.008$, $\eta_p^2 = 0.67$), a significant main effect of frequency ($p < 0.001$, $\eta_p^2 = 0.99$), but no significant time × frequency interaction ($p = 0.37$, $\eta_p^2 = 0.07$). Post-hoc paired *t*-tests revealed significant reductions in torque from Pre to Post. At lower frequencies (1-15 Hz), torque values recovered to baseline by 48 h ($p > 0.05$ vs. Pre). At higher frequencies (20-50 Hz), torque remained significantly lower than Pre at 48 h ($p < 0.05$), although values increased significantly between 24 h and 48 h ($p < 0.05$). Recovery of torque to baseline values was evident by 5 and 7 d across all frequencies (Figure 7.7).

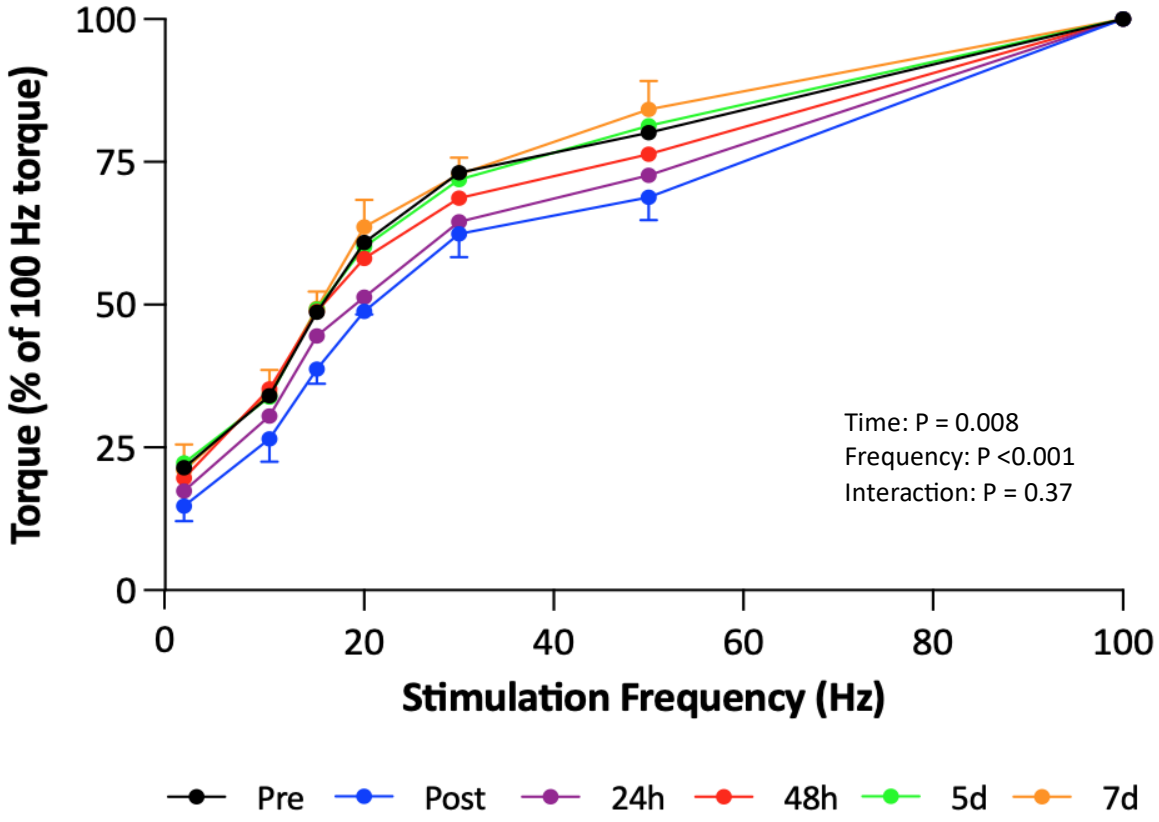

Figure 7.7. Torque–frequency relationship of palmitoylethanolamide (PEA) group, all frequencies were normalised to torque at 100 Hz. Data are shown for each time point: Pre (black line), Post (blue line), 24h (purple line), 48h (red line), 5d (green line), and 7d (orange line). Frequencies tested were 1, 10, 15, 20, 30, and 50 Hz. Values are mean ± SD.

Ibu

In the Ibu group, a two-way repeated-measures ANOVA revealed a significant main effect of time on torque-frequency in the Ibu ($p < 0.001$, $\eta_p^2 = 0.89$), a significant main effect of frequency ($p = 0.003$, $\eta_p^2 = 0.91$), but no significant time × frequency interaction ($p = 0.13$, $\eta_p^2 = 0.37$). Post-hoc paired *t*-tests revealed significant reductions in torque from Pre to Post across all frequencies ($p < 0.05$). At lower frequencies (1-15 Hz), torque showed partial recovery by 48 h, with values no longer significantly different from Pre ($p > 0.05$). At higher frequencies (20-50 Hz), torque remained significantly lower than Pre at 48 h ($p < 0.05$), although values increased significantly from 24 h to 48 h ($p < 0.05$). Recovery of torque to baseline values was evident by 5 and 7 d across all frequencies (Figure 7.8).

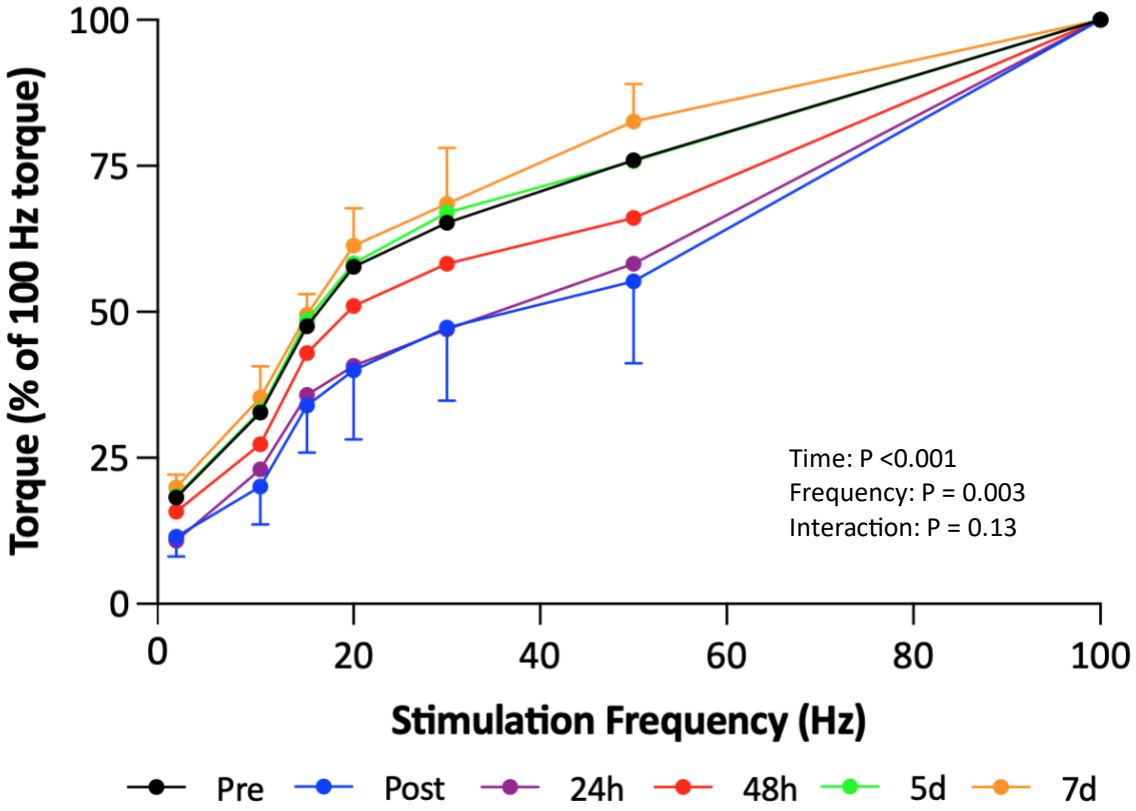

Figure 7.8. Torque–frequency relationship of ibuprofen (Ibu) group, all frequencies were normalised to torque at 100 Hz. Data are shown for each time point: Pre (black line), Post (blue line), 24h (purple line), 48h (red line), 5d (green line), and 7d (orange line). Frequencies tested were 1, 10, 15, 20, 30, and 50 Hz. Values are mean ± SD.

7.4.4 Pain

We first examined peak pain scores, defined as the highest VAS value reported by each participant across the 7-day recovery period, and then calculated the mean peak pain score within each condition. A one-way ANOVA was conducted to assess differences in peak pain scores between conditions. There was no significant effect of condition on peak pain (p = 0.322, η_p^2 =0.03), indicating that peak pain did not differ significantly between groups. Next, we examined individual daily pain scores to capture the time course of pain resolution across all participants and conditions. A two-way mixed ANOVA revealed a significant main effect of time on individual pain scores across time (p <0.001, η_p^2 = 0.86), with pain scores progressively decreasing over time. Pairwise (Fisher's LSD) indicated that pain was significantly reduced

from day 3 (p = 0.010), and further declined at days 4, 5, 6, and 7 (p < 0.001, respectively) compared to day 1 post-exercise. Additionally, pain scores continued to significantly decrease between days 2 to 5, 3 to 5 and 4 to 6 (p < 0.001, respectively). No significant interaction between time and condition was observed (p = 0.229, η_p^2 = 0.21), nor was there a significant main effect of condition (p = 0.455, η_p^2 = 0.12) on pain scores. However, pairwise (Fisher's LSD) comparisons at day 7 revealed significantly lower pain scores in both the PEA and IBU conditions compared to placebo (p < 0.001), suggesting potential condition-specific effects at this later time point.

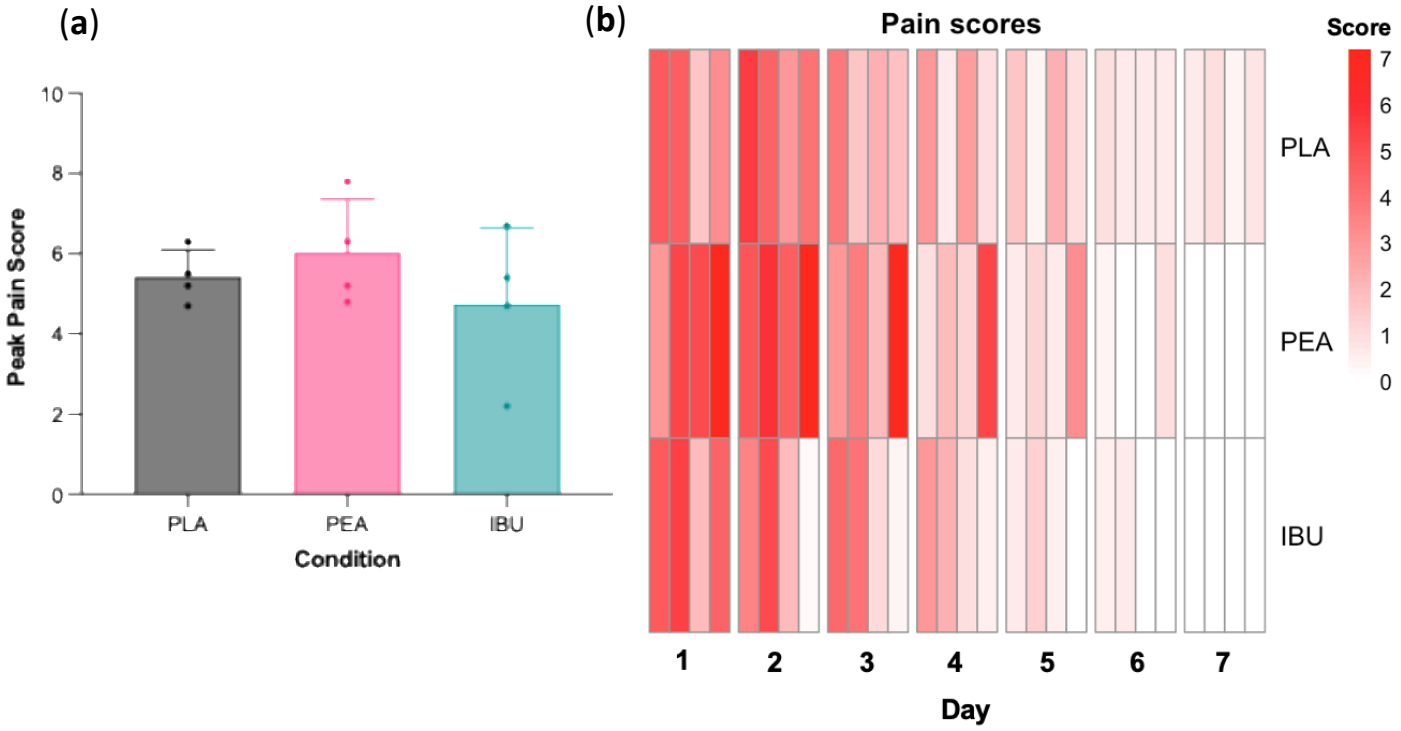

Figure 7.9. Pain as assessed via the visual analogue scale (VAS) following the final DR session. (**a**) Peak pain scores across conditions. Bar chart showing mean (±SD) peak pain scores within each condition: placebo (PLA), palmitoylethanolamide (PEA), and ibuprofen (IBU). (**b**) Individual pain scores within condition across time. Heatmap displaying self-reported pain scores for each participant across all time points within conditions. Darker red indicates higher pain scores, whilst white represents no pain.

7.4.5 Kidney Function

We first investigated estimated glomerular filtration rate (eGFR), as this marker is commonly used to assess kidney function. A two-way mixed ANOVA revealed a

significant main effect of time on eGFR ($p < 0.001$) (Figure 7.10 (d)). Post-hoc comparisons (Bonferroni-corrected) indicated a significant decrease in eGFR immediately post-exercise compared to pre-exercise ($p < 0.001$). eGFR values were significantly elevated at 24 h, 48 h, 5 d, and 7 d compared to the immediate post-exercise time point (all $p < 0.001$). No significant interaction between time and condition was observed ($p = 0.707$), and there was no significant main effect of condition on eGFR ($p = 0.521$). Next, we analysed sodium, urea and potassium levels to determine whether exercise or supplementation influenced these additional markers of kidney function. No significant main effect of time was observed for sodium levels ($p = 0.681$), nor was there a significant interaction ($p = 0.105$) or main effect of condition ($p = 0.13$) (Figure 7.10 (a)). Similarly, no significant main effect of time was observed for urea levels ($p = 0.314$), with no significant interaction ($p = 0.964$) or condition effect ($p = 0.88$) (Figure 7.10 (b)). Potassium levels also showed no significant main effect of time ($p = 0.64$), interaction ($p = 0.714$), or condition effect ($p = 0.544$) (Figure 7.10 (c)).

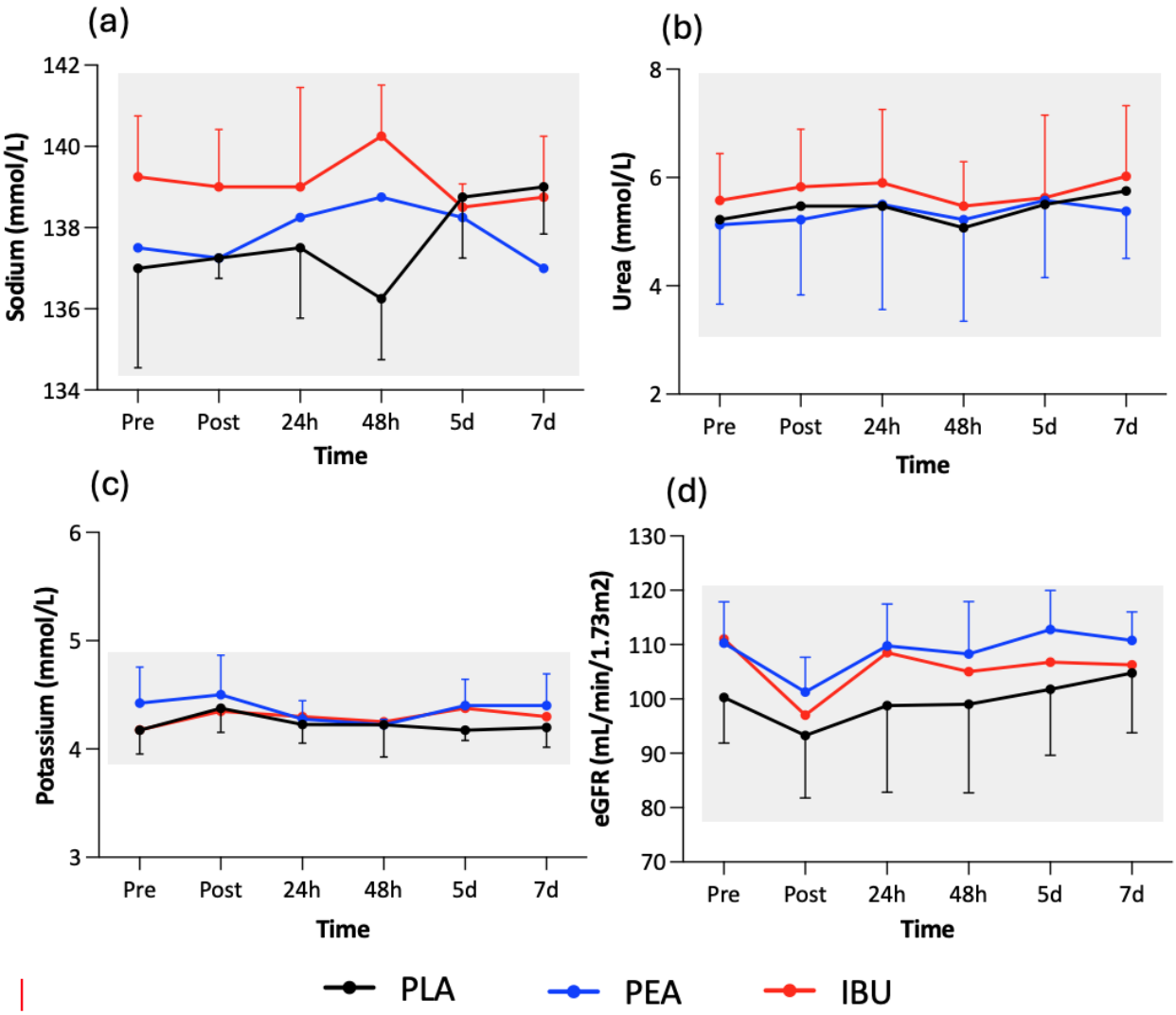

Figure 7.10. Changes in blood (a) sodium (mmol/L), (b) urea (mmol/L), (c) potassium (mmol/L), and (d) estimated glomerular filtration rate (eGFR) (mL/min/1.73m2) across time. Shaded areas represent average ranges for healthy adults (for context only). Data represented as mean ± SEM.

7.5 Discussion

The present study evaluated the effect of daily PEA supplementation (600mg/day for 10 days) on symptoms of EIMD following a 50-minute downhill run (at -17% gradient) compared to Ibuprofen (Ibu). It was hypothesized that PEA would demonstrate comparable analgesic efficacy to Ibu in reducing perceived muscle pain following EIMD, and would not impair the recovery of neuromuscular function, while maintaining a superior safety profile with respect to markers of renal function compared to Ibu. However, neither PEA nor Ibu significantly

altered the recovery trajectory of muscle function following downhill running, as indicated by comparable decrements and recovery patterns across all functional assessments. While no overall significant effect of condition on perceived muscle pain (PMP) was observed, both PEA and Ibu groups reported complete resolution of soreness by day 7, whereas pain persisted in the PLA group. This suggests that PEA may contribute to a faster resolution of pain and facilitation of recovery, both of which hold particular relevance for ultra-endurance athletes, where pain is often regarded as a primary factor limiting performance. Additionally, neither treatment adversely affected markers of renal function, suggesting both interventions were well tolerated under experimental conditions.

The exercise protocol used in the present study elicited moderate muscle damage, demonstrated by a sustained ~20% decrease in isometric maximal voluntary torque up to 48 hours post-exercise, and accompanied by a substantial increase in perceived muscle pain. According to Paulsen et al. (2012), muscle damage severity can be inferred from the magnitude and duration of strength loss, with reductions of 20-50% and prolonged recovery (>48h) indicative of moderate damage. Similarly, Coratella et al. (2024) reported comparable strength deficits and soreness following a 30-min downhill run (10 kmh^{-1}, at -20% gradient) on a motorised treadmill, supporting the use of this protocol as a valid model for inducing moderate muscle damage. Although prior training exposure can influence the magnitude of the damage response and may increase the likelihood of observing beneficial effects of the interventions, the structured training phase was implemented in a controlled manner to standardise participants' conditioning and ensure a comparable level of muscle damage across groups.

Assessment of neuromuscular function revealed that the downhill running protocol induced both central and peripheral fatigue. Voluntary activation decreased significantly immediately post-exercise and remained suppressed up to 48 hours, indicating impaired neural drive from the central nervous system to the working muscles, a protective mechanism thought to reduce further muscle damage during the acute recovery phase (Millet et al., 2003, Garnier et al., 2018). Analysis of the torque-frequency relationship revealed significant low-frequency fatigue, characterised by disproportionate reductions in evoked torque at lower stimulation frequencies, indicating peripheral fatigue consistent with impaired excitation-contraction

coupling, which may arise from structural damage to muscle fibers (Edwards et al., 1977). Although muscle function declined substantially post-exercise across all groups, recovery trajectories did not differ between conditions. Moderate effect sizes for time × condition interactions in voluntary activation and evoked torque suggest that potential treatment effects cannot be excluded, however, the absence of consistent functional improvements across all neuromuscular measures indicates that neither intervention meaningfully improved recovery. These findings align with prior work using resistance-based protocols, which similarly reported no improvements in post-exercise measures of muscle function with PEA supplementation. For example, Mallard et al. (2020) administered 300mg/day of PEA over three days surrounding a bout of unaccustomed resistance exercise and observed no effect on muscle soreness, functional recovery, or systemic inflammation. The authors proposed that the short supplementation period and insufficient volume of exercise may have limited the potential to observe an effect. More recently, Schouten et al. (2024) investigated a higher PEA dose (600mg/day) administered over seven days in recreationally active males performing eccentric contractions of the knee extensors. While the protocol resulted in moderate reductions in muscle force, no group differences were observed, likely because the crossover design of the study induced a repeated bout effect (RBE) that diminished muscle damage in the second trial, potentially obscuring any therapeutic effects of PEA. Accordingly, the present study sought to minimise the influence of the RBE and standardise adaptations to downhill running (DR) across participants by incorporating a structured training programme (see Section 7.3.4), providing clearer evidence that neither PEA nor Ibu exerted a significant effect on muscle function recovery.

Pain is a hallmark symptom of EIMD, a major driver of NSAID use among athletes, and is widely regarded as a primary limiter of performance in ultra-endurance events (Tiller and Millet, 2025). In the present study, perceived muscle pain (PMP) declined over time across all conditions, with significantly lower scores at day 7 in both the PEA and Ibu groups compared to PLA. While no main effect of condition or condition x time interaction was observed, the moderate effect sizes reported highlight condition-related influences that may not have been detected due to the small sample size. Nonetheless, the late-phase difference may indicate a delayed analgesic response. While some studies have reported no effect of PEA on muscle soreness following eccentric exercise (Mallard et al., 2020, Huschtscha et al., 2024), Schouten

et al. (2024) observed a trend toward lower ratings of muscle soreness on day 3 in the PEA condition compared to PLA ($p = 0.066$). The delayed reduction in PMP observed in both Schouten et al. (2024) and the present study suggests a potential analgesic effect of PEA during later stages of recovery. Notably, the reduction in PMP observed with PEA was comparable to that of Ibu. Supporting this, a recent systematic review and meta-analysis of 11 trials including 774 participants reported a 1.68-fold reduction in self-reported pain following PEA supplementation (400–1200 mg/day) compared to control (Lang-Illievich et al., 2023). However, as the included studies focused primarily on chronic medical and pain conditions (e.g., multiple sclerosis, osteoarthritis), the underlying mechanisms of pain, and the response to PEA, may differ from those associated with acute EIMD. From a practical perspective, even a modest reduction in late-phase pain may be highly relevant for multi-day or prolonged endurance events, where persistent muscle pain during later stages can impair performance and recovery (Hoffman and Fogard, 2011, Tiller and Millet, 2025). However, these findings should be interpreted with caution due to the small sample size in each group ($n = 4$) and can only be confirmed in future studies with larger sample sizes.

Kidney function was assessed in the current study, due to growing concerns regarding NSAID-associated renal complications during ultra-endurance events, where dehydration, heat stress, and prolonged exertion can exacerbate renal vulnerability (Wharam et al., 2006, Tidmas et al., 2022). While no significant differences in renal markers were observed between groups, a significant post-exercise decline in estimated glomerular filtration rate (eGFR) was recorded. This is likely due to the acute redistribution of blood flow away from the kidneys during intense exercise, where renal blood flow, eGFR, and urine output can decline by 30-60% (Zambraski et al., 1996, Baker et al., 2005), rather than reflecting any pathological impairments. eGFR values returned to baseline within 24h, and no meaningful changes were detected in other markers of kidney function, including sodium, potassium, and urea, all of which remained with normal reference ranges for healthy individuals of this age group (see Figure 7.10). Although NSAID use is commonly associated with acute kidney injury (AKI), the evidence remains equivocal. A recent scoping review identified considerable variability in renal outcomes among ultra-endurance athletes, with some studies reporting transient reductions in kidney function and others finding no adverse effects (Pannone and Abbott, 2024). Importantly, while no differences in kidney markers were observed between

conditions in this study, the established profile of adverse effects associated with NSAID use across diverse populations, combined with the absence of reported renal or other adverse effects for PEA, indicates that PEA may offer a safer alternative for managing EIMD symptoms.

7.6 Limitations

The present study has some limitations that should be addressed. As previously mentioned, the sample size and number per condition (4) due to the between-subjects design of the study is rather small. As such, findings should be interpreted with caution, and further studies with larger sample sizes are needed to validate these preliminary observations. Although the study included physically active individuals, participants were not elite athletes. While this improves generalisability to recreational populations, it limits applicability to elite sport, where trained muscle is less susceptible to exercise-induced damage (Newton et al., 2008), and the potential for observing an augmented response to nutritional or pharmacological interventions may be reduced in comparison to untrained individuals.

In addition, plasma PEA and Ibuprofen concentrations were not evaluated in the current study. Compliance to supplement intake was monitored by supervising morning doses, reminding participants to take evening doses, and requesting that supplement containers be returned at the end of the study to verify adherence. Although plasma PEA concentrations were not assessed in the present study, prior research has demonstrated that a single 300 mg dose of Levagen+ results in an approximate twofold increase from baseline, with elevated levels sustained for at least 4 hours (Briskey et al., 2020). Given that the current study administered 300 mg of Levagen+ twice daily, it is highly likely that this supplementation protocol effectively elevated plasma PEA levels.

Another potential limitation of the present study is the comparison between the two doses of PEA and Ibuprofen. Whilst both doses were chosen based on previous evidence demonstrating efficacy and safety (Huschtscha et al., 2024, Roberts et al., 2024b), they represent different pharmacological compounds with distinct mechanisms of action and pharmacokinetic profiles. Therefore, this disparity may influence the relative efficacy of each

treatment, making direct comparisons challenging and further highlighting the need for dose-ranging studies to better match bioactive exposure and clarify comparative outcomes.

7.7 Conclusion

The present study demonstrates that daily supplementation with palmitoylethanolamide (PEA; 600 mg/day for 10 days) did not significantly enhance recovery of muscle function following a 50-minute downhill running bout. Neither PEA nor ibuprofen (Ibu; 800 mg/day for 10 days) altered the recovery trajectory of neuromuscular function, with all conditions displaying comparable impairments in both central (voluntary activation) and peripheral (torque-frequency relationship) mechanisms of fatigue. While no overall treatment effect on perceived muscle pain was observed, the complete resolution of pain by day 7 in both the PEA and Ibu groups compared to placebo suggests a potential delayed analgesic effect that warrants further investigation. Importantly, no adverse changes in renal function were observed with either intervention under the acute dosing conditions of this study, with the transient post-exercise decline in estimated glomerular filtration rate reflecting normal physiological responses to exercise rather than treatment-related nephrotoxicity. However, given the well-established risks associated with repeated or chronic NSAID use in broader athletic contexts, PEA may represent a promising alternative for pain management in endurance athletes, particularly during multi-day events where cumulative NSAID exposure could pose greater risks. Future research is warranted in larger cohorts to confirm these findings and explore the broader therapeutic potential of PEA across different exercise modalities, dosing strategies, and athletic populations.

Chapter 8

Thesis Synthesis

This chapter provides a synthesis of the main aims and outcomes of the investigations described in this thesis. Limitations and future direction of research are also discussed.

8.1 Realisation of Aims

This thesis sought to advance understanding of the potential effects and applications of palmitoylethanolamide (PEA) in the context of skeletal muscle. The first aim was to explore the prevalence and perceptions of non-steroidal anti-inflammatory drug (NSAID) use among ultra-endurance runners, thereby highlighting the need for safer alternatives, such as PEA, to manage exercise-induced muscle damage (EIMD). Building on this, the second aim was to investigate the cellular mechanisms through which PEA may act on skeletal muscle, with particular focus on its influence on myogenesis and gene expression. To extend these findings to muscle protein metabolism, the third aim was to compare the effects of PEA and ibuprofen (Ibu) on protein synthesis and protein abundance in skeletal muscle cells, addressing concerns regarding the potential detrimental impact of NSAIDs on muscle adaptation and recovery. The fourth aim was to evaluate the translational relevance of PEA by assessing its efficacy as an alternative to NSAIDs for mitigating EIMD in humans, using a downhill running model to examine muscle function, soreness, and the safety profile of PEA supplementation. Collectively, these studies aimed to generate a comprehensive body of qualitative, mechanistic, and applied evidence to guide future practice, inform supplementation strategies, and support the development of safer approaches to promote effective recovery in exercise and sports settings.

8.1.1 Aim 1 – To investigate the prevalence and perceptions of NSAID use among ultra-endurance runners to assess the need for safer alternatives in managing EIMD.

This thesis contributes novel insight to the growing body of literature examining analgesic use in ultra-endurance sport by providing one of the most detailed examinations of NSAID use within the ultra-endurance running community. While previous research has typically reported prevalence figures without exploring underlying motivations, the mixed-methods approach used in **Chapter 4** enabled a more nuanced understanding of the cultural, behavioural, and performance-related drivers of use. The findings from this study highlight that while many athletes are aware of potential health risks, they continue to use NSAIDs for reasons linked to performance, recovery and pain management. Importantly, the observation that female athletes have sex-specific motivations for use highlights a gap in current guidance and reinforces the need for tailored education and alternative strategies. The finding that a

large majority of runners expressed willingness to adopt safer, low-risk alternatives underscores an opportunity to influence practice at both the individual and community level.

In light of these findings and the limitations of a cross-sectional, self-report survey design, the primary message is that NSAID use in ultra-endurance runners is not only a matter of individual behaviour but also reflects broader cultural norms and performance drivers. This reinforces the need for future research to move beyond simply documenting prevalence and instead understanding and implementing interventions that target behaviour change, educational outreach, and policy development. Addressing sex-specific drivers of use and evaluating the impact of structured education on analgesic and NSAID practices will be particularly important. At a policy level, governing bodies could have an influential impact by promoting evidence-based recovery strategies with limited adverse effects.

Together, these insights suggest that while NSAIDs remain a large part of ultra-endurance practice, there is a clear need and want among athletes for safer alternatives. Future research should therefore focus on developing and testing such alternatives, alongside behavioural and policy approaches that aim to change the norm around NSAID use, ultimately supporting athlete health and performance.

8.1.2 Aim 2 – To investigate the effects of PEA on C2C12 skeletal muscle myogenesis and gene expression in vitro.

This thesis is the first to investigate the cellular and molecular effects of PEA on skeletal muscle. Addressing a significant gap in the literature, this work explored both functional and transcriptomic responses using an established model of myogenesis. **In** Chapter 5, acute exposure to PEA revealed a concentration-dependent effect, with lower concentrations (10 µM) well-tolerated in differentiated myotubes, but higher doses (100 µM) impairing metabolic activity. At 10 µM, PEA influenced myogenic progression and gene expression, suggesting regulatory effects beyond PPARα activation and muscle-specific transcriptional pathways via enzymes such as Naaa. These findings highlight novel mechanisms through which PEA may influence skeletal muscle, providing a foundation for future mechanistic and translation research.

While this research is the first to investigate the cellular and molecular effects of PEA on skeletal muscle, several limitations must be addressed when interpreting findings to human muscle. While *in vitro* models provide valuable mechanistic insight, they cannot directly translate to *in vivo* outcomes. The supraphysiological concentrations of compounds, the use of a 2D murine cell line, the presence of residual unfused myoblasts and the absence of native muscle architecture limit the extent to which these findings reflect in vivo physiological responses (Dessauge et al., 2021). Consequently, three-dimensional (3D) culture systems are increasingly favoured for better modelling *in vivo* conditions and promoting more physiologically relevant cell behaviour (Ravi et al., 2015). Replication of the studies described in Chapter 5 of this thesis, utilising a 3D cell culture system will provide more physiological insights as to how PEA influences skeletal muscle myogenesis.

Future research should therefore focus on establishing physiologically relevant tissue concentrations of PEA, using techniques such as LC-MS/MS. Replicating these experiments in 3D muscle models, that better model tissue architecture, contractile activity, and metabolic activity, enabling more physiologically relevant assessments of PEA's effects on myogenesis. Integrated multi-omic approaches are also needed to comprehensively map the molecular networks through which PEA acts on skeletal muscle. Collectively, this chapter demonstrates distinct regulatory pathways through which PEA acts on skeletal muscle and emphasises the importance of translational studies to determine whether these effects can support muscle repair.

8.1.3 Aim 3 – To investigate the effects of PEA and the NSAID Ibuprofen on protein synthesis and protein abundance in C2C12 skeletal muscle myotubes in vitro.

Building on the transcriptomic work in **Chapter 5**, this thesis also investigated the effects of PEA on skeletal muscle at the protein level and compared responses to ibuprofen (Ibu), given evidence that NSAIDs can inhibit protein synthesis. By combining fractional synthesis rates (FSR) with abundance profiling, this is the first study to characterise how PEA and Ibu remodel the skeletal muscle proteome *in vitro*. Neither compound altered mixed-protein FSR, but both induced distinct proteome remodelling with Ibu upregulating contractile, ribosomal, and stress-response proteins and PEA selectively increasing the abundance of ribosomal and actin-

binding proteins. Both treatments increased 40S ribosomal protein abundance, significantly for PEA, resembling early adaptive responses to resistance exercise. Together, these findings suggest that PEA and Ibu promote ribosomal biogenesis and structural remodelling via distinct regulatory pathways.

Whilst it appears that PEA is capable of modulating proteomic pathways associated with muscle adaption, the limitations of the in vitro model impact the translational significance of these effects. The concentrations of both compounds used in this study exceed typical physiological plasma levels, and the simple *in vitro* model does not replicate the systemic, inflammatory, and tissue-level interactions that influence these compounds *in vivo*. As such, in vitro experiments should be primarily used as tools for identifying mechanistic pathways, rather than used as predictors of whole-body outcomes.

Future work should therefore employ models that bridge the gap between cellular insights and applied physiology. Validation in animal and human studies will be essential to establish whether the proteome changes observed here translate into functional outcomes such as muscle mass or recovery. Studies should also examine the effects of chronic or repeated dosing regimes, which may better capture the adaptations associated with training or clinical use. In addition, targeted investigations of key proteins identified in this study, including ribosomal subunits, and actin-binding proteins, could provide insight into novel pathways through which PEA may act as a safer alternative to NSAIDs. Overall, this work, paired with the findings in **Chapter 5**, provide evidence of PEA's molecular effects on skeletal muscle, extending insights from transcriptomic to protein-level regulation.

8.1.4 Aim 4 – To investigate the potential of PEA as an alternative to NSAIDs for alleviating symptoms of EIMD using an in vivo downhill running model.

Following the preceding molecular chapters, **Chapter 7** aimed to translate the findings into an exercise induced muscle damage (EIMD) context, addressing the need identified in **Chapter 4** for safer alternatives to NSAIDs. Using a downhill running protocol to induce moderate muscle damage, the study compared daily PEA supplementation with Ibu and placebo (PLA). While neither treatment improved functional recovery, both PEA and Ibu diminished perceived

muscle pain by day 7, suggesting a potential late-phase analgesic effect. This pattern aligns with previous reports of modest soreness reduction during later recovery stages with PEA supplementation and may have practical relevance for multi-day ultra-endurance events, where persistent muscle pain can impair performance. Importantly, no adverse renal effects were observed with either treatment; however, given the well-documented risks of chronic Ibu use, PEA may represent a safer option.

This study offers novel insight into the effects of PEA and Ibu supplementation following muscle-damaging exercise, however, several limitations must be acknowledged to appropriately interpret and contextualise the findings. The small sample size reduced statistical power, sex-specific responses could not be explored, and supplement adherence could not be completely verified. Furthermore, without pharmacokinetic data on compound concentrations and direct histological confirmation of muscle damage, the mechanisms underlying the observed effects remains unclear. These constraints highlight the need for larger sample sizes, more controlled cohorts, validated compliance tracking, pharmacokinetic measures and histological analyses to confirm and extend these findings.

Future research should therefore focus on including athletes and clinical populations to explore differences in response across sex, training status, and sport-specific demands. Replicating ultra-endurance race environments under physiological stressors such as heat, fatigue, and variable terrain would enhance ecological validity and clarify whether PEA's late-phase analgesic effects translate into performance benefits under real-world conditions, while also assessing potential stress on renal function under prolonged or repeated exertion. Incorporating pharmacokinetic analyses will be essential to confirm systemic exposure and dose-response relationships, while the inclusion of muscle protein-level measurements will aim to clarify mechanisms of action. Collectively, these measures will help determine whether the late-phase analgesic effects observed here can be translated into ultra-endurance settings, where persistent muscle pain is a major performance-limiting factor and whether PEA could be positioned as a practical, safe alternative to NSAIDs in sport and beyond.

8.2 Final Conclusions

NSAID use is highly prevalent among ultra-endurance athletes, driven by the need to manage pain and maintain performance, despite known evidence of associated health risks. This suggests a need for education and alternative strategies to mitigate pain and maintain performance. The work presented here demonstrates that in skeletal muscle, palmitoylethanolamide influences key molecular processes, including the regulation of inflammatory pathways and ribosomal biogenesis, without impairing protein synthesis or myogenic progression and importantly, in human subjects, PEA provided pain relief comparable to ibuprofen following exercise-induced muscle damage (EIMD), without evidence of negative effects on renal function or functional recovery.

Interestingly, although ibuprofen is often discussed in the context of potential negative effects on muscle adaptation, the findings of this thesis did not identify any adverse effects of ibuprofen in either in vitro or in vivo experiments. At the cellular level, ibuprofen unexpectedly increased the synthesis and abundance of ribosomal proteins and markers associated with translational capacity, responses generally associated with early adaptive remodelling. However, these observations should not be interpreted as evidence of a beneficial effect, as the experimental conditions applied here do not replicate in vivo pharmacokinetics or typical NSAID use patterns. Rather, they highlight that the interaction between NSAIDs and muscle adaptation may be more nuanced than traditionally assumed, and further research is required to clarify when and how ibuprofen influences skeletal muscle protein metabolism.

Collectively, these findings raise important questions as to whether PEA may serve not only as a symptomatic aid but with the potential to support adaptive processes in skeletal muscle. Given the significance of safe and effective recovery strategies in both athletic and clinical contexts, further exploration of PEA is warranted. Important questions remain regarding the pharmacokinetics and mechanistic actions of PEA in skeletal muscle, the optimal timing, dosing, and duration of PEA supplementation, and it's influence on long-term training adaptations. At present, the evidence in humans is limited, and PEA should not be considered a replacement for existing strategies but rather as an emerging area for future research. The

widespread use of NSAIDs remains a concern, and this thesis provides new insights into the effects of PEA on skeletal muscle and its potential role in the context of EIMD.

References

ABRAHAM, W. M. 1977. Factors in delayed muscle soreness. *Medicine and science in sports,* 9**,** 11-20.

ADAN, A., ALIZADA, G., KIRAZ, Y., BARAN, Y. & NALBANT, A. 2017. Flow cytometry: basic principles and applications. *Critical reviews in biotechnology,* 37**,** 163-176.

AHN, K., MCKINNEY, M. K. & CRAVATT, B. F. 2008. Enzymatic pathways that regulate endocannabinoid signaling in the nervous system. *Chem Rev,* 108**,** 1687-707.

ALHOUAYEK, M. & MUCCIOLI, G. G. 2014. Harnessing the anti-inflammatory potential of palmitoylethanolamide. *Drug Discovery Today,* 19**,** 1632-1639.

ALOE, L., LEON, A. & LEVI-MONTALCINI, R. 1993. A proposed autacoid mechanism controlling mastocyte behaviour. *Agents and actions,* 39**,** C145-C147.

AMBROSINO, P., SOLDOVIERI, M. V., RUSSO, C. & TAGLIALATELA, M. 2013. Activation and desensitization of TRPV1 channels in sensory neurons by the PPARα agonist palmitoylethanolamide. *British Journal of Pharmacology,* 168**,** 1430-1444.

ANNUNZIATA, C., LAMA, A., PIROZZI, C., CAVALIERE, G., TRINCHESE, G., DI GUIDA, F., NITRATO IZZO, A., CIMMINO, F., PACIELLO, O., DE BIASE, D., MURRU, E., BANNI, S., CALIGNANO, A., MOLLICA, M. P., MATTACE RASO, G. & MELI, R. 2020. Palmitoylethanolamide counteracts hepatic metabolic inflexibility modulating mitochondrial function and efficiency in diet-induced obese mice. *Faseb j,* 34**,** 350-364.

ARMSTRONG, R. 1984. Mechanisms of exercise-induced delayed onset muscular soreness: a brief review. *Medicine and science in sports and exercise,* 16**,** 529-538.

ARMSTRONG, R. 1990. Initial events in exercise-induced muscular injury. *Medicine and science in sports and exercise,* 22**,** 429-435.

ARMSTRONG, R., WARREN, G. & WARREN, J. 1991. Mechanisms of exercise-induced muscle fibre injury. *Sports medicine,* 12**,** 184-207.

ARTUKOGLU, B. B., BEYER, C., ZULOFF-SHANI, A., BRENER, E. & BLOCH, M. H. 2017. Efficacy of Palmitoylethanolamide for Pain: A Meta-Analysis. *Pain Physician,* 20**,** 353-362.

ASFOUR, H. A., ALLOUH, M. Z. & SAID, R. S. 2018. Myogenic regulatory factors: The orchestrators of myogenesis after 30 years of discovery. *Experimental Biology and Medicine,* 243**,** 118-128.

ASMUSSEN, E. 1953. Positive and negative muscular work. *Acta Physiologica Scandinavica,* 28**,** 364-382.

BACHUR, N. R., MASEK, K., MELMON, K. L. & UDENFRIEND, S. 1965. Fatty Acid Amides of Ethanolamine in Mammalian Tissues. *J Biol Chem,* 240**,** 1019-24.

BAKER, J., COTTER, J. D., GERRARD, D. F., BELL, M. L. & WALKER, R. J. 2005. Effects of indomethacin and celecoxib on renal function in athletes. *Med Sci Sports Exerc,* 37**,** 712-717.

BALENGA, N., MARTÍNEZ-PINILLA, E., KARGL, J., SCHRÖDER, R., PEINHAUPT, M., PLATZER, W., BÁLINT, Z., ZAMARBIDE, M., DOPESO-REYES, I. & RICOBARAZA, A. 2014. Heteromerization of GPR 55 and cannabinoid CB 2 receptors modulates signalling. *British journal of pharmacology,* 171**,** 5387-5406.

BECK, F., PLUMMER, S., SENIOR, P., BYRNE, S., GREEN, S. & BRAMMAR, W. 1992. The ontogeny of peroxisome-proliferator-activated receptor gene expression in the mouse and rat. *Proceedings of the Royal Society of London. Series B: Biological Sciences,* 247**,** 83-87.

BEELEN, M., BURKE, L. M., GIBALA, M. J. & VAN LOON, L. J. 2010. Nutritional strategies to promote postexercise recovery. *International journal of sport nutrition and exercise metabolism,* 20**,** 515-532.

BEGGIATO, S., TOMASINI, M. C. & FERRARO, L. 2019a. Palmitoylethanolamide (PEA) as a Potential Therapeutic Agent in Alzheimer's Disease. *Front Pharmacol,* 10**,** 821.

BEGGIATO, S., TOMASINI, M. C. & FERRARO, L. 2019b. Palmitoylethanolamide (PEA) as a potential therapeutic agent in Alzheimer's disease. *Frontiers in pharmacology,* 10**,** 821.

BELCASTRO, A. N., SHEWCHUK, L. D. & RAJ, D. A. 1998. Exercise-induced muscle injury: a calpain hypothesis. *Molecular and cellular biochemistry,* 179**,** 135-145.

BELL, P., MCHUGH, M., STEVENSON, E. & HOWATSON, G. 2014. The role of cherries in exercise and health. *Scandinavian journal of medicine & science in sports,* 24**,** 477-490.

BELLANTI, F., BUKKE, V. N., MOOLA, A., VILLANI, R., SCUDERI, C., STEARDO, L., PALOMBELLI, G., CANESE, R., BEGGIATO, S., ALTAMURA, M., VENDEMIALE, G., SERVIDDIO, G. & CASSANO, T. 2022. Effects of Ultramicronized Palmitoylethanolamide on Mitochondrial Bioenergetics, Cerebral Metabolism, and Glutamatergic Transmission: An Integrated Approach in a Triple Transgenic Mouse Model of Alzheimer's Disease. *Front Aging Neurosci,* 14**,** 890855.

BERGER, N. J., BEST, R., BEST, A. W., LANE, A. M., MILLET, G. Y., BARWOOD, M., MARCORA, S., WILSON, P. & BEARDEN, S. 2024. Limits of ultra: towards an interdisciplinary understanding of ultra-endurance running performance. *Sports Medicine,* 54**,** 73-93.

BERNARD, C., JOMARD, C., CHAZAUD, B. & GONDIN, J. 2023. Kinetics of skeletal muscle regeneration after mild and severe muscle damage induced by electrically-evoked lengthening contractions. *The FASEB Journal,* 37**,** e23107.

BHALA, N., EMBERSON, J., MERHI, A., ABRAMSON, S., ARBER, N., BARON, J., BOMBARDIER, C., CANNON, C., FARKOUH, M. & FITZGERALD, G. 2013. Vascular and upper gastrointestinal effects of non-steroidal anti-inflammatory drugs: meta-analyses of individual participant data from randomised trials. *Lancet (London, England),* 382**,** 769-779.

BILLAT, V. L., DEMARLE, A., SLAWINSKI, J., PAIVA, M. & KORALSZTEIN, J.-P. 2001. Physical and training characteristics of top-class marathon runners. *Medicine and science in sports and exercise,* 33**,** 2089-2097.

BLACKER, S. D., WILLIAMS, N. C., FALLOWFIELD, J. L., BILZON, J. L. & WILLEMS, M. E. 2010. Carbohydrate vs protein supplementation for recovery of neuromuscular function following prolonged load carriage. *Journal of the International Society of Sports Nutrition,* 7**,** 1-11.

BLAIVAS, M. & CARLSON, B. M. 1991. Muscle fiber branching—difference between grafts in old and young rats. *Mechanisms of ageing and development,* 60**,** 43-53.

BOCKHOLD, K. J., DAVID ROSENBLATT, J. & PARTRIDGE, T. A. 1998. Aging normal and dystrophic mouse muscle: analysis of myogenicity in cultures of living single

fibers. *Muscle & Nerve: Official Journal of the American Association of Electrodiagnostic Medicine,* 21**,** 173-183.
BONTEMPS, B., GRUET, M., LOUIS, J., OWENS, D. J., MIRÍC, S., ERSKINE, R. M. & VERCRUYSSEN, F. 2022. The time course of different neuromuscular adaptations to short-term downhill running training and their specific relationships with strength gains. *European Journal of Applied Physiology,* 122**,** 1071-1084.
BONTEMPS, B., VERCRUYSSEN, F., GRUET, M. & LOUIS, J. 2019. Commentaries on Viewpoint: Distinct modalities of eccentric exercise: different recipes, not the same dish. *Journal of Applied Physiology,* 127**,** 884-891.
BONTEMPS, B., VERCRUYSSEN, F., GRUET, M. & LOUIS, J. 2020. Downhill Running: What Are The Effects and How Can We Adapt? A Narrative Review. *Sports Med,* 50**,** 2083-2110.
BRAISSANT, O., FOUFELLE, F., SCOTTO, C., DAUÇA, M. & WAHLI, W. 1996. Differential expression of peroxisome proliferator-activated receptors (PPARs): tissue distribution of PPAR-alpha,-beta, and-gamma in the adult rat. *Endocrinology,* 137**,** 354-366.
BRAUN, T. & GAUTEL, M. 2011. Transcriptional mechanisms regulating skeletal muscle differentiation, growth and homeostasis. *Nature reviews Molecular cell biology,* 12**,** 349-361.
BRAUN, V. & CLARKE, V. 2006. Using thematic analysis in psychology. *Qualitative research in psychology,* 3**,** 77-101.
BRAUN, V. & CLARKE, V. 2016. (Mis) conceptualising themes, thematic analysis, and other problems with Fugard and Potts'(2015) sample-size tool for thematic analysis. *International Journal of social research methodology,* 19**,** 739-743.
BRENTANO, M. & MARTINS KRUEL, L. 2011. A review on strength exercise-induced muscle damage: applications, adaptation mechanisms and limitations. *J Sports Med Phys Fitness,* 51**,** 1-10.
BRISKEY, D., EBELT, P., STEELS, E., SUBAH, S., BOGODA, N. & RAO, A. 2022. Efficacy of palmitoylethanolamide (Levagen+ TM) compared to ibuprofen for reducing headache pain severity and duration in healthy adults: a double-blind, parallel, randomized clinical trial. *Food and Nutrition Sciences,* 13**,** 690-701.
BRISKEY, D., MALLARD, A. & RAO, A. 2020. Increased absorption of palmitoylethanolamide using a novel dispersion technology system (LipiSperse®). *J. Nutraceuticals Food Sci,* 5.
BRISKEY, D., ROCHE, G. & RAO, A. 2021. The Effect of a Dispersible Palmitoylethanolamide (Levagen+) Compared to a Placebo for Reducing Joint Pain in an Adult Population–A Randomised, Double-Blind Study. *Int. J. Nutr. Food Sci,* 10.
BROOKS, S. V., ZERBA, E. & FAULKNER, J. A. 1995. Injury to muscle fibres after single stretches of passive and maximally stimulated muscles in mice. *The Journal of physiology,* 488**,** 459-469.
BROWN, A. D., STEWART, C. E. & BURNISTON, J. G. 2022. Degradation of ribosomal and chaperone proteins is attenuated during the differentiation of replicatively aged C2C12 myoblasts. *Journal of Cachexia, Sarcopenia and Muscle,* 13**,** 2562-2575.

BYRNE, C., TWIST, C. & ESTON, R. 2004. Neuromuscular function after exercise-induced muscle damage: theoretical and applied implications. *Sports Med,* 34**,** 49-69.
CALDERÓN, J. C., BOLAÑOS, P. & CAPUTO, C. 2014. The excitation–contraction coupling mechanism in skeletal muscle. *Biophysical reviews,* 6**,** 133-160.
CAMERA, D. M., BURNISTON, J. G., POGSON, M. A., SMILES, W. J. & HAWLEY, J. A. 2017. Dynamic proteome profiling of individual proteins in human skeletal muscle after a high-fat diet and resistance exercise. *The FASEB Journal,* 31**,** 5478-5494.
CANNON, J. G. & ST. PIERRE, B. A. 1998. Cytokines in exertion-induced skeletal muscle injury. *Molecular and cellular biochemistry,* 179**,** 159-168.
CARLSON, B. M. & FAULKNER, J. A. 1983. The regeneration of skeletal muscle fibers following injury: a review. *Medicine and science in sports and exercise,* 15**,** 187-198.
CELORRIO, M., ROJO-BUSTAMANTE, E., FERNÁNDEZ-SUÁREZ, D., SÁEZ, E., DE MENDOZA, A. E.-H., MÜLLER, C. E., RAMÍREZ, M. J., OYARZÁBAL, J., FRANCO, R. & AYMERICH, M. S. 2017. GPR55: A therapeutic target for Parkinson's disease? *Neuropharmacology,* 125**,** 319-332.
CHAIAMNUAY, S., ALLISON, J. J. & CURTIS, J. R. 2006. Risks versus benefits of cyclooxygenase-2-selective nonsteroidal antiinflammatory drugs. *American journal of health-system pharmacy,* 63**,** 1837-1851.
CHARGÉ, S. B. & RUDNICKI, M. A. 2004. Cellular and molecular regulation of muscle regeneration. *Physiological reviews,* 84**,** 209-238.
CHAZAUD, B. 2016. Inflammation during skeletal muscle regeneration and tissue remodeling: application to exercise-induced muscle damage management. *Immunology and cell biology,* 94**,** 140-145.
CHEUNG, K., HUME, P. & MAXWELL, L. 2003. Delayed onset muscle soreness: Treatment Strategies and Performance Factors. ncbi. nlm. nih. gov. 2015. September.
CLARKE, R. V. & CORNISH, D. B. 2017. Modeling offenders' decisions: A framework for research and policy. *Crime Opportunity Theories*. Routledge.
CLARKSON, P. M. & HUBAL, M. J. 2002. Exercise-induced muscle damage in humans. *American journal of physical medicine & rehabilitation,* 81**,** S52-S69.
COATES, A. M., BERARD, J. A., KING, T. J. & BURR, J. F. 2021. Physiological determinants of ultramarathon trail-running performance. *International journal of sports physiology and performance,* 16**,** 1454-1461.
COBURN, A. F. & MOORE, L. V. 1943. Nutrition as a conditioning factor in the rheumatic state. *American Journal of Diseases of Children,* 65**,** 744-756.
COBURN, A. F., TRULSON, M. F. & MOORE, L. V. 1954. [Further study of the effect of the administration of egg yolk on susceptibility of children to rheumatic infection]. *Minerva Med,* 45**,** 1534-6.
COCHRANE-SNYMAN, K. C., CRUZ, C., MORALES, J. & COLES, M. 2021. The effects of cannabidiol oil on noninvasive measures of muscle damage in men. *Medicine & Science in Sports & Exercise,* 53**,** 1460-1472.
COHEN, J. 2013. *Statistical power analysis for the behavioral sciences*, routledge.

CONNOLLY, D., MCHUGH, M. & PADILLA-ZAKOUR, O. 2006. Efficacy of a tart cherry juice blend in preventing the symptoms of muscle damage. *British journal of sports medicine,* 40**,** 679-683.
CORATELLA, G., VARESCO, G., ROZAND, V., CUINET, B., SANSONI, V., LOMBARDI, G., VERNILLO, G. & MOUROT, L. 2024. Downhill running increases markers of muscle damage and impairs the maximal voluntary force production as well as the late phase of the rate of voluntary force development. *European Journal of Applied Physiology,* 124**,** 1875-1883.
CORONA, B. T., BALOG, E. M., DOYLE, J. A., RUPP, J. C., LUKE, R. C. & INGALLS, C. P. 2010. Junctophilin damage contributes to early strength deficits and EC coupling failure after eccentric contractions. *American Journal of Physiology-Cell Physiology,* 298**,** C365-C376.
CORRIGAN, B. & KAZLAUAKAA, R. 2000. Drug testing at the Sydney Olympics. *Medical journal of Australia,* 173**,** 312-313.
CORRIGAN, B. & KAZLAUSKAS, R. 2003. Medication use in athletes selected for doping control at the Sydney Olympics (2000). *Clinical Journal of Sport Medicine,* 13**,** 33-40.
COSTA, B., COMELLI, F., BETTONI, I., COLLEONI, M. & GIAGNONI, G. 2008. The endogenous fatty acid amide, palmitoylethanolamide, has anti-allodynic and anti-hyperalgesic effects in a murine model of neuropathic pain: involvement of CB1, TRPV1 and PPARγ receptors and neurotrophic factors. *Pain,* 139**,** 541-550.
COSTA, B., CONTI, S., GIAGNONI, G. & COLLEONI, M. 2002. Therapeutic effect of the endogenous fatty acid amide, palmitoylethanolamide, in rat acute inflammation: inhibition of nitric oxide and cyclo-oxygenase systems. *Br J Pharmacol,* 137**,** 413-20.
COVINGTON, M. B. 2004. Omega-3 fatty acids. *American family physician,* 70**,** 133-140.
CRAVATT, B. F., GIANG, D. K., MAYFIELD, S. P., BOGER, D. L., LERNER, R. A. & GILULA, N. B. 1996. Molecular characterization of an enzyme that degrades neuromodulatory fatty-acid amides. *Nature,* 384**,** 83-7.
CRISCO, J. J., JOKL, P., HEINEN, G. T., CONNELL, M. D. & PANJABI, M. M. 1994. A muscle contusion injury model: biomechanics, physiology, and histology. *The American journal of sports medicine,* 22**,** 702-710.
D'AGOSTINO, G., RUSSO, R., AVAGLIANO, C., CRISTIANO, C., MELI, R. & CALIGNANO, A. 2012. Palmitoylethanolamide protects against the amyloid-β25-35-induced learning and memory impairment in mice, an experimental model of Alzheimer disease. *Neuropsychopharmacology,* 37**,** 1784-92.
D'ALOIA, A., MOLTENI, L., GULLO, F., BRESCIANI, E., ARTUSA, V., RIZZI, L., CERIANI, M., MEANTI, R., LECCHI, M. & COCO, S. 2021. Palmitoylethanolamide modulation of microglia activation: characterization of mechanisms of action and implication for its neuroprotective effects. *International journal of molecular sciences,* 22**,** 3054.
DAMAS, F., NOSAKA, K., LIBARDI, C. A., CHEN, T. C. & UGRINOWITSCH, C. 2016. Susceptibility to exercise-induced muscle damage: a cluster analysis with a large sample. *International journal of sports medicine,* 37**,** 633-640.
DAVIS, M. P., BEHM, B., MEHTA, Z. & FERNANDEZ, C. 2019. The potential benefits of palmitoylethanolamide in palliation: a qualitative systematic review. *American Journal of Hospice and Palliative Medicine®,* 36**,** 1134-1154.

DAYNES, R. A. & JONES, D. C. 2002. Emerging roles of PPARs in inflammation and immunity. *Nature Reviews Immunology,* 2**,** 748-759.
DE FILIPPIS, D., LUONGO, L., CIPRIANO, M., PALAZZO, E., CINELLI, M. P., DE NOVELLIS, V., MAIONE, S. & IUVONE, T. 2011. Palmitoylethanolamide reduces granuloma-induced hyperalgesia by modulation of mast cell activation in rats. *Molecular pain,* 7**,** 1744-8069-7-3.
DE PETROCELLIS, L., DAVIS, J. B. & DI MARZO, V. 2001. Palmitoylethanolamide enhances anandamide stimulation of human vanilloid VR1 receptors. *FEBS Letters,* 506**,** 253-256.
DE VRIES, H. A. 1967. Quantitative electromyographic investigation of the spasm theory of muscle pain. *Ins. Counsel J.,* 34**,** 455.
DESSAUGE, F., SCHLEDER, C., PERRUCHOT, M.-H. & ROUGER, K. 2021. 3D in vitro models of skeletal muscle: myopshere, myobundle and bioprinted muscle construct. *Veterinary Research,* 52**,** 72.
DI CESARE MANNELLI, L., D'AGOSTINO, G., PACINI, A., RUSSO, R., ZANARDELLI, M., GHELARDINI, C. & CALIGNANO, A. 2013a. Palmitoylethanolamide is a disease-modifying agent in peripheral neuropathy: pain relief and neuroprotection share a PPAR-alpha-mediated mechanism. *Mediators of Inflammation,* 2013.
DI CESARE MANNELLI, L., D'AGOSTINO, G., PACINI, A., RUSSO, R., ZANARDELLI, M., GHELARDINI, C. & CALIGNANO, A. 2013b. Palmitoylethanolamide Is a Disease-Modifying Agent in Peripheral Neuropathy: Pain Relief and Neuroprotection Share a PPAR-Alpha-Mediated Mechanism. *Mediators of Inflammation,* 2013**,** 328797.
DIEKMANN, A. & PREISENDÖRFER, P. 2003. Green and greenback: The behavioral effects of environmental attitudes in low-cost and high-cost situations. *Rationality and Society,* 15**,** 441-472.
DILORENZO, F. M., DRAGER, C. J. & RANKIN, J. W. 2014. Docosahexaenoic acid affects markers of inflammation and muscle damage after eccentric exercise. *The Journal of Strength & Conditioning Research,* 28**,** 2768-2774.
DOUGLAS, J., PEARSON, S., ROSS, A. & MCGUIGAN, M. 2017. Eccentric exercise: physiological characteristics and acute responses. *Sports Medicine,* 47**,** 663-675.
DUNCAN, C. 1987. Role of calcium in triggering rapid ultrastructural damage in muscle: a study with chemically skinned fibres. *Journal of Cell Science,* 87**,** 581-594.
EBBELING, C. B. & CLARKSON, P. M. 1989. Exercise-induced muscle damage and adaptation. *Sports Med,* 7**,** 207-34.
EDWARDS, R., HILL, D., JONES, D. & MERTON, P. 1977. Fatigue of long duration in human skeletal muscle after exercise. *The Journal of physiology,* 272**,** 769-778.
EMERSON, D. M., CHEN, S. C., KELLY, M. R., PARNELL, B. & TORRES-MCGEHEE, T. M. 2021. Non-steroidal anti-inflammatory drugs on core body temperature during exercise: A systematic review. *Journal of Exercise Science & Fitness,* 19**,** 127-133.
ERICSSON, K. A., KRAMPE, R. T. & TESCH-RÖMER, C. 1993. The role of deliberate practice in the acquisition of expert performance. *Psychological review,* 100**,** 363.

ERSKINE, R. M., JONES, D. A., MAGANARIS, C. N. & DEGENS, H. 2009. In vivo specific tension of the human quadriceps femoris muscle. *European journal of applied physiology,* 106**,** 827-838.
ERSKINE, R. M., JONES, D. A., WILLIAMS, A. G., STEWART, C. E. & DEGENS, H. 2010. Inter-individual variability in the adaptation of human muscle specific tension to progressive resistance training. *European journal of applied physiology,* 110**,** 1117-1125.
EVANGELISTA, M., CILLI, V., DE VITIS, R., MILITERNO, A. & FANFANI, F. 2018. Ultra-micronized palmitoylethanolamide effects on sleep-wake rhythm and neuropathic pain phenotypes in patients with carpal tunnel syndrome: an open-label, randomized controlled study. *CNS & Neurological Disorders-Drug Targets (Formerly Current Drug Targets-CNS & Neurological Disorders),* 17**,** 291-298.
FAULKNER, J. A. 2003. Terminology for contractions of muscles during shortening, while isometric, and during lengthening. *Journal of Applied Physiology,* 95**,** 455-459.
FIELDING, R., MANFREDI, T., DING, W., FIATARONE, M., EVANS, W. & CANNON, J. G. 1993. Acute phase response in exercise. III. Neutrophil and IL-1 beta accumulation in skeletal muscle. *American Journal of Physiology-Regulatory, Integrative and Comparative Physiology,* 265**,** R166-R172.
FRIDEN, J. & LIEBER, R. L. 1992. Structural and mechanical basis of exercise-induced muscle injury. *Medicine & Science in Sports & Exercise,* 24**,** 521-530.
FU, X., WANG, H. & HU, P. 2015. Stem cell activation in skeletal muscle regeneration. *Cellular and Molecular Life Sciences,* 72**,** 1663-1677.
GABRIELSSON, L., MATTSSON, S. & FOWLER, C. J. 2016. Palmitoylethanolamide for the treatment of pain: pharmacokinetics, safety and efficacy. *Br J Clin Pharmacol,* 82**,** 932-42.
GARNIER, Y. M., LEPERS, R., DUBAU, Q., PAGEAUX, B. & PAIZIS, C. 2018. Neuromuscular and perceptual responses to moderate-intensity incline, level and decline treadmill exercise. *European Journal of Applied Physiology,* 118**,** 2039-2053.
GARRETT JR, W. E., SEABER, A. V., BOSWICK, J., URBANIAK, J. R. & GOLDNER, J. L. 1984. Recovery of skeletal muscle after laceration and repair. *The Journal of hand surgery,* 9**,** 683-692.
GATTI, A., LAZZARI, M., GIANFELICE, V., DI PAOLO, A., SABATO, E. & SABATO, A. F. 2012. Palmitoylethanolamide in the treatment of chronic pain caused by different etiopathogenesis. *Pain Medicine,* 13**,** 1121-1130.
GHLICHLOO, I. & GERRIETS, V. 2019. Nonsteroidal anti-inflammatory drugs (NSAIDs).
GIANDOLINI, M., VERNILLO, G., SAMOZINO, P., HORVAIS, N., EDWARDS, W. B., MORIN, J.-B. & MILLET, G. Y. 2016. Fatigue associated with prolonged graded running. *European journal of applied physiology,* 116**,** 1859-1873.
GISSEL, H. & CLAUSEN, T. 2001. Excitation-induced Ca2+ influx and skeletal muscle cell damage. *Acta Physiologica Scandinavica,* 171**,** 327-334.
GIZARD, F., AMANT, C., BARBIER, O., BELLOSTA, S., ROBILLARD, R., PERCEVAULT, F., SEVESTRE, H., KRIMPENFORT, P., CORSINI, A. & ROCHETTE, J. 2005. PPARα inhibits vascular smooth muscle cell proliferation underlying intimal hyperplasia by inducing the tumor suppressor p16 INK4a. *The Journal of clinical investigation,* 115**,** 3228-3238.

GLASS, D. J. 2005. Skeletal muscle hypertrophy and atrophy signaling pathways. *Int J Biochem Cell Biol,* 37**,** 1974-84.
GORSKI, T., CADORE, E. L., PINTO, S. S., DA SILVA, E. M., CORREA, C. S., BELTRAMI, F. G. & KRUEL, L. M. 2011. Use of NSAIDs in triathletes: prevalence, level of awareness and reasons for use. *British journal of sports medicine,* 45**,** 85-90.
GRAHAM, G. G. & SCOTT, K. F. 2021. Limitations of drug concentrations used in cell culture studies for understanding clinical responses of NSAIDs. *Inflammopharmacology***,** 1-18.
GRAY, P., CHAPPELL, A., JENKINSON, A. M., THIES, F. & GRAY, S. R. 2014. Fish oil supplementation reduces markers of oxidative stress but not muscle soreness after eccentric exercise. *International journal of sport nutrition and exercise metabolism,* 24**,** 206-214.
GREEN, S. & WAHLI, W. 1994. Peroxisome proliferator-activated receptors: finding the orphan a home. *Molecular and cellular endocrinology,* 100**,** 149-153.
GRIFFIN, T. J., GYGI, S. P., IDEKER, T., RIST, B., ENG, J., HOOD, L. & AEBERSOLD, R. 2002. Complementary profiling of gene expression at the transcriptome and proteome levels in saccharomyces cerevisiae* S. *Molecular & Cellular Proteomics,* 1**,** 323-333.
GROUNDS, M. 1991. Towards understanding skeletal muscle regeneration. *Pathology-Research and Practice,* 187**,** 1-22.
GUIDA, F., LUONGO, L., BOCCELLA, S., GIORDANO, M., ROMANO, R., BELLINI, G., MANZO, I., FURIANO, A., RIZZO, A. & IMPERATORE, R. 2017. Palmitoylethanolamide induces microglia changes associated with increased migration and phagocytic activity: involvement of the CB2 receptor. *Scientific reports,* 7**,** 375.
GUIDA, G., DE MARTINO, M., DE FABIANI, A., CANTIERI, L., ALEXANDRE, A., VASSALLO, G., ROGAI, M., LANAIA, F. & PETROSINO, S. 2010. La palmitoiletanolamida (Normast®) en el dolor neuropático crónico por lumbociatalgia de tipo compresivo: Estudio clínico multicéntrico. *Dolor. Investigación Clínica & Terapéutica,* 25**,** 35-42.
GULICK, D. T. & KIMURA, I. F. 1996. Delayed onset muscle soreness: what is it and how do we treat it? *Journal of Sport Rehabilitation,* 5**,** 234-243.
GURLEY, B. J., MURPHY, T. P., GUL, W., WALKER, L. A. & ELSOHLY, M. 2020. Content versus label claims in cannabidiol (CBD)-containing products obtained from commercial outlets in the state of Mississippi. *Journal of dietary supplements,* 17**,** 599-607.
HAEFELI, M. & ELFERING, A. 2006. Pain assessment. *European spine journal,* 15**,** S17-S24.
HAGAN, R., SMITH, M. & GETTMAN, L. 1981. Marathon performance in relation to maximal aerobic power and training indices. *Medicine and Science in Sports and Exercise,* 13**,** 185-189.
HATCHETT, A., ARMSTRONG, K., HUGHES, B. & PARR, B. 2020. The influence cannabidiol on delayed onset of muscle soreness. *Int. J. Phys. Educ. Sports Health,* 7**,** 89-94.
HAUER, D., SCHELLING, G., GOLA, H., CAMPOLONGO, P., MORATH, J., ROOZENDAAL, B., HAMUNI, G., KARABATSIAKIS, A., ATSAK, P. & VOGESER, M. 2013. Plasma

concentrations of endocannabinoids and related primary fatty acid amides in patients with post-traumatic stress disorder. *Plos one,* 8**,** e62741.
HEATON, L. E., DAVIS, J. K., RAWSON, E. S., NUCCIO, R. P., WITARD, O. C., STEIN, K. W., BAAR, K., CARTER, J. M. & BAKER, L. B. 2017. Selected in-season nutritional strategies to enhance recovery for team sport athletes: a practical overview. *Sports medicine,* 47**,** 2201-2218.
HESSELINK, J. M. K. & HEKKER, T. A. 2012. Therapeutic utility of palmitoylethanolamide in the treatment of neuropathic pain associated with various pathological conditions: a case series. *Journal of Pain Research***,** 437-442.
HINDI, S. M. & MILLAY, D. P. 2022. All for one and one for all: Regenerating skeletal muscle. *Cold Spring Harbor perspectives in biology,* 14**,** a040824.
HODGSON, L., WALTER, E., VENN, R., GALLOWAY, R., PITSILADIS, Y., SARDAT, F. & FORNI, L. 2017. Acute kidney injury associated with endurance events—is it a cause for concern? A systematic review. *BMJ Open Sport & Exercise Medicine,* 3.
HOFFMAN, M. D. & FOGARD, K. 2011. Factors related to successful completion of a 161-km ultramarathon. *International journal of sports physiology and performance,* 6**,** 25-37.
HOLGADO, D., HOPKER, J., SANABRIA, D. & ZABALA, M. 2018. Analgesics and sport performance: beyond the pain-modulating effects. *PM&R,* 10**,** 72-82.
HOLMES, W. E., ANGEL, T. E., LI, K. W. & HELLERSTEIN, M. K. 2015. Dynamic Proteomics: In Vivo Proteome-Wide Measurement of Protein Kinetics Using Metabolic Labeling. *Methods Enzymol,* 561**,** 219-76.
HOPPELER, H., BAUM, O., LURMAN, G. & MUELLER, M. 2011. Molecular mechanisms of muscle plasticity with exercise. *Comprehensive Physiology,* 1**,** 1383-1412.
HOPPELER, H. & HERZOG, W. 2014. Eccentric exercise: many questions unanswered. American Physiological Society Bethesda, MD.
HOUGH, T. 1902. Ergographic studies in muscular soreness. *American physical education review,* 7**,** 1-17.
HOWATSON, G. & VAN SOMEREN, K. A. 2008. The prevention and treatment of exercise-induced muscle damage. *Sports medicine,* 38**,** 483-503.
HUARD, J., LI, Y. & FU, F. H. 2002. Muscle injuries and repair: current trends in research. *JBJS,* 84**,** 822-832.
HUGHES, S. M., CHI, M. M.-Y., LOWRY, O. H. & GUNDERSEN, K. 1999. Myogenin induces a shift of enzyme activity from glycolytic to oxidative metabolism in muscles of transgenic mice. *The Journal of cell biology,* 145**,** 633-642.
HUSCHTSCHA, Z., SILVER, J., GERHARDY, M., URWIN, C. S., KENNEY, N., LE, V. H., FYFE, J. J., FEROS, S. A., BETIK, A. C. & SHAW, C. S. 2024. The Effect of Palmitoylethanolamide (PEA) on Skeletal Muscle Hypertrophy, Strength, and Power in Response to Resistance Training in Healthy Active Adults: A Double-Blind Randomized Control Trial. *Sports Medicine-Open,* 10**,** 66.
HYLDAHL, R. D. & HUBAL, M. J. 2014. Lengthening our perspective: morphological, cellular, and molecular responses to eccentric exercise. *Muscle & nerve,* 49**,** 155-170.
HYLDAHL, R. D., OLSON, T., WELLING, T., GROSCOST, L. & PARCELL, A. C. 2014. Satellite cell activity is differentially affected by contraction mode in human muscle following a work-matched bout of exercise. *Frontiers in physiology,* 5**,** 485.

IANNOTTI, F. A., DI MARZO, V. & PETROSINO, S. 2016. Endocannabinoids and endocannabinoid-related mediators: Targets, metabolism and role in neurological disorders. *Progress in lipid research,* 62**,** 107-128.
ILCHENKO, S., HADDAD, A., SADANA, P., RECCHIA, F. A., SADYGOV, R. G. & KASUMOV, T. 2019. Calculation of the Protein Turnover Rate Using the Number of Incorporated 2H Atoms and Proteomics Analysis of a Single Labeled Sample. *Analytical Chemistry,* 91**,** 14340-14351.
IMPELLIZZERI, D., BRUSCHETTA, G., CORDARO, M., CRUPI, R., SIRACUSA, R., ESPOSITO, E. & CUZZOCREA, S. 2014a. Micronized/ultramicronized palmitoylethanolamide displays superior oral efficacy compared to nonmicronized palmitoylethanolamide in a rat model of inflammatory pain. *Journal of neuroinflammation,* 11**,** 1-9.
IMPELLIZZERI, D., BRUSCHETTA, G., CORDARO, M., CRUPI, R., SIRACUSA, R., ESPOSITO, E. & CUZZOCREA, S. 2014b. Micronized/ultramicronized palmitoylethanolamide displays superior oral efficacy compared to nonmicronized palmitoylethanolamide in a rat model of inflammatory pain. *J Neuroinflammation,* 11**,** 136.
INKER, L. A., ENEANYA, N. D., CORESH, J., TIGHIOUART, H., WANG, D., SANG, Y., CREWS, D. C., DORIA, A., ESTRELLA, M. M. & FROISSART, M. 2021. New creatinine-and cystatin C–based equations to estimate GFR without race. *New England Journal of Medicine,* 385**,** 1737-1749.
ISSEMANN, I. & GREEN, S. 1990. Activation of a member of the steroid hormone receptor superfamily by peroxisome proliferators. *Nature,* 347**,** 645-650.
JACKMAN, S. R., WITARD, O. C., JEUKENDRUP, A. E. & TIPTON, K. D. 2010. Branched-chain amino acid ingestion can ameliorate soreness from eccentric exercise. *Medicine & Science in Sports & Exercise,* 42**,** 962-970.
JESSEN, S., QUESADA, J. P., DI CREDICO, A., MORENO-JUSTICIA, R., WILSON, R., JACOBSON, G., BANGSBO, J., DESHMUKH, A. S. & HOSTRUP, M. 2024. Beta2-Adrenergic Stimulation Induces Resistance Training-Like Adaptations in Human Skeletal Muscle: Potential Role of KLHL41. *Scandinavian Journal of Medicine & Science in Sports,* 34**,** e14736.
JOHNSON, E., KILGORE, M. & BABALONIS, S. 2022. Cannabidiol (CBD) product contamination: quantitative analysis of Δ9-tetrahydrocannabinol (Δ9-THC) concentrations found in commercially available CBD products. *Drug and alcohol dependence,* 237**,** 109522.
JONES, R., RUBIN, G., BERENBAUM, F. & SCHEIMAN, J. 2008. Gastrointestinal and cardiovascular risks of nonsteroidal anti-inflammatory drugs. *The American journal of medicine,* 121**,** 464-474.
JOSLIN, J., LLOYD, J., KOTLYAR, T. & WOJCIK, S. 2013. NSAID and other analgesic use by endurance runners during training, competition and recovery. *South African Journal of Sports Medicine,* 25**,** 101-104.
JOURIS, K. B., MCDANIEL, J. L. & WEISS, E. P. 2011. The effect of omega-3 fatty acid supplementation on the inflammatory response to eccentric strength exercise. *Journal of sports science & medicine,* 10**,** 432.
KAHLICH, R., KLÍMA, J., CIHLA, F., FRANKOVÁ, V., MASEK, K., ROSICKÝ, M., MATOUSEK, F. & BRUTHANS, J. 1979. Studies on prophylactic efficacy of N-2-hydroxyethyl palmitamide (Impulsin) in acute respiratory infections.

Serologically controlled field trials. *Journal of hygiene, epidemiology, microbiology, and immunology,* 23**,** 11-24.
KARALAKI, M., FILI, S., PHILIPPOU, A. & KOUTSILIERIS, M. 2009. Muscle regeneration: cellular and molecular events. *In vivo,* 23**,** 779-796.
KASPER, A. M., SPARKS, S. A., HOOKS, M., SKEER, M., WEBB, B., NIA, H., MORTON, J. P. & CLOSE, G. L. 2020. High prevalence of cannabidiol use within male professional rugby union and league players: a quest for pain relief and enhanced recovery. *International journal of sport nutrition and exercise metabolism,* 30**,** 315-322.
KELLY, B. & O'NEILL, L. A. 2015. Metabolic reprogramming in macrophages and dendritic cells in innate immunity. *Cell research,* 25**,** 771-784.
KEPPEL HESSELINK, J. 2013. Professor Rita Levi-Montalcini on nerve growth factor, mast cells and palmitoylethanolamide, an endogenous antiinflammatory and analgesic compound. *J Pain Relief,* 2**,** 1000114.
KEPPEL HESSELINK, J., DE BOER, T. & WITKAMP, R. F. 2013. Palmitoylethanolamide: a natural body-own anti-inflammatory agent, effective and safe against influenza and common cold. *International journal of inflammation,* 2013.
KIRKENDALL, D. T. 1990. Mechanisms of peripheral fatigue. *Medicine and science in sports and exercise,* 22**,** 444-449.
KISLINGER, T., GRAMOLINI, A. O., PAN, Y., RAHMAN, K., MACLENNAN, D. H. & EMILI, A. 2005. Proteome Dynamics during C2C12 Myoblast Differentiation* S. *Molecular & cellular proteomics,* 4**,** 887-901.
KONRAD, M., NIEMAN, D. C., HENSON, D. A., KENNERLY, K. M., JIN, F. & WALLNER-LIEBMANN, S. J. 2011. The acute effect of ingesting a quercetin-based supplement on exercise-induced inflammation and immune changes in runners. *International journal of sport nutrition and exercise metabolism,* 21**,** 338-346.
KRENTZ, J. R., QUEST, B., FARTHING, J. P., QUEST, D. W. & CHILIBECK, P. D. 2008. The effects of ibuprofen on muscle hypertrophy, strength, and soreness during resistance training. *Applied Physiology, Nutrition, and Metabolism,* 33**,** 470-475.
KUCHINKE, K. P. 1997. Employee expertises the status of the theory and the literature. *Performance improvement quarterly,* 10**,** 72-86.
KUEHL JR, F., JACOB, T., GANLEY, O., ORMOND, R. & MEISINGER, M. 1957. The identification of N-(2-hydroxyethyl)-palmitamide as a naturally occurring anti-inflammatory agent. *Journal of the American Chemical Society,* 79**,** 5577-5578.
LAMBERT, D. M., VANDEVOORDE, S., JONSSON, K. O. & FOWLER, C. J. 2002. The palmitoylethanolamide family: a new class of anti-inflammatory agents? *Curr Med Chem,* 9**,** 663-74.
LAMBERT, G. P., BOYLAN, M., LAVENTURE, J.-P., BULL, A. & LANSPA, S. 2007. Effect of aspirin and ibuprofen on GI permeability during exercise. *International journal of sports medicine***,** 722-726.
LAMON, S., MORABITO, A., ARENTSON-LANTZ, E., KNOWLES, O., VINCENT, G. E., CONDO, D., ALEXANDER, S. E., GARNHAM, A., PADDON-JONES, D. & AISBETT, B. 2021. The effect of acute sleep deprivation on skeletal muscle protein synthesis and the hormonal environment. *Physiological reports,* 9**,** e14660.
LANG-ILLIEVICH, K., KLIVINYI, C., LASSER, C., BRENNA, C. T., SZILAGYI, I. S. & BORNEMANN-CIMENTI, H. 2023. Palmitoylethanolamide in the Treatment of

Chronic Pain: A Systematic Review and Meta-Analysis of Double-Blind Randomized Controlled Trials. *Nutrients,* 15**,** 1350.
LANG-ILLIEVICH, K., KLIVINYI, C., RUMPOLD-SEITLINGER, G., DORN, C. & BORNEMANN-CIMENTI, H. 2022. The effect of palmitoylethanolamide on pain intensity, central and peripheral sensitization, and pain modulation in healthy volunteers—a randomized, double-blinded, placebo-controlled crossover trial. *Nutrients,* 14**,** 4084.
LAUCKNER, J. E., JENSEN, J. B., CHEN, H.-Y., LU, H.-C., HILLE, B. & MACKIE, K. 2008. GPR55 is a cannabinoid receptor that increases intracellular calcium and inhibits M current. *Proceedings of the national Academy of sciences,* 105**,** 2699-2704.
LEVI-MONTALCINI, R., SKAPER, S. D., DAL TOSO, R., PETRELLI, L. & LEON, A. 1996. Nerve growth factor: from neurotrophin to neurokine. *Trends in neurosciences,* 19**,** 514-520.
LEWIS, P. B., RUBY, D. & BUSH-JOSEPH, C. A. 2012. Muscle soreness and delayed-onset muscle soreness. *Clinics in sports medicine,* 31**,** 255-262.
LEYK, D., RÜTHER, T., HARTMANN, N., VITS, E., STAUDT, M. & HOFFMANN, M. A. 2023. Analgesic use in sports: results of a systematic literature review. *Deutsches Ärzteblatt International,* 120**,** 155.
LI, H., MALHOTRA, S. & KUMAR, A. 2008. Nuclear factor-kappa B signaling in skeletal muscle atrophy. *J Mol Med (Berl),* 86**,** 1113-26.
LIEN, S.-C., WEI, S.-Y., CHANG, S.-F., CHANG, M. D.-T., CHANG, J.-Y. & CHIU, J.-J. 2013. Activation of PPAR-α induces cell cycle arrest and inhibits transforming growth factor-β1 induction of smooth muscle cell phenotype in 10T1/2 mesenchymal cells. *Cellular signalling,* 25**,** 1252-1263.
LILJA, M., MANDIĆ, M., APRÓ, W., MELIN, M., OLSSON, K., ROSENBORG, S., GUSTAFSSON, T. & LUNDBERG, T. R. 2018. High doses of anti-inflammatory drugs compromise muscle strength and hypertrophic adaptations to resistance training in young adults. *Acta Physiologica,* 222**,** e12948.
LIN, J. H., COCCHETTO, D. M. & DUGGAN, D. E. 1987. Protein binding as a primary determinant of the clinical pharmacokinetic properties of non-steroidal anti-inflammatory drugs. *Clinical pharmacokinetics,* 12**,** 402-432.
LINDHARDSEN, J., GISLASON, G. H., JACOBSEN, S., AHLEHOFF, O., OLSEN, A.-M. S., MADSEN, O. R., TORP-PEDERSEN, C. & HANSEN, P. R. 2014. Non-steroidal anti-inflammatory drugs and risk of cardiovascular disease in patients with rheumatoid arthritis: a nationwide cohort study. *Annals of the rheumatic diseases,* 73**,** 1515-1521.
LINDSTEDT, S. L., LASTAYO, P. & REICH, T. 2001. When active muscles lengthen: properties and consequences of eccentric contractions. *Physiology,* 16**,** 256-261.
LO VERME, J., FU, J., ASTARITA, G., LA RANA, G., RUSSO, R., CALIGNANO, A. & PIOMELLI, D. 2005. The nuclear receptor peroxisome proliferator-activated receptor-alpha mediates the anti-inflammatory actions of palmitoylethanolamide. *Mol Pharmacol,* 67**,** 15-9.
LONG, D. & MARTIN, A. 1956. Factor in arachis oil depressing sensitivity to tuberculin in BCG-infected guineapigs. *Lancet***,** 464-6.

LOVE, M. I., HUBER, W. & ANDERS, S. 2014. Moderated estimation of fold change and dispersion for RNA-seq data with DESeq2. *Genome biology,* 15**,** 550.
LOVERME, J., LA RANA, G., RUSSO, R., CALIGNANO, A. & PIOMELLI, D. 2005. The search for the palmitoylethanolamide receptor. *Life sciences,* 77**,** 1685-1698.
MACHADO BERGAMASCHI, M., HELENA COSTA QUEIROZ, R., WALDO ZUARDI, A. & CRIPPA, A. S. 2011. Safety and side effects of cannabidiol, a Cannabis sativa constituent. *Current drug safety,* 6**,** 237-249.
MACINTYRE, D. L., REID, W. D. & MCKENZIE, D. C. 1995a. Delayed muscle soreness. *Sports medicine,* 20**,** 24-40.
MACINTYRE, D. L., REID, W. D. & MCKENZIE, D. C. 1995b. Delayed muscle soreness: the inflammatory response to muscle injury and its clinical implications. *Sports medicine,* 20**,** 24-40.
MACLENNAN, D. H. & KRANIAS, E. G. 2003. Phospholamban: a crucial regulator of cardiac contractility. *Nature reviews Molecular cell biology,* 4**,** 566-577.
MALCOLM, D. 2009. Medical uncertainty and clinician–athlete relations: The management of concussion injuries in rugby union. *Sociology of sport journal,* 26**,** 191-210.
MALLARD, A., BRISKEY, D., RICHARDS, A., MILLS, D. & RAO, A. 2020. The Effect of Orally Dosed Levagen+ (palmitoylethanolamide) on Exercise Recovery in Healthy Males-A Double-Blind, Randomized, Placebo-Controlled Study. *Nutrients,* 12.
MALM, C., SJÖDIN, B., SJÖBERG, B., LENKEI, R., RENSTRÖM, P., LUNDBERG, I. E. & EKBLOM, B. 2004. Leukocytes, cytokines, growth factors and hormones in human skeletal muscle and blood after uphill or downhill running. *The Journal of physiology,* 556**,** 983-1000.
MARINI, I., LAVINIA BARTOLUCCI, M., BORTOLOTTI, F., ROSARIA GATTO, M. & ALESSANDRI BONETTI, G. 2012. Palmitoylethanolamide versus a nonsteroidal anti-inflammatory drug in the treatment of temporomandibular joint inflammatory pain. *Journal of orofacial pain,* 26**,** 99.
MARKUS, I., CONSTANTINI, K., HOFFMAN, J., BARTOLOMEI, S. & GEPNER, Y. 2021. Exercise-induced muscle damage: Mechanism, assessment and nutritional factors to accelerate recovery. *European journal of applied physiology,* 121**,** 969-992.
MARSH, D. R., CRISWELL, D. S., CARSON, J. A. & BOOTH, F. W. 1997. Myogenic regulatory factors during regeneration of skeletal muscle in young, adult, and old rats. *Journal of applied physiology,* 83**,** 1270-1275.
MARSHALL, P. W., LOVELL, R., JEPPESEN, G. K., ANDERSEN, K. & SIEGLER, J. C. 2014. Hamstring muscle fatigue and central motor output during a simulated soccer match. *PloS one,* 9**,** e102753.
MARTÍNEZ, S., AGUILÓ, A., MORENO, C., LOZANO, L. & TAULER, P. 2017. Use of non-steroidal anti-inflammatory drugs among participants in a mountain ultramarathon event. *Sports,* 5**,** 11.
MARTINEZ-NAVARRO, I., MONTOYA-VIECO, A., COLLADO, E., HERNANDO, B. & HERNANDO, C. 2022. Ultra trail performance is differently predicted by endurance variables in men and women. *International journal of sports medicine,* 43**,** 600-607.
MARTÍNEZ-PINILLA, E., AGUINAGA, D., NAVARRO, G., RICO, A. J., OYARZÁBAL, J., SÁNCHEZ-ARIAS, J. A., LANCIEGO, J. L. & FRANCO, R. 2019. Targeting CB 1 and

GPR55 endocannabinoid receptors as a potential neuroprotective approach for Parkinson's disease. *Molecular Neurobiology,* 56**,** 5900-5910.
MAŠEK, K., PERLÍK, F., KLÍMA, J. & KAHLICH, R. 1974. Prophylactic efficacy of N-2-hydroxyethyl palmitamide (Impulsin®) in acute respiratory tract infections. *European journal of clinical pharmacology,* 7**,** 415-419.
MATSUDA, L. A., LOLAIT, S. J., BROWNSTEIN, M. J., YOUNG, A. C. & BONNER, T. I. 1990. Structure of a cannabinoid receptor and functional expression of the cloned cDNA. *Nature,* 346**,** 561-564.
MAUGHAN, R. & LEIPER, J. 1983. Aerobic capacity and fractional utilisation of aerobic capacity in elite and non-elite male and female marathon runners. *European journal of applied physiology and occupational physiology,* 52**,** 80-87.
MAUKSCH, S., VON DER GRACHT, H. A. & GORDON, T. J. 2020. Who is an expert for foresight? A review of identification methods. *Technological Forecasting and Social Change,* 154**,** 119982.
MAURO, A. 1961. Satellite cell of skeletal muscle fibers. *The Journal of biophysical and biochemical cytology,* 9**,** 493.
MCCARTHY, J. J., MULA, J., MIYAZAKI, M., ERFANI, R., GARRISON, K., FAROOQUI, A. B., SRIKUEA, R., LAWSON, B. A., GRIMES, B. & KELLER, C. 2011. Effective fiber hypertrophy in satellite cell-depleted skeletal muscle. *Development,* 138**,** 3657-3666.
MCCARTNEY, D., BENSON, M. J., DESBROW, B., IRWIN, C., SURAEV, A. & MCGREGOR, I. S. 2020. Cannabidiol and sports performance: a narrative review of relevant evidence and recommendations for future research. *Sports medicine-open,* 6**,** 1-18.
MCCULLY, K. K. & FAULKNER, J. A. 1986. Characteristics of lengthening contractions associated with injury to skeletal muscle fibers. *Journal of Applied Physiology,* 61**,** 293-299.
MCDUFF, D., STULL, T., CASTALDELLI-MAIA, J. M., HITCHCOCK, M. E., HAINLINE, B. & REARDON, C. L. 2019. Recreational and ergogenic substance use and substance use disorders in elite athletes: a narrative review. *British journal of sports medicine,* 53**,** 754-760.
MCFARLAN, J. T., YOSHIDA, Y., JAIN, S. S., HAN, X.-X., SNOOK, L. A., LALLY, J., SMITH, B. K., GLATZ, J. F., LUIKEN, J. J. & SAYER, R. A. 2012. In vivo, fatty acid translocase (CD36) critically regulates skeletal muscle fuel selection, exercise performance, and training-induced adaptation of fatty acid oxidation. *Journal of Biological Chemistry,* 287**,** 23502-23516.
MCHUGH, M. P., CONNOLLY, D. A., ESTON, R. G. & GLEIM, G. W. 2000. Electromyographic analysis of exercise resulting in symptoms of muscle damage. *J Sports Sci,* 18**,** 163-72.
MCKAY, A. K., STELLINGWERFF, T., SMITH, E. S., MARTIN, D. T., MUJIKA, I., GOOSEY-TOLFREY, V. L., SHEPPARD, J. & BURKE, L. M. 2021. Defining training and performance caliber: a participant classification framework. *International journal of sports physiology and performance,* 17**,** 317-331.
MECHOULAM, R. & HANUŠ, L. 2002. Cannabidiol: an overview of some chemical and pharmacological aspects. Part I: chemical aspects. *Chemistry and physics of lipids,* 121**,** 35-43.

MELO, F., CAREY, D. J. & BRANDAN, E. 1996. Extracellular matrix is required for skeletal muscle differentiation but not myogenin expression. *Journal of cellular biochemistry,* 62**,** 227-239.
MELZER, M., ELBE, A.-M. & STRAHLER, K. 2022. Athletes' use of analgesics is related to doping attitudes, competitive anxiety, and situational opportunity. *Frontiers in Sports and Active Living,* 4**,** 849117.
MENDHAM, A. E., DONGES, C. E., LIBERTS, E. A. & DUFFIELD, R. 2011. Effects of mode and intensity on the acute exercise-induced IL-6 and CRP responses in a sedentary, overweight population. *European journal of applied physiology,* 111**,** 1035-1045.
MIKKELSEN, U., SCHJERLING, P., HELMARK, I. C., REITELSEDER, S., HOLM, L., SKOVGAARD, D., LANGBERG, H., KJÆR, M. & HEINEMEIER, K. 2011. Local NSAID infusion does not affect protein synthesis and gene expression in human muscle after eccentric exercise. *Scandinavian journal of medicine & science in sports,* 21**,** 630-644.
MIKKELSEN, U. R., LANGBERG, H., HELMARK, I. C., SKOVGAARD, D., ANDERSEN, L. L., KJAER, M. & MACKEY, A. L. 2009. Local NSAID infusion inhibits satellite cell proliferation in human skeletal muscle after eccentric exercise. *Journal of applied physiology,* 107**,** 1600-1611.
MILLET, G. Y., MARTIN, V., LATTIER, G. & BALLAY, Y. 2003. Mechanisms contributing to knee extensor strength loss after prolonged running exercise. *Journal of Applied Physiology,* 94**,** 193-198.
MORGAN, D. L. & ALLEN, D. G. 1999. Early events in stretch-induced muscle damage. *J Appl Physiol (1985),* 87**,** 2007-15.
MURASE, S., TERAZAWA, E., HIRATE, K., YAMANAKA, H., KANDA, H., NOGUCHI, K., OTA, H., QUEME, F., TAGUCHI, T. & MIZUMURA, K. 2013. Upregulated glial cell line-derived neurotrophic factor through cyclooxygenase-2 activation in the muscle is required for mechanical hyperalgesia after exercise in rats. *The Journal of physiology,* 591**,** 3035-3048.
MURASE, S., TERAZAWA, E., QUEME, F., OTA, H., MATSUDA, T., HIRATE, K., KOZAKI, Y., KATANOSAKA, K., TAGUCHI, T. & URAI, H. 2010. Bradykinin and nerve growth factor play pivotal roles in muscular mechanical hyperalgesia after exercise (delayed-onset muscle soreness). *Journal of Neuroscience,* 30**,** 3752-3761.
MYBURGH, K. H. 2014. Polyphenol supplementation: benefits for exercise performance or oxidative stress? *Sports Medicine,* 44**,** 57-70.
NAM, J. H., PARK, E. S., WON, S.-Y., LEE, Y. A., KIM, K. I., JEONG, J. Y., BAEK, J. Y., CHO, E. J., JIN, M. & CHUNG, Y. C. 2015. TRPV1 on astrocytes rescues nigral dopamine neurons in Parkinson's disease via CNTF. *Brain,* 138**,** 3610-3622.
NEEDHAM, R. D. & DE LOË, R. C. 1990. The policy Delphi: purpose, structure, and application. *Canadian Geographer/Le Géographe Canadien,* 34**,** 133-142.
NEMALI, M. R., USUDA, N., REDDY, M. K., OYASU, K., HASHIMOTO, T., OSUMI, T., RAO, M. S. & REDDY, J. K. 1988. Comparison of constitutive and inducible levels of expression of peroxisomal β-oxidation and catalase genes in liver and extrahepatic tissues of rat. *Cancer research,* 48**,** 5316-5324.
NEWHAM, D., MILLS, K., QUIGLEY, R. & EDWARDS, R. 1982. Muscle pain and tenderness after exercise. *Aust J Sports Med Exerc Sci,* 14**,** 129-31.

NEWTON, M. J., MORGAN, G. T., SACCO, P., CHAPMAN, D. W. & NOSAKA, K. 2008. Comparison of responses to strenuous eccentric exercise of the elbow flexors between resistance-trained and untrained men. *The Journal of Strength & Conditioning Research,* 22**,** 597-607.

NGUYEN, H. X. & TIDBALL, J. G. 2003. Interactions between neutrophils and macrophages promote macrophage killing of rat muscle cells in vitro. *The Journal of physiology,* 547**,** 125-132.

NIE, H., MADELEINE, P., ARENDT-NIELSEN, L. & GRAVEN-NIELSEN, T. 2009. Temporal summation of pressure pain during muscle hyperalgesia evoked by nerve growth factor and eccentric contractions. *European Journal of Pain,* 13**,** 704-710.

NIELSEN, J., MADSEN, K., JØRGENSEN, L. & SAHLIN, K. 2005. Effects of lengthening contraction on calcium kinetics and skeletal muscle contractility in humans. *Acta Physiologica Scandinavica,* 184**,** 203-214.

NIEMAN, D. C., HENSON, D. A., DAVIS, J. M., ANGELA MURPHY, E., JENKINS, D. P., GROSS, S. J., CARMICHAEL, M. D., QUINDRY, J. C., DUMKE, C. L. & UTTER, A. C. 2007a. Quercetin's influence on exercise-induced changes in plasma cytokines and muscle and leukocyte cytokine mRNA. *Journal of Applied Physiology,* 103**,** 1728-1735.

NIEMAN, D. C., HENSON, D. A., DAVIS, J. M., DUMKE, C. L., GROSS, S. J., JENKINS, D. P., MURPHY, E. A., CARMICHAEL, M. D., QUINDRY, J. C. & MCANULTY, S. R. 2007b. Quercetin ingestion does not alter cytokine changes in athletes competing in the Western States Endurance Run. *Journal of Interferon & Cytokine Research,* 27**,** 1003-1012.

NOONAN, T. J. & GARRETT JR, W. E. 1992. Injuries at the myotendinous junction. *Clinics in Sports Medicine,* 11**,** 783-806.

NOSAKA, K. 2006. Effects of amino acid supplementation on muscle soreness and damage. *International journal of sport nutrition and exercise metabolism,* 16**,** 620-635.

NOSAKA, K. & CLARKSON, P. M. 1996. Variability in serum creatine kinase response after eccentric exercise of the elbow flexors. *International journal of sports medicine,* 17**,** 120-127.

NOSAKA, K., NEWTON, M. & SACCO, P. 2002. Muscle damage and soreness after endurance exercise of the elbow flexors. *Medicine & Science in Sports & Exercise,* 34**,** 920-927.

NUNEZ, R. 2001. DNA measurement and cell cycle analysis by flow cytometry. *Current issues in molecular biology,* 3**,** 67-70.

O'FALLON, K. S., KAUSHIK, D., MICHNIAK-KOHN, B., DUNNE, C. P., ZAMBRASKI, E. J. & CLARKSON, P. M. 2012. Effects of quercetin supplementation on markers of muscle damage and inflammation after eccentric exercise. *International journal of sport nutrition and exercise metabolism,* 22**,** 430-437.

O'NEILL, L. A. & PEARCE, E. J. 2016. Immunometabolism governs dendritic cell and macrophage function. *Journal of Experimental Medicine,* 213**,** 15-23.

ORIMO, S., HIYAMUTA, E., ARAHATA, K. & SUGITA, H. 1991. Analysis of inflammatory cells and complement C3 in bupivacaine-induced myonecrosis. *Muscle & Nerve: Official Journal of the American Association of Electrodiagnostic Medicine,* 14**,** 515-520.

OVERBYE, M. 2021. Walking the line? An investigation into elite athletes' sport-related use of painkillers and their willingness to use analgesics to train or compete when injured. *International Review for the Sociology of Sport,* 56**,** 1091-1115.
OVERDEVEST, E., WOUTERS, J. A., WOLFS, K. H., VAN LEEUWEN, J. J. & POSSEMIERS, S. 2018. Citrus flavonoid supplementation improves exercise performance in trained athletes. *Journal of sports science & medicine,* 17**,** 24.
OWENS, D. J., TWIST, C., COBLEY, J. N., HOWATSON, G. & CLOSE, G. L. 2019. Exercise-induced muscle damage: What is it, what causes it and what are the nutritional solutions? *Eur J Sport Sci,* 19**,** 71-85.
PAGANO, E., VENNERI, T., LUCARIELLO, G., CICIA, D., BRANCALEONE, V., NANÌ, M. F., CACCIOLA, N. A., CAPASSO, R., IZZO, A. A. & BORRELLI, F. 2021. Palmitoylethanolamide reduces colon cancer cell proliferation and migration, influences tumor cell cycle and exerts in vivo chemopreventive effects. *Cancers,* 13**,** 1923.
PALADINI, A., FUSCO, M., CENACCHI, T., SCHIEVANO, C., PIROLI, A. & VARRASSI, G. 2016. Palmitoylethanolamide, a Special Food for Medical Purposes, in the Treatment of Chronic Pain: A Pooled Data Meta-analysis. *Pain Physician,* 19**,** 11-24.
PALMER, R. 1990. Prostaglandins and the control of muscle protein synthesis and degradation. *Prostaglandins, leukotrienes and essential fatty acids,* 39**,** 95-104.
PANNONE, E. & ABBOTT, R. 2024. What is known about the health effects of non-steroidal anti-inflammatory drug (NSAID) use in marathon and ultraendurance running: a scoping review. *BMJ Open Sport & Exercise Medicine,* 10.
PASIAKOS, S. M., LIEBERMAN, H. R. & MCLELLAN, T. M. 2014. Effects of protein supplements on muscle damage, soreness and recovery of muscle function and physical performance: a systematic review. *Sports medicine,* 44**,** 655-670.
PASTOR, F. S., BESSON, T., VARESCO, G., PARENT, A., FANGET, M., KORAL, J., FOSCHIA, C., RUPP, T., RIMAUD, D. & FÉASSON, L. 2022. Performance determinants in trail-running races of different distances. *International journal of sports physiology and performance,* 17**,** 844-851.
PATERNITI, I., IMPELLIZZERI, D., CRUPI, R., MORABITO, R., CAMPOLO, M., ESPOSITO, E. & CUZZOCREA, S. 2013. Molecular evidence for the involvement of PPAR-δ and PPAR-γ in anti-inflammatory and neuroprotective activities of palmitoylethanolamide after spinal cord trauma. *Journal of neuroinflammation,* 10**,** 787.
PAULSEN, G., RAMER MIKKELSEN, U., RAASTAD, T. & PEAKE, J. M. 2012. Leucocytes, cytokines and satellite cells: what role do they play in muscle damage and regeneration following eccentric exercise? *Exercise immunology review,* 18.
PEAKE, J., NOSAKA, K. K., MUTHALIB, M. & SUZUKI, K. 2006. Systemic inflammatory responses to maximal versus submaximal lengthening contractions of the elbow flexors.
PEAKE, J. M., NEUBAUER, O., DELLA GATTA, P. A. & NOSAKA, K. 2017. Muscle damage and inflammation during recovery from exercise. *J Appl Physiol (1985),* 122**,** 559-570.
PETROSINO, S., CORDARO, M., VERDE, R., SCHIANO MORIELLO, A., MARCOLONGO, G., SCHIEVANO, C., SIRACUSA, R., PISCITELLI, F., PERITORE, A. F. & CRUPI, R.

2018. Oral ultramicronized palmitoylethanolamide: plasma and tissue levels and spinal anti-hyperalgesic effect. *Frontiers in Pharmacology,* 9**,** 249.
PETROSINO, S. & DI MARZO, V. 2017a. The pharmacology of palmitoylethanolamide and first data on the therapeutic efficacy of some of its new formulations. *British journal of pharmacology,* 174**,** 1349-1365.
PETROSINO, S. & DI MARZO, V. 2017b. The pharmacology of palmitoylethanolamide and first data on the therapeutic efficacy of some of its new formulations. *Br J Pharmacol,* 174**,** 1349-1365.
PETROSINO, S. & SCHIANO MORIELLO, A. 2020. Palmitoylethanolamide: a nutritional approach to keep neuroinflammation within physiological boundaries—a systematic review. *International Journal of Molecular Sciences,* 21**,** 9526.
PETROSINO, S., SCHIANO MORIELLO, A., CERRATO, S., FUSCO, M., PUIGDEMONT, A., DE PETROCELLIS, L. & DI MARZO, V. 2016. The anti-inflammatory mediator palmitoylethanolamide enhances the levels of 2-arachidonoyl-glycerol and potentiates its actions at TRPV1 cation channels. *Br J Pharmacol,* 173**,** 1154-62.
PETROSINO, S., SCHIANO MORIELLO, A., VERDE, R., ALLARÀ, M., IMPERATORE, R., LIGRESTI, A., MAHMOUD, A. M., PERITORE, A. F., IANNOTTI, F. A. & DI MARZO, V. 2019. Palmitoylethanolamide counteracts substance P-induced mast cell activation in vitro by stimulating diacylglycerol lipase activity. *Journal of Neuroinflammation,* 16**,** 1-16.
PHILLIPS, S. M. 2011. The science of muscle hypertrophy: making dietary protein count. *Proceedings of the nutrition society,* 70**,** 100-103.
PHILPOTT, J. D., DONNELLY, C., WALSHE, I. H., DICK, J., DR, S., GALLOWAY, K. D. & WITARD, O. C. Adding Fish Oil to Whey Protein, Leucine and Carbohydrate Over a 6 Week. *International Journal of Sport Nutrition*.
PIZZA, F. X., PETERSON, J. M., BAAS, J. H. & KOH, T. J. 2005. Neutrophils contribute to muscle injury and impair its resolution after lengthening contractions in mice. *The Journal of physiology,* 562**,** 899-913.
PROSKE, U. & MORGAN, D. L. 2001. Muscle damage from eccentric exercise: mechanism, mechanical signs, adaptation and clinical applications. *J Physiol,* 537**,** 333-45.
RAASTAD, T., OWE, S. G., PAULSEN, G., ENNS, D., OVERGAARD, K., CRAMERI, R., KIIL, S., BELCASTRO, A., BERGERSEN, L. H. & HALLÉN, J. 2010. Changes in calpain activity, muscle structure, and function after eccentric exercise.
RAINSFORD, K. 2009. Ibuprofen: pharmacology, efficacy and safety. *Inflammopharmacology,* 17**,** 275-342.
RANKIN, L. & FOWLER, C. J. 2020. The basal pharmacology of palmitoylethanolamide. *International Journal of Molecular Sciences,* 21**,** 7942.
RAVI, M., PARAMESH, V., KAVIYA, S., ANURADHA, E. & SOLOMON, F. P. 2015. 3D cell culture systems: advantages and applications. *Journal of cellular physiology,* 230**,** 16-26.
READ, D., SMITH, A. C. & SKINNER, J. 2023. Theorising painkiller (mis) use in football using Bourdieu's practice theory and physical capital. *International Review for the Sociology of Sport,* 58**,** 66-86.
RELAIX, F. & ZAMMIT, P. S. 2012. Satellite cells are essential for skeletal muscle regeneration: the cell on the edge returns centre stage. *Development,* 139**,** 2845-2856.

REYNOLDS, J., NOAKES, T., SCHWELLNUS, M., WINDT, A. & BOWERBANK, P. 1995. Non-steroidal antiinflammatory drugs fail to enhance healing of acute hamstring injuries treated with physiotherapy. *South African Medical Journal,* 85.

RIEGER, A. M. & BARREDA, D. R. 2016. Accurate assessment of cell death by imaging flow cytometry. *Imaging Flow Cytometry: Methods and Protocols*, 209-220.

RINNE, P., GUILLAMAT-PRATS, R., RAMI, M., BINDILA, L., RING, L., LYYTIKÄINEN, L.-P., RAITOHARJU, E., OKSALA, N., LEHTIMÄKI, T. & WEBER, C. 2018. Palmitoylethanolamide promotes a proresolving macrophage phenotype and attenuates atherosclerotic plaque formation. *Arteriosclerosis, thrombosis, and vascular biology,* 38, 2562-2575.

ROBERTS, B. M., GEDDIS, A. V. & MATHENY JR, R. W. 2024a. The dose-response effects of flurbiprofen, indomethacin, ibuprofen, and naproxen on primary skeletal muscle cells. *Journal of the International Society of Sports Nutrition,* 21, 2302046.

ROBERTS, B. M., SCZUROSKI, C. E., CALDWELL, A. R., ZEPPETELLI, D. J., SMITH, N. I., PECORELLI, V. P., GWIN, J. A., HUGHES, J. M. & STAAB, J. S. 2024b. NSAIDs do not prevent exercise-induced performance deficits or alleviate muscle soreness: A placebo-controlled randomized, double-blinded, cross-over study. *Journal of science and medicine in sport,* 27, 287-292.

RODEMANN, H. & GOLDBERG, A. 1982. Arachidonic acid, prostaglandin E2 and F2 alpha influence rates of protein turnover in skeletal and cardiac muscle. *Journal of Biological Chemistry,* 257, 1632-1638.

RODERICK, M. 2006. Adding insult to injury: workplace injury in English professional football. *Sociology of health & illness,* 28, 76-97.

ROJAS-VALVERDE, D. 2021. Potential role of cannabidiol on sports recovery: a narrative review. *Frontiers in Physiology,* 12, 722550.

ROSENBERG, H. F. & GALLIN, J. I. 1993. Neutrophil-specific granule deficiency includes eosinophils. *Blood,* 82, 268-273.

ROSS, R. A. 2003. Anandamide and vanilloid TRPV1 receptors. *British journal of pharmacology,* 140, 790-801.

RUSSO, E. B., GUY, G. W. & ROBSON, P. J. 2007. Cannabis, pain, and sleep: lessons from therapeutic clinical trials of Sativex®, a cannabis-based medicine. *Chemistry & biodiversity,* 4, 1729-1743.

SADYGOV, R. G. 2020a. Partial isotope profiles are sufficient for protein turnover analysis using closed-form equations of mass isotopomer dynamics. *Analytical chemistry,* 92, 14747-14753.

SADYGOV, R. G. 2020b. Partial Isotope Profiles Are Sufficient for Protein Turnover Analysis Using Closed-Form Equations of Mass Isotopomer Dynamics. *Anal Chem,* 92, 14747-14753.

SANDRI, M. 2013. Protein breakdown in muscle wasting: role of autophagy-lysosome and ubiquitin-proteasome. *The international journal of biochemistry & cell biology,* 45, 2121-2129.

SAWZDARGO, M., NGUYEN, T., LEE, D. K., LYNCH, K. R., CHENG, R., HENG, H. H., GEORGE, S. R. & O'DOWD, B. F. 1999. Identification and cloning of three novel human G protein-coupled receptor genes GPR52, ΨGPR53 and GPR55: GPR55 is extensively expressed in human brain. *Molecular brain research,* 64, 193-198.

SAXTON, J. & DONNELLY, A. 1995. Light concentric exercise during recovery from exercise-induced muscle damage. *International journal of sports medicine,* 16**,** 347-351.
SCALVINI, L., GHIDINI, A., LODOLA, A., CALLEGARI, D., RIVARA, S., PIOMELLI, D. & MOR, M. 2020. N-Acylethanolamine Acid Amidase (NAAA): Mechanism of Palmitoylethanolamide Hydrolysis Revealed by Mechanistic Simulations. *ACS Catalysis,* 10**,** 11797-11813.
SCHEER, V., BASSET, P., GIOVANELLI, N., VERNILLO, G., MILLET, G. P. & COSTA, R. J. 2020. Defining off-road running: a position statement from the ultra sports science foundation. *International journal of sports medicine,* 41**,** 275-284.
SCHIAFFINO, S., BORMIOLI, S. P. & ALOISI, M. 1979. Fibre branching and formation of new fibres during compensatory muscle hypertrophy. *Muscle regeneration***,** 177-188.
SCHOENFELD, B. J. 2012. The Use of Nonsteroidal anti-inflammatory drugs for exercise-induced muscle damage. *Sports medicine,* 42**,** 1017-1028.
SCHOUTEN, M., DALLE, S., COSTAMAGNA, D., RAMAEKERS, M., BOGAERTS, S., THIENEN, R. V., PEERS, K., THOMIS, M. & KOPPO, K. 2024. Palmitoylethanolamide Does Not Affect Recovery from Exercise-Induced Muscle Damage in Healthy Males.
SCHULTZ, E., GIBSON, M. C. & CHAMPION, T. 1978. Satellite cells are mitotically quiescent in mature mouse muscle: an EM and radioautographic study. *Journal of Experimental Zoology,* 206**,** 451-456.
SCHWANE, J. A., JOHNSON, S. R., VANDENAKKER, C. B. & ARMSTRONG, R. B. 1983. Delayed-onset muscular soreness and plasma CPK and LDH activities after downhill running. *Med Sci Sports Exerc,* 15**,** 51-6.
SHARIR, H. & ABOOD, M. E. 2010. Pharmacological characterization of GPR55, a putative cannabinoid receptor. *Pharmacology & therapeutics,* 126**,** 301-313.
SHEN, W., PRISK, V., LI, Y., FOSTER, W. & HUARD, J. 2006. Inhibited skeletal muscle healing in cyclooxygenase-2 gene-deficient mice: the role of PGE2 and PGF2α. *Journal of applied physiology,* 101**,** 1215-1221.
SISIGNANO, M. & GEISSLINGER, G. 2023. Rethinking the use of NSAIDs in early acute pain. *Trends in Pharmacological Sciences*.
SJODIN, B. & SVEDENHAG, J. 1985. Applied physiology of marathon running. *Sports medicine,* 2**,** 83-99.
SKAPER, S. D., FACCI, L., BARBIERATO, M., ZUSSO, M., BRUSCHETTA, G., IMPELLIZZERI, D., CUZZOCREA, S. & GIUSTI, P. 2015. N-Palmitoylethanolamine and Neuroinflammation: a Novel Therapeutic Strategy of Resolution. *Mol Neurobiol,* 52**,** 1034-42.
SMITH JR, M. & JACKSON, C. 1990. 199 Delayed Onset Muscle Soreness (doms), Serum Creatine Kinase (sck), And Creatine Kinase-mb (ck-mb) Related To Performance Measurements In Football. *Medicine & Science in Sports & Exercise,* 22**,** S34.
SMITH, L. L. 1991. Acute inflammation: the underlying mechanism in delayed onset muscle soreness? *Medicine and science in sports and exercise,* 23**,** 542-551.
SNOW, M. H. 1977. Myogenic cell formation in regenerating rat skeletal muscle injured by mincing II. An autoradiographic study. *The Anatomical Record,* 188**,** 201-217.
SORICHTER, S., KOLLER, A., HAID, C., WICKE, K., JUDMAIER, W., WERNER, P. & RAAS, E. 1995. Light concentric exercise and heavy eccentric muscle loading: effects

on CK, MRI and Markers of Inflammation. *International journal of sports medicine,* 16**,** 288-292.
SORICHTER, S., MAIR, J., KOLLER, A., GEBERT, W., RAMA, D., CALZOLARI, C., ARTNER-DWORZAK, E. & PUSCHENDORF, B. 1997. Skeletal troponin I as a marker of exercise-induced muscle damage. *Journal of applied physiology,* 83**,** 1076-1082.
SORICHTER, S., PUSCHENDORF, B. & MAIR, J. 1999. Skeletal muscle injury induced by eccentric muscle action: muscle proteins as markers of muscle fiber injury. *Exercise immunology review,* 5**,** 5-21.
SOUTHORN, B. G. & PALMER, R. M. 1990. Inhibitors of phospholipase A2 block the stimulation of protein synthesis by insulin in L6 myoblasts. *Biochemical journal,* 270**,** 737-739.
SRISAWAT, K., STEAD, C. A., HESKETH, K., POGSON, M., STRAUSS, J. A., COCKS, M., SIEKMANN, I., PHILLIPS, S. M., LISBOA, P. J. & SHEPHERD, S. 2024. People with obesity exhibit losses in muscle proteostasis that are partly improved by exercise training. *Proteomics,* 24**,** 2300395.
STAMPANONI BASSI, M., GENTILE, A., IEZZI, E., ZAGAGLIA, S., MUSELLA, A., SIMONELLI, I., GILIO, L., FURLAN, R., FINARDI, A. & MARFIA, G. A. 2019. Transient receptor potential vanilloid 1 modulates central inflammation in multiple sclerosis. *Frontiers in neurology,* 10**,** 416781.
STANSFIELD, B. N., BROWN, A. D., STEWART, C. E. & BURNISTON, J. G. 2021. Dynamic profiling of protein mole synthesis rates during C2C12 myoblast differentiation. *Proteomics,* 21**,** 2000071.
STEAD, C. A., HESKETH, S. J., THOMAS, A. C., VIGGARS, M. R., SUTHERLAND, H., JARVIS, J. C. & BURNISTON, J. G. 2025. Dynamic time course of muscle proteome adaptation to programmed resistance training in rats. *American Journal of Physiology-Cell Physiology*.
STEENSBERG, A., VAN HALL, G., OSADA, T., SACCHETTI, M., SALTIN, B. & PEDERSEN, B. K. 2000. Production of interleukin-6 in contracting human skeletal muscles can account for the exercise-induced increase in plasma interleukin-6. Wiley Online Library.
STEINHARDT, R. A., BI, G. & ALDERTON, J. M. 1994. Cell membrane resealing by a vesicular mechanism similar to neurotransmitter release. *Science,* 263**,** 390-393.
SUMNERS, D. P., DYER, A., FOX, P., MILEVA, K. N. & BOWTELL, J. 2011. Montmorency cherry juice reduces muscle damage caused by intensive strength exercise.
SUZIC LAZIC, J., DIKIC, N., RADIVOJEVIC, N., MAZIC, S., RADOVANOVIC, D., MITROVIC, N., LAZIC, M., ZIVANIC, S. & SUZIC, S. 2011. Dietary supplements and medications in elite sport–polypharmacy or real need? *Scandinavian journal of medicine & science in sports,* 21**,** 260-267.
SZCZYGLOWSKI, M. K., ADE, C. J., CAMPBELL, J. A. & BLACK, C. D. 2017. The effects of exercise-induced muscle damage on critical torque. *European Journal of Applied Physiology,* 117**,** 2225-2236.
SZKLARCZYK, D., KIRSCH, R., KOUTROULI, M., NASTOU, K., MEHRYARY, F., HACHILIF, R., GABLE, A. L., FANG, T., DONCHEVA, N. T. & PYYSALO, S. 2023. The STRING database in 2023: protein–protein association networks and functional enrichment analyses for any sequenced genome of interest. *Nucleic acids research,* 51**,** D638-D646.

TAIOLI, E. 2007. Use of permitted drugs in Italian professional soccer players. *British journal of sports medicine,* 41**,** 439-441.
TARTIBIAN, B., MALEKI, B. H. & ABBASI, A. 2009. The effects of ingestion of omega-3 fatty acids on perceived pain and external symptoms of delayed onset muscle soreness in untrained men. *Clinical Journal of Sport Medicine,* 19**,** 115-119.
THORPE, R., BLOCKMAN, M., TALBERG, H. & BURGESS, T. 2022. The knowledge and attitudes of South African-based runners regarding the use of analgesics during training and competition. *South African Journal of Sports Medicine,* 34**,** 1-6.
TIDBALL, J. G. 2005. Inflammatory processes in muscle injury and repair. *American Journal of Physiology-Regulatory, Integrative and Comparative Physiology,* 288**,** R345-R353.
TIDBALL, J. G. 2011. Mechanisms of muscle injury, repair, and regeneration. *Comprehensive physiology***,** 2029-2062.
TIDBALL, J. G. & VILLALTA, S. A. 2010. Regulatory interactions between muscle and the immune system during muscle regeneration. *American Journal of Physiology-Regulatory, Integrative and Comparative Physiology,* 298**,** R1173-R1187.
TIDMAS, V., BRAZIER, J., BOTTOMS, L., MUNIZ, D., DESAI, T., HAWKINS, J., SRIDHARAN, S. & FARRINGTON, K. 2022. Ultra-endurance participation and acute kidney injury: a narrative review. *International Journal of Environmental Research and Public Health,* 19**,** 16887.
TILLER, N. B. & MILLET, G. Y. 2025. Decoding ultramarathon: muscle damage as the main impediment to performance. *Sports Medicine,* 55**,** 535-543.
TILLER, N. B., ROBERTS, J. D., BEASLEY, L., CHAPMAN, S., PINTO, J. M., SMITH, L., WIFFIN, M., RUSSELL, M., SPARKS, S. A. & DUCKWORTH, L. 2019. International Society of Sports Nutrition Position Stand: Nutritional considerations for single-stage ultra-marathon training and racing. *Journal of the International Society of Sports Nutrition,* 16**,** 50.
TRAPPE, T., FLUCKEY, J., WHITE, F., LAMBERT, C. & EVANS, W. 2001. Skeletal muscle PGF2αand PGE2 in response to eccentric resistance exercise: influence of ibuprofen and acetaminophen. *The Journal of Clinical Endocrinology & Metabolism,* 86**,** 5067-5070.
TRAPPE, T. A., CARROLL, C. C., DICKINSON, J. M., LEMOINE, J. K., HAUS, J. M., SULLIVAN, B. E., LEE, J. D., JEMIOLO, B., WEINHEIMER, E. M. & HOLLON, C. J. 2011. Influence of acetaminophen and ibuprofen on skeletal muscle adaptations to resistance exercise in older adults. *American Journal of Physiology-Regulatory, Integrative and Comparative Physiology,* 300**,** R655-R662.
TRAPPE, T. A. & LIU, S. Z. 2013. Effects of prostaglandins and COX-inhibiting drugs on skeletal muscle adaptations to exercise. *Journal of Applied Physiology,* 115**,** 909-919.
TRAPPE, T. A., RATCHFORD, S. M., BROWER, B. E., LIU, S. Z., LAVIN, K. M., CARROLL, C. C., JEMIOLO, B. & TRAPPE, S. W. 2016. COX inhibitor influence on skeletal muscle fiber size and metabolic adaptations to resistance exercise in older adults. *Journals of Gerontology Series A: Biomedical Sciences and Medical Sciences,* 71**,** 1289-1294.
TRAPPE, T. A., WHITE, F., LAMBERT, C. P., CESAR, D., HELLERSTEIN, M. & EVANS, W. J. 2002. Effect of ibuprofen and acetaminophen on postexercise muscle protein

synthesis. *American Journal of Physiology-Endocrinology and Metabolism,* 282**,** E551-E556.
TSAO, R. 2010. Chemistry and biochemistry of dietary polyphenols. *Nutrients,* 2**,** 1231-1246.
TSCHOLL PH, M., GARD, S. & SCHINDLER, M. 2017. A sensible approach to the use of NSAIDs in sports medicine. *Schweiz Z Med Traumatol,* 65**,** 15-20.
TSITSIMPIKOU, C., TSIOKANOS, A., TSAROUHAS, K., SCHAMASCH, P., FITCH, K. D., VALASIADIS, D. & JAMURTAS, A. 2009. Medication use by athletes at the Athens 2004 Summer Olympic Games. *Clinical journal of sport medicine,* 19**,** 33-38.
TSUBOI, K., SUN, Y. X., OKAMOTO, Y., ARAKI, N., TONAI, T. & UEDA, N. 2005. Molecular characterization of N-acylethanolamine-hydrolyzing acid amidase, a novel member of the choloylglycine hydrolase family with structural and functional similarity to acid ceramidase. *J Biol Chem,* 280**,** 11082-92.
TSUCHIYA, Y., YANAGIMOTO, K., NAKAZATO, K., HAYAMIZU, K. & OCHI, E. 2016. Eicosapentaenoic and docosahexaenoic acids-rich fish oil supplementation attenuates strength loss and limited joint range of motion after eccentric contractions: a randomized, double-blind, placebo-controlled, parallel-group trial. *European journal of applied physiology,* 116**,** 1179-1188.
UEDA, N., LIU, Q. & YAMANAKA, K. 2001. Marked activation of the N-acylphosphatidylethanolamine-hydrolyzing phosphodiesterase by divalent cations. *Biochimica et Biophysica Acta (BBA)-Molecular and Cell Biology of Lipids,* 1532**,** 121-127.
UEDA, N., TSUBOI, K. & UYAMA, T. 2010. N-acylethanolamine metabolism with special reference to N-acylethanolamine-hydrolyzing acid amidase (NAAA). *Prog Lipid Res,* 49**,** 299-315.
VACONDIO, F., BASSI, M., SILVA, C., CASTELLI, R., CARMI, C., SCALVINI, L., LODOLA, A., VIVO, V., FLAMMINI, L. & BAROCELLI, E. 2015. Amino acid derivatives as palmitoylethanolamide prodrugs: synthesis, in vitro metabolism and in vivo plasma profile in rats. *PLoS One,* 10**,** e0128699.
VAIA, M., PETROSINO, S., DE FILIPPIS, D., NEGRO, L., GUARINO, A., CARNUCCIO, R., DI MARZO, V. & IUVONE, T. 2016. Palmitoylethanolamide reduces inflammation and itch in a mouse model of contact allergic dermatitis. *European journal of pharmacology,* 791**,** 669-674.
VAN WIJCK, K., LENAERTS, K., VAN BIJNEN, A. A., BOONEN, B., VAN LOON, L. J., DEJONG, C. H. & BUURMAN, W. A. 2012. Aggravation of exercise-induced intestinal injury by Ibuprofen in athletes. *Medicine & Science in Sports & Exercise,* 44**,** 2257-2262.
VANDENBURGH, H. H., HATFALUDY, S., SOHAR, I. & SHANSKY, J. 1990. Stretch-induced prostaglandins and protein turnover in cultured skeletal muscle. *American Journal of Physiology-Cell Physiology,* 259**,** C232-C240.
VELIÇA, P. & BUNCE, C. M. 2011. A quick, simple and unbiased method to quantify C2C12 myogenic differentiation. *Muscle & nerve,* 44**,** 366-370.
VERBURG, E., MURPHY, R. M., STEPHENSON, D. G. & LAMB, G. D. 2005. Disruption of excitation–contraction coupling and titin by endogenous Ca2+-activated proteases in toad muscle fibres. *The Journal of physiology,* 564**,** 775-790.
VERME, J. L., FU, J., ASTARITA, G., LA RANA, G., RUSSO, R., CALIGNANO, A. & PIOMELLI, D. 2005. The nuclear receptor peroxisome proliferator-activated

receptor-α mediates the anti-inflammatory actions of palmitoylethanolamide. *Molecular pharmacology,* 67**,** 15-19.
WANG, Z., GERSTEIN, M. & SNYDER, M. 2009. RNA-Seq: a revolutionary tool for transcriptomics. *Nature reviews genetics,* 10**,** 57-63.
WARDEN, S. J. 2005. Cyclo-oxygenase-2 inhibitors: beneficial or detrimental for athletes with acute musculoskeletal injuries? *Sports Medicine,* 35**,** 271-283.
WARDEN, S. J. 2009. Prophylactic misuse and recommended use of non-steroidal anti-inflammatory drugs by athletes. British Association of Sport and Excercise Medicine.
WARDEN, S. J. 2010. Prophylactic use of NSAIDs by athletes: a risk/benefit assessment. *The Physician and sportsmedicine,* 38**,** 132-138.
WARNER, D. C., SCHNEPF, G., BARRETT, M. S., DIAN, D. & SWIGONSKI, N. L. 2002. Prevalence, attitudes, and behaviors related to the use of nonsteroidal anti-inflammatory drugs (NSAIDs) in student athletes. *Journal of Adolescent Health,* 30**,** 150-153.
WARREN, G. L., INGALLS, C. P., LOWE, D. A. & ARMSTRONG, R. 2002. What mechanisms contribute to the strength loss that occurs during and in the recovery from skeletal muscle injury? *Journal of Orthopaedic & Sports Physical Therapy,* 32**,** 58-64.
WARREN, G. L., LOWE, D. A. & ARMSTRONG, R. B. 1999. Measurement tools used in the study of eccentric contraction-induced injury. *Sports medicine,* 27**,** 43-59.
WHALEN, R. G., HARRIS, J. B., BUTLER-BROWNE, G. S. & SESODIA, S. 1990. Expression of myosin isoforms during notexin-induced regeneration of rat soleus muscles. *Developmental biology,* 141**,** 24-40.
WHARAM, P. C., SPEEDY, D. B., NOAKES, T. D., THOMPSON, J., REID, S. A. & HOLTZHAUSEN, L.-M. 2006. NSAID use increases the risk of developing hyponatremia during an Ironman triathlon. *Medicine and Science in Sports and Exercise,* 38**,** 618-622.
WILLOUGHBY, D., MCFARLIN, B. & BOIS, C. 2003. Interleukin-6 expression after repeated bouts of eccentric exercise. *International journal of sports medicine,* 24**,** 15-21.
WIŚNIEWSKI, J. R., ZOUGMAN, A., NAGARAJ, N. & MANN, M. 2009. Universal sample preparation method for proteome analysis. *Nature methods,* 6**,** 359-362.
WOJCIK, J. R., WALBERG-RANKIN, J., SMITH, L. L. & GWAZDAUSKAS, F. 2001. Comparison of carbohydrate and milk-based beverages on muscle damage and glycogen following exercise. *International journal of sport nutrition and exercise metabolism,* 11**,** 406-419.
WOLEDGE, R. C., CURTIN, N. A. & HOMSHER, E. 1985. Energetic aspects of muscle contraction. *Monographs of the physiological society,* 41**,** 1-357.
YAFFE, D. & SAXEL, O. 1977. Serial passaging and differentiation of myogenic cells isolated from dystrophic mouse muscle. *Nature,* 270**,** 725-727.
YASUDA, T., SAKAMOTO, K., NOSAKA, K., WADA, M. & KATSUTA, S. 1997. Loss of sarcoplasmic reticulum membrane integrity after eccentric contractions. *Acta physiologica scandinavica,* 161**,** 581-582.
YIN, H., PRICE, F. & RUDNICKI, M. A. 2013. Satellite cells and the muscle stem cell niche. *Physiological reviews,* 93**,** 23-67.

YU, G., WANG, L.-G., HAN, Y. & HE, Q.-Y. 2012. clusterProfiler: an R package for comparing biological themes among gene clusters. *Omics: a journal of integrative biology,* 16**,** 284-287.

ZAMBRASKI, E., COLLETTI, A., RAHE, T. & VOGL, H. 1996. Effects of acetaminophen versus ibuprofen on renal function in normal and sodium depleted subjects. *Physiologist,* 39**,** A53.

ZHAO, R. & TSANG, S. Y. 2017. Versatile roles of intracellularly located TRPV1 channel. *Journal of Cellular Physiology,* 232**,** 1957-1965.

ZILTENER, J.-L., LEAL, S. & FOURNIER, P.-E. 2010. Non-steroidal anti-inflammatory drugs for athletes: an update. *Annals of physical and rehabilitation medicine,* 53**,** 278-288.

ZYGMUNT, P. M., ERMUND, A., MOVAHED, P., ANDERSSON, D. A., SIMONSEN, C., JÖNSSON, B. A., BLOMGREN, A., BIRNIR, B., BEVAN, S. & ESCHALIER, A. 2013. Monoacylglycerols activate TRPV1–a link between phospholipase C and TRPV1. *PloS one,* 8**,** e81618.